GRADUATE SCHOOL OF NATURAL AND APPLIED SCIENCES

PhD THESIS

May, 2019

REPUBLIC OF TURKEY
YILDIZ TECHNICAL UNIVERSITY
GRADUATE SCHOOL OF NATURAL AND APPLIED SCIENCES

GREEN SYNTHESIS OF METAL NANOPARTICLES, THEIR CHEMICAL AND BIOCHEMICAL CHARACTERIZATIONS

ISRAT JAHAN

PHD THESIS
DEPARTMENT OF BIOENGINEERING
PROGRAM OF BIOENGINEERING

ADVISER
PROF. DR. IBRAHIM IŞILDAK

ISTANBUL, 2019

REPUBLIC OF TURKEY

YILDIZ TECHNICAL UNIVERSITY

GRADUATE SCHOOL OF NATURAL AND APPLIED SCIENCES

GREEN SYNTHESIS OF METAL NANOPARTICLES, THEIR CHEMICAL AND BIOCHEMICAL CHARACTERIZATIONS

A thesis submitted by Israt JAHAN in partial fulfilment of the requirements for the degree of **DOCTOR OF PHILOSOPHY** is approved by the committee on 06.05.2019 in Department of Bioengineering, Bioengineering Program.

Thesis Adviser

Prof. Dr. Ibrahim IŞILDAK

Yıldız Technical University

Approved By the Examining Committee

Prof. Dr. Ibrahim IŞILDAK

Yıldız Technical University _____

Assoc. Prof. Didem ÖZÇİMEN, Member

Yıldız Technical University _____

Assoc. Prof. Dr. Kazım Yalçın ARĞA, Member

Marmara University _____

Prof. Dr. Musa TÜRKER, Member

Yıldız Technical University _____

Prof. Dr. İbrahim DEMİRTAŞ, Member

Çankırı Karatekin University _____

ACKNOWLEDGEMENTS

research at YTU campus. I would also like to express my gratitude to Prof. Dr. Musa TÜRKER, the chairman of the Department of Bioengineering and other faculty members in our department for their help and encouragement throughout my Ph.D. program at Yıldız Technical University. I am grateful that I have had the privilege to work with these dynamic and energetic researchers.

I am ever grateful to my family for their sacrifice and endless support to fulfil my dreams and wishes. Albeit this would not be enough, I would like to present my gratitude to my mother, my father, my mother-in-law, my brother Dider, my sister Nowshin and my brother-in-law Jafor. Especially, I am grateful to my husband Dr. Abu Bakar SIDDIQ, for his companionship, endless support and immeasurable sacrifice, which have allowed me to complete the long process of research work presented in this thesis as well as at least a small contribution I present to enrich scientific research in Turkey.

Despite the invaluable help from the people listed above, the research and results presented in this thesis is entirely my own. No one else but I am the one who is responsible for all of its errors and mistakes.

April, 2019

Israt JAHAN

TABLE OF CONTENTS

CHAPTER 5

LIST OF SYMBOLS

%	Percentage
&	And
~	Approximately
±	Error
°C	Degree centigrade
Å	Degree Angstrom
et al.	And others
etc.	Etcetera
gm	Gram (s)
h	Hour (s)
L	Liter (s)
M	Mole (s)
mg/g	Milligram per gram
mg/l	Milligram per liter
min.	Minute (s)
ml	Milliliter (s)
mM	Millimolar (s)
mm	Millimeter (s)
nm	Nanometer (s)
no.	Number
pH	Power of hydrogen
rpm	Revolution per minutes
v/v %	Volume/ volume percentage concentration
w/v %	Weight/volume percentage concentration
W	Watt
λ	Wavelength
μg	Microgram (s)
μl	Microliter (s)
μM	Micromole (s)

LIST OF ABBREVIATIONS

ACS   American Chemical Society
AFM   Atomic Force Microscopy
CFU   Colony forming unit
DLS   Dynamic light scattering
DMEM   Eagle's minimal essential medium
DNA   Deoxyribonucleic acid
EDS/EDX   Energy dispersive X-ray spectroscopy
ELISA   Enzyme-Linked Immunosorbent Assay
FBS   Fetal Bovine Serum
HRTEM   High-resolution transmission electron microscopy
IR   Infra-Red
ISO   International Organization for Standardization
JCPDS   Joint Committee on powder diffraction standards
MEF   Metal-enhanced fluorescence
NADPH   Nicotinamide adenine dinucleotide phosphate
NPs   Nanoparticles
PBS   Phosphate-buffered saline
RNA   Ribonucleic acid
ROS   Reactive oxygen species
SEM   Scanning Electron Microscopy
SERS   Surface-enhanced Raman scattering
SPR   Surface Plasmon Resonance
TEM   Transmission Electron Microscopy
TMV   Tobacco Mosaic Virus
UV-Vis   Ultra violet visible
XRD   X- ray diffraction
XTT   Tetrazolium chloride
YTU   Yıldız Technical University

LIST OF FIGURES

xii

LIST OF TABLES

ABSTRACT

GREEN SYNTHESIS OF METAL NANOPARTICLES, THEIR CHEMICAL AND BIOCHEMICAL CHARACTERIZATIONS

Israt JAHAN

Department of Bioengineering

PhD Thesis

Adviser: Prof. Dr. Ibrahim IŞILDAK

Nanotechnology has been a flourishing field by being concentrated on the fabrication, characterization, manipulation and the exploitation of materials at the nanometre scale. There is also an expanding commercial demand for nanoparticles, particularly the metallic nanoparticles because of their wide-ranging capacity to be used in various sectors. Conventional methods for nanoparticle synthesis are quite expensive as well as they produce nanoparticles with toxic residues. The existence of these contaminated toxic residues with synthesized NPs can create potential risks such as ecological imbalance, carcinogenicity and cytotoxicity which might limit their clinical and biomedical applications. Hence, there is a new branch in contemporary scientific approach which is called nanobiotechnology. Along with the chemical and physical processes, this new scientific branch particularly deals the principles of biology for the production of particles at nano-levels of specific functions. Providing that they utilize simple, moderately low-priced and effortlessly scaled-up nontoxic materials for comparatively a large-scale fabrication, the bio-based techniques for the production of NPs are economic as well as environmentally. Besides, the green syntheses of NPs with microwave-assisted heating technique offer some extra benefits. This is due to the reason that it reveals increased reaction kinetics and boosts reaction rates which eventually accelerate higher yields along with the desirable quality.

Considering these facts, scopes and benefits, the main aim of this study has been to fabricate silver and copper nanoparticles via plant extracts, as reducing, capping and stabilizing agents. In this investigation, microwave irradiation scheme with two optimized parameters (time and temperature) has been used for facile and fast phytosynthesis of NPs. Aqueous extracts of *Malus pumila* (apple) pulp, *Cuminum cyminum* (cumin) seeds, *Zingiber officinale* (ginger) rhizome, *Rosa santana* (rose) petals, *Citrus sinensis* (orange) peel and *Citrus limon* (lemon) peel have been used to

synthesize AgNPs whereas *Camellia sinensis* (green tea), *Zingiber officinale* (ginger) rhizome, *Citrus sinensis* (orange) juice and *Pinus brutia* (Turkish pine) bark extracts were used for CuNPs synthesis.

After successful syntheses, the quantity and quality of nanoparticles have been screened by UV-Vis spectroscopy, X-Ray Diffraction (XRD) analysis, Fourier Transforms Infrared (FTIR) spectroscopy, Transmission Electron Microscopy (TEM) and particle size distribution and Zeta potential measurement. The TEM micrographs confirmed the presence of nearly spherical or oval shaped nanoparticles (AgNPs & CuNPs). For AgNPs, the smallest size ranged (1.84 - 20.57 nm) nanoparticles (CcAgNPs) with the mean diameter of 14.30 nm were obtained from *Cuminum cyminum* (cumin) seed extract while the largest size ranged (7.5 - 69.83 nm) nanoparticles (ClAgNPs) with the average diameter of 41.86 nm were found using *Citrus limon* (lemon) peel extract. On the other hand, for CuNPs, the smallest size ranged (6.93 - 20.70 nm) nanoparticles (CisCuNPs) with the average diameter of 17.58 nm were observed from *Citrus sinensis* (orange) juice extract and the largest particle size ranged (17.59 - 149.92 nm) nanoparticles (CasCuNPs) with the average diameter of 45.30 nm were achieved from *Camellia sinensis* (green tea).

Antibacterial prospective and potentials of both silver and copper NPs have been investigated against Gram-positive (*Staphylococcus aureus*) along with Gram-negative (*Escherichia coli*) bacteria. It has been found that the nanoparticle samples with smallest particle size range and highest potential value showed the best antibacterial activities. Therefore, the silver nanoparticle (CcAgNPs) obtained from *Cuminum cyminum* seed extract showed the highest antibacterial activity against *S. aureus* and *E. coli* with the maximum inhibition zones of 12.53 mm and 10.30 mm in diameter, respectively. Similarly, the copper nanoparticles (CisCuNPs) using *Citrus sinensis* juice extract showed the maximum antibacterial activity with the highest inhibition zones of 12.60 mm and 10.83 mm in diameter against *S. aureus* and *E. coli*, respectively. Considering the overall outcomes, it is remarkable that silver nanoparticles showed stronger antibacterial activity then copper nanoparticles.

In this study, the in-vitro cytotoxic effects of both AgNPs and CuNPs have also been monitored against healthy, regular normal mouse fibroblasts cell line (L929) by means of XTT assay. According to results, the cell viability has not been found significantly affected with increased concentrations (0.1 - 5μg/mL) of nanoparticles; hence it is noticeable and apparent that, none of the phytosynthesized nanoparticles has toxic effect on L929 cells in given concentrations.

Keywords: Green synthesis, Microwave-assisted synthesis, silver, copper, metallic nanoparticles, antibacterial activity, cytotoxicity

YILDIZ TECHNICAL UNIVERSITY

GRADUATE SCHOOL OF NATURAL AND APPLIED SCIENCES

YEŞİL METAL NANOPARTİKÜL SENTEZİ, KİMYASAL VE BİYOKİMYASAL KARAKTERİZASYONU

Israt JAHAN

Biyomühendislik Anabilim Dalı

Doktora Tezi

Tez Danışmanı: Prof. Dr. Ibrahim IŞILDAK

Nanoteknoloji, nanometre ölçeğinde malzemelerin üretilmesi, karakterizasyonu, manipülasyonu ve kullanımına odaklanarak gelişen bir alandır. Nanopartiküllerin, özellikle metalik nanopartiküllerin çeşitli alanlarda geniş ve kapsamlı uygulanabilir olması nedeniyle bu nanopartiküllere yüksek bir ticari talep mevcuttur. Nanopartikül sentezi için konvensiyonel yöntemler, nanopartikülleri toksik kalıntılar ile birlikte üretmesinin yanı sıra oldukça pahalıdır. Nanopartiküller üzerindeki bu toksik kalıntıların varlığı, çevresel toksisite, sitotoksisite ve kanserojenite gibi klinik ve biyomedikal uygulamaları sınırlayabilecek potansiyel riskler oluşturabilir. Bu nedenle günümüzdeki bilimsel yaklaşımlarında, biyolojinin prensiplerini kimyasal ve fiziksel süreçlerle birleştirerek, nano-boyutlu partiküllerin spesifik fonksiyonlarla üretilmesi için nanobiyoteknoloji adı verilen yeni bir bilim dalı ortaya çıkmıştır. Nanopartiküllerin sentezi için biyolojik yöntemler hem ekonomik hem de çevresel olarak yeşildir. Çünkü daha büyük ölçekli üretim için bu uygulamalarda nispeten ucuz, basit ve kolayca ölçeklendirilebilen toksik olmayan malzemeler kullanılmaktadır. Öte yandan, nanoparçacıkların mikrodalga destekli ısıtma tekniği ile yeşil sentezi ise bu uygulamalarda ek faydalar sağlamaktadır. Bunun nedeni ise, bu tekniğin istenen kalite ile birlikte daha yüksek verime sebebp olan yüksek reaksiyon kinetiği ve yüksek reaksiyon hızları sağlamasıdır.

Bu sebepleri, kapsamları ve avantajları ele aldığımızda bu çalışmanın temel amacı, bitkisel ekstraklarını indirgeyici, kapaklayıcı ve stabilize edici maddeler olarak kullanılması ile gümüş ve bakır nanoparçacıkların sentezlenmezi olarak belirlendi. Çalışmada, nanoparçacıkların kolay ve hızlı fitosentezi için iki paramtre (zaman ve sıcaklık) yönünden optimize edilmiş olan mikrodalga ışınlama yöntemi kullanılmıştır.

Gümüş nanoparçacıkların (AgNPs) sentezi için taze *Malus pumila* (elma), *Cuminum cyminum* (kimyon) tozu, taze *Zingiber officinale* (zencefil), *Rosa santana* (gül) taçyaprağı, *Citrus limon* (limon) kabuğu ve *Citrus sinensis* (portakal) kabuğun sulu ekstraksiyonu kullanırken, bakır nanoparçaların (CuNPs) sentezi için taze *Zingiber officinale* (zencefil), kuru *Camellia sinensis* (yeşil çay), *Citrus sinensis* (portakal) suyu ve *Pinus brutia* (Kızılçam) kabuğun ekstraksiyonu kullanılmıştır. Başarılı sentez işlemlerinden sonra, nanopartiküllerin miktarı ve kalitesi UV-Vis spektroskopisi, Fourier Transforms İnfrared (FTIR) spektroskopisi, X-Işını Kırınımı (XRD) analizi, Transmisyon Elektron Mikroskobu (TEM), Partiküllerin Boyut Ölçümü ve Zeta Potansiyel Ölçümü (Zeta sizer) ile karakterize edilmiştir. TEM mikrografları ile neredeyse yuvarlak veya oval şekilli nanopartiküllerin (AgNPs & CuNPs) varlığı doğrulanmıştır. AgNP'ler için, ortalama çapı 41,86 nm ile birlike en büyük boyutlu olan (7,5 - 69,83 nm) nanopartiküller (ClAgNP) *Citrus limon* kabuğu ekstraksiyondan elde edilirken, *Cuminum cyminum* çekirdeği kabuğu ekstraksiyondan ortalama çapı 14,30 nm ile birlikte en küçük boyutlu (1,84 - 20,80 nm) nanopartiküller (CcAgNP) tespit edilmiştir. Öte yandan CuNP'ler için, ortalama çapı 45,30 nm ile birlike en büyük boyutlu olan (17,59 - 149,92 nm) nanopartiküller (CasCuNP) *Camellia sinensis* ekstraksiyondan elde edilirken, *Citrus sinensis* suyudan ortalama çapı 17,58 nm ile birlikte en küçük boyutlu (6,93 - 20,70 nm) nanopartiküller (CisCuNP) tespit edilmiştir.

Hem AgNP hem de CuNP'lerin antibateriyel potansiyelleri Gram pozitif (*Staphylococcus aureus*) ve Gram negatif (*Escherichia coli*) bakterilere karşı test edilmiştir. En küçük parçacık büyüklüğü aralığına ve en yüksek potansiyel değere sahip nanopartikül örneklerinin en iyi antibakteriyel aktiviteleri gösterdiği gözlenmiştir. Böylece, kimyon tohumu ekstraksiyondan elde edilen gümüş nanoparçacık (CcAgNP), 12,53 mm maksimum inhibisyon zonlarıyla10,30 mm çapındaki sırasıyla *S. aureus* ve *E. coli*'ye karşı en yüksek antibakteriyel etkinliği göstermektedir. Aynı şekilde, portakal suyu ekstraksiyondan elde edilen bakır nanoparçacık (CisCuNP), 12,60 mm maksimum inhibisyon zonlarıyla10,83 mm çapındaki sırasıyla *S. aureus* ve *E. coli*'e karşı en yüksek antibakteriyel etkinliği göstermektedir. Dolayısıyla, genel sonuçlar göz önüne alındığında, bakır nanoparçacıkların aksine gümüş nanoparçacıkların daha güçlü antibakteriyel aktivite gösterdiği söz konusudur.

Bu çalışmada, ayrıca, hem AgNP hem de CuNP'lerin in vitro sitotoksik etkilerin, XTT testi ile normal fare fibroblast hücre hattı (L929) üzerinde belirlenmiştir. Sonuçlara göre, nanopartiküllerin artan konsantrasyonlarından (0,1 - 5,0 µg/mL) hücre canlılığı önemli ölçüde etkilenmemiştir; Dolayısıyla, fitosentezlenmiş nanopartiküllerin hiçbirinin, verilen konsantrasyonlarda L929 hücreleri üzerinde toksik etkisi olmadığı açıktır.

Anahtar Kelimeler: Yeşil sentez, Mikrodalga destekli sentez, gümüş, bakır, metalik nanopartiküller, antibakteriyel aktivite, sitotoksisite

YILDIZ TEKNİK ÜNİVERSİTESİ FEN BİLİMLERİ ENSTİTÜSÜ

CHAPTER 1

INTRODUCTION

1.1 Literature Review

The prefix 'Nano' of the Nanotechnology was actually coined from the Greek originated word 'Nanos', meaning the dwarf or miniature. This is a theoretical and applied science at the molecular level mainly covering and focusing the exploration, manufacture, categorization and the use of materials below 100 nanometres. In other ways, 'nanotechnology' compels the capability to include components of molecular size and precise machine. While giving a talk called "There's Plenty of Room at the Bottom", the idea of nanotechnology first came from a physicist Richard Feynman in 1959 [1].

According to the National Science Foundation (NSF) in the U.S., nanotechnology enhances the ability to comprehend, operate and control matter at molecular level of particular atom [2]. It is a rising field which can be used in almost every field of scientific inventions. Currently, the branches of nanotechnology are being expanded and extended to large a number of areas including catalysis, mechanics, biomedical, beverage, cosmetics, photo-electrochemical application which could bang the international market [1].

Furthermore, green nanotechnology is the branch of nanotechnology that increases environmental sustainability by utilizing eco-friendly methods to manufacture green Nano-products that reduce negative facet [3]. Nanotechnology appliances are vastly appropriate for biological research applications mainly because of their specific properties.

The significance of the use of green or bio-nanotechnology comes from the advantages that it can use biological resources to fabricate metallic nanoparticles. Albeit having

many conventional schemes available for the fabrication of metallic nanoparticles assuring high purity and expected quality of the nanostructured materials, these methods are often reasonably costly, damaging, unsafe, unhealthy and environmentally harmful. Therefore, bio-based green synthesis by means of biological materials such as plant, algae, fungi, bacteria and viruses has gradually been a matter of extra attention as well as been believed to be biocompatible and lucrative process among scientific community [4]. Consequently, the biosynthesis of metallic nanoparticles has been a vast area of study with the potential and impending functions as well as the applications for utilizing and implementing different developments of advanced technologies [5]. However, the main aim of green nanotechnological research has been to reduce environmental and human health hazards and to enhance the application of more environmentally friendly Nano-products as the substitute of existing toxic products.

1.2 Objective of the Thesis

The primary objective of this study has been:

1. The evaluation of the potential use of plant parts as well as biological wastes (e.g. orange and lemon peel, rose petals and pine bark) as synthesizing agents for the production of silver (AgNPs) and copper (CuNPs) nanoparticles.

2. To phytosynthesize silver nanoparticles (AgNPs) and copper nanoparticles (CuNPs) under microwave irradiation (by green synthesis method).

3. To perform details chemical and biochemical characterizations of biosynthesized silver (AgNPs) and copper (CuNPs) nanoparticles.

4. To observe and thoroughly estimate the antimicrobial potential of both biosynthesized silver (AgNPs) and copper (CuNPs) nanoparticles against the species *Escherichia coli* and *Staphylococcus aureus.*

5. To investigate *in vitro* cytotoxic activities of the biosynthesized silver (AgNPs) and copper (CuNPs) nanoparticles.

1.3 Hypothesis

A standard protocol can be established from this research suitable for synthesizing silver and copper nanoparticles using green technology assisted by microwave irradiation. This research protocol can be both non-toxic and economical. In this

protocol, moreover, diverse verity of plants and fruits are possible to be exploited directly as the reducing and capping agent for the syntheses of silver (AgNPs) and copper (CuNPs) nanoparticles. Utilization of microwave-assisted synthesis could be helpful to produce nanoparticles with desired properties. Comparison between the antibacterial potential of these nanoparticles at very low concentration against the species *Escherichia coli* and *Staphylococcus aureus* could also be possible from this experiment. Moreover, the *in vitro* cytotoxic studies of the phytosynthesized silver nanoparticles (AgNPs) and copper nanoparticles (CuNPs) by this promising protocol could unfold a novel phase of the secure exercise of nanostructured materials and their applications in diverse sectors, particularly in the medical field.

GENERAL INFORMATION

2.1 Nanotechnology

Nanotechnology allocates the materials sized between 1 to 100 nm (1 nm = 10^{-9} of a meter) (Figure 2.1). This technology offers the capability to create materials with desirable properties mainly controlling their size and shape. This promotes multi-scaled research by using nanomaterials. This technology is therefore considered to be one of the latest advanced branches of science emerging from the multi-disciplinary sciences, mainly of physical, chemical, biological and engineering [7]. Furthermore, this innovative field is being spread to the number of areas including beverages, cosmetics, biomedical applications, production of drugs, different types of health care facilities, environmental safety, catalytic analysis, mechanics, development of different types of devices, space industries as well as various types industrial uses [8].
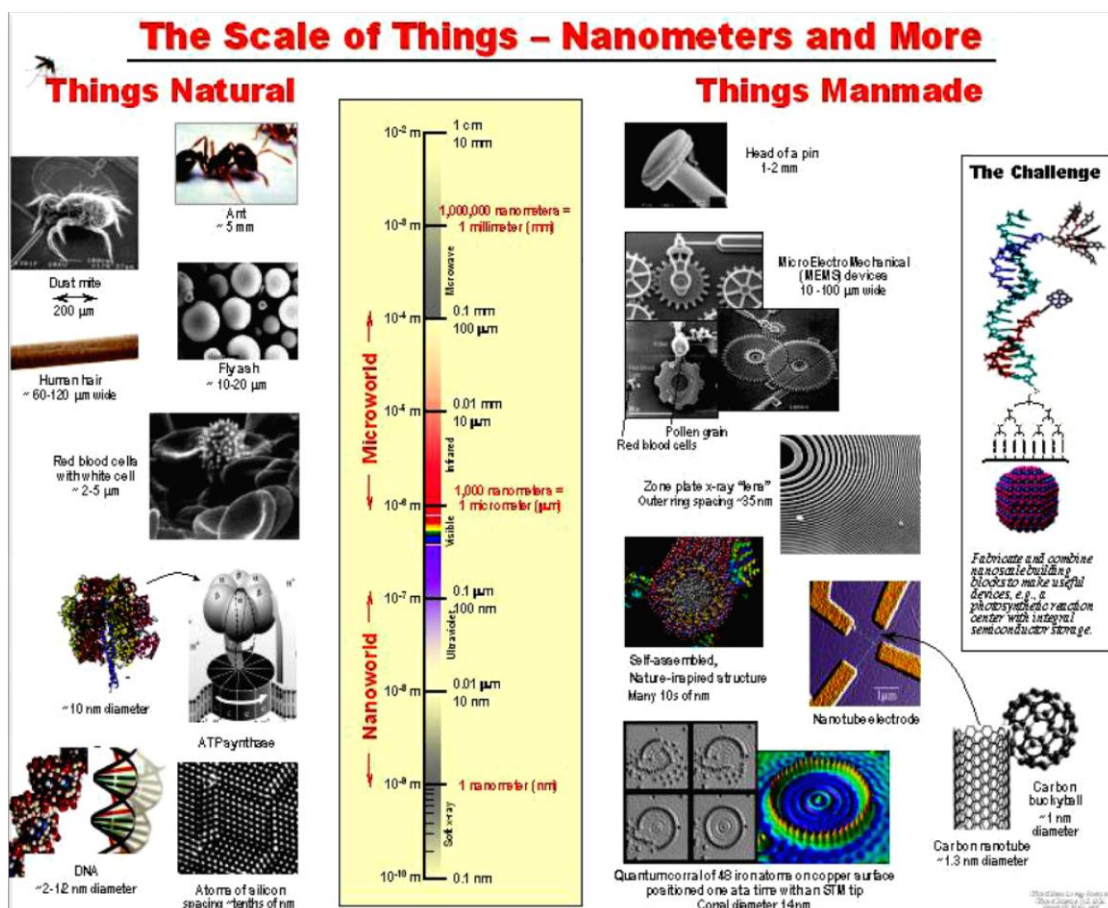
Figure 2.1 Diagram indicating the relative scale of nanosized objects of the various natural and artificial occurring objects [9].

2.2 Background of Nanotechnology

Indeed, it is evident that people from different parts of the ancient world were practicing various kinds of Nano-level process for the production of nanosized objects and used them in practical application long before the beginning of modern "nanoera". For instance, organic resources such as wool, silk, cotton and flax of a size ranged between 1 and 20 nanometres were found to be used at least around 1000 BC. The use of metallic nanoparticles, on the other hand, seems to have started in ancient Egypt and Mesopotamia back in the 14th and 13th centuries BC, mainly with the beginning of glass-making. In fact, some of the red coloured glasses were made by using either of metallic copper nanoparticles or cuprous oxide nanoparticles [10]. Moreover, the ancient Egyptians used a special type of hair dyeing paste mixed with sulphur and Nano-galenite particles. Even surprisingly, a steady dyeing was reported to be obtained from this Nano-based hair dyeing paste [11].

On the other hand, the production of multi-coloured stained-glasses, which were used in the church windows, was reported to accomplish at a high-quality level during the medieval time in Europe. In the manufacturing process of these various types of coloured glasses, particularly gold and other kinds of nanometals were used as special additives for the making of the red-coloured stained-glass [12].

However, in modern science, the concepts of nanotechnology first came to the light in 1959 by renowned physicist Richard Feynman which was given the place to be the father of modern nanoscience. However, N. Taniguchi (1974) applied the word "nanotechnology" in scientific research purpose in 1974 [13]. Following this, the ideas of nanotechnological approach were put forward by a number of important discoveries and inventions particularly during the second half of 1980s and early 1990s. The efforts and inventions of these contributory scientists eventually promoted and spread a conceptual ground of nanotechnology into conventional scientific protocols. Since then, considerable numbers of new, contributory and innovative scientific applications of nanotechnological researches have begun to flourish all over the world [14].

A chronological brief description of important events of the development of nanotechnology is given below in Table 2.1.

Table 2.1 A chronological brief of the key events of the nanotechnology [15].

• ~ 2000 Years ago	Greeks and Romans were using sulphide based nanocrystals as very useful supplements of hair dye.
• ~ 1000 Years ago	Along with some other nanoparticles of different sizes, gold was used to produce different colours in the making process of stained-glass windows used in medieval church.
• 1959	The concept of modern nanotechnology first came to the light by Richard Feynman.
• 1974	For the first time, Taniguchi uses the term "Nanotechnology"
• 1981	Development of Scanning Tunnelling Microscope

Table 2.1 A chronological brief of the key events of the nanotechnology [15]
(Continued).

• 1985	C_{60} (Buckyball) was discovered by Scientists at the University of Sussex and Rice University
• 1986	K. Eric Drexler's "Engines of Creation" became the first book on nanotechnology.
	Binnig, Quate and Gerbe invented Atomic Force Microscope (AFM), one of the important tools being used in nanoscience.
• 1991	Sumio Iijima first invented Carbon (C) nanotubes.
• 1999	"Nanomedicine", the first book on nano-medicine was written by R. Freitas.
• 2000	The establishment of "National Nanotechnology Initiative (NNI)", in the U.S.

2.3 Nanoparticles (NPs) or Nanostructured Materials (NSMs)

The term "Nanoparticles" is used to describe the set of particles or the substances through smaller dimension less than approximately 100 nm, at any rate, for one dimension which could be exploited as building blocks in nano-researches [16]. More than a few terms have been tended for describing nanoparticles; such as nanoscale materials, nanosized particles, nanomaterials, nanosized materials, nanostructured materials, nanoscale particles, and nano-objects etc.

Nanoparticles are complex molecules having mainly of three layers i.e. (a) surface or outer layer, (b) shell layer and (c) the core [17]. The surface or outer layer might be functionalized having a variety of small molecules, ions, surfactants, and polymers with it. The shell layer diverges according to the nature of nanoparticles. However, they might be natural or manufactured as well as chemically diverse from the core in every aspect. On the other hand, the core is actually the central portion of NPs that eventually refers to the nanoparticle itself. Consequently, this complex active structure of NPs provides various unique and suitable physicochemical properties.

2.3.1 Classifications of Nanostructured Materials (NSMs)

Nanoparticles are broadly categorized in different groups according to their size and shape, morphological structure, composition, origin, dimensionality, uniformity, and agglomeration. Therefore, NPs can be tubular, spherical and irregular in their shape. They further can be observed in aggregated, fused and agglomerated in form and structure. Depending on their various categories, different classes of nanoparticles are narrated below-

2.3.1.1 Classification of Nanoparticles or Nanostructured Materials based on The Number of Dimensions

For the first time, Gleiter gave the classification idea of NPs or NSMs in 1995, and further was explained by Skorokhod in 2000 [18]. Nevertheless, Gleiter and Skorokhod scheme didn't take into account the dimensional structures of NPs such as fullerenes, nanotubes, and nanoflowers and that's why, this classification was not entirely measured and counted. Late on, Pokropivny and Skorokhod offered a modified classification system for nanostructured materials, where 0D, 1D, 2D and 3D NSMs were included [19].

Dimensionality refers to shape or morphology of nanomaterials, which can broadly classify the Nanostructured Materials (NSMs) into four categories: Zero-dimensional Nanostructured Materials, One-dimensional Nanostructured Materials, Two-dimensional Nanostructured Materials, and Three-dimensional Nanostructured Materials (Figure 2.2). According to the dimensions, various prominent features and examples of four categories of NSMs are explained in Table 2.2 and Figure 2.3:

Table 2.2 Dimensional systems of nanostructured materials (NSMs) [19].

Nanostructured Materials (NSMs)	Characteristics	Examples
Zero dimensional NSMs (0D)	a) The electrons in the materials are confined in their motion in all three directions (Figure. 2.3a). b) 1 to 100 nm range in all three dimensions .	nanospheres, Nanoclusters
One dimensional NSMs (1D)	a) The electrons in the materials can easily move in one direction and confined in their motion in two directions (Figure. 2.3b). b) Usually this category includes needle like-shaped nanomaterials.	Nanofibers, Nanorods, Nanowires
Two dimensional NSMs (2D)	a) Electrons are free to travel in two directions and confined in one direction (Figure. 2.3c). b) These NSMs exhibit plate-like shapes.	Nanofilms, nanoplates and branched structures.
Three dimensional NSMs (3D)	a) In 3-D system, the electrons free to move in all three directions as a result of having three arbitrarily dimensions (Figure. 2.3d). b) This type is also called Bulk nanomaterials possess a nanocrystalline at the nanoscale. c) 3-D nanomaterials can contain bundles nanotubes and of nanowires, dispersions of nanoparticles as well as multi-nanolayers.	Nanoballs, nanocoils, nanocones, nanopillers and nanoflowers
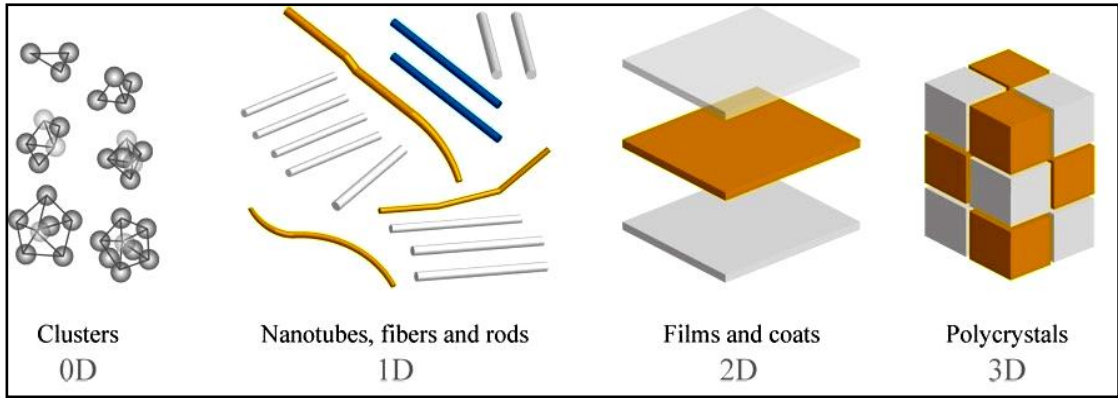
Figure 2.2 Heterogeneous nanostructured materials with different morphologies [20].
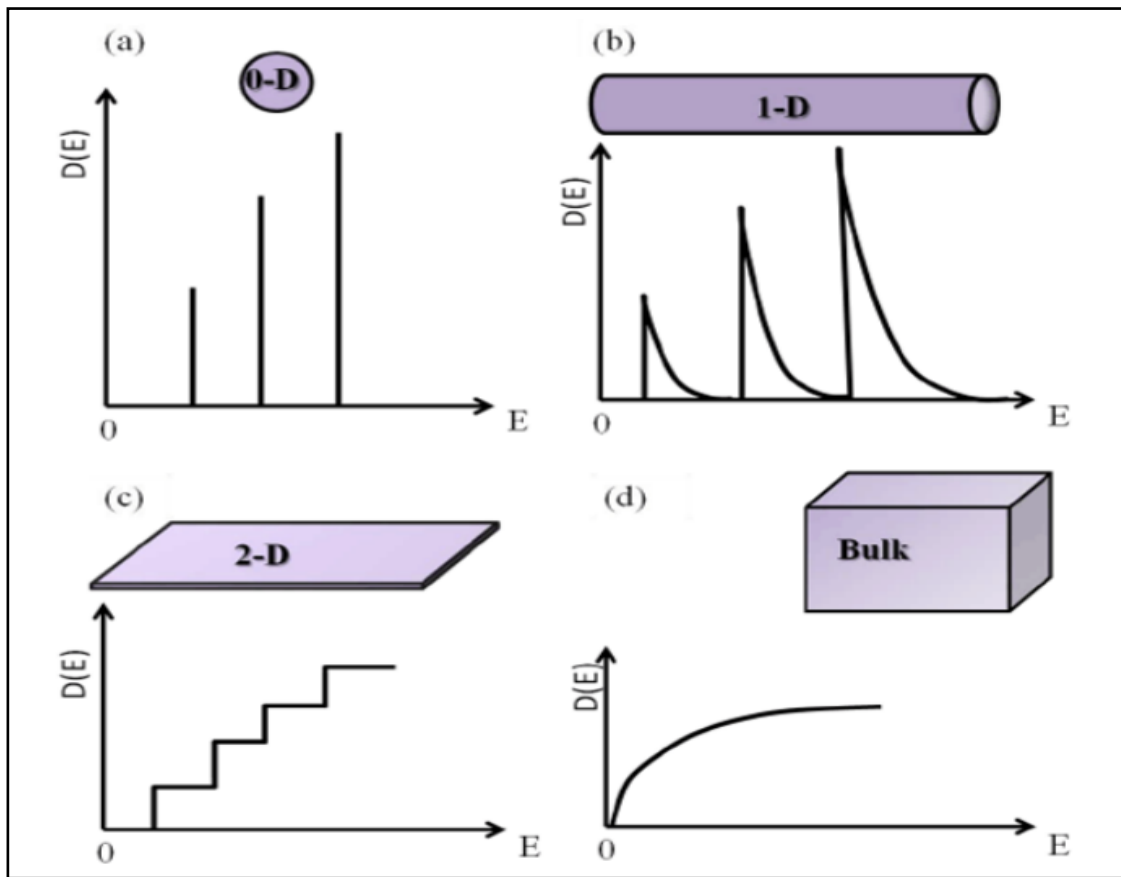
Figure 2.3 Schematic representation of (a) zero-dimension, (b) one- dimension, (c) two-dimension and (d) three-dimension systems with their corresponding density of states [21].

2.3.1.2 Classification of NPs or NSMs based on their Properties

Depending on their chemical, biochemical and physical properties, several recognized and familiar classes of NPs are mentioned in Table 2.3:

Table 2.3 Various features of different NP groups and their applications.

Nanoparticles (NPs)	Features	Usages
Carbon-based NPs	a) Contain single or multiple layered allotropic crystalline carbon sheets with remarkable strength and unique electrical properties (conducting, semi conducting, or insulating). These crystals sheets form a globular hollow cage or tubular structures [22]. b) Two best examples of carbon-based NPs groups can be the Fullerenes and carbon nanotubes (CNTs).	Commercially used as nanocomposites such as efficient gas adsorbents for environmental remediation [23], fillers and as the supportive medium for different inorganic and organic catalysts [24].
Metallic NPs	a) Made of stable, alkali, pure and significant metals precursors e.g. copper (Cu), gold (Au), silver (Ag) etc. [25]. b) These nanoparticles have unique optoelectrical properties because of their characteristic Localized Surface Plasmon Resonance (LSPR).	Highly sensitive diagnostic assays, drug and gene delivery, radiotherapy enhancement, thermal ablation etc.

Table 2.3 Various features of different NP groups and their applications (continued).

Nanoparticles (NPs)	Features	Usages
Ceramics NPs	a) These are non-metallic inorganic NPs. b) Can be found as the solid state with polycrystalline, amorphous, porous or hollow structures [26].	Catalysis, photocatalysis, photodegradation of dyes, and imaging applications [27].
Semiconductor NPs	a) These nanomaterials have properties between metals and non-metals. b) They also possess wide bandgaps. With bandgap tuning, they further show significant alteration in their properties [28].	They are very important materials in electronic devices, photo optics and photo catalysis [29].
Polymeric NPs	a) Usually biodegradable, biocompatible and organic based NPs with nanospheres or Nano-capsular shape [30].	Due to their biodegradable and biocompatible properties, they could be applied for the suitable carrier in controlling and sustaining drug delivery.
Lipid-based NPs	a) Normally, a lipid NP is characteristically spherical (diameter ranging from 10 to 1000 nm) consists of a solid core made of lipid and a matrix contains soluble lipophilic molecules [31].	Effectively using in many biomedical purposes such as drug carriers and delivery and RNA release in cancer therapy [32].

2.3.1.3 Classification of NPs based on Source of Origin

Nano structured materials (NSMs) or nanoparticles (NPs) can be derived from natural or man-made (engineered or incidental) sources. Based on their source of origin, nano-structured particles could be grouped into two categories, i.e. (a) Natural NPs and (b) Engineered NPs.

These nano-structured materials could be found in the natural minerals where they are capable of synthesizing by natural routes like biodegradation or/and biomineralization [33]. Additionally, under in-vivo condition, Nano-structured materials (NSMs) can be created throughout diverse natural events like volcanic eruption, erosion, marine wave strokes, forest fires, natural weathering of rocks etc.

On the other hand, nanoparticles can also be produced through usual human actions in everyday life like automobile exhaust, welding fumes, fuel (coal) combustion, industrial effluents etc. This type of NPs is known as incidental NPs. In this day and age, the Nano-scaled particles have been engineered to provide definite intentions, intended for the profits of mankind. The vast range of engineered Nano-structured materials (NSMs) is being created with unlike characteristics like unique physical, chemical and biochemical nature as well as distinctive morphology, dispersion status, and modified surface area; and therefore, contributing to build a significant dynamic area of science [33].

2.4 Metallic Nanoparticles

Nanoparticles which are synthesized either by destructive methods or constructive techniques, from their metal salts and reduced to zero-valent nanometric sizes atoms are called metallic nanoparticles. In 1857, Faraday recognized the existence of metal based nanoparticles in solution and quantitative details of their colour were specified by Mie in 1908 [34]. The term metal or metallic nanoparticle is used for describing nanosized metals consist of a number of atoms or molecules with their dimensions such as length, width or thickness in nanometres.

Even though, almost all the metals can be synthesized into their metallic nanoparticles but some metal also can be used to produce their metal oxides based nanoparticles i.e. Copper oxides (CuO & Cu_2O), Iron oxide (Fe_2O_3), Aluminium oxide (Al_2O_3), Silicon dioxide (SiO_2), Titanium oxide (TiO_2), Zinc oxide (ZnO),Cerium oxide (CeO_2),

Magnetite (Fe_3O_4) etc. In contrast to the bulk materials, the metallic nanoparticles particularly possess distinctive properties [34]. Such as-

a) Sizes, as low as within the range of 10 to 100 nm,

b) Distinctive unique structures like spherical and cylindrical,

c) Crystalline and amorphous structures,

d) Surface characteristics like pore size, high surface area, large surface energies etc.

e) Diverse colour of the particles,

f) Specific surface charge and surface charge density. The conversion involving molecular to metallic states that helps to provide definite electronic configuration (local density of states LDOS);

g) The ability to store excess electrons.

h) Highly Reactive and sensitive to environmental factors, for example humidity, air, high temperature, sunlight etc.

2.4.1 Silver Nanoparticles (AgNPs)

Silver (Ag) is a soft and white glossy malleable metal. It has an atomic mass of 107.862 and atomic number of 47. It is a first-rated conductor of electricity and heat as well as also able to reflect light very well. This lustrous is widely preferred as a catalyst for different significant oxidation reactions.

Silver nanoparticles have different shape for instance cubes, triangular, rods, pentagonal and prism. Moreover, silver nanoparticles itself are insoluble in water while the silver salts such as silver nitrate ($AgNO_3$) and silver chloride (AgCl) are soluble in water. The particle size of a silver nanoparticle (AgNP) is usually smaller than 100 nm and each nanoparticle contains approximately 20-15,000 atoms [35]. However, these nanoparticles have unique and remarkable properties such as dispersion capacity, well-developed surface, chemical and functional stability, excellent electrical conductivity with high electrical double layer capacitance, catalytic activity, non-linear optical behaviour associated with the SPR etc. Moreover, the structure and morphology possess strong influence on their above mentioned unique and remarkable properties [36].

2.4.2 Copper Nanoparticles (CuNPs)

Copper (Cu) is a red-orange coloured transition metal. It has an atomic mass of 63.546 and an atomic number of 29. This metal comprises two oxides forms, i.e. cupric oxide (CuO) and cuprous oxide (Cu_2O). These two oxides contain distinct colours, crystal structures as well as unique physical and electrical properties. Copper possesses metallic lustre. Moreover, it is comparatively more plentiful in the Earth's crust (the 8th). The metal further shows various types of characteristic features for example, high corrosion resistance, high electrical conductivity, high thermal conductivity, good ductility and malleability. Therefore, copper has been utilized in contribution of the humanity for several millennia [37]. It is also considered to an inevitable element in contemporary world. For instance, it has been used in associated plumbing and modern household water piping prior to other metals along with is being chosen for most vehicle radiators and air conditioners.

On the other hand, a copper nanoparticle is a copper based blackish brown or black coloured metal particle [38]. This particle is 1 to 100 nm in size and therefore been a particle of sought-after as a consequence of its high melting point, high electrical conductivity, low electrochemical migration behaviour as well as low material cost [39].

Like many other metallic nanoparticles, on the other hand, copper nanoparticles can also be formed both in through artificial synthesis as well as natural processes. Sometimes the copper nanoparticles (CuNPs) require encapsulation by organic or inorganic compounds to prevent oxidation [40], since the particles (CuNPs) can easily oxidize into oxides (CuO & Cu_2O).

2.5 Syntheses of Metallic Nanoparticles

Metallic NPs are formed through the reduction of metal salt to zero-valent metal atoms. The diameter of the metallic nanoparticle is influenced by various factors like strength of the metal-metal bonds, nature of solvent, synthesis conditions, the redox potential between the metal salts and the reducing agent, type of stabilizing agent used, temperature etc. [41]. Majority metals are capable of creating into their metallic NPs. However, the on the whole, frequently exercised metals intended for nanoparticle production are silver (Ag), iron (Fe), gold (Au), copper (Cu), lead (Pb), aluminium (Al), cadmium (Cd), cobalt (Co) and zinc (Zn) [42].

Various methods and protocols are applied to create nanoparticles. However, all of these methods could largely be classified into two chief groups, i.e. (1) Bottom-up synthesis and (2) Top-down synthesis [43]. These chief groups could further be categorized into three subgroups (i.e. biological, physical and chemical schemes methods) according to their reaction condition, operation, and adopted protocols (Figure 2.4).
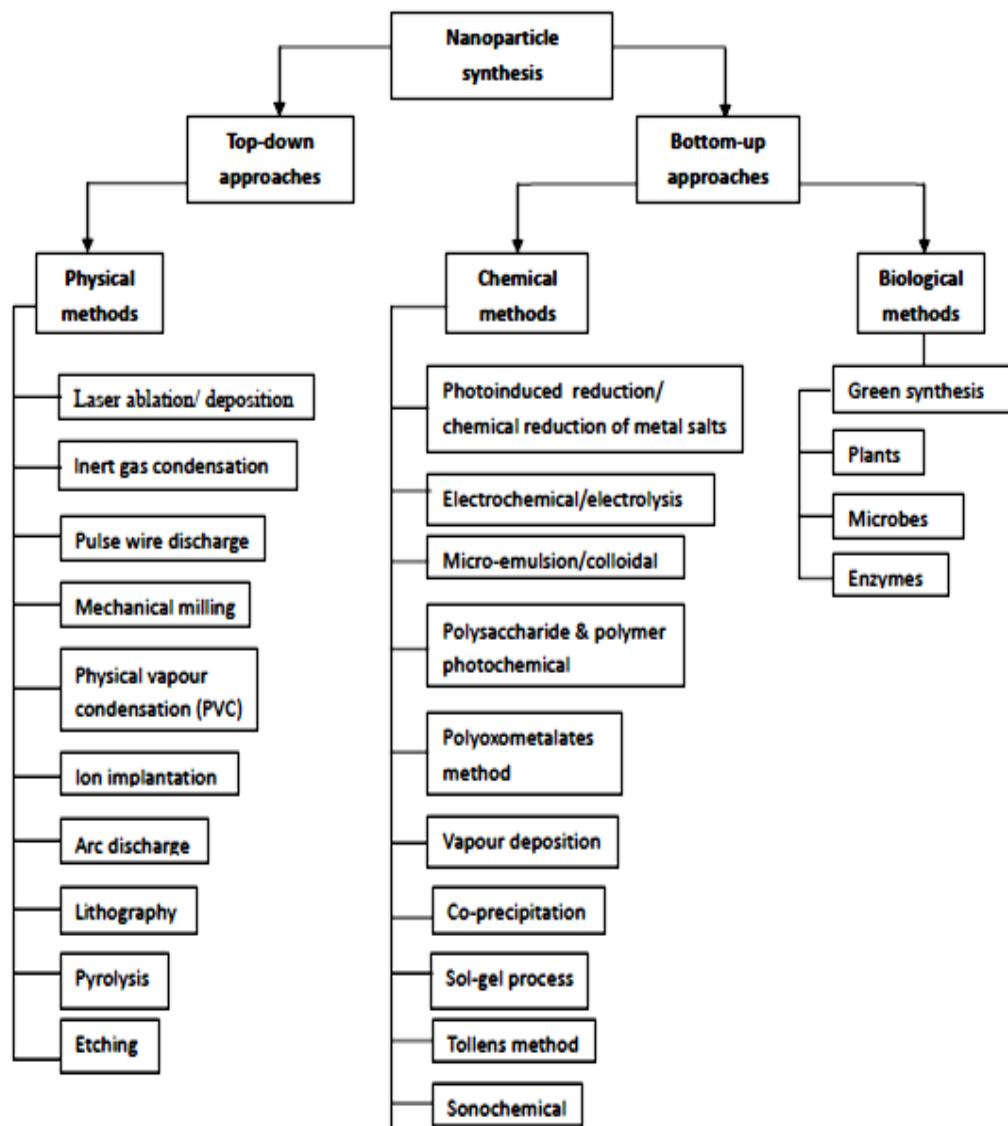
Figure 2.4 The representation of different types of nanoparticles synthesis methods [44].

2.5.1 Top-down Synthesis

For "top–down" synthesis, destructive approach is employed. In this method, bulk state metals or larger molecules are systematically broken down into extra smaller particles. Therefore, these extra small particles become very suitable to be converted into metal nanoparticles of desired dimensions (Figure 2.5). In top-down manufacturing, moreover, particle assembly and formation is controlled by a pattern or matrix [45]. All examples of this approach basically represent the physical methods such like evaporation-condensation, pyrolysis, laser ablation grinding, physical vapour deposition (PVD) and also other kinds of decomposition techniques.

Various types of metallic nanoparticles e.g. gold (Au), cadmium sulphide (CdS), silver (Ag) and lead sulphide (PbS) have been synthesized in the past, particularly by using the evaporation-condensation method [46]. Ultrasound has also been used in the fabrication of novel nanomaterials. However, this physical synthesis method as a nanoparticle producer can be helpful for enduring experiments related to inhalation toxicity studies [47].

Comparing to other protocols, the physical methods are beneficial because of the uniformity of nanoparticle distribution as well as absence of chemical solvent contamination throughout the synthesis [48]. Hence, for various types of advanced applications, pure, clean and contamination free metal particles and colloids can be fabricated from these useful techniques [49].

2.5.2 Bottom–up Synthesis

In contrast of the Top-down Synthesis, nanoparticles are created from moderately smaller and simpler molecules (atoms) in the 'bottom–up', also called 'building-up' synthesis (Figure 2.5). This synthesis system involves the assembly of small substances to synthesize nanoparticles through chemical or biological methods with the help of reduction and sedimentation mechanisms [50].

In this processes, the aqueous metal ions which are the precursor of metal salts play the vital role for nanoparticle production. Different reducing agents convert these metal ions to metal particles. Consequently, a change in colour occurs in the mixture that basically specifies the construction of nanoparticles. However, using protective agents to stabilize dispersive synthesized NPs is very crucial and significant while preparing

them. Hence, to avoid agglomeration, various stabilizers are added to the synthesis mediums which protect by shielding the particles [51]. In General, both biological approaches and chemical methods like photoinduced reduction, vapour deposition, sol-gel process, tollens method etc. are cheaper in comparison with physical methods.

The most common example of the Bottom–up synthesis by far is the fabrication of silver (Ag) nanoparticles with a controlled size (50-200 nm) through the modified one-stepped Tollens method [52].
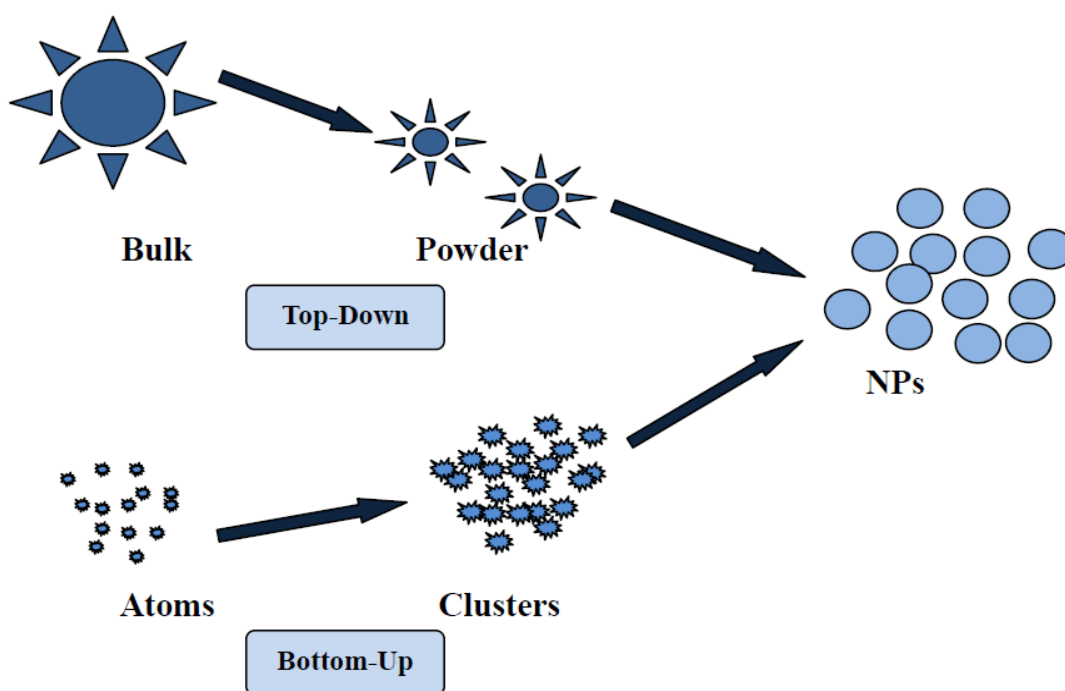
Figure 2.5 Diagrammatic illustration of the top-down and bottom-up syntheses of NPs [44].

2.6 Biological Approach for Metallic Nanoparticle Fabrication

Nanoparticles are fabricated with the help of a diverse range of scientific protocols both of physical and chemical as well as their hybrid and modified procedures [53]. Conventional methods of these protocols could be useful to commercially manufacture an outsized amount of nanoparticles comparatively within shorter time-period. However, manufacturing nanoparticles by using these protocols sometimes might produce toxic by-products which are eventually environmental hazards. Moreover, there are more advanced, easier and more efficient techniques are available nowadays

so far. Besides, the physical methods require expensive instrumentations, high pressure and temperature that demand enormous consumption of energy [54], [55]. With all of the disadvantages mentioned above, nevertheless, both physical and chemical schemes enclose some limitations to maintain the desirable shape, size, quality and quantity of nanoparticles along with their further functionalization [56].

Therefore, alternative method for nanoparticle synthesis which is less expensive and uses environmentally friendly resources, produces non-toxic waste products and with high yield of nanoparticles would be ideal that every researcher in nanoparticle synthesis is aiming to attain [57], [58]. This has promoted the opportunity to come forward with the idea of nano-biotechnology which is also called as 'green chemistry'.

As a consequence, in the 1990's, along with the development and advancements in the field of nanotechnology, another concept was evolving known as "Green chemistry". To develop this concept, the Green Chemistry Institute was included in 1997 and turned out to be a part of the American Chemical Society (ACS) in 2001. In recent years, moreover, scientists have used biomaterials as inexpensive raw materials for the fabrication of various kinds of nanoparticles [59].

Based on several aspects and conditions, fabricating nanoparticles with the help of green protocols are therefore far superior and advantageous comparing to the fabrication and production of nanoparticles in the course of conventional physical and chemical methods. Below, the benefits of the alternative protocols or the green syntheses of nanoparticle production are expressed in Figure 2.6.

19
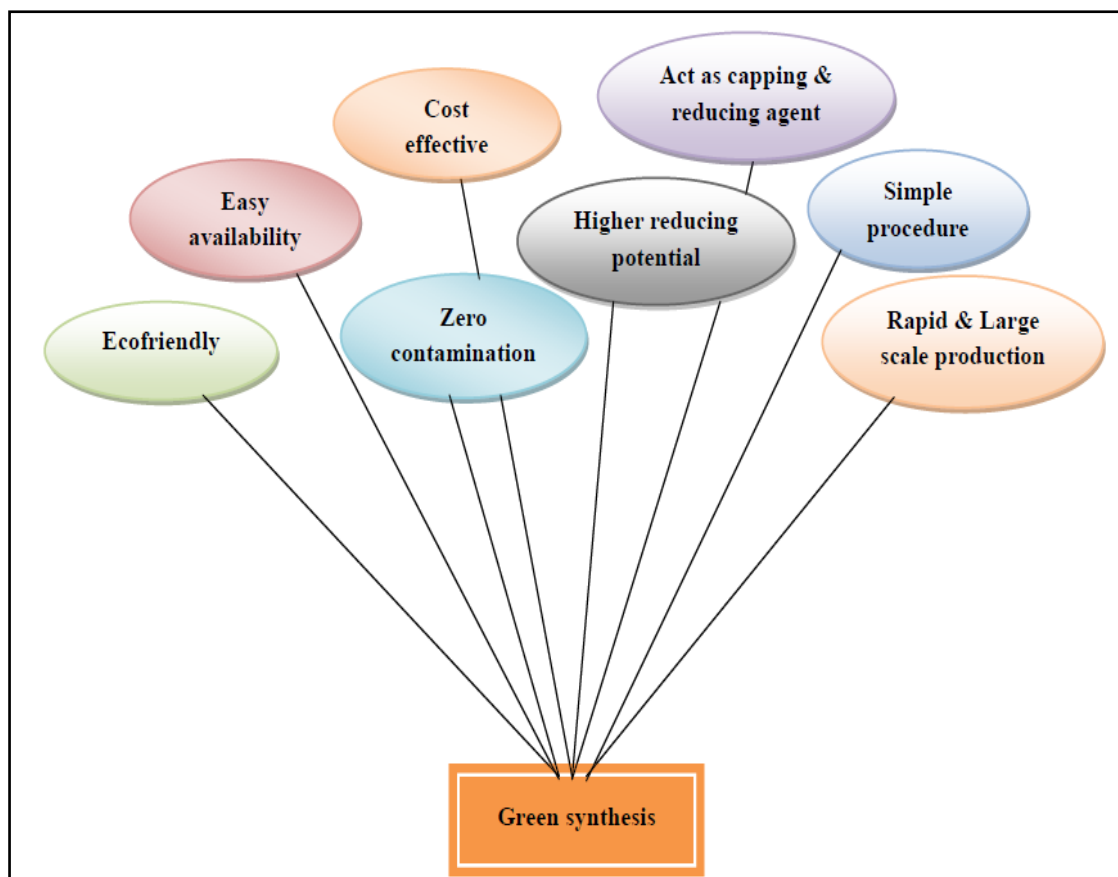
Figure 2.6 Advantages of alternative protocols or the green synthesis [44].

As designed in Figure 2.7, the green nanobiotechnology could generally be categorized into bottom-up synthesis. Using biological resources such as plants, microorganisms, and viruses as well as their by-products, for example, proteins and lipids, this green nanobiotechnology synthesize nanomaterials or nanoparticles with the help of reduction or oxidation reaction [60]. The two main goals of green nanobiotechnology or green chemistry are,

☐ Producing nanomaterials without affectingthe human health or the environment.

☐ Producing nanomaterials that offer resolutions to the environmental problem.
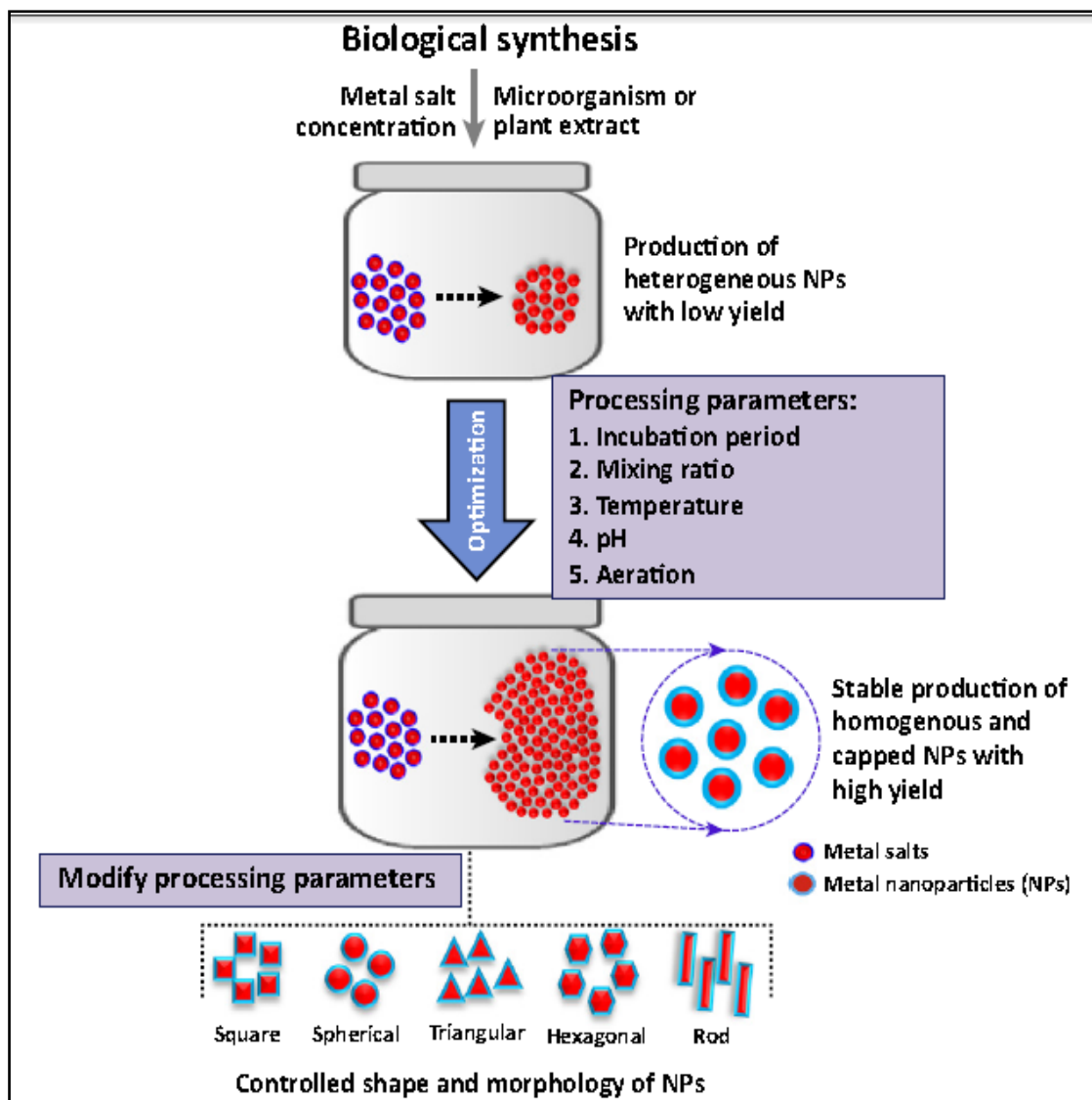
Figure 2.7 Schematic representation of bio-based synthesis process [61].

However, a brief discussion of biological approach using a variety of living materials is given below:

2.6.1 Synthesis of Metallic NPs using Virus, Bacteria and Yeast

Different microorganisms like virus, bacteria, actinomycetes and yeast have the capability to synthesize different metallic nanoparticles due to their high growth rate and genetic modification/manipulation tendency as well as the capacity to accumulate heavy metals. A range of reductase and metal-resistant enzymes and proteins, cofactors and other molecules of these microbes are proficient of reducing metal ions to metallic nanoparticles with a fine size diameter distribution [62].

It has been confirmed that diverse bacterial genera have been applied for metallic nanoparticle synthesis, i.e. *Pseudomonas, Bacillus sp., Lactobacillus, Escherichia, Klebsiella sp., Enterobacter sp., Aeromonas sp., Corynebacterium sp., Weissella sp., Rhodobacter sp., Rhodococcus sp., Trichoderma, Brevibacterium sp., Streptomyces sp., Desulfovibrio sp., Rhodopseudomonas, Sargassum sp., Shewanella sp., Plectonemaboryanum sp., Pyrobaculum sp.* etc.[63], [64]. Furthermore, similar potential for producing AgNPs with the particles size ranges from 35 to 46 nm has been showed by using *Pseudomonas stutzeri* AG259 [65]. Likewise, *Serratia sp.* was also used to synthesize copper oxide (CuO) nanoparticles. This bacterium was isolated from the midgut of an insect, *Stibara* sp. [66].

On the other hand, Virus proteins have been worked as biological particles to extend the biological synthesis of nanoparticles [67]. For Instance, It has been found that TMV could able to the mineralize sulphide and crystalline nanowires [68].

2.6.2 Fabrication of Metallic NPs using Fungus

Different genera of fungi are being considered as significant agents on behalf of the biological fabrication of nanoparticles by reason of the fact that they are highly tolerant to adverse conditions, economically viable and   have the capacity of bioaccumulation, therefore, could produce substantial amounts of NPs [53], [69].

Furthermore, the mechanism of NPs fabrication by this microorganism is done as follows i.e. attachment of metal ions to the outside layer of the fungal cells; the consequent enzymatic reduction (enzymes like nitrate reductase, and /-NADPH-dependent reductase) of the metallic ions to nano-metals by the fungal cell system [70]. For instance, fungal reductase enzymes from *Penicillium* spp. and *Fusarium oxysporum* have been found to play vital roles in nanoparticle syntheses [71]. Furthermore, Mukherjee *et al* have also investigated the fabrication of highly stable nanocrystalline silver particles using an agriculturally important *Trichoderma asperellum* species which is also considered as non-pathogenic fungus [72]. Additionally, copper (Cu) nanoparticles have also been produced by the extracellular mechanisms of three *Penicillium* spp. (*Penicillium citrinum*, *P. waksmanii* and *P. aurantiogriseum*) [73].

2.6.3 Synthesis of Metallic Nanoparticles using Algae

Some information is offered for algae as a "Biofactory" for the nanoparticles synthesis. Lower groups (Cyanobacteria, eukaryotic genera) of algae such as *Cladophora prolifera, Rhizoclonium heiroglyphicum, Spirulina subsalsa, S. platensis, Lyngbya majuscule, Chlorella vulgaris, Sargassum fluitans* and *Padina pavonica* have been utilized for biorecovery of gold (Au) NPs [74], [75], [76]. In addition, some available marine groups of algae, such as *Chlorella salina, Chaetoceros calcitrans, Isochrysis galbana* have also been engaged for the reduction of Ag^+ to AgNPs [77].

Nevertheless, nanoparticles synthesis using microorganisms are slower and low productive. On the other hand, the maintenance for synthesis procedures using lower group of organisms are also time consuming as because of the extra complex steps are needed to follow through the process, such as microbial maintenance, sampling, isolation and culturing. Therefore, the utilization of plant source raw materials to fabricate metallic NPs has become a immense and significant option which is reasonable, practicable and feasible [78].

2.6.4 Plant-mediated Syntheses of Metallic Nanoparticles

Not long ago, plant based fabrication of metallic NPs, particularly silver (Ag), gold (Au) and copper (Cu) nanoparticles has turned into a significant topic and has gained extra attention by the researches, working in the field of phytonanotechnology or bionanotechnology. It is being taken a better option for NPs production as plants are boasted with some advanced features, including biocompatibility, scalability [79]. Moreover, plant-mediated biosynthesis is easier and rapid since the natural reducing factors are ready and thereby, could effortlessly be supplied by the plants. Furthermore, water can be used as a universal solvent in the reducing medium to accelerate the synthesizing process [80].

Primarily, the entire plants had been utilized for the production of metal nanoparticles. However, isolated pure phytocompounds like cellulose, starch, glucose, etc. or dried biomass were utilized for silver (Ag) nanoparticle production [81]. On the other hand, the entire plant and/or their parts, i.e. roots, leaves, barks, stems, fruits, peels, fruit pulps, seeds as well as secretory substance like gums, volatile oils, rubber, pigments have already been reported for green synthesis of different NPs [82] (Figure 2.8).
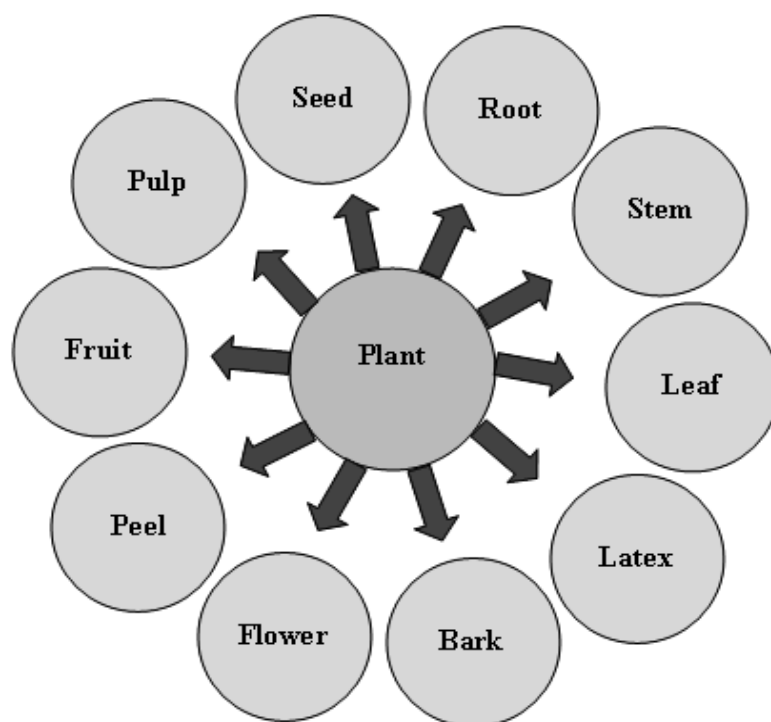
Figure 2.8 Various parts of plants used in green synthesis of NPs [44].

Besides, plants possess primary metabolites such as amino acids, acyl lipids, peptides, proteins, reducing sugars, phytosterols, vitamins etc. over and above the secondary metabolites like alkaloids, terpenoids, tannins, phenolic compounds, heterocyclic compounds, tannins and resins which could act the crucial aspects for reducing metallic ions to NPs [83], [84], [85]. Furthermore, the general biobased metallic nanoparticle reduction mechanism process is followed by 3 main steps [85] as pointed up in Figure 2.9.
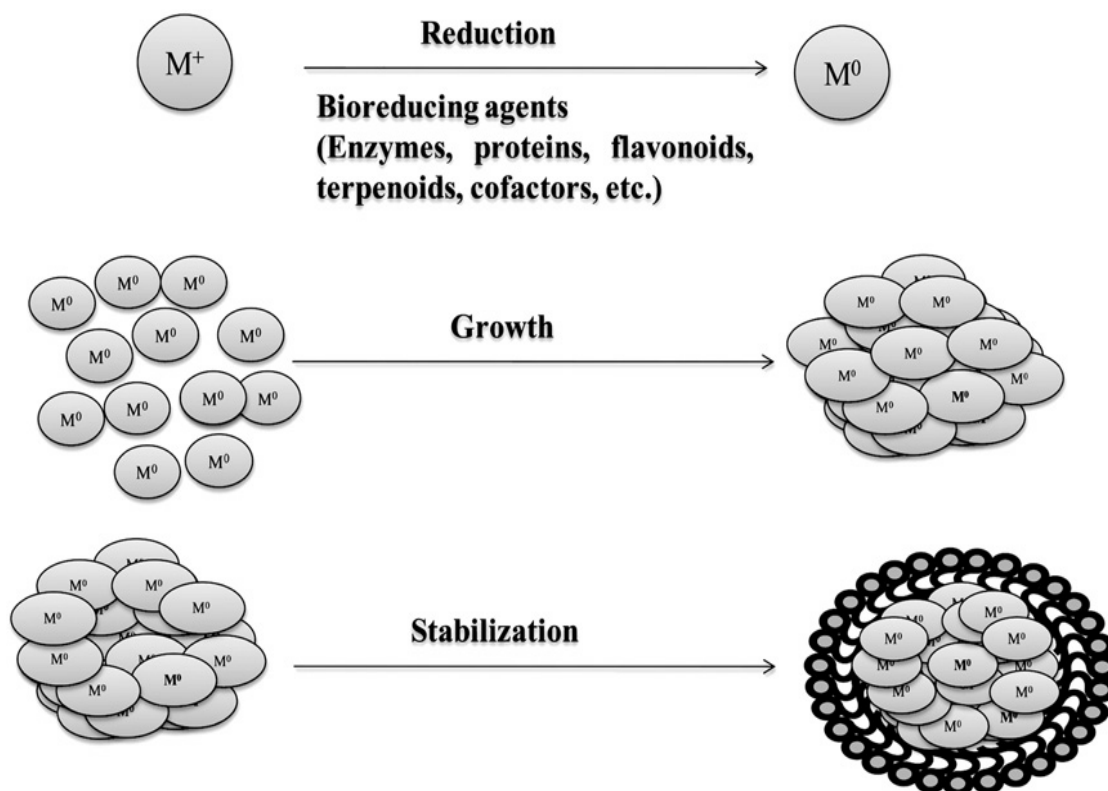
Figure 2.9 Consecutive diagram of plant-mediated (bio-based) metallic nanoparticle reduction mechanism (M+-metal ion) [86].

However, a brief summary of some reports of plant-mediated metallic nanoparticle fabrication by using a number of plants parts is describing in Table 2.4.

Table 2.4 List of plant species, their parts used and some mentionable features of NPs for plant-mediated syntheses of metallic NPs.

Biological resources	Plant parts	Obtained NPs	Shapes and size (nm)	References
Ginkgo biloba	Leaves	Copper	Spherical; 15–20 nm	[87]
Azadirachta indica	Leaves	Silver	41–60 nm	[88]
Pinus densiflora	Cones	Silver	Oval but few triangular; 30–80 nm	[89]

25

Table 2.4 List of plant species, their parts used and some mentionable features of NPs for plant-mediated syntheses of metallic NPs les (continued).

Biological resources	Plant parts	Obtained NPs	Shapes and size (nm)	References
Orange and pineapple	Fruits	Silver	Spherical; 10–300 nm	[90]
Nelumbo nucifera	Leaves	Silver	spherical, triangular; 25–80 nm	[91]
Allium sativum	Cloves and Bulbs	Silver	spherical; 7–8 nm	[92]
Aloe vera	Leaves	Silver	spherical; 34–102 nm	[93]
Citrus medica	Fruits	Copper	20 nm	[94]
Lawsonia inermis	Leaves	Iron	Hexagonal; 21 nm	[95]
Artocarpus gomezianus	Fruits	Zinc	Spherical; >20 nm	[96]
Euphorbiaceae	latex	Silver & Copper	18 nm Ag; 10.5 nm Cu	[97]
Citrus sinensis	peel	Silver	spherical; 10±1 nm (at 60 °C); 35±2 nm (at 25 °C)	[98]
Rosa rugosa	Leaves	Silver & Gold	30–60 nm Ag; 50–250 nm Au	[99]
Carica papaya	Fruits	Silver	25–50 nm	[100]

Table 2.4 List of plant species, their parts used and some mentionable features of NPs for plant-mediated syntheses of metallic NPs (continued).

Biological resources	Plant parts	Obtained NPs	Shapes and size (nm)	References
Cymbopogon sp. (lemongrass)	Leaves	Gold	spherical or triangular; 200–500 nm	[101]
Jatropha curcas L.	latex	Lead	10–12.5 nm	[102]
Mentha piperita (peppermint)	Whole plant	Silver	spherical; 5–150 nm	[103]
Syzygium cumini	Seeds	Silver	spherical; 29–92 nm	[104]
Musa paradisiacal	Peel	Silver	20 nm	[105]
Geranium sp.	Leaves	Gold	16–40 nm	[106]

2.7 Factors Affecting the Formation of NPs

Quite a few factors can influence the creation, categorization and appliance of nanoparticles while manufacturing the metallic nanoparticles. Among them, the most important physical and chemical parameters are the pH of reaction mixture, reaction temperature, duration of reaction and agitation, pressure, reactant concentration, content of the reducing agent, environment, proximity and above all the protocols that are followed for the synthesis process [107]. The sections following present a glimpse of some of those dominant factors.

2.7.1 Particular Method or Technique

Different schemes have been intended for the fabrication of metal NPs. This could include the physical techniques of using mechanical and photolytic procedures, the chemical protocols with the help of various organic or inorganic chemicals as well as the biological protocols using different kinds living organisms and bio-based raw materials. However, each of these procedures has its certain advantages and

disadvantages. Providing that the biological protocols mainly use nontoxic and environmentally benign materials, they are economically cheap, eco-friendly, safe, having less side effects as well as more reliable and convenient than the protocols used in traditional methods [108]. Additionally, the preference of technique used to purify the fabricated metallic nanoparticles can influence nanoparticle quantity and quality.

2.7.2 Influence and Effect of pH

The pH value of the redaction solution is very influential in the course of nanoparticle fabrications. Studies have shown that pH of the solution medium has propensity to construct variability in the morphology of synthesized nanomaterials [109]. On the contrary of the high pH values, larger particles have a propensity to be fabricated particularly at lower acidic pH values [110]. There is example, conversely, of rod-shaped AuNPs fabrication by using the common oat (*Avena sativa*). In this case, it has been found that larger sized gold nanoparticles (25nm to 85 nm) were synthesized at pH 2, whereas comparatively smaller sized gold nanoparticles (5 to 20 nm) were synthesized at pH 3 to 4 [111]. Therefore, it is strongly evident that the dimension of NPs may possibly be monitored by altering the pH of the reaction solution. On the other hand, some studies also present the effect of pH on the structure and morphology of the synthesized silver nanoparticles (AgNPs) [112].

2.7.3 Influence of Reaction Temperature

In all kinds of methods, temperature is also a vital cause that influences the morphology and yield of fabricated nanoparticles. The highest temperature ($>350^{\circ}$C) is needed in physical processes, whereas less than 350°C is require chemical schemes [113]. Generally, using green technology for the synthesis of nanoparticles requires ambient temperature or temperatures less than 100°C and the temperature during synthesis established the nature of the nanoparticles [114]. For instance, by using the sweet orange peel extract (*Citrus sinensis*), Ag nanoparticles with mean dimension of just about 35 nm has been produced at a reaction temperature of 25°C. However, the average particle size in this synthesis was reduced to 10 nm while the reaction heat was amplified to 60°C [98]. On the other hand, it has been illustrated that higher temperatures moreover, influence the structural form of gold nanoparticles. For example the rod-like and plate-like gold nanoparticles (AuNPs) have been formed at

higher temperature whereas spherical-shaped gold nanoparticles (AuNPs) have been produced predominantly at lower temperatures [115, 116].

2.7.4 Influence of Reaction Time

While using green technology, the reaction condition like time also comprises an immense effect upon the quality and type of synthesized metallic NPs [117]. The variations in the time may affect the synthesis process in many ways. For example, particles might shrivel or grow during long storage; the aggregation of particles might also occur due to long time storage [118]. There is also example that a quick colour change occurred within 2 minute, while synthesizing spherical silver nanoparticles (AgNPs) using pineapple (*Ananas comosus*) extract. The reaction sustained up to 5 min and however, subsequently only an insignificant difference in colour may possibly be monitored [119].

2.7.5 Influence of Pressure

Pressure also becomes an important factor while synthesizing nanoparticles. The shape and size can be affected by the pressure applied to the reaction medium [120]. It has been found that the metal ions reduction rate occurs much faster at ambient pressure conditions using biological agents [121].

2.7.6 Effects of Reactant Concentration

In green chemistry, the formation of metallic nanoparticles has extensively been influenced by the concentration and density of bio-particles occurs in the plant extracts. A recent study has demonstrated the difference in concentration of sundried camphor leaf extract (*Cinnamomum camphora*) in the synthesis medium; possibly possess significant influence on the morphology of Ag and Au synthesized nanoparticles [122]. Similarly another study shows that, the ratio of gold triangular plates to spherical nanoparticles was influenced depending on the amount of chloroaurate ions containing the extract from the juicy leaves of *Aloe vera* (Asphodelaceae) in the synthesis medium of fabrication process [81].

2.7.7 Chemical Constitute of Reducing and Stabilizing Agent

A variety of living systems (e.g. plants) are being exercised as reducing, synthesizing and stabilizing mediators, meant for the nanoparticle syntheses. These living systems are rich in secondary metabolites. However, the substances of these secondary metabolites diverge according to their types, parts as well as the procedures which have been followed for their extraction [123]. Correspondingly, different microorganisms produce distinctive extracellular and intracellular enzymes of different quantities which might affect the synthesis of nanoparticle [124].

2.7.8 Environment

The surrounding environment especially humidity also operates as important factor for the construction of synthesized NPs. Additionally; the environment also influences the chemical and physical structure of the synthesized nanoparticles. In the biological system, a single nanoparticle would quickly become core-shell nanoparticles by reacting with other materials. Quick changes might also occur when it absorbs materials by the oxidation or corrosion process in its environment [125]. For instance, the crystalline nature of the zinc sulphide nanoparticles changed immediately when their surrounding has been changed from a wet environment into a dry circumstance.

2.8 Characterization of Nanoparticles

The chemical, biochemical and physical components of NPs are extremely important for their performances, their applications and their interaction with living systems. On the other hand, the key features of nanomaterials like structure, morphology, surface energy, surface composition, surface charge, and the morphology subsist crucially significant as well as needed to be well examined for the better understanding of the behaviours of nanomaterials in vivo [126]. Therefore, a range of sophisticated analytical techniques is commonly applied for the categorization and determination of the properties of nanoparticles.

Some of the frequently used microscopy and spectroscopy techniques are, UV-Visible Spectroscopy (UV-vis), Fourier Transform Infrared Spectroscopy (FT-IR), Atomic Force Microscopy (AFM), Scanning Electron Microscopy (SEM), Transmission Electron Microscopy (TEM), Energy Dispersive Spectroscopy (EDS), Dynamic Light Scattering (DLS), Powder X-ray Diffraction (XRD) and Raman Spectroscopy.

A glimpse of the several techniques which are used for the evaluation of the physical and chemical characterizations of nanoparticles is presented below.

2.8.1 UV-Visible Absorption Technique

UV-Visible Absorbance Spectroscopy covers a visible range of among 380 nm and 800 nm and an UV range of among 190 and 380 nm. Both of these two categories of radiation interact with substance by promoting electronic transitions that could vary between the ground state to a higher energy state.

Metallic nanoparticles from a minimum size range of 2 nm to a maximum size range of around 100 nm can be monitored by using the wavelengths of between 300 and 800 nm that are in general, being used for characterization [127]. UV-Visible Spectroscopy gives information regarding to the structure, size, stability, concentration and aggregation of the nanoparticles. It could even give the information about the bio-conjugation the nanoparticles if the absorption profiles are different [128]. On the other hand, in a process of estimating the combined oscillations of conduction electrons in response to electromagnetic emissions as well as measuring the Plasmon resonance, the UV-Visible Spectroscopy is also been applied to prove the formation of metallic nanoparticles. Metal nanoparticles commonly have specific absorbance bands in characteristic spectra. For example, while the silver nanoparticles (AgNPs) demonstrate an absorbance peak of between 400 and 450 nm, the gold nanoparticles (AuNPs) present a specific absorbance peak of between 500 and 550 nm [129], [130].

2.8.2 Fourier Transform Infrared Spectroscopy (FTIR)

Since nearly all molecules are capable of absorbing infra-red light, their absorption spactra can be used as molecular fingerprints of the sample that show how the sample absorbs light at each wavelength [131]. The infrared emission spectrum, photoconductivity, absorption, or Raman scattering of a gas, liquid, or solid can be estimated and calculated by using FT-IR analysis; this because of the fact that all of these substances have distinct characteristic vibrational frequencies in the infra-red range.

Fourier transform infrared spectroscopy (FTIR) with a significant I.R. region between $4000 - 670$ cm^{-1} is capable of identifying chemical information i.e functional groups, side chains, and cross-links of the NPs, and thereby, helps to elucidate the possible

molecules which might accountable for capping and stabilization of the nanoparticles. Hence, this is able to facilitate nanoparticle synthesis using green technology [132].

In FTIR technique, conventionally, the absorption spectra for the solid nanoparticles samples can obtain through the formation of thin, translucent potassium bromide (KBr) pellets containing the specimens of interest. The KBr mixtures are placed in a vacuum line prior to pellet construction and the spectra are obtained after purging in dry air conditions corrected to a reference blank sample (KBr) [133]. However, there is a latest method that has been developed in recent time and called the Attenuated Total Reflection (ATR)–FTIR Spectroscopy. When it comes into contact with a sample, the intensity of the reflected IR beam changes. Consequently, this method provides the result peaks representing the chemical functional groups of the sample. In an ATR–FTIR system, an IR beams are focussed onto an optically dense internal reflection element (IRE) crystal with a high refractive index at a certain angle. This internal reflectance generates a transitory wave that broadens away from the exterior layer of the crystal that achieves the contact of the specimens with the crystal [134]. ATR is ideal not only for strongly absorbing or thick solids samples i.e natural powders, but also for liquid analysis i.e free-flowing aqueous solutions [135].

In a recent study, copper nanoparticles (CuNPs) have been synthesized with the use of the secondary bio-compounds, the rubber or latex of *Euphorbiaceae*. The FTIR measurements have been carried out in this study, to identify the possible interactions between the nanoparticles and polypeptides that are present in steam latex of a plant. This is due to the fact that the functional group of enzymes, proteins, peptides and amino acids are significant markers for IR peak graphs [97].

2.8.3 X-ray Diffraction (XRD) Technique

A wide range of X-ray based approches and techniques have been invented which could be useful for characterization of NPs. However, among all these instruments, X-ray diffraction (XRD) has gained extra attention due to the capacity of its evaluation functions and facilities to measure the crystallinity and size of synthesized nanoparticles [131]. It has been considered as a very important key instrument to generate and evaluate the tertiary structures with mean size allocation over and above the crystallinity of particles at molecular levels [127].

According to Bragg's law, the diffraction peaks of molecules, extracted from XRD analysis merely illustrate the reflection of beam onto the crystalline planes of an inspected sample [136]. For achieving the result, the composition and lattice parameters of the diffracted powdered samples are analyzed through computing the angle of diffraction, once, X-ray beam is prepared to incident on them. Particle size is determined using the Scherrer formula. This formula counts the interplanar spacing ($d_{calculated}$) values and XRD reflection peaks to calculate mean particle size [137]. Furthermore, size distributions and crystallinity of particles depend on the width of reflection peaks. Internationally, a standard database is being employed to compare the examined XRD pattern that confirms the identification and chemical composition of the samples. Additionally this data also considered as crystallographic data that could be utilize to resolve the structural information of the examined specimens [138].

Albeit X-ray diffraction (XRD) practice is considered as an indisputable, well-known technique, there are some remarkable rising difficulties for structural analysis of molecules. This is due to the fact that XRD shows limitations to conclude the structural information in growing crystals. Additionally, this practice verifies the state of the materials by evaluating and extracting the results from a single conformation scheme confirmation state which might limits the relevance of this technique [139]. Furthermore, in comparisons with the electron diffractions procedure, another weakness of this X-ray diffraction is to generate reflection planes for molecules with low atomic number due to the low intensity of X-ray of XRD [140].

2.8.4 EDX technique/Energy Dispersive X-ray Spectroscopy

Energy Dispersive X-ray Spectroscopy (EDX, XEDS or EDXS), also known as Energy Dispersive X-ray Microanalysis (EDXMA/ EDXA). It is a systematic methodical practice, applicable and designed for the chemical characterization of samples at molecular levels which is being regarded as one of the alternatives of XRF to study very small scales; i.e. at the atomic or micro or even nano levels. It has become an accommodating analytical device that interact some resource of X-ray excitation features with the sample molecules which might open the window of opportunity of the appliance of this device in plentiful areas of materials science and microelectronics along with the branches of biotechnology specially for the characterization of nanoparticles constructed with green nanotechnology [141].

In the EDX setup, four chief working components are the excitation and interesting source (x-ray electron beam), the EDX detector, the pulse processor and the analyser. A detector inside the instrument works as convertor that adapts the X-ray beams/energy and converts into voltage beams or signal. These voltage signals are transferred in to the processor. The pulse processor is capable of measuring the signals and surpasses them into an analyzer to exhibit data for examination and analysis [142].

It is established that each and every element possesses a distinctive, distinguishing and characteristic atomic structure. This uniqueness of the elements works as the crucial basic principle of the characterization function of this practice that allows x-rays beams to identify and recognize the atomic structure distinctively [143].

Characterization of molecules by EDX, XEDS or EDXS EDS schemes are quite easy and the data regenerated from these instruments show high degree of reproducibility. Moreover, this useful instrument is easy to handle and very simple with lasting operation. However, major leading complexities in this system are the lack of skilled enthusiastic analysts. The general error made by EDX learners might lead to the misidentification of the extracted peaks or data. Furthermore, this approach has relied too much on automated systems instead of manual investigation [144].

2.8.5 TEM technique or Transmission Electron Microscopy

Transmission Electron Microscopy (TEM) inserts images that are simple, easy to resolve the morphology and chemical status of materials at nanolevel; therefore this technique is very popular, effective and commonly used method for differentiating and analyzing nanomaterials [145]. TEM has advantages over other microscopic imaging system due to the fact that this microscopy inserts enhanced spatial focus and higher resolution quality images with additional supplementary analytical measurements [146].

Nevertheless, during the specimen preparation for TEM analysis, this method usually requires extremely ultrathin section of the sample on average not more than 100 nm for electron transmittance which is time consuming, extremely complex and complicated; and demands skilful technicians [147]. Those samples containing thin films are equipped on to a carbon-coated copper grid by applying dropping method. A tiny quantity of the sample in liquid form is dropped on the grid; waited for few minutes to stale down the specimen on the grid and then removed the additional solution by using

the blotting paper [143]. Nonetheless, Organic polymers, biological specimens, and similar materials may need special treatment with heavy atom labels in order to obtain sufficient image contrast.

In addition, the Transmission electron microscopy utilizes a high voltage electron beam to illuminate the specimen and generate a micrographic image. An electron gun in the instrument initiates and accelerates these electron beams and then transmitted through the specimen on the conducting grid. These transmitted electron beams holds and carries all the morphological information of the samples that could be recorded by fluorescence screen or CCD camera and revealed into the micrographic images. Furthermore, the magnification of Transmission electron microscopy (TEM) is resolved by adjusting the distance between the lens and the ultrathin section of the sample and the distance between lens and its image plane [148].

Nevertheless, some additional features such as the surface atomic arrangement of crystalline nanoparticles, microstructures of atoms are possible to examine by utilizing HRTEM (High-resolution Transmission Electron Microscopy) [149].

2.8.6 SEM technique or Scanning Electron Microscopy

SEM scheme is another method, supportive to reveal and evaluate the morphology and atomic composition of the samples as well as the topographic details of the outer layer of the materials at nanolevel. It is a surface imaging mode wherein through direct visualization, light sources and glass lenses work combinedly to illuminate or light up and visualize the molecular samples and to manufacture magnified images [149].

Inside the SEM device, the electron beams interact with the sample surface. This interaction aid and facilitate the beams to scan and inspect transversely the sample surface. This overall scanning of the molecules works to create higher resolution images of much [150]. The SEM device has special condenser lenses along with some other functional features like a vacuum system and an electron gun. With the help of specially functionalized lenses, SEM constructs 3 types of prime images: backscattered electron image, exterior X-ray map and secondary e-image (electron based image) [151].

This method offers several advantages for morphological analysis of material at nano level. In addition, SEM practice is very realistic and practical and could be applied

directly to reveal the nano-scaled facts of nanomaterials; i.e. the form, dimension and size distribution of NPs. Moreover, a three-dimensional appearance can be displayed using this microscopic technique [152].

Despite these advantages, this technique is costly, time consuming. The performance of SEM practice also generates several drawbacks. It has disclosed that, the three-dimensional images offer limited and scarcity in information regarding the mean size distribution and accurate density of population number [153]. In addition, for this analysis, the solution of the nanoparticles must be dried in powder form. The dried and powdered sample further must be mounted or glued on a filter membrane or a conducting grid holder. A thin layer made of various conductive materials is used for the coating the dried and powdered sample. This ultrathin layer helps obtain clear images of particles at molecular levels. On the other hand, materials like graphite, iridium, palladium alloy, osmium, gold alloy, gold, platinum, chromium, or even tungsten could be to best conductive sources of this thin layer [154].

Moreover, it is necessary to wait and put the sample filter in open air for the samples to be dried up after the mounting or gluing the specimens. Throughout this drying process, the specimen might shrink and retract. Here, this shrinking effect could bring changes in the characteristic features of nanomaterials [155]. Furthermore, for a successful and fruitful analysis, the nanoparticles must be capable of resisting the unfavourable effects of the electron beam and vacuum pressure, which can damage Nano-polymers [149].

2.9 Application of Metallic Nanoparticles

Nanotechnology has become one of the most influential and beneficiary technologies in all branches of scientific contribution. This technology mainly relies on the synthesis, intonation and modulation of particles in nano-level. On the other hand, considerable amount of alteration and modifications of the metallic properties is required for the synthesis of metallic nanoparticle [156]. Albeit this is a very effective and very popular research protocols in contemporary science, different nanomaterials especially the metallic NPs in fact have been exploited in every part of the humankind as well as by many civilization for thousands of years. However, it is still a matter of discussion whether the ancient people used various kinds of nanoparticles knowingly or accidentally. It is further reported that gold nanoparticles were considered to be very

useful particles for colouring the wine glasses. They are also regarded to be very valuable substance for the cure of certain ailments [157].

Information storage device have also been developed by using metallic nanomaterials. The advantage of these types of devices is that they can record the information in a nanoscale layer. Additionally, different kinds of sensors and biosensors could be designed by using these very effective and unique nanoparticle properties [158].

Walter and co-workers have developed devices using nanoparticle for optical, electronic and sensor applications [159]. On the other hand, nanosensors, which are particularly made of nano-scale particles, have been manufactured particularly to trace the heavy metal particles such as mercury, mycobacterial and algal toxins present in drinking water [160]. In recent times, scientists have also developed nanosensors for hormonal regulation. They are also manufacturing nanosensors for the detection of viruses, very harmful agricultural pests and also the nutrient levels of the soil. Even different kinds of nanosensors are being used for the monitoring and detection of the stress factors like oxygen distribution as well as concentration level of a plant hormone named auxin [161]. Additionally, semiconductor nanoparticles are more efficient and proficient for computer devices, solar cells and for electricity production (photovoltaics).

In recent time, with the help of highly developed technologies, scientists have increasingly become successful monitoring physiochemical characteristics of nanoparticles. Scientists have also been able to identify that, some of these characteristics are virtually responsible for the control of the morphological features of these nano-scale particles. Moreover, these monitored NPs are currently being used in diverse *in vitro* applications (Figure 2.10).
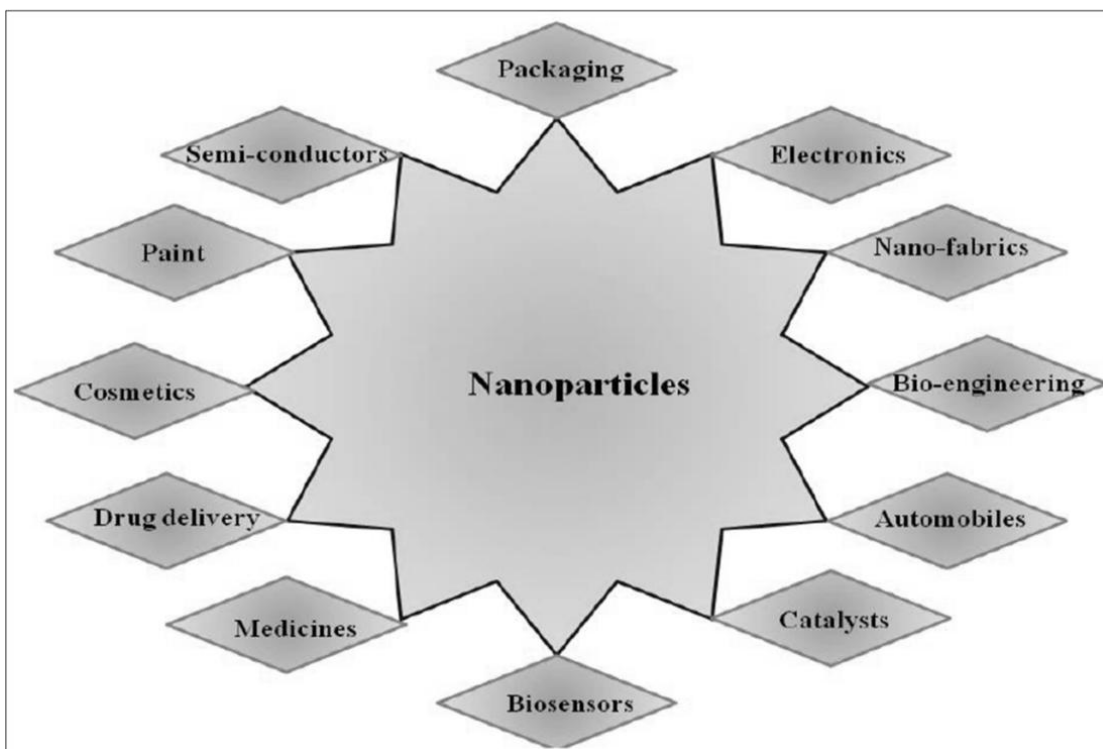
Figure 2.10 Overview applications of nanoparticles [162].

Nonetheless, when nanomaterials in powder form are supplemented with polymer matrix, the activity of polymer-complex might enhance by the reason of the amalgamation of two originator material characteristics like strength and lightweight. Hence, as a result of such properties, various products with advanced features like fire-retardant nanocomposites and/or wear resistant coatings have been expanded for various application purposes [163].

The production of particular types of very important drugs such as doxorubicin, paclitaxel and methotrexate has currently been possible with the help of metallic nanoparticles for example gold nanoparticles (AuNPs). AuNPs have also been utilized for angiogenesis, for the detection of tumour, for the detection and cure of various kinds of genetic disease as well as for the diagnosis of genetic disorders. They are also used as highly significant components for the photothermal therapy as well as photo-imaging [164].

Conversely, iron oxide nanoparticles have been applied for magnetic resonance imaging, different types of therapies for the cure of cancer, for tissue repair, for the production of specific drugs, for the labelling of cell and for hyperthermia. These

nanoparticles are also being used particularly for the detoxification of biological fluids [165], [166], [167].

The zinc nanoparticles (ZnNPs) and titanium nanoparticles (TiNPs) are also being used as valuable elements in different crucial fields. For example, they have been widely used in the cosmetic sectors, for the manufacture of biomedical productions, for the manufacture of biocompatible products, for the manufacture of self-cleansing products, for the manufacture of skincare products as well as for the dermatological treatments. The zinc nanoparticles as well as the titanium nanoparticles are also being used as ultraviolet (UV)-blocking agents in particular of sunstone cream and skincare treatments. They are also being considered to be useful for various types of modern processing applications because of their nontoxic nature [168], [169].

The silver nanoparticles (AgNPs), on the other hand, also have different types of applications. They have particularly been exploited for many antimicrobial purposes, anticancer treatments as well as the applications of antiseptic treatments. They further are being used as a valuable product of anti-inflammatory applications [170].

On the other hand, the palladium nanoparticles (PdNPs) and the copper (CuNPs) nanoparticles are considered to be highly potential and sometimes inevitable elements for various kinds of manufacture and industrial applications. For example, they are widely being exploited in polymers, for the production of batteries, for the manufacture of optical limiting devices. Besides they are used in plastics plasmonic wave guides [171], [87]. The palladium nanoparticles (PdNPs) and the copper (CuNPs) nanoparticles are also reported to have antimicrobial potentials against numerous groups of pathogenic microorganisms.

Besides of the specific applications of certain metal nanoparticles (i.e. AuNPs, ZnNPs, AgNPs, PdNPs, CuNPs etc.), the metallic nanoparticles in general have also been applied in the spatial analysis of various biomolecules, particularly for the visualization with higher resolution and sensitivity [172].

The Figure 2.11 confirms the frequent usages of different metallic NPs in biotechnological applications.
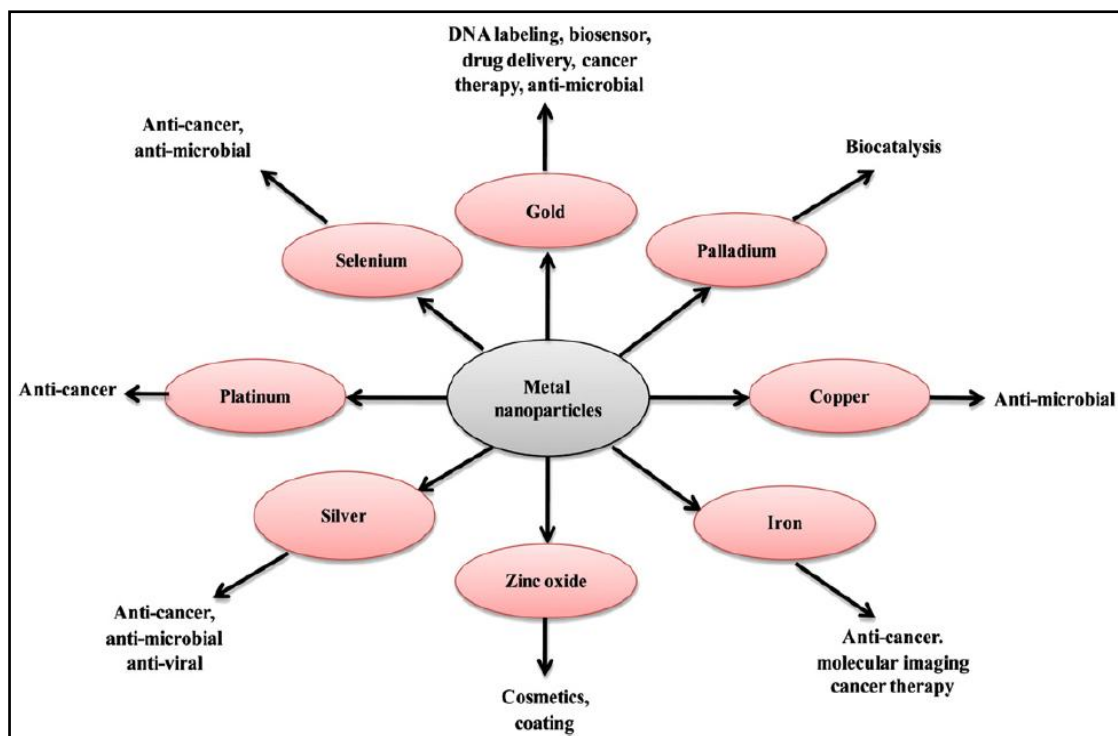
Figure 2.11 The metallic nanoparticles and their functions in biotechnology [173].

Until the present day, researchers have so far investigated huge amount of efforts for the establishment of different kinds of suitable techniques for nanoparticle productions. Making this process for a use of eco-friendly and environmentally safe use was also among the main aspirations of these efforts by scientists. Therefore, synthesizing nanoparticles by biological means like different types of fungi, different types of bacteria as well as yeast has been a new trend in scientific communities, designed for the fabrication of nanoparticles. Besides, various kinds of plants that have the multi-scale advantages such well-defined morphology, non-toxicity, reproducibility in production, easy scaling-up have also been popularly exploited as very useful biological means for the fabrication of nanoparticle. Consequently, with the help of various kinds of biomaterials, the biosynthesis of nanoparticles has popularly been taken place in different types of scientific ventures. Experiments and applications in biomedical sectors, different types of inventions and productions for agricultural benefits, different types of experiments and initiatives for environmental safety and environmental health as well as different types of experiments and applications in physiochemical sectors have been the most frequent ones among these cutting-edge biosyntheses of nanoparticles (Figure 2.12).
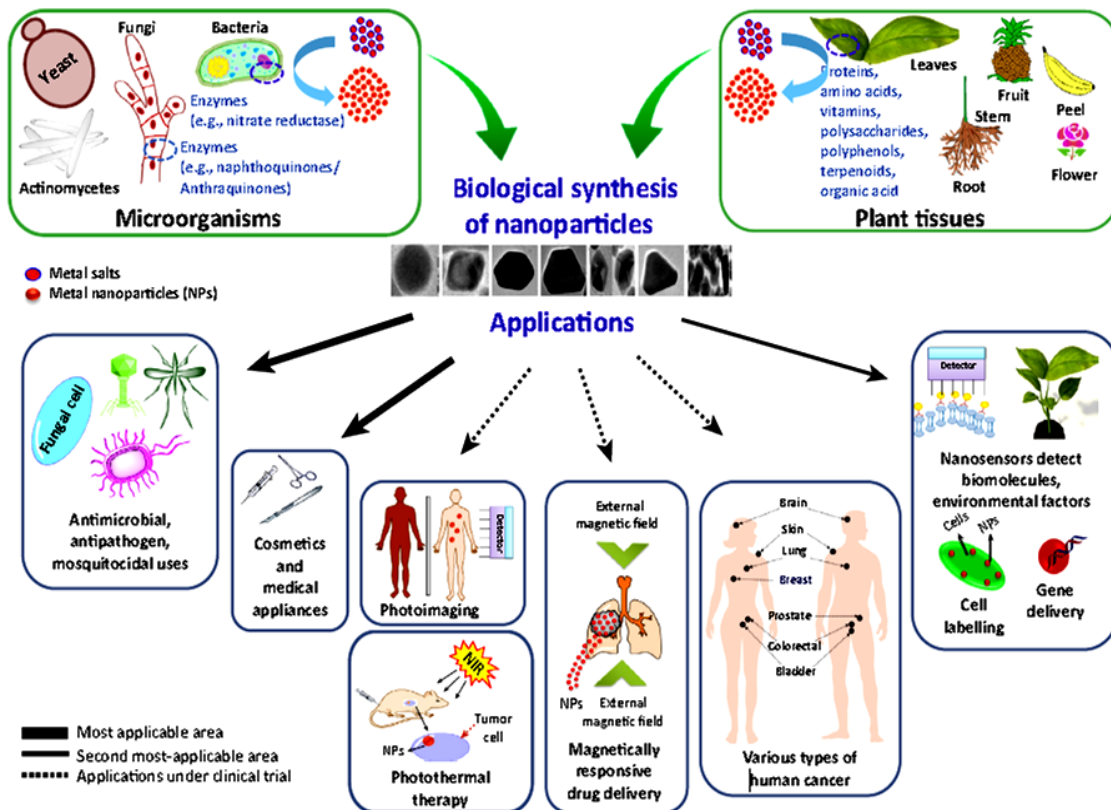
Figure 2.12 Applications of bio-based synthesized metallic nanoparticles [61].

However, the sections mentioned below are pointing out the applications of both silver and copper nanoparticles in various aspects-

2.9.1 Application of Silver Nanoparticles (AgNPs)

Compared to ion and bulk parent materials, AgNPs have distinct optical, mecanical chemical and biochemical properties. Moreover, these exclusive properties of silver nanoparticles revels remarkable properties like increased catalytic activity. It happens as a consequence of their morphologies with exceedingly active facades [174], [175]. That is why the silver nanoparticles (AgNPs) have been among one of the most attractive nanomaterials which are preferably being used in commercialization applications (Figure 2.13). Moreover, the silver nanoparticles (AgNPs) have widely been exploited as a very suitable anti-bacterial agent particularly in the health industries [176]. They have also been the basic material for electronic manufacturing, particularly for the advancement of cutting-edge electronic products, optical devices as well as various kinds of sensors [177]. On the other hand, the silver nanoparticles (AgNPs) have an extensive assortment of applications particularly for the purpose of food

storage, coating purposes textile sectors [178]. The significant facts that the silver nanoparticles (AgNPs) have gradually become the inevitable particles in various kinds of environmental applications in contemporary world. Furthermore, according to different research and commercial sectors, a brief description of applications of silver nanoparticles are given below-
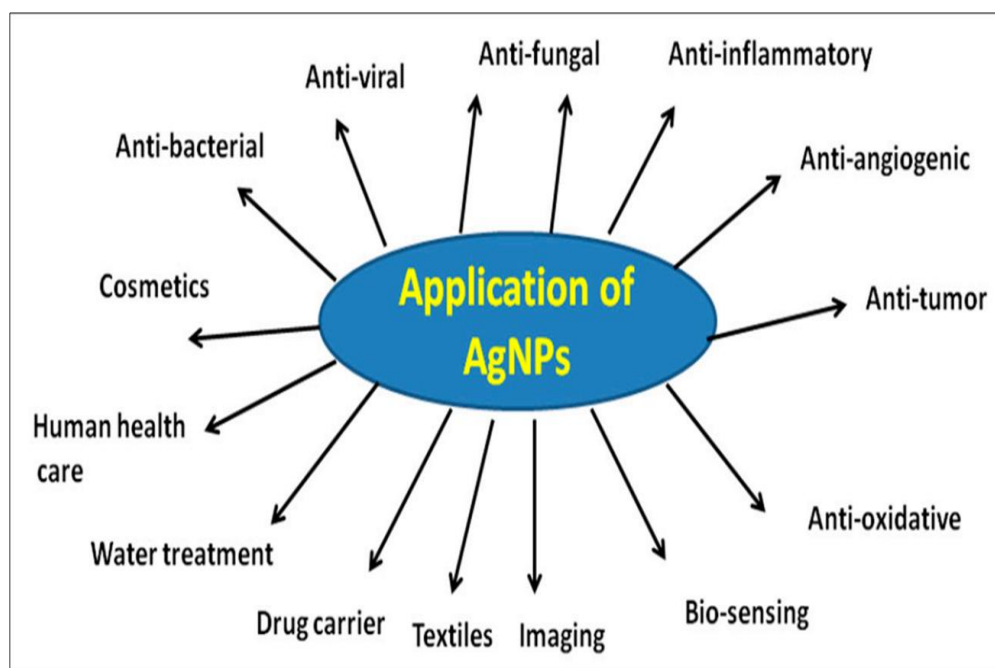
Figure 2.13 Various applications of AgNPs [179].

2.9.1.1 AgNPs as Sensors

To focus the nature of the peptide, peptide capped silver nanoparticle has been used widely by past societies particularly for the colorimetric sensing system. The system works by the capping rates as well as the other effects of the peptides on silver nanoparticles. Moreover, fluorescent sensors which are based on the silver nanoparticles have a very high efficiency. These sensors are able to overcome the limitations in detection process [180].

2.9.1.2 Optical Probes

Silver nanoparticles reveal more advantages in contrast to other gracious metal nanoparticles. For instance, using silver nanoparticles (AgNPs) provides the benefits of their sharper extinction bands, the benefits of the higher extinction coefficients, as well as benefits of their high field enhancements [127]. Therefore, silver nanoparticles

(AgNPs) have extensively been employed as probes both for the Metal-Enhanced Fluorescence (MEF) as well as the Surface-Enhanced Raman Scattering (SERS).

2.9.1.3 Antibacterial Agent

Silver nanoparticles have broad-spectrum antimicrobial ability and therefore, it turns out to be the main extensively exercised sanitizing nano-materials for medical services, personal care products, food packaging, refrigerator exterior making and textile purposes [181].

2.9.1.4 Catalyst

AgNPs have been exhibited to enhance the catalytic redox features for biological agents like dyes, in addition to chemical agents like benzene. In addition, adsorption ability of the reactant species to the catalytic substrate and the substance atmosphere of the AgNPs play an essential function in their catalytic characteristics. In general, silver nanoparticles have widely been used as the catalyst with titanium dioxide particularly for the chemical reactions [182].

2.9.1.5 Environmental Purposes

There is a huge concern of the silver nanoparticles (AgNPs), nanodots or nanopowder for different applications of the wastewater treatment. They further have great potentialities for various kinds of utilities applied in biological systems [183]. For instance, the nitrifying bacteria show susceptibility for inhibition by nano-scale silver particles. These particular silver nanoparticles (AgNPs) are typically of 1-40 nanometres (nm) in size. However, they can have the mean particle dimension of 2-10 nm that commonly ranges with a explicit surface area of about 1 $m^2\,g^{-1}$ [184].

2.9.1.6 Household Applications

The silver nanoparticles (AgNPs), along with the colloidal silver, have also been widely exploited in various types of household utilities, particularly of electrical and electronic machines. For instance the Samsung, one of the leading brands for household appliances, have maintained that the exploitation of metallic AgNPs in washing machines may facilitate to purify water; therefore, these machines could be capable of sterilizing garments throughout the washing and rinsing course of action. It is further

claimed that, because of this, the washing machine may have the capacity to clean the dirty clothes without any use of hot water [185].

2.9.2 Application of Copper Nanoparticles (CuNPs)

Copper is of metallic elements due to mainly of their historical application for various kinds of facilities. The earliest use of these particular nanoparticles (i.e. CuNPs) perhaps goes back to the manufacturing process of colour glasses and ceramics during the 9th century in ancient Mesopotamia [37]. The preference of copper nanoparticles (CuNPs) over silver nanoparticles (AgNPs) is because of the physical and chemical stability, the lower cost of copper than silver, and ease of mixing with polymers [186]. Hence, CuNPs have great applications as antimicrobial materials [187], super strong materials [188], heat transfer systems [189], sensors [190], and catalysts [191]. A brief description of applications of copper nanoparticles are given below-

2.9.2.1 Copper Nanoparticles for Water Purification

Even though there are some beneficial microbes in all ground waters, but, on the other hand, some harmful microorganisms (e.g. bacteria, protozoa, viruses) may cause disease which is a foremost threat to human race. Water-borne pathogen contamination and the provision of safe drinking water have become a significant human-health concern throughout the world. As a consequence, the numbers of disinfectant procedures have increased since some microbes are resistant to older antimicrobial agents. In such case, Point-of-use (POU) water purification offers an inexpensive and suitable way to reduce exposure to pathogenic microorganisms [192]. Paper-based filters coated with biocidal agents like nanoparticles do not require energy and therefore, are easy to produce and distribute to remote locations [193]. Recently, copper nanoparticles have been employed as a disinfectant for drinking water [194].

2.9.2.2 Effective Antimicrobial Agent

Copper nanoparticles can easily interact with other particles like polymers, sepiolite, carbon, and polyurethane foam. They possess this significant capacity owing to their very reactive high surface to the volume ratio. Therefore, it is possible to increase their antimicrobial efficiency. Because of its bio-compatibility, it is very possible to develop the copper-based bio-pesticide into an efficient delivery system. This could further be

in use for the copper-based fungicides which is more advantageous particularly for the protection of plants [195]. On the other hand, it has been found that at low melting point, the 100% recycled soda-lime-silica glass powder which contains the copper nanoparticles (CuNPs) possess efficient antimicrobial actions against the gram-negative and the gram-positive bacteria. With this additive of copper nanoparticles (CuNPs), the glass powder has also the efficiency of antimicrobial activity against yeast as well as fungi [196].

2.9.2.3 CuNPs as Catalyst

Copper nanoparticles are also widely used as catalyst due to the irreversible and renewable surface, the large surface-to-volume ratio, over and above, the changes in microelectrode potential values. Therefore the stabilized copper nanoparticles offer suitable catalytic properties [197]. The performance of biodiesel in automotive engines is limited due to its high nitrogen oxide emission. For diesel engine, CuNPs within the range of 40–50 nm have been used as the fuel additive with soya bean bio-diesel (B10) which exhibit better engine performance and reduced nitrogen oxide emission compared to other formulations [198].

2.9.2.4 In Sensor System

Metallic copper nanoparticles provide flexible interface activity by reason of its special properties like great catalytic activities, high stability against aggregation, bio compatibility, and hydrophilic character. Therefore, the copper nanoparticles (CuNPs) and their composites can be very useful for different kinds of applications of biosensors. Moreover, the copper nanoparticles (CuNPs) and their composites have highly functional potentials to be used for the manufacture of electrochemical sensors [199].

A glucose sensor is one of the best examples of using copper nanoparticles in sensor system. The sensor does not require any enzyme if the copper nanoparticles (CuNPs) are used in glucose sensor. Therefore, dealings with the enzyme degradation as well as the enzyme and denaturation are no longer required in this process.

If a glucose sample is added to a polyacrylamide hydrogel that contains the copper nanoparticles (CuNPs), the CuNPs in the sensor diffract the incident light. However, figuring on the amount of glucose, CuNPs may diffract the incident light from couple

of dissimilar angle. Alternatively, the hydrogel becomes swollen. This is due to the fact that the phenylboronic acid assemblages on the gel polymers can combine with the glucose molecules. Consequently, the CuNPs move apart and thereby, the gel becomes red in colour. However, the colour may change its variations from red to orange, from orange to yellow, or from yellow to green, depending on the gradual decrease of the glucose levels [200]. To present it in a more clear way, an illustration of this sensor system is revealed in Figure 2.14 below:
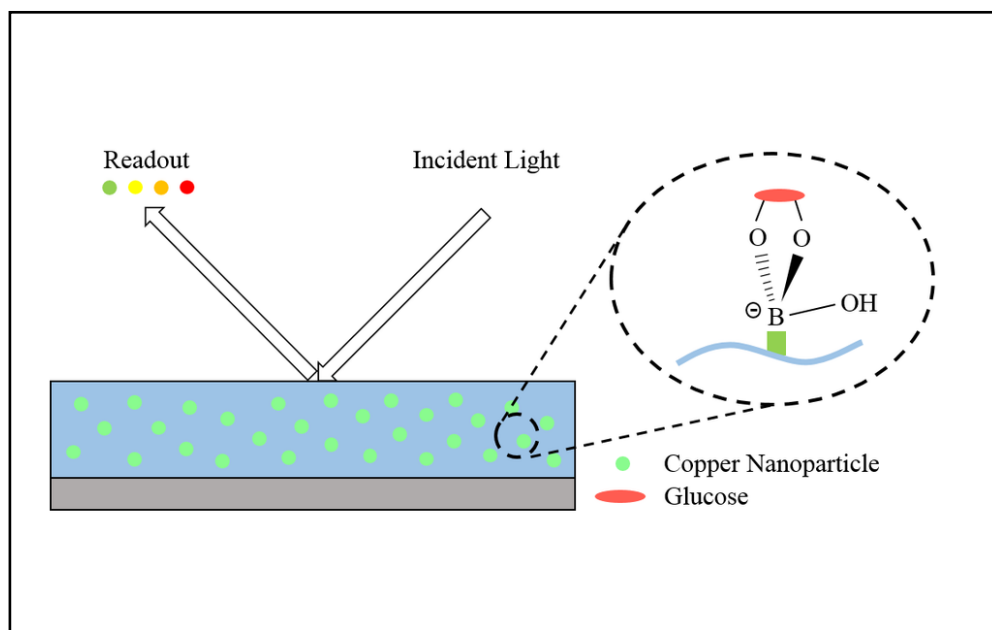
Figure 2.14 Mechanism of copper nanoparticles in glucose sensor [200].

2.10 Antimicrobial Mechanism of Nanoparticles

It has been observed that various prominent metals at their nano levels along with some important nanometals oxides showed their remarkable and significant actions against diverse microbial strains. Some of the mentionable metals and oxidized form of metals are silver (Ag), gold (Au), copper (Cu), zinc oxide (ZnO), copper oxide (CuO), silver oxide (Ag_2O), magnesium oxide (MgO) and titanium dioxide (TiO_2) have been conducted as nanomaterials and accounted as prominent agents for controlling harmful or unwanted organisms at micro level [201], [202]. Therefore, these important abundant metals and oxidized metals as nanomaterials have been broadly exploited like antimicrobial agents and intended for hundreds of years. Thus, form a long period of time; metals have been being applied effectively in various sectors like medical procedures, agricultural management and industrial purposes.

Besides their usages and applications, scientist have also been searching and conducting experiments to reveal a clear explanation of the mechanism of metal and metal oxide NPs against microorganisms. Nevertheless, the mechanism of antimicrobial activity is not clear and still controversial as there are not sufficient existing literatures that could support it.

However, two most accepted hypothetical mechanisms of antimicrobial activity are: Mechanism 1: antimicrobial activity using oxidative stress or catalytic effects that produced by Reactive Oxygen Species (ROS) of NPs. Mechanism 2: ionic mimicry; antimicrobial toxicity on account of the production of metallic ions by NPs [203], [204].

Figure 2.15 illustrates a brief outline of the promising mechanisms related to the antimicrobial behaviour or actions of metallic nanoparticles as well as a details and informative explanation of this hypothesis is discussing below:

The first mechanism: antimicrobial activity using oxidative stress produced by Reactive Oxygen Species (ROS) which is accelerated by the reduction potential activity of metallic NPs. Metals have the capability to involve and participate in RS (Redox Reactions). By creating this Redox Reactions, metals gain electrons from donors [205]. Electron containing redox-activated metals could consequently play a vital role for antimicrobial mechanism by different processes. These activated metallic electrons could function as catalytic cofactors which might interrupt the activities of microbial cell enzymes.

On the other hand, these metallic electrons could also work as catalyzing Reactive Oxygen Species (ROS). The exterior surface or outer layer of NPs constructs the Reactive Oxygen Species (ROS) that might produces oxidative stress [205]. In addition, different free radicals (e.g. $^1O_2$, $OH^•$ etc.), ions, minute molecules for example H_2O_2, superoxide ($O_2^{•-}$) etc. also promote the activities of Reactive Oxygen Species (ROS). The ROS containing outer layer of organic metallic nanoparticle could change the ionic balance of bacterial cells. As a consequence, these ROS-induced bacteria with ionic imbalance could not function properly and disturb by the damaging of cellular membrane as a result of membrane lipid peroxidation. These bacterial proteins, lipids and DNA also could not function properly due to the oxidative stress or oxidative lesions [206], [207].

The remarkable example of oxidative stress induced antimicrobial activity was noticed in *Escherichia coli* by silver oxide (Ag_2O) nanoparticles. It has found that these NPs stimulated the oxidative stress oxidative stress that damages the bacterial DNA; interrupts the bacterial cell cycles that hampers the cell growth and ultimately promotes the death of the cell [208].

Likewise, CuO NPs could also account for this mechanism. It is established that CuO nanoparticles encompass the capability of regenerating Reactive Oxygen Species (ROS) while it come to the contact of bacterial cells. The evident shows that in case of both *Staphylococcus aureus* and *E. coli,* the CuO NPs release free radicals and superoxide ions when these NPs are absorbed by the surfaces of bacterial cells [209].
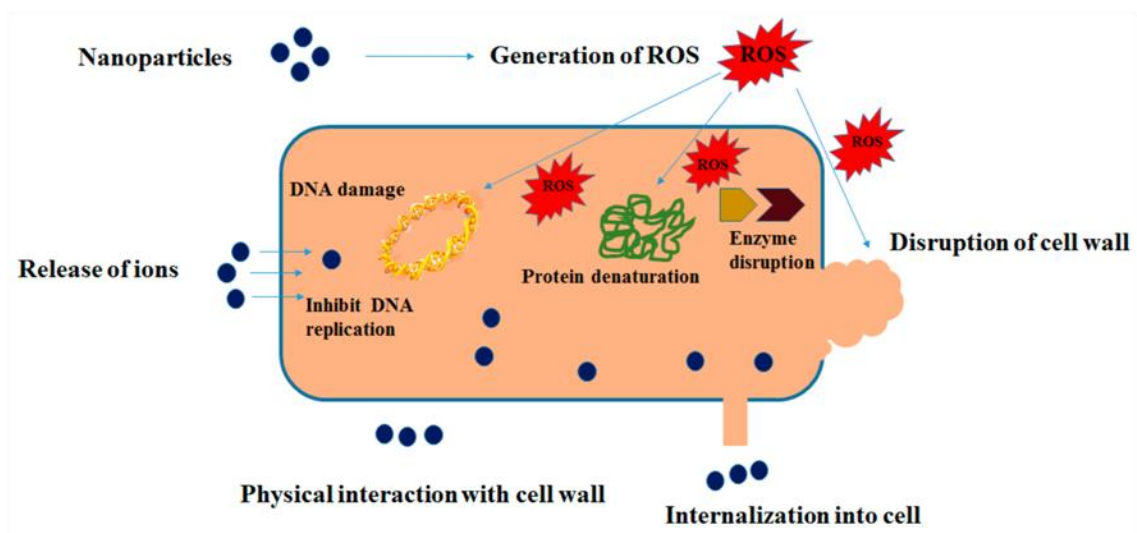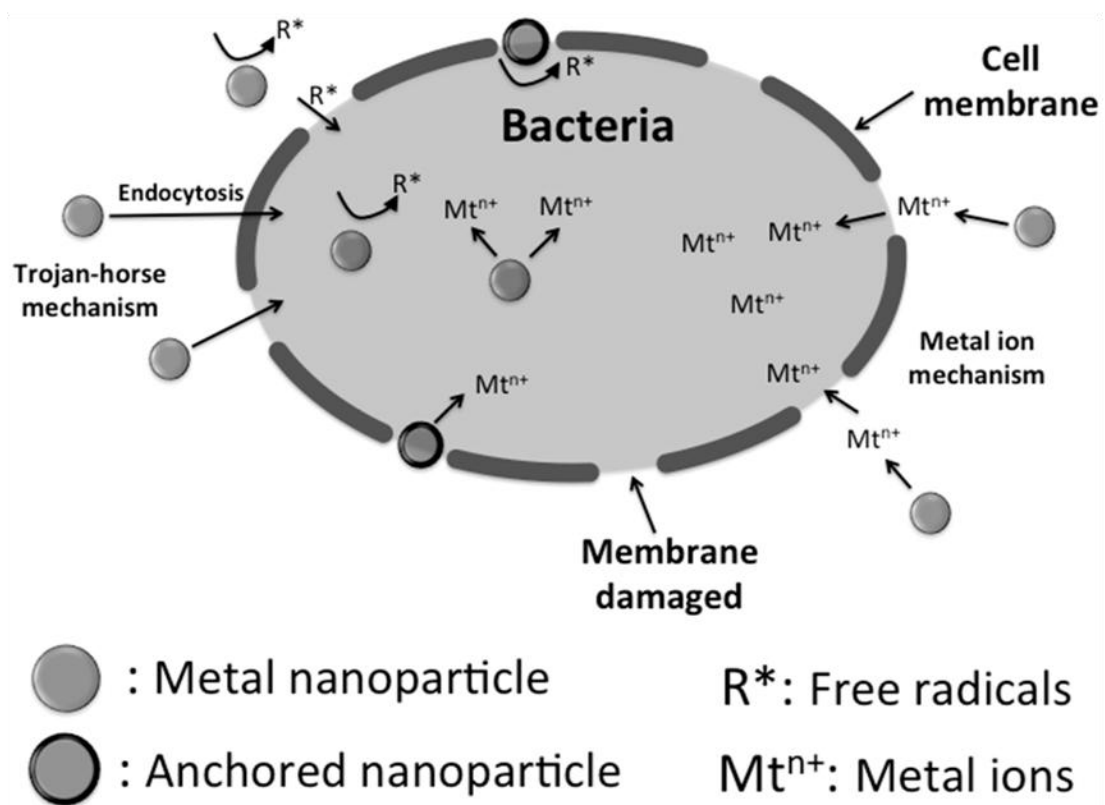
Figure 2.15 A diagrammatic outline of various mechanisms behind the antimicrobial behaviour of metallic nanoparticles [210], [211].

Several mechanisms on ROS regarding copper-induced bacterial cellular toxicity have been developed to explain how this NP works as bactericidal agent. It is believed that CuNPs produce both free cuprous (Cu^+) and cupric (Cu^{++}) ions which could involve in redox reactions [212]. The cupric (Cu^{++}) ions reduced to cuprous (Cu^+) ions in the existence of several reducing factors (e.g. ascorbic acid) and the superoxide ($O_2^{•-}$).

This ionic reduction induces and catalyzes the free radical reaction that forms hydroxyl radicals from hydrogen peroxide via the Haber-Weiss reactions [213]

In the existence of either superoxide ($O_2^{\bullet-}$) or other reducing agents like ascorbic acid, Cu^{2+} can be reduced to Cu^+ catalyzing the formation of hydroxyl radicals from hydrogen peroxide (H_2O_2) according to the Haber-Weiss reaction formula [213]:

$$O_2^{\bullet-} + Cu^{2+} \rightarrow O_2 + Cu^+$$

$$Cu^+ + H_2O_2 \rightarrow Cu^{2+} + OH^- + OH^{\bullet}$$
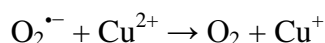
However, the hydroxyl radical ($OH^{\bullet}$) is so potential and influential that It might capable of functioning as common oxidizing radical factor. This radical could easily react with nearly all biological components and molecules [214].

On the other hand, the second mechanism: Mechanism 2: ionic mimicry; antimicrobial toxicity in consequence of the production of metallic ions by nanoparticles is established on the nature of metallic NPs' donor atom specificity, selectivity and convergence/speciation. Inside the microbial cells, a strong and interactive force works for metallic ions that might help them to bind easily with some atoms/molecule of donors i.e. S, O, and N [215]. In fact, these external ions from metallic NPs along or with the help of their donor binding complexes might reinstate and substitute novel metallic ions working for the regular functions of different biomolecules of the bacterial cellulose [194]. This trend is described either molecular impersonation if the metal complexes involved or ionic mimicry when metal ions are implicated in this process [215].

Likewise, metal nanoparticles are also capable of substituting some functional non-catalytic sites of the bacterial enzymes that can easily bind metallic ions. There metal-binding sites with metallic ions however could easy inhibit the functions and activities of these enzymes. As a result of malfunctioning enzymes, the conformational isomerism structures of polypeptides, proteins, DNA and RNA could be altered. These irregularities may cause defects in oxidative phosphorylation and other important pathways which could lead to osmotic imbalance [205]. For instance, with the aid of lipid radicals and oxygen, ions of copper nanoparticles are capable of excessing the peroxidative functions and activities of membrane [214].

Nevertheless, independent on the abovementioned mechanisms, another possible bactericidal mechanism might be interpreted as the intracellular regulation of biocidal

ions from metallic NPs inside the bacterial cell membrane. This is providing that the bacterial cell membranes hold macromolecules which are loaded with extremely electronegative functional groups. These natively charged functional groups serve as metal binding sites that could attach and absorb some of the bactericidal metallic ions that might cause bactericidal toxicity [205], [216].

Some evidences have recommended that few metallic nanoparticles, mostly AgNPs are capable of attaching, anchoring and penetrating the bacterial cell wall [217]. This theory has suggested that metal ions first damage the cell membrane after attaching with it. And subsequently penetrate into the intracellular region of bacterial cell; dissipate the chemiosmotic potential of the cell membrane that could change the cell membrane permeability. This altered membrane permeability leads to proton leakage throughout the cell membrane that causes disruption on the bacterial electron transport chain reaction [205]. Additionally, ions from silver nanoparticles (AgNPs) are also capable of interacting with the thiol groups (R-S-R′) of many essential proteins and enzymes of bacterial cells. This interaction causes inactivation of these essential molecules' functions. Some of the malfunctioning enzymes inhabit respiratory system and hence causes the death of the bacterial cell [218].

 Furthermore, silver (Ag) is a soft acid. It has a natural affinity to respond and interact with a soft base [219]. Bacterial cells especially cell membranes are largely consist of some important soft base; i.e. phosphorus and sulphur. Sulphur and phosphorus are also the major components of nucleic acids. Therefore, the ionic silver nanoparticles after anchoring into the bacterial cells easily react with those based that subsequently change the membrane functions as well as interrupt the DNA replication of the bacteria, destroy the DNA which eventually terminate the bacterial growth and thus, lead to cell death [220] (Figure 2.16).
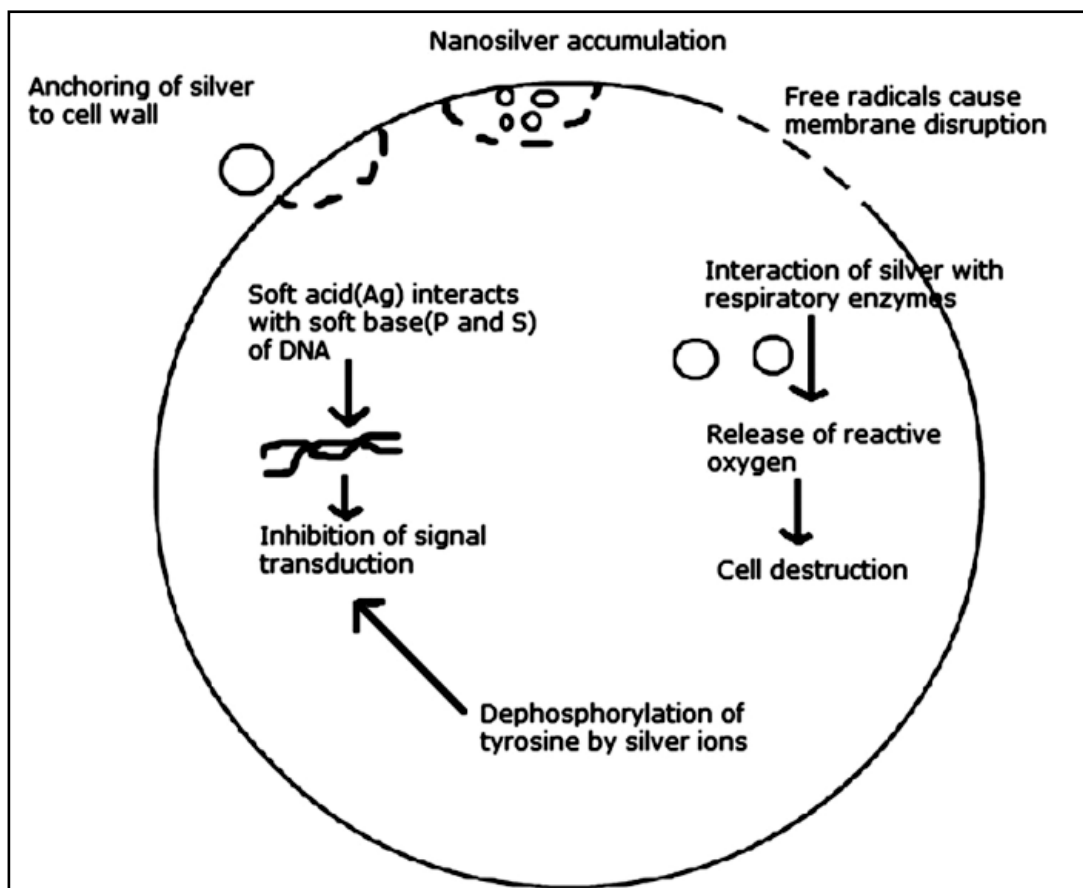
Figure 2.16 Hypothetical modes of action of ionic nanosilver inside the bacterial cell [207].

In addition, in a comparison to the larger particles of bulk materials, nanoparticles are able to dissolve more rapidly in a specified solution with desirable concentration of volume. Therefore, this advantage favours the nanometals releasing a huge amount of ions [221]. For that reason, based on the abovementioned antimicrobial mechanisms, nanoparticles ought to perform rapidly as antimicrobial agent with relatively stronger antimicrobial effects rather than their bulk forms; i.e. metallic microparticles or metal surfaces. In case of copper nanoparticles, it has been experimented that in distilled water the nanoparticle as their ionic form dissolve rapidly as compared with microparticles [222].

On the other hand, morphological and physiochemical properties of nanoparticles are also play vital factors for their bactericidal properties [223]. Nanoparticles with smaller size distribution trend to show stronger antimicrobial effect [224], [225]. Furthermore, the potential values of NPs also influence their bactericidal properties. Nano-metallic

particle surface with high potential charge could rapidly bind with surfaces of bacterial cells which might increase of the bactericidal effect [226].

Nevertheless, the shapes of the metallic nanoparticles; i.e. globular, oval, triangular or irregular structured nanoparticles also influence their antimicrobial actions [227]. As it is reported that with the comparison of rod-shaped silver nanoparticles, truncated triangular and spherical shaped AgNPs showed stronger antibacterial effects [227].

2.10.1 AgNPs and CuNPs as Antimicrobial Agent

Copper and silver nanoparticles have gained extra attention attracted in recent time due to their remarkable chemical, physical and biochemical properties along with their huge applications in electrical, optical, catalytic, and biological sectors [228], [229]. These nanoparticles have been utilized either singly as their pure forms or polymeric states holding up a variety of suitable elements, like carbon compounds, polyurethane foam, polymers etc. which have been successfully exercised for bactericidal purposes [100], [230].

Silver is usually applied in its nitrate types to influence antimicrobial effect however while AgNPs have been applied, an enormous enhanced antimicrobial effect has been observed due to the high surface area of silver nanoparticles, offered additional availability for the microorganisms to be exposed to [231]. Silver NPs are illustrated as 'oligodynamic' for the reason that, the ions of these NPs are proficient to cause not only bactericidal (antibacterial) impact but also bacteriostatic (growth inhibition) effect [232]. However, it is a safe inorganic antimicrobial agent that has a low toxicity towards animal cells.

Silver at nanoscale has demonstrated antibacterial, antifungal and antiviral activities and is capable of killing about 650 microorganisms that cause diseases [231]. The antimicrobial features of AgNPs are influential, stable, deep-rooted and well-known; thereby these NPs have been extensively applied for diverse relevance because of their distinctive features which aid plentiful antimicrobial appliances [217].

Silver nanoparticles synthesized either chemically or biologically, are capable of inhibiting both Gram-negative and Gram-positive bacteria besides against yeasts. But, stronger antibacterial activity has been observed against Gram-negative bacteria that might be accredited to the presence of an additional external surface layer on top of the

peptidoglycan of the thicker cell wall of Gram-positive bacteria. These outer layers of the bacteria have been distinguished as extremely resistant and impermeable that might interrupt the access of metallic ions into the bacterial cell [233]. However, Gram-positive bacteria have polysaccharides in their cell wall called teichoic acid, which is negatively charged and have facilitated the passage of the positive metal ions [231].

Additionally, along with the bactericidal activities, Nano-silver is very efficient and a fast-operative fungicide against a wide spectrum of universal fungal genera such as *Saccharomyces, Aspergillus* and *Candida* [234]. Silver nanoparticle synthesized by using the plant *Svensonia hyderabadensis* leaf extract has shown its antifungal effect against *Fusarium oxysporum, Aspergillus niger, Curvularia lunata* and *Rhizopus arrhizus* [235]. Moreover, Silver nanoparticles synthesized using green chemistry especially from plant resources have been utilized for evaluating their antimicrobial potentials against different microbes as describing in Table 2.5.

Table 2.5 Antimicrobial activities of AgNPs synthesized using plant materials.

Biobased units (Plant extracts)	Microorganisms	References
Aloe vera	*Escherichia coli*	[236]
Coconut (*Cocous nucifera*)	*Pseudomonas aeruginosa, Salmonella paratyphi, Klebsiella pneumoniae*, and *Bacillus subtilis*	[237]
Camellia sinensis	*Escherichia coli*	[238]
Alternanthera dentate	*Pseudomonas aeruginosa, Escherichia coli, Klebsiella pneumoniae*, *Enterococcus faecalis*	[239]
Lemon grass (*Cymbopogan citrates*)	*Pseudomonas aeruginosa, Escherichia coli, Proteus mirabilis, Shigella flexaneri, Shigella sonnei, Klebsiella pneumonia*	[240]

Table 2.5 Antimicrobial activities of AgNPs synthesized using plant materials
(continued).

Biobased units (Plant extracts)	Microorganisms	References
Bindii (*Tribulus terrestris*)	*Pseudomonas aeruginosa, Streptococcus pyogens, Bacillus subtilis, Escherichia coli, Staphylococcus aureus*	[241]
Spreading hogweed (*Boerhavia diffusa*)	*Flavobacterium branchiophilum, Pseudomonas Fluorescens, Aeromonas hydrophila*	[242]

On the other hand, copper or copper oxide NPs have offered noteworthy pledge as bactericidal mediator albeit very few evidences have accounted for the antimicrobial properties of these NPs [243]. Copper nanoparticles are very involuntary, capable of interacting easily with other molecules on account of their elevated surface area to volume ratio which might enhance their antimicrobial effectiveness [244]. Copper in colloidal forms have been exercised as an antimicrobial mediator for several decades. For instance, the bactericidal activities of CuNPs were confirmed against various species of bacteria, for example *Bacillus subtilis* and methicillin-resistant *Pseudomonas aeruginosa* (MRSA), *Pseudomonas aeruginosa* and *Salmonella enteric* as well as some yeast species like *Candida albicans* [245].

Furthermore, Beyth *et al*. showed that CuNPs have a high antimicrobial activity against *Anthrax bacterium* and *Bacillus subtilis* as because these microbes are rich of carboxyl and amines groups on their outer layers of the cell which offers better affinity of copper nanoparticles as their ionic form to these groups [246]. Yoon *et al.* evaluated the antibacterial properties of both copper and silver NPs by means of *B. subtilis* and *E. coli* strains and in this case the CuNPs have proved better antibacterial potential in contrast of the AgNPs [247]. However, handling metallic copper nanoparticles is quite challenging because of its intense susceptibility to the air. When copper nanoparticles

expose to the air they trend to form an oxidized layer which may reduce their antimicrobial potential, remarkably [244], [248].

Along with the abovementioned reason, the bactericidal action of copper nanoparticles is also contingent on the stage of agglomeration of CuNPs. By reducing and decreasing agglomeration, it possible to achieve smaller sized copper nanoparticles that might be able to provide more obtainable surface area and increase the solubility of copper ions; hence, facilitate the interaction with bacterial cell which offers increased availability of CuNPs as antimicrobial agent [244].

2.11 Cytotoxicity of Nanoparticles

Rapid advancement in the field of nanotechnology lead to fabricate nano-sized materials with diverse chemical, biochemical and physical characteristics in contrast to their bulk form [249]. Albeit this is a very effective and very popular research protocols in contemporary science, different nanomaterials especially the metallic NPs in fact have been exploited in almost all parts of the world as well as by many civilization for thousands of years.

Human exposure to different nanoparticles is unavoidable and inevitable as it acquires various applications in almost all aspects of mankind; i.e. from cosmetics to medical goods to water purification and renewable energy capture like solar energy [250]. Due to rising extensive interaction and exposure of nanomaterials with human body, the possible threat to human safety has become the considerable matter of concern and therefore, research on nanotoxicology is now gaining more attention [251]. The major concern is that in the workplace where worker handle nanomaterials may have the adverse effects of acute or chronic exposure.

Furthermore, in nanoparticle research, particle size has a vital and significant role to determine important and specific biological behaviour of nanomaterials. Nanoparticles with larger surface area create the number of surface molecules or atoms that amplify exponentially and offer high reactivity [252]. Therefore, small sized nanoparticles with larger surface area have been widely utilized in industry, and hence, there is a high chance in this case that these NPs could easily interact directly with macromolecules such as protein, DNA, RNA etc. Besides, NPs could easily pass through the nostril respiratory system and inhale into the lung. This could make it a possible organ system for accumulation of nanoparticle intake inside the human body. After inhaling in to the

lung, such tiny particles rapidly absorbed by the cells found mainly on the internal surfaces of the air cavities, alveolar cells. This absorption by the air cavities might induce toxic effects on human body [253].

Additionally, exposure to NPs might be related to an increased risk of different cancers. Even though the accurate mechanisms are not yet studied, there are some evidences that same mechanisms of these NPs inside the bacterial cells could also take place inside the human body. The surface or outer layer of nanoparticles constructs the Reactive Oxygen Species (ROS) that might produces oxidative stress [205]. This oxidative stress might be a significant reason in the carcinogenetic effects of metals on human body [254]. Furthermore, in an advanced study, it has been found that in the NT2 human testicular embryonic carcinoma cells, AgNPs with particle size of 200 nm have some negative effects on Human DNA. These have evidently caused a concentration-dependent increase in DNA strand breaks of these carcinoma cell lines [255]. Researchers have also shown that AgNPs decreased cell viability. AgNPs have been applied on apoptotic bodies, DNA fragmentation and sub-G1 hypo-diploid cells to test their cytotoxic activity [255].

Moreover, in another finding it has been shown that AgNPs damage mitochondrial function, mainly by altering mitochondrial membrane permeability, which effect on the oxidative phosphorylation system [256]. Collectively, abovementioned findings indicate that silver nanoparticles have potential cytotoxic effects that might cause significant cell damage in case of long term exposure to these NPs [257]. However, now a day, by overlooking all these negative facts and risk, silver nanoparticles have become the most common metallic NPs among all and are extensively utilized in various purchasable products, for example cosmetics, healthcare proposes, household goods, clothing, pesticides etc. Since AgNPs have been found to an effective antimicrobial agent, it is introduced into different food-contacting supplies, like food containers made of plastic, storage bags, exterior surface of the refrigerators into the washing machine and chopping boards [258].

Afterward, copper is being considered as one of the essential nutritional element for human body. If the intake of Cu surpasses the level of requirement however, it might have some lethal effects such as jaundice, hemolysis that ultimately could be dreadful for human life [259].

It has been observed that CuNPs are supplementary cytotoxic than their larger microparticles. This might be the reason of having easy penetration capability of NPs inside the human system through inhalation, skin contact, and ingestion [260]. The effect of CuNPs on dorsal root ganglion (DRG) of louse was studied by Prabhu et al. (2010).

For cell viability, this study uncovered that the treatment with increasing sizes (40, 60, and 80 nm) and concentrations (10–100 μM) of nano-Cu showed the significant toxic effect compared to unexposed control cultures. Additionally, they also stated that higher concentration and small-sized nanoparticles exerted the maximum toxic effects [260]. However, albeit metallic nanoparticles are extensively used, the long-term fate of these NPs in biological environments is not well understood. Once metallic nanoparticles have entered cells, they may not induce DNA damage themselves but instead deteriorate cell cycle over time, release metallic ions that could induce genotoxicity [261].

MATERIALS AND METHODS

3.1 Materials

The present study entitled "Green synthesis of metal nanoparticles, their chemical and biochemical characterizations" was performed in the Polymeric biomaterials and macromolecular synthesis laboratory, Department of Bioengineering, Yildiz Technical University, Istanbul, Turkey. The details of materials, devices and chemicals used have been elaborated and were as follows-

3.1.1 Devices and Instrument

Table 3.1 Names of devices and equipment needed for the experiments.

Devices and equipment	Brand/Trademark
Ultrasonic bath	Bandelin, SONOREX SUPER
Centrifuge machine	Sigma 2-16PK centrifuge
Water Purification Systems (ultrasonic water purifier)	Purelab flex, veolia water solutions & technologies
Food-grade blender	Tefal Master Blend HB114B30 700 W
Laboratory-grade microwave	Milestone Microsynth microwave labstation
Incubator	Friocell, USA
Magnetic Stirrer	VWR

Table 3.1 Names of devices and equipment needed for the experiments (continued).

Vortex machine	Isolab
pH meter	Mettler Toledo
Laboratory-grade freezer	+4 ° C refrigerator with glass cover -20 ° C refrigerator LIEBHERR
Class II sterile cabinet (laminar flow)	Esco
UV-vis spectroscopy	Shimadzu UV-1700 spectrophotometer
XRD	PANalytical Empyrean model
Zeta analyzer	Zeta-sizer nano ZS, Malvern Instruments Ltd., U.K.
TEM	TEM 1400 (JEOL, Tokyo, Japan)
FTIR	Shimadzu IR Prestige-21 FTIR-ATR & JASCO, FT/ IR-6300 spectrometer (Tokyo, Japan).
Autoclave	Core
CO_2 Incubator	Memmert
Inverted Microscope	Nikon
Micro-plate reader	BioTek Instruments
Multiplate reader	Lab-Line Instruments, Melrose Park, IL, USA
Sterile pipette (5,10 & 25 ml)	LpItalianaSpa
Serological pipette gun	Thermo
Sterile 15 and 50 ml falcon tubes	Isolab

Table 3.1 Names of devices and equipment needed for the experiments (continued).

10, 100, 1000 µl micropipettes	Isolab
Disposable Pipette Tips 1-10, 10-100, 100-1000 µl	Isolab
Centrifuge tubes 1, 2, 15, 50 ml	Eppendorf, ISOLAB
ELISA 24, 48 and 96 well plates	VWR
50-1000 ml autoclavable glass bottles	Isolab
250-1000 ml Erlenmeyer flasks	Isolab
0.22 µm and 0.45 µm Syringe Filters	Merck Millipore
Filter paper	Whatman No.1 & Whatman No.5

3.1.2 Chemicals

Table 3.2 Names of chemicals needed for the experiments.

Name of the chemicals	Brand/trademark
Silver nitrate ($AgNO_3$)	Sigma-Aldrich
Copper sulphate pentahydrate ($CuSO_4.5H_2O$)	Sigma-Aldrich
L- Ascorbic acid	Merck
Ethanol	Merck
Nutrient Agar	Merck

Table 3.2 Names of chemicals needed for the experiments (continued).

Agar	Sigma-Aldrich
Nutrient broth	Merck
Muller Hinton Broth	MHB; BD, Auckland, New Zealand
Muller Hinton Agar	MHA, Merck
Barium chloride dehydrate ($BaCl_2.2H_2O$)	Sigma-Aldrich
Sulphuric acid (H_2SO_4)	Merck
Penicillium-Streptomycin (PEST)	Biochrom-AG (Penicillium/Streptomycin: 10,000 unit/1000 μl/ml)
Trypan Blue powder (Dye content ~40%)	Sigma-Aldrich
L-Glutamine	Biological industries
Fetal Bovine Serum (FBS)	Biochrom AG
Sodium Chloride (NaCl)	Sigma-Aldrich
Potassium Chloride (KCl)	Sigma-Aldrich
Hydrochloric Acid (HCl)	Merck
Disodium Phosphate (Na_2HPO_4)	Sigma-Aldrich
Monopotassium Phosphate (KH_2PO_4)	Sigma-Aldrich
DMEM/ F12 mixed with F12 1.1 (Dulbecco's Modified Eagle Medium: Nutrient mixture F-12)	Sigma-Aldrich

3.2 Methods

3.2.1 Plant Extract Preparations

Various plant materials have been used for aqueous extract preparation which has utilized as synthesizing agent as reducing and stabilizing forces in the fabrication of silver and copper NPs. Extract preparation procedures are described in detail as blows:

3.2.1.1 From Apple (*Malus pumila*) Pulp

Fresh yellow delicious apples (*Malus pumila*) have been collected from the local market (Figure 3.1). The fruits have been washed separately and properly with running tap water to eliminate the unwanted dust particles and again, washed several times thoroughly with ultra-purified water. Using a sterilized kitchen paring knife, the fruits have been peeled off and 100 gm of its pulp has been sliced into small pieces. Then, these seedless pieces have been put into a food grade kitchen blender, ground well to make pulp paste. Afterwards, the paste has been transferred in a conical flask. After adding equal volume of ultra-purified water, the mixer has been seated approximately for 3 minutes with a maximum power level of 700 W into a microwave (laboratory-grade) for irradiation to extract the biomolecules present in apple pulp. And then, after cooling down at room temperature, the pulp suspension has been centrifuged for 15 min at 5000 rpm to collect the supernatant (pale yellow coloured). Then the pulp extract has been filtered well using Whatman No. 1 filter paper to eliminate the impurities. The final extract has been stored in the freezer at 4°C for further experiments.

3.2.1.2 From Cumin (*Cuminum cyminum*) Seeds

Dried cumin (*Cuminum cyminum*) seed powder has been purchased from the local spice shops (Figure 3.2). About 10 gm of powdered cumin seed has been added in 100 ml of ultra-purified water and subsequently, for 20 minutes, the solution has been placed into an ultrasonic bath at 70°C for heating. After cooling down at room temperature, the resulting suspension has been centrifuged for 15 min at 5000 rpm. After centrifuge, a visible yellowish-brown coloured supernatant has been collected and filtered well using Whatman No. 1 filter paper to remove the stringy discarded particles. Lastly, the final cumin seed extract has been stored in the freezer at 4°C for further experiments
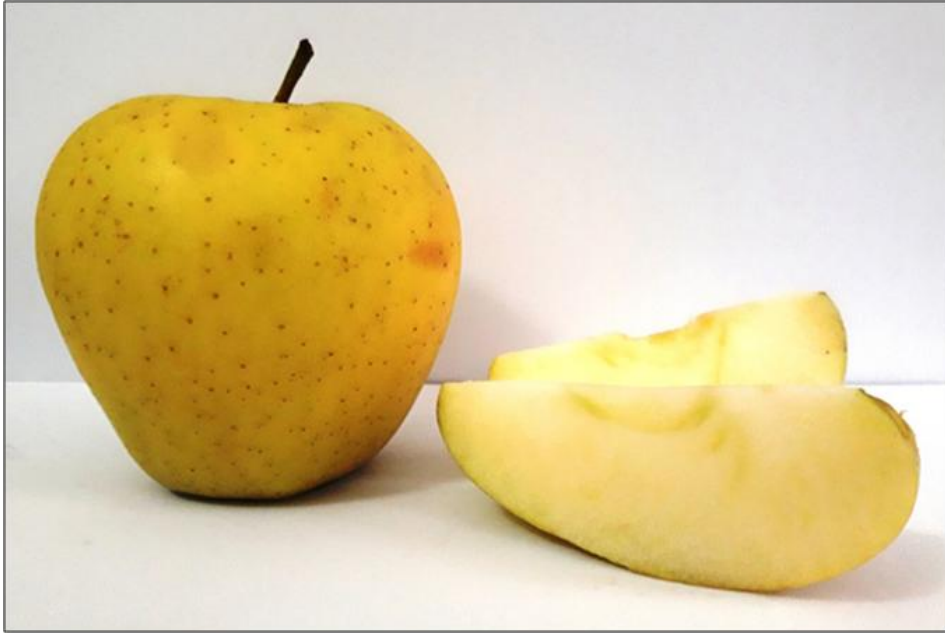
Figure 3.1 Yellow delicious apple (*Malus pumila*).

Figure 3.2 Cumin (*Cuminum cyminum*) seed powder.

3.2.1.3 From Fresh Ginger (*Zingiber officinale*) Rhizome

Fresh ginger (*Zingiber officinale*) rhizomes have been collected from the local market (Figure 3.3). 100 gm of fresh rhizomes have been washed separately and properly with running tap water to eliminate the unwanted dust particles and again, washed several times thoroughly with ultra-purified water. Using a sterilized kitchen paring knife, the rhizomes have been peeled off and sliced into small pieces. Then, these ginger rhizome

pieces have been put into a food grade kitchen blender, ground well to make a paste. Afterwards, the paste has been transferred in a conical flask. 100 ml of ultra-purified water has been added into to flask and with a highest heating level of 700 W the mixture has been placed into a microwave (laboratory-grade) for irradiation approximately about 5 minutes to extract the biomolecules present in the mixture. Finally, the resulting suspension has been centrifuged for 10 min at 5000 rpm, after cooling, and afterwards, has collected the pale-yellow coloured supernatant. The ginger rhizome extract has been then filtered with Whatman No. 1filter paper to eliminate the fibrous impurities and stored at 4°C for further use.

Figure 3.3 Fresh ginger (*Zingiber officinale*) rhizome.

3.2.1.4 From Fresh Rose (*Rosa santana*) Flower Petals

Fresh rose (*Rosa santana*) flowers have been collected from the campus of Yildiz Technical University, Davudpasa, Istanbul, Turkey (Figure 3.4). 10 gm of dustless flower petals have been isolated and thoroughly, rinsed thrice with ultra-purified deionized water before processing, and after that, have been chopped into very small pieces using a sterilized kitchen paring knife. These chopped pieces have been then placed into a food grade kitchen blender, ground well with 50 mL of ultra-purified deionized water. The petal suspension has been then placed at 80°C of in an ultrasonic bath for heating for about 60 min. In the end, And then, after cooling down at room

temperature, the resulting suspension has been centrifuged for 10 min at 5000 rpm, collected the wine-red coloured supernatant. Afterwards, the collected supernatant has been filtered well by using Whatman No. 1filter paper to eliminate the unwanted large particles and stored in frezzer at 4°C for further use.

Figure 3.4 Rose (*Rosa santana*) flowers.

3.2.1.5 From Lemon (*Citrus limon*) Peel

Fresh lemon (*Citrus limon*) have been collected from the local market (Figure 3.5). Fruits have been thoroughly rinsed thrice, with ultra-purified deionized water to remove the dust particles. Then using a sterilized kitchen paring knife, the yellow coloured peel segments have been taken away from the lemon fruits and shortly after the cutting off, the peels have been chopped into small pieces. Around 5 gm of the sliced peels have been shifted into a conical flask. The shifting has been done as quickly as possible to diminish evaporation rates of the reagents like volatile oil, available in the lemon peel. 50 ml of ultra-purified deionized water has been added to peels and the aqueous mixture has been placed into the microwave (laboratory-grade) for heating for approximately 2 minutes with highest irradiation level of 700 W to extract the biomolecules. After cooling down, the solution has been filtered properly by

using Whatman No. 1 filter paper to eliminate the fibrous discarded particles. The aqueous extract has been then refrigerated at 4°C for further use.

Figure 3.5 Fresh lemon (*Citrus limon*).

3.2.1.6 From Orange (*Citrus sinensis*) Peel

Fresh orange (*Citrus sinensis*) have been collected from the local market (Figure 3.6). Fruits have been thoroughly rinsed thrice, with ultra-purified deionized water to remove the dust particles. Using a sterilized kitchen paring knife, the orange coloured peel segments have been cut away from the fruits and shortly after the cutting off, the peels have been chopped into small pieces. Around 5 grams of the sliced peels have been shifted into a conical flask. The shifting has been done as quickly as possible to diminish evaporation rates of the reagents like volatile oil, available in the orange peel. 50 ml of ultra-purified deionized water has been added to peels and the aqueous mixture has been placed into the microwave (laboratory-grade) for heating for approximately 2 minutes with highest irradiation level of 700 W to extract the biomolecules. After cooling down, the solution has been filtered properly by using Whatman No. 1 filter paper to eliminate the fibrous discarded particles. The aqueous extract has been then refrigerated at 4°C for further use.
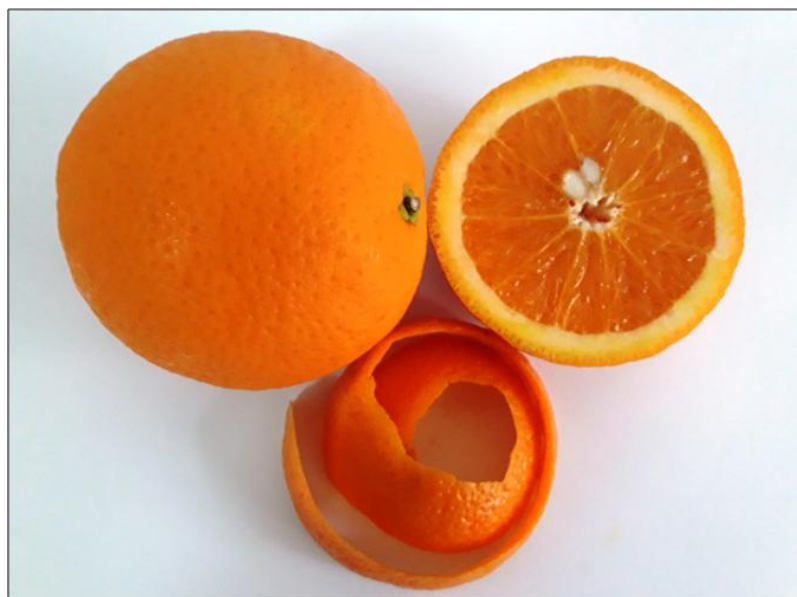
Figure 3.6 Fresh orange (*Citrus sinensis*).

3.2.1.7 From Orange (*Citrus sinensis*) Juice

The leftover peeled-off fresh orange fruits have been used to prepare juice extract. Using a sterilized kitchen paring knife, the peeled-off orange fruits have been sliced and then, squeezed properly to take out the juice. Afterwards, the squeezed orange juice has been centrifuged at 5000 rpm for 10 min to collect the supernatant. The aqueous solution of orange juice has then filtered well using Whatman No. 1filter paper. In a clean and dried vessel, the light-yellow coloured solution has been collected and stored at 4°C for further uses.

3.2.1.8 From Green Tea (*Camellia sinensis*)

Dried green tea (*Camellia sinensis*) leaves have been purchased from the local market (Figure 3.7). Using a 250 ml Erlenmeyer flask, 10 gm of dried leaves have been mixed well with 100 ml ultra-purified deionized water. On the electric heater, the mixture has been then placed for heating at 80°C for 20 min. A magnetic stirring bar has been used in the liquid for continuous spinning. After cooling down, the mixture has been filtered carefully by using Whatman No. 1 filter paper to remove unwanted large particles and stored at 4°C for further use.

Figure 3.7 Dried green tea (*Camellia sinensis*) leaves.

3.2.1.9 From Turkish Pine (*Pinus brutia*) Bark

The bark specimens of the *Pinus brutia* have been collected from the Yildiz Park, Besiktas, Istanbul, Turkey (Figure 3.8). The barks have been collected in the spring (in between April and May). The collected bark specimens have been thoroughly washed for several times with ultra-purified deionized water before processing. The rinsed barks have been dried at room temperature; put into a conventional food grade kitchen grinder and ground finely to get the powder form and then, stored in air-tight containers at 4°C for further use. In a 250 ml Erlenmeyer flask, 10 gm of bark powders has been mixed properly with 100 ml ultra-purified deionized water. At 80°C, the mixture has been placed on the electric heater for heating for about 30 min. A magnetic stirring bar has been used in the liquid for continuous spinning. After attaining the room temperature, by using Whatman No. 1 filter paper, the boiled solution has been filtered to obtain the aqueous pine bark extract, stored at 4°C and later, used for metallic nanoparticle productions.

Figure 3.8 Turkish pine (*Pinus brutia*).

3.2.2 Biosynthesis of Nanoparticles

In the present experiment, both silver and copper nanoparticles (AgNPs &CuNPs) have been fabricated by using the microwave irradiation in a single step, directed by means of the schemes of green chemistry. Different plant-based extracted stock solutions have been utilized within 1 week of preparation for the syntheses.

Moreover, the temperature, time range and other experimental parameters have been optimized and standardized after several trails. Each synthesis cycle using the following plant extracts has been repeated several times to establish the protocol and to achieve the desired amounts of NPs.

3.2.2.1 Biosynthesis of Silver Nanoparticles (AgNPs)

AgNPs have been fabricated from silver nitrate ($AgNO_3$) salt using apple (*Malus pumila*) pulp, cumin (*Cuminum cyminum*) seed, fresh ginger (*Zingiber officinale*) rhizome, rose (*Rosa santana*) petal, lemon (*Citrus limon*) and orange (*Citrus sinensis*) peel extracts.

The fabrications of AgNPs have been conducted separately for each plant extract. Syntheses of AgNPs have been started by integrating 0.017 g of silver nitrate ($AgNO_3$; 1mM) with 90ml of ultra-purified deionized water and 10 ml of each plant extract. With a magnetic stirring bar, the reaction mixtures have been placed into the microwave (laboratory-grade) for 25 minutes at a temperature of 90°C with a highest heating level of 300 W. The colour change in the synthesis medium has primarily indicated the production of AgNPs.

70

Following the successful finishing point of the phytosynthesis process, the synthesized samples have been filtered by means of Whatman Grade No.5 filter paper with 2.5μm pore size to eliminate large discarded particles in the sample solutions. At 4°C, the colloidal suspensions of the fabricated AgNPs have been centrifuged at 5000 rpm for 15 minutes and then, washed with ultra-purified water to eliminate unwanted plant extract residues. These centrifugation and washing steps have been repeated 3-4 times to get pure, plant-debris free precipitate of NPs. Finally, the purified AgNPs have been placed for drying process under vacuum condition and stocked in dark coloured vials and stored at 4°C for further experiments.

3.2.2.2 Biosynthesis of Copper Nanoparticles (CuNPs)

For copper nanoparticles synthesis, copper sulphate pentahydrate ($CuSO_4.5H_2O$) salt has been used as basic precursors whereas different concentrations of plant extracts from fresh ginger (*Zingiber officinale*) rhizome, green tea (*Camellia sinensis*), orange (*Citrus sinensis*) juice and Turkish pine (*Pinus brutia*) bark have been played as reducing, synthesizing and stabilizing factors. Depends on the plant types, the fabrication process were slightly different.

To synthesize CuNPs by utilizing orange juice extract, 1mM of copper (II) sulphate pentahydrate ($CuSO_4.5H_2O$) aqueous solution has been prepared using ultra purified deionized water. Afterward, 1mM copper sulphate solution and orange juice extract has been acquired in 1:2 ratios and the solution has been adjusted to microwave irradiation at 700 W for 5 minutes, then, stirred up properly and again, has been placed to microwave irradiation system for 10 min with continuous stirring by magnetic stirrers. The formation of dark blackish brown colloid in the reaction mixture has indicated the copper nanoparticles creation and the completion of the reaction.

On the other hand, for the fabrication of CuNPs using ginger rhizome extract, 75 ml of the freshly acquired ginger rhizome extract has been mixed up with 100 ml of the freshly prepared 1mM $CuSO_4.5H_2O$ solution. Then, for 2 minutes, the mixture has been subjected to the microwave system at 700 W. Afterward, 5 ml of 10% L-ascorbic acid solution has been stirred up properly with the mixture and then again, placed into microwave heating with continuous stirring by magnetic stirrers for 15 min until dark blackish brown colloid has been formed which has indicated the copper nanoparticles formation and the completion of the reaction.

In case of CuNPs production by using green tea and Turkish pine bark extract, 50 ml of the fresh plant extracts have been added to 50 ml of the freshly prepared 1mM $CuSO_4.5H_2O$ solutions. Then, for 2 minutes, the mixture has been subjected to microwave system at 700 W. Afterward, 5 ml of 10% L-ascorbic acid solution has been stirred up properly with the mixture and then again, placed into microwave heating with continuous stirring by magnetic stirrers for15 min until dark blackish brown colloid has been formed which has indicated the copper nanoparticles formation and the completion of the reaction.

Following the successful finishing point of the phytosynthesis process, the synthesized CuNPs samples have been filtered by means of Whatman Grade No.5 filter paper with 2.5μm pore size to eliminate large discarded particles in the sample solutions. At 4°C, the colloidal suspensions of the fabricated CuNPs have been centrifuged at 5000 rpm for 15 minutes and then, washed with ultra-purified water to eliminate unwanted plant extract residues. These centrifugation and washing steps have been repeated 3-4 times to get pure, plant-debris free precipitate of NPs. Finally, the purified CuNPs have been placed for drying process under vacuum condition and stocked in a dark coloured vials and stored at 4°C for further experiments.

To produce CuNPs by using ginger rhizome, green tea and Turkish pine bark extracts, plant extracts have played the role as stabilizer and reducing agent while L-ascorbic acid at low concentration has worked as an anti-oxidant agent. It is well known that orange juice is rich of vitamin C which is the substitute of ascorbic acid (AA) and therefore, no additional L-ascorbic acid solution has been needed to add for CuNPs synthesis [262].

3.2.3 Methods of Characterization

3.2.3.1 UV-Vis Spectrophotometer Analysis

To monitor the completion of bioreduction of metal ions, the optical properties of phytosynthesized silver and copper nanoparticles have been monitored by using UV-vis spectrophotometer (Shimadzu UV-1700 double beam scanning UV-vis spectrophotometer). For the documentation of UV-vis Spectroscopic outcomes, about 1 cm path length UV-vis quartz cell has been employed, and the spectra have been collected over a range of 300 - 800 nm. For preparing the sample for UV- vis analysis,

1 ml of solution containing synthesized NPs have been diluted with 2 ml of ultra-purified deionized water, with the aim of normalizing absorbance to approximately 2 AU and subsequent scan in UV-visible (vis) spectra. Ultra-purified deionized water has been utilized as the blank and the spectra have been taken shortly after the completion of the syntheses.

3.2.3.2 X-ray Diffraction (XRD) Study

The composition of obtained silver and copper nanoparticles using various plant extracts have been examined through an X-ray diffraction scheme (PANalytical Empyrean model) with CuKα radiation (k-1.54 A). The XRD patterns of metallic silver and copper NPs have been calculated with a step size of 0.02 over the range of 2h from 10° to 90°. The Origin 8.5 software has been used to regenerate the XRD graphs.

3.2.3.3 Fourier Transform Infrared (FTIR) Spectroscopic Studies

The specifications and identifications of biomolecules of plant extracts which might reduce and stabilize the phytosynthesized nanoparticles are most important characterization criteria. These biomolecules along with their functional groups also remain attached with the NPs; hence, the presence of these influential functional groups has been studied by using FTIR spectrometer. For silver nanoparticles, IR spectroscopic measurements have been conducted by Attenuated Total Reflection (ATR) method via Shimadzu IR Prestige-21 FTIR-ATR instrument in the 600–4000 cm^{-1} range. On the contrary, FTIR investigations of the dried CuNPs have been conducted with the potassium bromide (KBr) pellet (FTIR grade) method. The powdered CuNPs and KBr have been acquired in 1:50 ratio and IR absorption spectra have been recorded in the wave range between 400 cm^{-1} and 4000 cm^{-1} with the help of the instrument Jasco FT/ IR-6300 Fourier transform infrared spectrometer (JASCO, Tokyo, Japan).

3.2.3.4 Transmission Electron Microscopy (TEM)

The morphology of both silver and copper nanoparticles has been revealed by using the transmission electron microscopy (TEM) that has been conducted at an increased speed voltage of 120 kV. Designed for TEM analysis experiments, small amount of nanoparticle suspensions have been placed drop by drop on the copper grids. For better

adjustment during the specimens' preparation, extra solutions have been eliminated with clean blotting paper, and then kept for drying at room temperature for 30-45 minutes. After drying, the specimens have been handled for TEM imaging. Additionally, in some cases, the width of size distribution of the phytosynthesized NPs has been determined by measuring the randomly selected particles from TEM micrographs using J image software.

3.2.3.5 Size Distribution and Zeta Potential Analysis

A zeta analyzer has been employed for determining the polydispersity, size distribution and zeta potential of both copper and silver nanoparticles. All phytosynthesized powdered samples have been dispersed in ultra-purified deionized water, subsequently for ultra-sonication in ultra-sonic bath for 15 min at 30°C. After getting homogenous solution, the suspensions have been filtered by means of 2.5µm pore sized Whatman Filter Paper Grade No.5 to remove large aggregated particles. The filtered solutions have been diluted for 3 to 4 times by ultra-purified water and the particle distributions in liquors have been studied in a computer-controlled particle/zeta analyzer.

3.2.4 Antibacterial Activity Study

The antibacterial potentials of phytosynthesized AgNPs and CuNPs have been experimented against both Gram-negative (*Escherichia coli*) and Gram-positive (*Staphylococcus aureus*) bacteria through agar well diffusion method. For the experiment, under mentioned steps have been pursued-

3.2.4.1 Preparation of Nutrient Media and Chemical Solutions

• Nutrient Agar Medium

Nutrient Agar is a wide-ranging and well-designed nutrient medium that contains many nutrients needed for the microbial growth and used for the cultivation and maintenance of a wide range of non-fastidious microbes in addition to enumeration of microorganisms in sewage, dairy products, water and other materials [263]. The cream to yellow homogeneous free flowing nutrient agar powder contains the following components (Table 3.3)

Table 3.3 Chemical compositions of nutrient agar powdered medium [264].

Ingredients	Amounts (gm/L)
Peptone	5.0 gm
Sodium chloride	5.0 gm
Beef extract/ yeast extract	1.5 gm
HM peptone B#	1.5 gm
Agar	15.0 gm

The medium has been prepared by placing 28 grams of the dehydrated agar powder into 1 litter of ultra-purified water. Then, to dissolve all components, the nutrient containing mixture has been placed for heating with continuous stirring. Afterwards, the medium has been brought to the boiling point for one minute to dissolve entirely. At room temperature by using 1N NaOH, the pH has been adjusted to 6.8 ± 0.2. After that, for 15 minutes, the medium has been autoclaved at 121°C with 15 lbs pressure to complete the sterilization. Afterward, it has been cooled to around 45-50°C (122 °F). Then, in an aseptic condition, the warm medium has been poured into Petri dishes and then, as soon as possible, the medium containing Petri dishes have been covered instantly. Until the solidification of agar medium, the plates have been left on the sterile surface and afterwards, these plates have been stored upside down and have been refrigerated until used.

- **Mueller Hinton Broth (MHB)**

Mueller Hinton broth is a fluid medium that is utilized particularly for the growth and cultivation of microorganisms. It can also be applied for preparing dilutions of microorganisms for antibacterial tests [265]. In this experiment, Hinton broth (MHB; BD, Auckland, New Zealand) powdered media was used that contains the following ingredients (Table 3.4)

Table 3.4 Chemical compositions of Hinton broth powdered medium [266].

Ingredients	Amounts (gm/L)
Beef extract (infusion from)	2.0 gm
Casein acid hydrolysate	17.5 gm
starch	1.5 gm

Mueller Hinton broth medium has been prepared by suspending powdered medium (21 gm) into one litter (1000 ml) of distilled water. The continuous shaking has been done to mix the powder well and has been heated with frequent agitation to dissolve properly. The medium has been then boiled for one minute for complete dissolution. The pH has been adjusted at 7.3 ± 0.1 at room temperature using 1N NaOH. Then the media has been dispensed into appropriate containers or test tubes that have been autoclaved at 121°C with 15 lbs pressure for 15 minutes to complete the sterilization. And lastly, after allowing for cooling to room temperature, the containers with broth media have been stored at 2-8 ℃ for further use.

- **Mueller Hinton Agar (MHA)**

Mueller Hinton Agar is the same formulation of Mueller Hinton broth, with the added agar. It has become the ideal medium for microbial studies specially for antimicrobial susceptibility testing. For agar well diffusion assay, powdered Mueller Hinton agar (MHA, Lab M, UK) medium has been utilized that contains the following ingredients (Table 3.5).

Table 3.5 Chemical compositions of Mueller Hinton agar medium [266].

Ingredients	Amounts (gm/L)
beef extract, infusion from	2.0 gm
casein hydrolysate	17.5 gm
starch	1.5 gm
agar	17.0 gm

Mueller Hinton agar medium has been prepared by mixing 38 gm of the powdered medium with one litter (1000 ml) of ultra-purified deionized water. The continuous shaking has been done to mix the powder well and heated with frequent agitation to dissolve properly. It has been then boiled for one minute for complete dissolution. The pH has been adjusted at 7.3 ± 0.1 at room temperature using 1N NaOH. After that, for 15 minutes, the medium has been autoclaved at 121°C with 15 lbs pressure to complete the sterilization. Afterward, it has been cooled to around 45-50°C (122 °F). Afterward, it has been cooled to around 45-50°C (122 °F). Then, in an aseptic condition, the warm medium has been poured into Petri dishes and then, as soon as possible, the medium containing Petri dishes have been covered instantly. Until the solidification of agar medium, the plates have been left on the sterile surface. Finally, after allowing for cooling to room temperature, the dishes with solidified agar have been stored upside down and are refrigerated (at 2-8 ºC) until used for the antibacterial test.

- **Preparation of Barium Chloride Dehydrate (BaCl$_2$.2H$_2$O), 1.175% (wt/vol)**

1.175 g of BaCl$_2$.2H$_2$O was weighted out and place into a 100ml volumetric flask. 50 ml of ultra-purified deionized water has been added within the flask and the continuous mixing has been done to dissolve the powder well. The mixture has been then adjusted to 100 ml by adding more ultra-purified deionized water that has been stored at 25°C for further use.

- **Preparation of Sulphuric Acid (H$_2$SO$_4$), 1% (vol/vol)**

90 ml of ultra-purified deionized water has been added into a 100ml volumetric flask. By using a 1.0 ml volumetric pipette 1.0 ml of concentrated sulphuric acid has been measured and added into the water. Then, the mixture has been adjusted to 100 ml by adding deionized water. Subsequently, the solution has been transferred to a screw-cap glass bottle and stored it at 25°C for further use.

- **McFarland Standard**

For standardizing microbial testing, McFarland standards have been utilized as a standard indication to adjust the estimated amount of bacterial in a liquid suspension. The McFarland Standard is used to compare the turbidity of the test suspension. It is a solution of a chemical mixture of specified amounts of sulphuric acid and barium

chloride that reacts together and forms a fine barium sulphate precipitate that origins turbidity in the solution. For this experiment, to prepare a 0.5 McFarland standard solution, 0.05 mL of 1.175% barium chloride dihydrate ($BaCl_2.2H_2O$) has been mixed with 9.95 mL of 1% sulphuric acid (H_2SO_4). This mixture can provide an optical density equivalent to the density of a bacterial suspension colony (1.5×10^8) forming units (CFU/ml) [267].

3.2.4.2 Culture Collection

Lyophilized cultures of *Staphylococcus aureus* (ATCC 25923) and *Escherichia coli* (ATCC 25922) bacteria have been supplied from Microbiologics Inc. (Saint Cloud, MN, USA). Nutrient agar medium has been utilized to grow, cultivate the bacteria as well as to sustain the bacterial strains.

3.2.4.3 Preparation of Inoculums

Each bacterial strain has been transferred from the stock cultures and has been inoculated into separate cation-adjusted Mueller Hinton broth media. At 37 °C, these broth media have been incubated for a period of 24 h. Autoclaved bacteriological loops have been used for bacterial inoculation. Well-developed and distinctively separated bacterial colonies have been used as inoculums.

3.2.4.4 Agar Well Diffusion Method

The antimicrobial performances of both AgNPs and CuNPs have been tested using agar well diffusion bioassay. After 24 hours of inoculation, freshly cultured bacterial suspensions have been compared and adjusted to 0.5 McFarland turbidity standard colony forming units (1.5×10^8, CFU/mL). This standardization procedure has been performed through evaluating the transparency of the lines on the Wickerham card in the presence of good lighting. Subsequently, several holes or wells with approximately 6 to 7 mm diameter have been made aseptically on each Muller–Hinton agar medium by using a sterile gel puncher. After that, the 100 µL of bacterial inoculums as suspension forms have been transferred to cation-adjusted autoclaved Mueller Hinton agar containing Petri dish. Using the sterile drigalski spatula, the plating has been performed through spreading the samples evenly over the upper surface of agar medium into the plates and by rotating the petridish underneath at the same time. Then,

these plates have been put on the sterile surface for air drying at room temperature. 5µg of each powdered nanoparticle samples have been suspended in 5 mL of ultra-purified deionized water. By using sterile syringe filters with a 0.22 µm pore size, the suspensions have been filtrated that applied as the working concentration. Afterward, using this micropipette, a volume of 50 µL of aliquot parts of nanoparticle solution of both AgNPs and CuNPs has been used to pour into every single well of the medium.

Later, the agar plates have been incubated at 37°C for a period of 24 h. After incubation, by using a calliper, the zones of inhibition have been calculated in diameter by millimetres (mm) which have been distinguished by the transparent regions around the wells. Throughout the course of these experiments, gentamicin (Oxoid, 10µg/sensidisc) has been used as reference antibacterial agents, respectively. Sterile double distilled water alone (20 µL) has been applied as negative control. The experimental bioassay has been repeated in triplicate to verify the obtained results.

3.2.5 Cytotoxicity Study of Biosynthesized Nanoparticles

The cytotoxic effects of phytosynthesized silver and copper NPs have been done by following the under mentioned steps-

3.2.5.1 Preparation of Chemical Solutions

• **Preparation of Phosphate-buffered Saline (PBS Buffer) Solution**

PBS is a buffer that is salty in nature, contains sodium chloride (NCl), sodium phosphate (Na_2HPO_4), potassium phosphate (KH_2PO_4) and potassium chloride (KCl).

For preparing 100 ml of PBS buffer solution, at first, 80 ml deionized ultra-purified water has been taken and then 0.8 gm of NaCl, 0.144 gm of Na_2HPO_4, 0.024 gm of KH_2PO_4 and 0.02 gm of KCl have been added, cautiously. Afterward, the chemical containing aqueous solution has been mixed well and fixed the pH at 7.4 by using HCl. In the end, the volume has been adjusted to 100 ml by adding ultra-purified deionized water. Then, the solution has been distributed into aliquots and sterilize through autoclaving at 121°C for 20 min (liquid cycle). Finally, it has been stored at room temperature for further use.

• Trypan Blue (0.4% TB) Solution Preparation

Trypan blue powder is soluble in water. Trypan blue solutions have been prepared in PBS buffer or phosphate buffered saline solution at the concentration of 0.4%.

Initially, 1gm trypan blue powder (40% dye content) has been weighted and added into 100 ml autoclaved PBS buffer solution. The mixture has been then put into a slow boil and dissolved completely by constant stirring. After cooling at room temperature, it has been filtered with 0.22 microns of pore sized sterile membrane filter to obtain desired 0.4% TB solution.

For testing cell viability and observing viable and nonviable cells, 10 μl of 0.4% trypan blue stock solution has been taken and diluted with 90 μl deionized sterile water which functioned as the counting solution. 98 μl of the counting solution and 2 μl of cell suspension have been mixed to give 100 ml of the mixture and examined instantly under a microscope at low magnification.

3.2.5.2 Cell Culture

A mouse fibroblast cell line (L929) has been used for *in-vitro* toxicity experiments. The cell line has been cultured in a DMEM-F12 medium supplemented with 5 ml 1% L-Glutamine, 2.5 ml 0.5% Penicillin-Streptomycin and 10% Fetal Bovine Serum. The culture has been incubated at 37°C (5% CO_2) and cell multiplication and proliferation has been daily observed. Fully confluent cells have been aseptically detached from surface of cell culture vessel via trypsinization (application of TB solution). Detached cells have been centrifuged at 5,000 rpm for 5 min and the supernatant have been removed and the cell number has been counted with Thoma slides using a hemocytometer by placing the cells suspension (50-100 cells per large square of the hemacytometer counting chamber) on the stage of an inverted microscope using the 10X objective.

3.2.5.3 *In-vitro* Cytotoxicity of Phytosynthesized Nanoparticles

The cultured L929 cells have been used for cytotoxicity experiments of green synthesized silver and copper nanoparticles. Cultured viable cells (10^4) have been seeded in every well of sterile 96-well flat bottom microplates. All nanoparticle samples have been added to cultured cells (n=5) at altered proportions (0.1 μg/mL, 0.25

μg/mL, 0.5 μg/mL 1μg/mL, 2.5μg/mL, and 5μg/mL). After exposing both AgNPs and CuNPs at different concentrations, the cultured cells have been incubated for 24 hours at 37°C (5% CO_2) and afterward, followed by the replacement of the medium with 100 ml fresh medium that contain 100μL of 2,3-Bis-(2-Methoxy-4-Nitro-5-Sulfophenyl)-2H-Tetrazolium-5-Carboxanilide (XTT) solution in DMEM (0.5 mg/ml concentration with 7.5 μg/mL Phenazine methosulfate). Again then, the suspension containing plates have been incubated for additional 4 h at 37°C. Lastly, after incubation, by means of a multiplate reader, the optical density of the cell suspensions has been measured at 450 nm.

The cell viability (%) has been calculated by using Equation 3.1 as follows:

$$\%\text{Cell viability} = \frac{\text{Optical density of sample}}{\text{Optical density of control}} \times 100 \qquad (3.1)$$

4.1 Synthesis and Characterization of Silver Nanoparticles

Freshly prepared plant based extracts have been used to create silver nanoparticles. When plant extracts had been mixed with silver nitrate ($AgNO_3$) salt solutions in desirable proportions, metal ions were reduced into metal nanoparticles. After syntheses, different characterization techniques have been used to evaluate the quantity and quality of phytosynthesized AgNPs.

4.1.1 Silver Nanoparticle Synthesis

Formation and fabrication of silver nanoparticles has been followed by an immediate colour alteration of the reaction after a certain time of period. Table 4.1 represents the initial colour changes of reaction mixture of silver nanoparticle synthesis using various plant materials.

Table 4.1 Colour changes of solutions during silver nanoparticle synthesis using different plant extract.

No.	Solution	Colour change		Colour intensity (AgNPs solution)
		Before synthesis	**After synthesis**	
1.	Yellow delicious apple (*Malus pumila*) pulp extract	Pale Yellow	Reddish brown	++
	1mM AgNO₃ solution	Colourless	**(Figure 4.1)**	

Table 4.1 Colour changes of solutions during silver nanoparticles synthesis using different plant extract (continued).

No.	Solution	Colour change		Colour intensity (AgNPs solution)
		Before synthesis	After synthesis	
2.	Cumin (*Cuminum cyminum*) seed extract	Light brown	Dark brown **(Figure 4.2)**	++
	1mM AgNO$_3$ solution	Colourless		
3.	Fresh ginger (*Zingiber officinale*) rhizome extract	Pale yellow	Dark yellowish brown **(Figure 4.3)**	+
	1mM AgNO$_3$ solution	Colourless		
4.	Rose (*Rosa santana)* petal extract	Wine red	Greenish Black **(Figure 4.4)**	+++
	1mM AgNO$_3$ solution	Colourless		
5.	Lemon *(Citrus limon)* peel extract	Yellow	Black **(Figure 4.5)**	+++
	1mM AgNO$_3$ solution	Colourless		
6.	Orange *(Citrus sinensis*) peel extract	Dark yellow	Black **(Figure 4.6)**	+++
	1mM AgNO$_3$ solution	Colourless		

Colour intensity/potency: Light colour: +, Dark colour: ++, Deep dark colour: +++

Figure 4.1 Photographic representation of silver nanoparticle synthesis. A. AgNO$_3$ solution; B. aqueous extract of yellow delicious apple pulp; C. green synthesized silver nanoparticles (MpAgNPs).
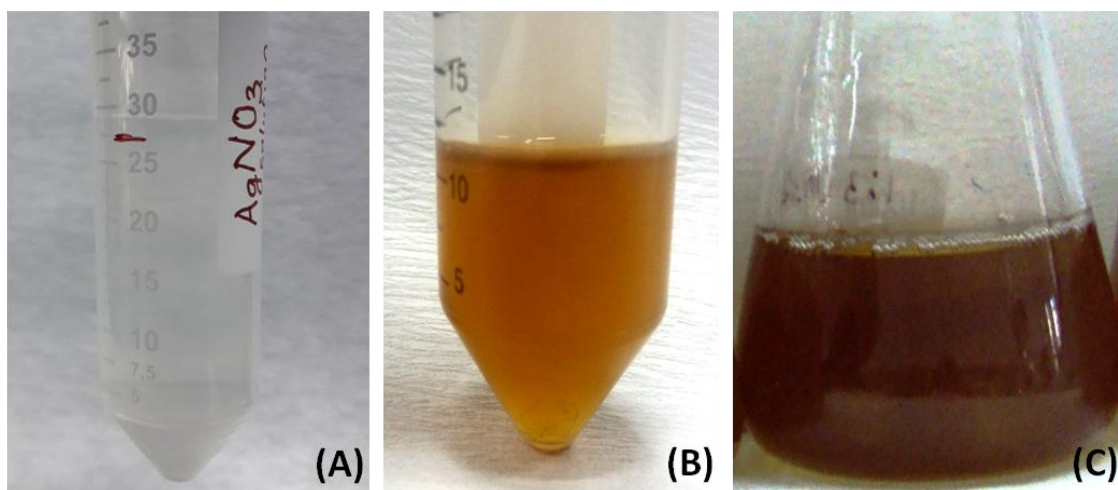
Figure 4.2 Photographic representation of silver nanoparticle synthesis. A. AgNO$_3$ solution; B. aqueous extract of cumin seed; C. green synthesized silver nanoparticles (CcAgNPs).
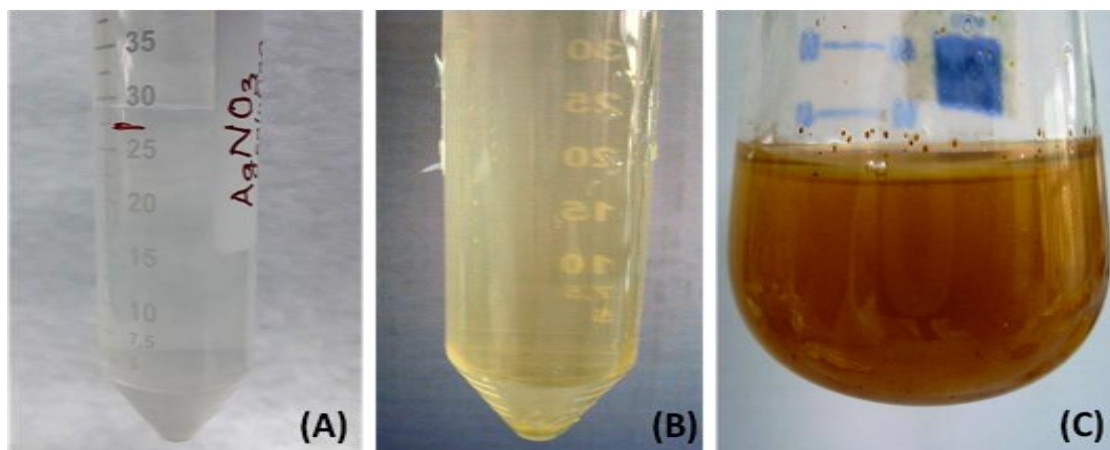
Figure 4.3 Photographic representation of silver nanoparticle synthesis. A. AgNO$_3$ solution; B. aqueous extract of fresh ginger rhizome; C. green synthesized silver nanoparticles (ZoAgNPs).
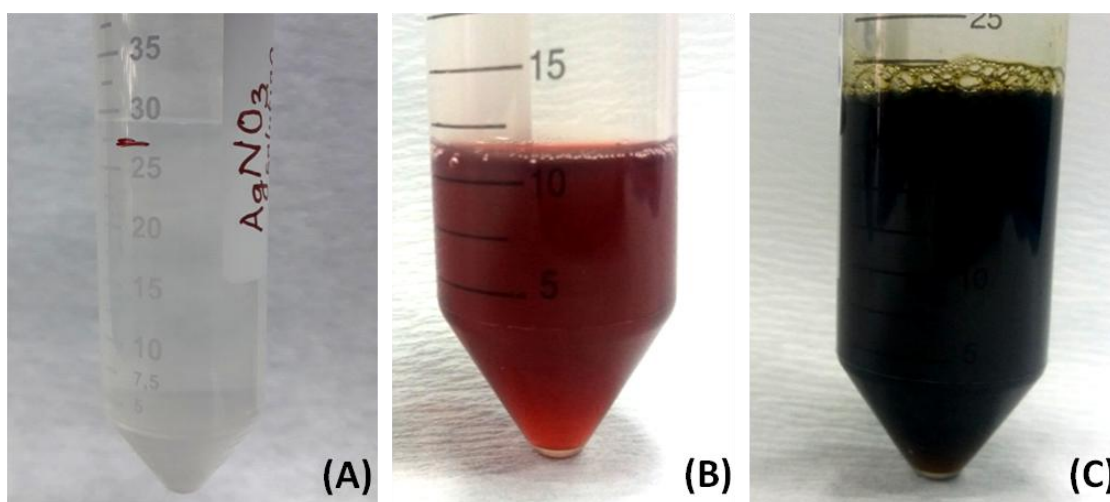
Figure 4.4 Photographic representation of silver nanoparticle synthesis. A. AgNO$_3$ solution; B. aqueous rose petal extract; C. green synthesized silver nanoparticles (RsAgNPs).
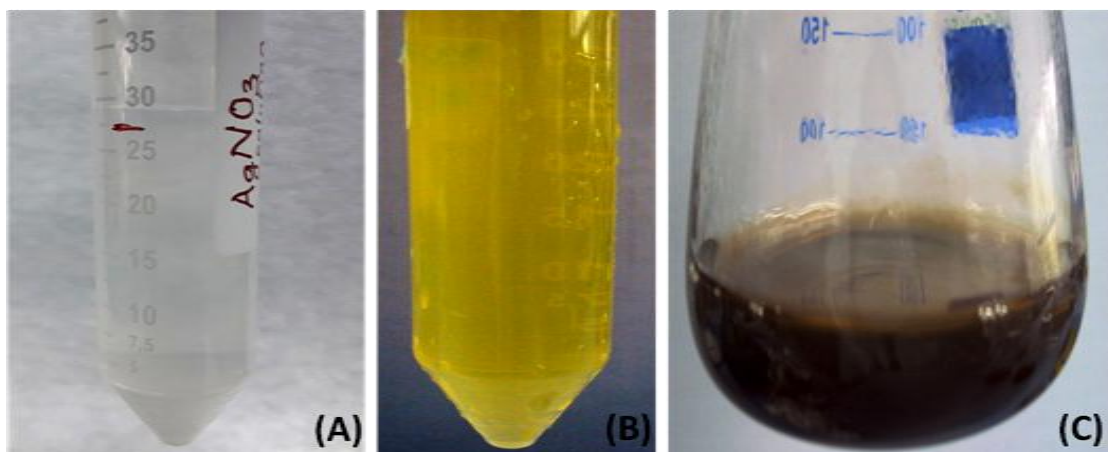
Figure 4.5 Photographic representation of silver nanoparticle synthesis. A. AgNO$_3$ solution; B. aqueous extract of lemon peel; C. green synthesized silver nanoparticles (ClAgNPs).
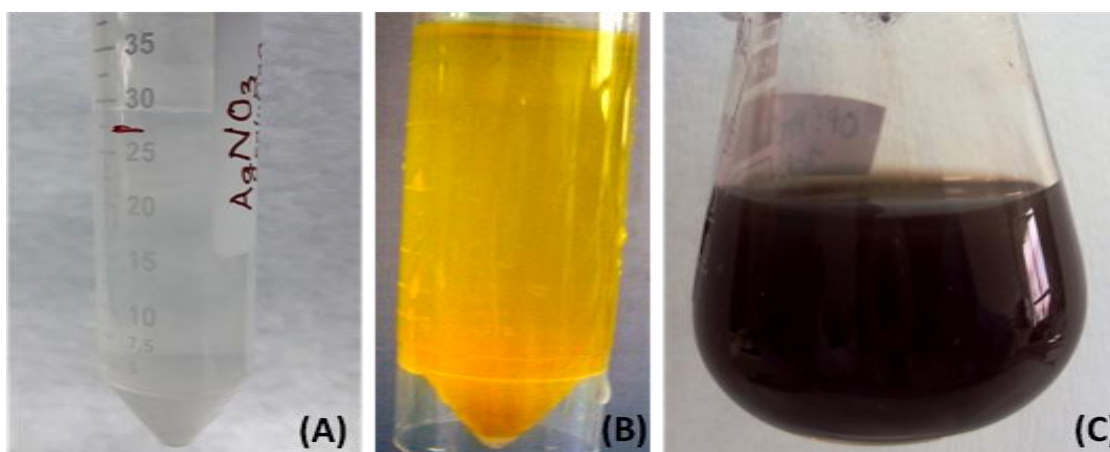
Figure 4.6 Photographic representation of silver nanoparticle synthesis. A. AgNO$_3$ solution; B. aqueous extract of orange peel; C. green synthesized silver nanoparticles (CsAgNPs).

4.1.2 Silver Nanoparticle Characterizations

4.1.2.1 UV-Visible Absorption Spectroscopic Study

The progress of formation of silver nanoparticles has been monitored by UV-Vis spectroscopy. It is an important and reliable process of investigation for the structural characterization of metallic NPs. The UV-Vis spectroscopy has been monitored the bio-reduction of silver ions in aqueous solutions and the recorded spectra have

confirmed the distinguishing Surface Plasmon Resonance (SPR) spectra with absorbance at 300 – 800 nm. The sharp peaks of silver nanoparticles have been observed at 440 nm, 439 nm and 441nm for yellow delicious apple pulp (MpAgNPs), cumin seed (CcAgNPs), fresh ginger rhizome (ZoAgNPs), respectively (Figure 4.7, Figure 4.8 & Figure 4.9) whereas in case of rose petal (RsAgNPs) the band has found at 438 nm (Figure 4.10) and for orange peel (CsAgNPs) the peak has showed at 435 nm (Figure 4.12). On the other hand, the spectrum in the Figure 4.11 of the ClAgNPs using lemon peel extract has provided the SPR band at 445 nm.
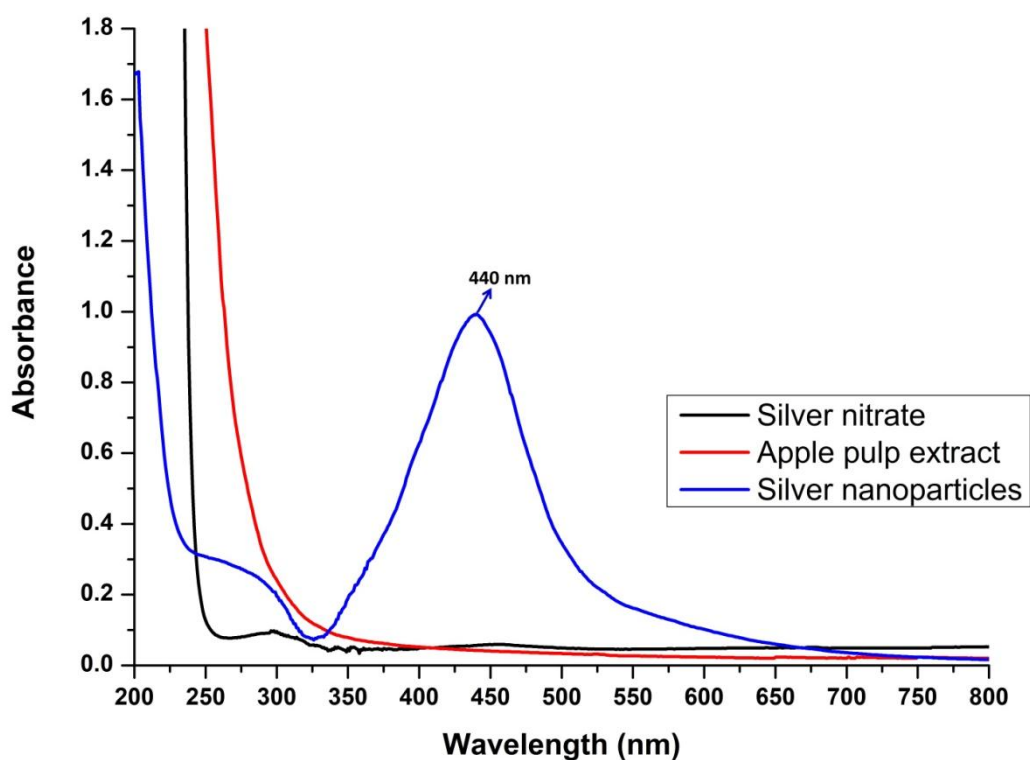
Figure 4.7 UV-visible absorbance maxima of biosynthesized MpAgNPs at 440 nm.
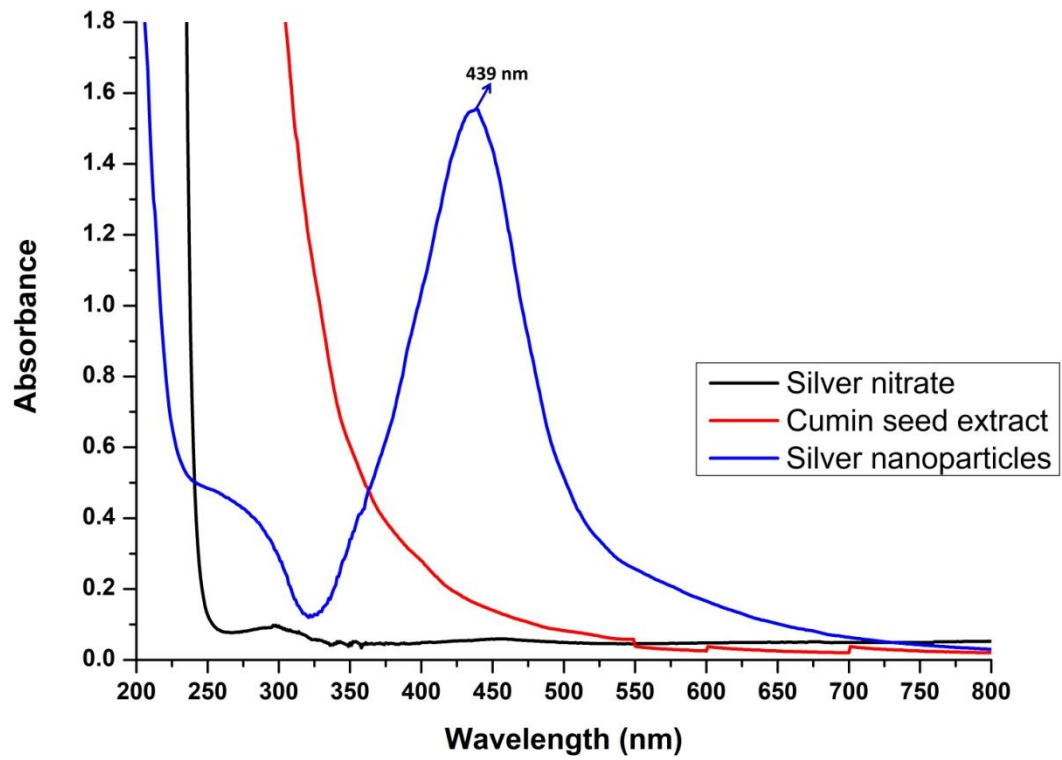
Figure 4.8 UV-visible absorbance maxima of biosynthesized CcAgNPs at 439 nm.
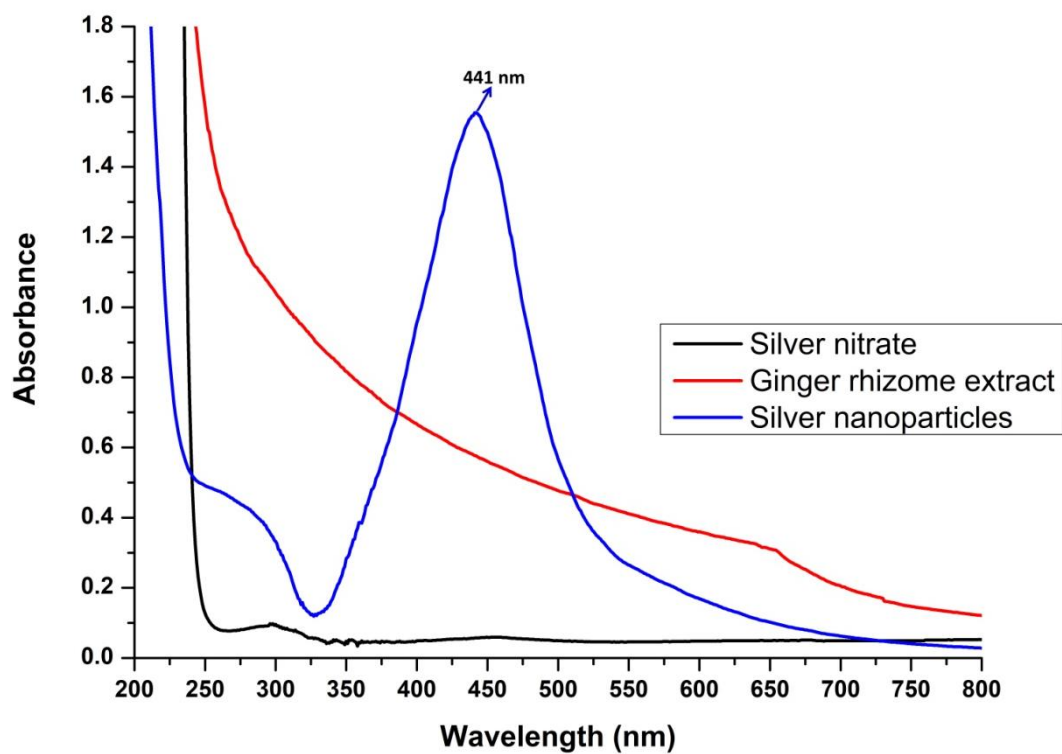
Figure 4.9 UV-visible absorbance maxima of biosynthesized ZoAgNPs at 441 nm.
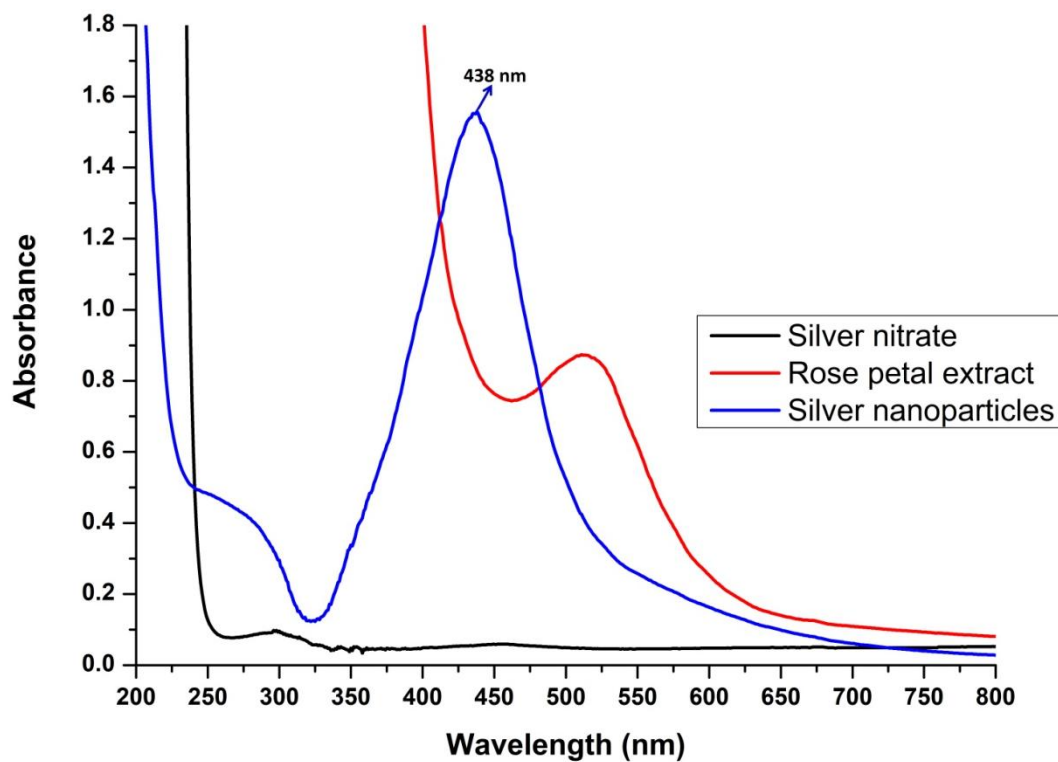
Figure 4.10 UV-visible absorbance maxima of biosynthesized RsAgNPs 438 nm.
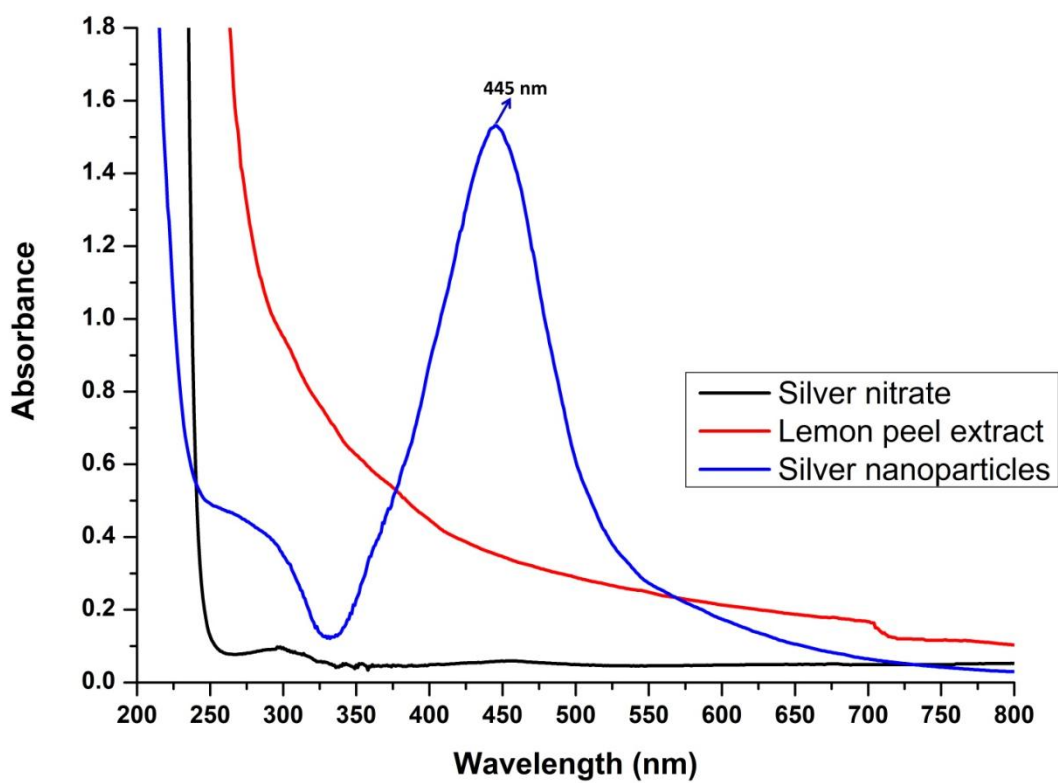
Figure 4.11 UV-visible absorbance maxima of biosynthesized ClAgNPs at 445 nm.
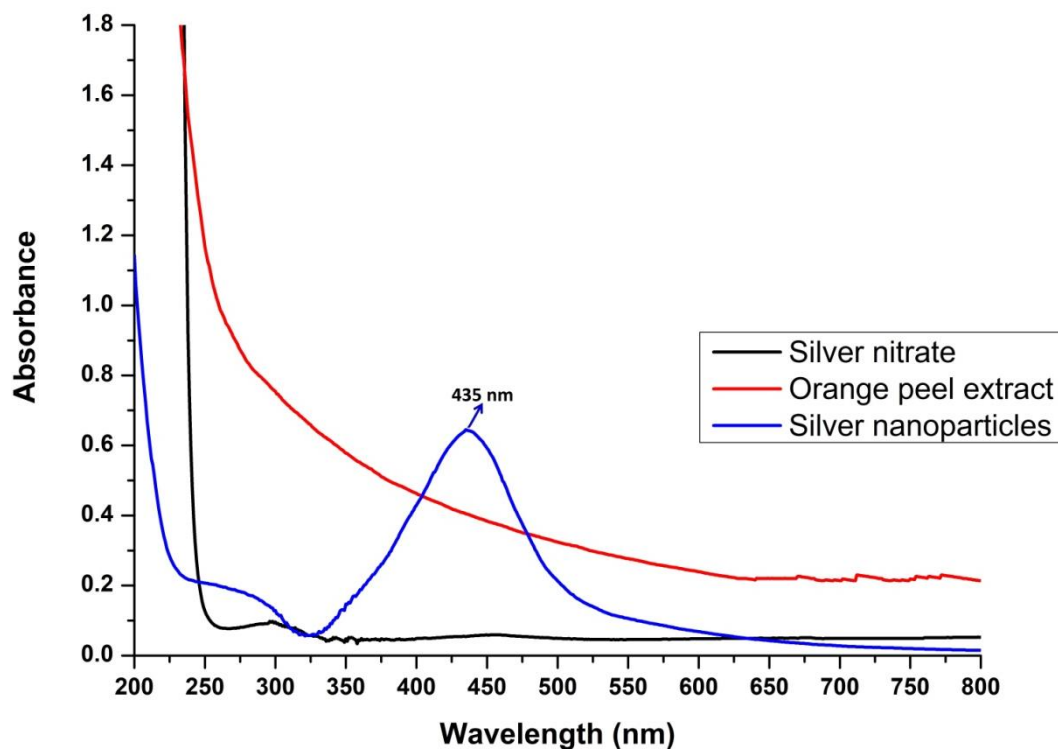
Figure 4.12 UV-visible absorbance maxima of biosynthesized CsAgNPs at 435 nm.

4.1.2.2 X-ray Diffraction (XRD) Study

To reveal the presence of crystallinity in the phytosynthesized AgNPs by using different plant extracts, X-ray diffraction (XRD) analysis has been conducted as a very important key instrument. The diffracted intensities were documented from 20° to 90°.

All silver nanoparticle samples have showed four strong reflections correspond to the planes of (111), (200), (220) and (311), respectively. These planes are the characteristic Bragg's diffraction plans for metallic silver with face-centered cubic crystalline structures which support or coordinate the database of the JCPDS (Joint Committee on Powder Diffraction Standards) file no: 04–0783 [268]. Moreover, details summary of XRD analysis of synthesized silver nanoparticle sample is describing below:

X-ray diffraction (XRD) graph of biosynthesized MpAgNPs by fresh yellow delicious apple (*Malus pumila*) pulp extract is illustrated in Figure 4.13. Strong peaks have been observed at 38.13°, 44.29°, 64.48° and 77.49° with the interplanar spacing ($d_{calculated}$) values are 2.360, 2.046, 1.446 and 1.230 Å.
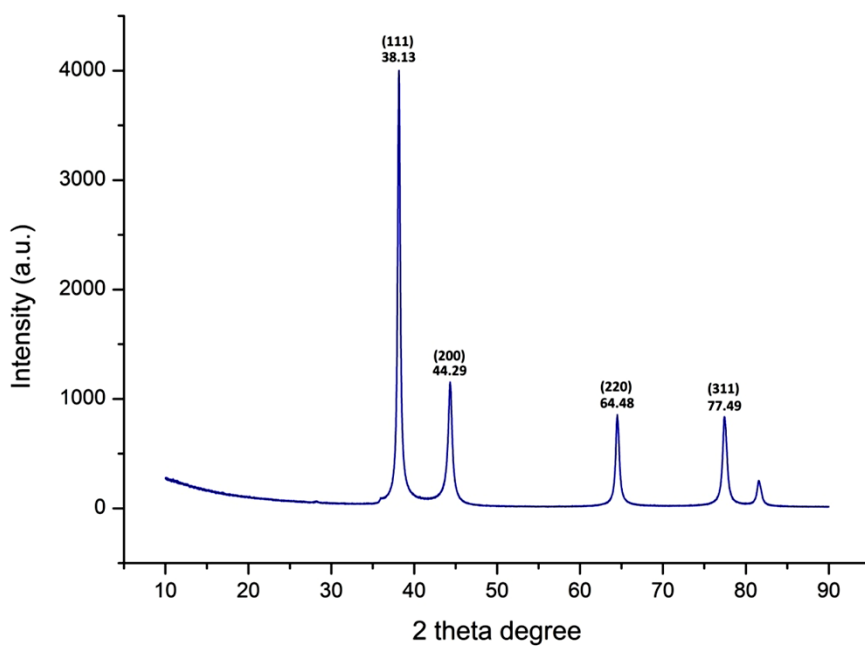
Figure 4.13 XRD pattern of biosynthesized MpAgNPs.

Figure 4.14 exhibits the XRD pattern of biosynthesized CcAgNPs using cumin (*Cuminum cyminum*) seeds extract. Strong peaks have been detected at 38.10°, 44.37°, 64.50° and 77.44° together with the interplanar spacing ($d_{calculated}$) values are 2.362, 2.043, 1.444 and 1.233 Å.
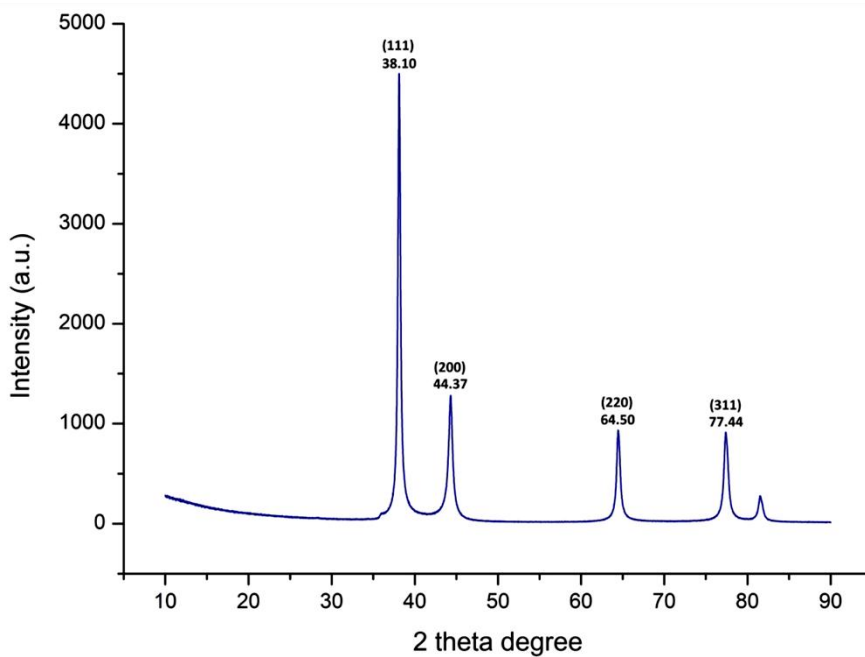
Figure 4.14 XRD pattern of biosynthesized CcAgNPs.

XRD outcomes of biosynthesized ZoAgNPs by fresh ginger (*Zingiber officinale*) rhizome extract is demonstrated in Figure 4.15. Significant peaks have been found at 38.13°, 44.31°, 64.55° and 77.51° along with the interplanar spacing ($d_{calculated}$) values of 2.360, 2.044, 1.443 and 1.231 Å.
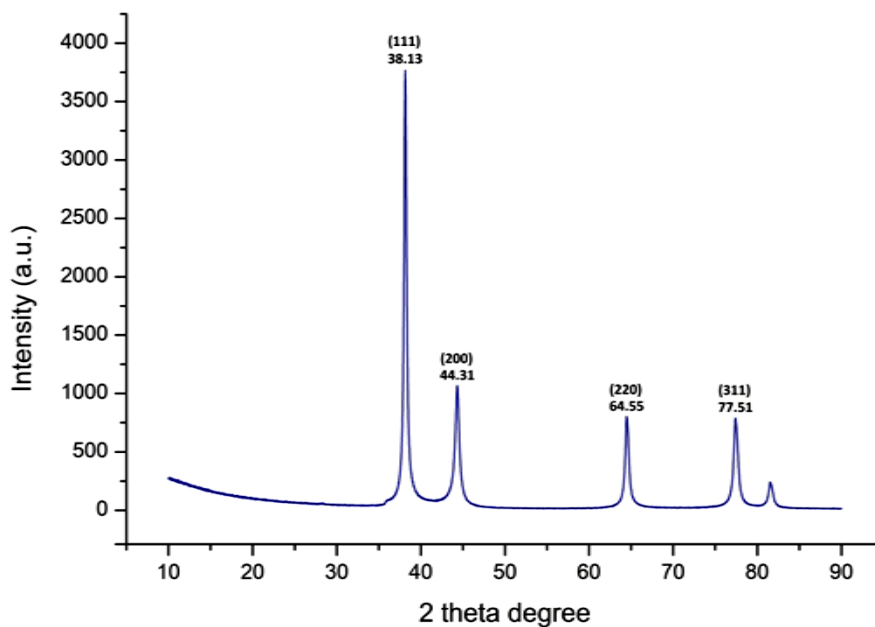
Figure 4.15 XRD pattern of biosynthesized ZoAgNPs.

XRD results of biosynthesized RsAgNPs by fresh rose (*Rosa santana*) petals extract is showed in Figure 4.16. Four strong reflections have been showed at 38.10°, 44.25°, 64.44° and 77.38° through the interplanar spacing ($d_{calculated}$) values are 2.361, 2.0461, 1.445 and 1.232 Å.
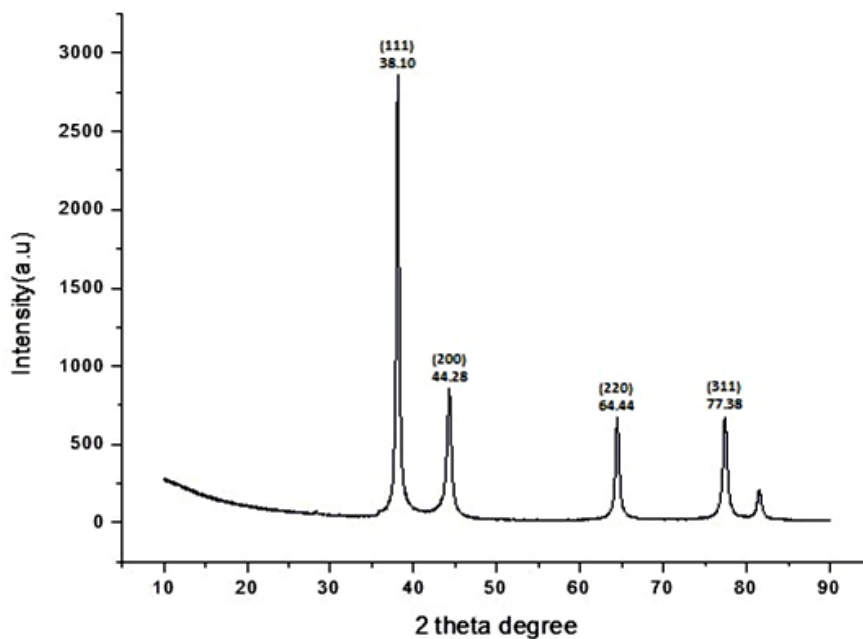
Figure 4.16 XRD pattern of biosynthesized RsAgNPs.

Figure 4.17 revealed the XRD outline of biosynthesized ClAgNPs using lemon (*Citrus limon*) peel extract. Four significant reflections have been observed at 38.11°, 44.30°, 64.54° and 77.50°. The interplanar spacing ($d_{calculated}$) values are 2.364, 2.046, 1.444 and 1.234 Å.
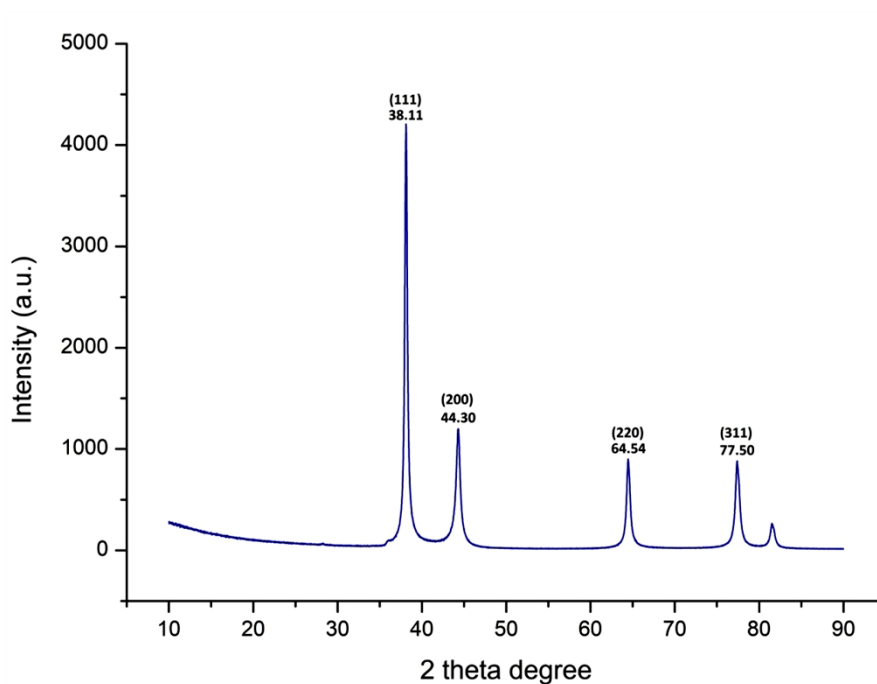
Figure 4.17 XRD pattern of biosynthesized ClAgNPs.

XRD analysis of biosynthesized CsAgNPs using orange (*Citrus sinensis*) peel extract is demonstrated in Figure 4.18. Diffraction peaks have been found at 38.14°, 44.32°, 64.46° and 77.51° together with the interplanar spacing ($d_{calculated}$) values are 2.359, 2.044, 1.440 and 1.231 Å.
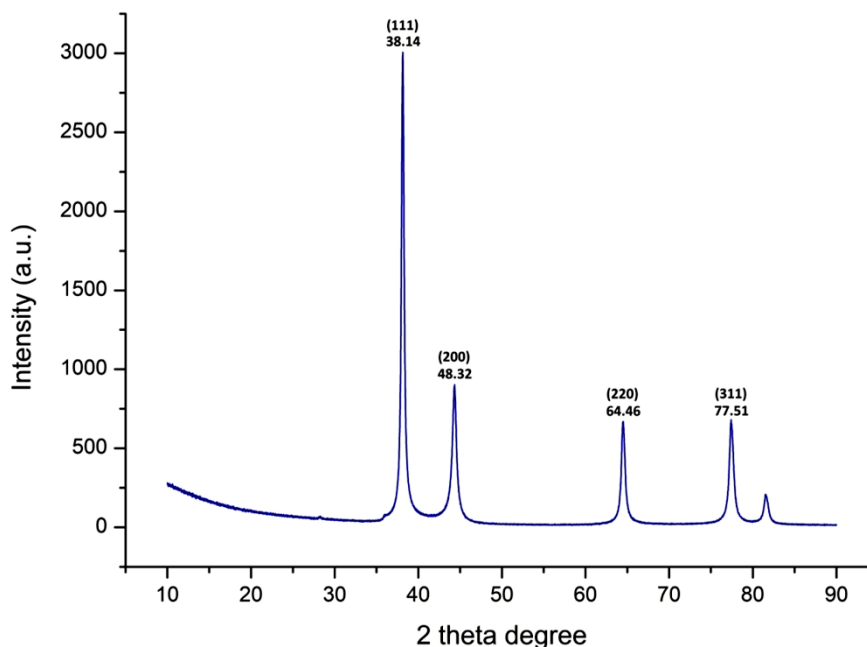
Figure 4.18 XRD pattern of biosynthesized CsAgNPs.

4.1.2.3 Fourier-Transform Infrared Spectroscopic (FTIR) Analysis

IR spectroscopic measurements of phytosynthesized metallic silver nanoparticle samples have been carried out to reveal the potential biomolecules available in yellow delicious apple (*Malus pumila*) pulp, cumin (*Cuminum cyminum*) seed, fresh ginger (*Zingiber officinale*) rhizome, fresh rose (*Rosa santana*) flower petal, lemon (*Citrus limon*) peel and orange (*Citrus sinensis*) peel extracts which might play significant roles as reducing, synthesizing, capping and stabilizing factors for AgNPs syntheses.

• FTIR Study of MpAgNPs Biosynthesized using Fresh Yellow Delicious Apple pulp extract

The FTIR spectrum of MpAgNPs (Figure 4.19) has illustrated the band at 3381.21 cm^{-1} corresponds to aliphatic primary amine stretching (N-H). The band that has found at 1641.42 cm^{-1}, responsible for strong alkene monosubstituted (C=C) bond; a strong C-O stretching primary alcohol bond shows the peak at 1055.06 cm^{-1}. The spectrum at

94

972.12 cm^{-1} represents a strong alkene disubstituted (trans) bond whereas the stretch of medium alkene (C=C) trisubstituted at 794.67 cm^{-1}.
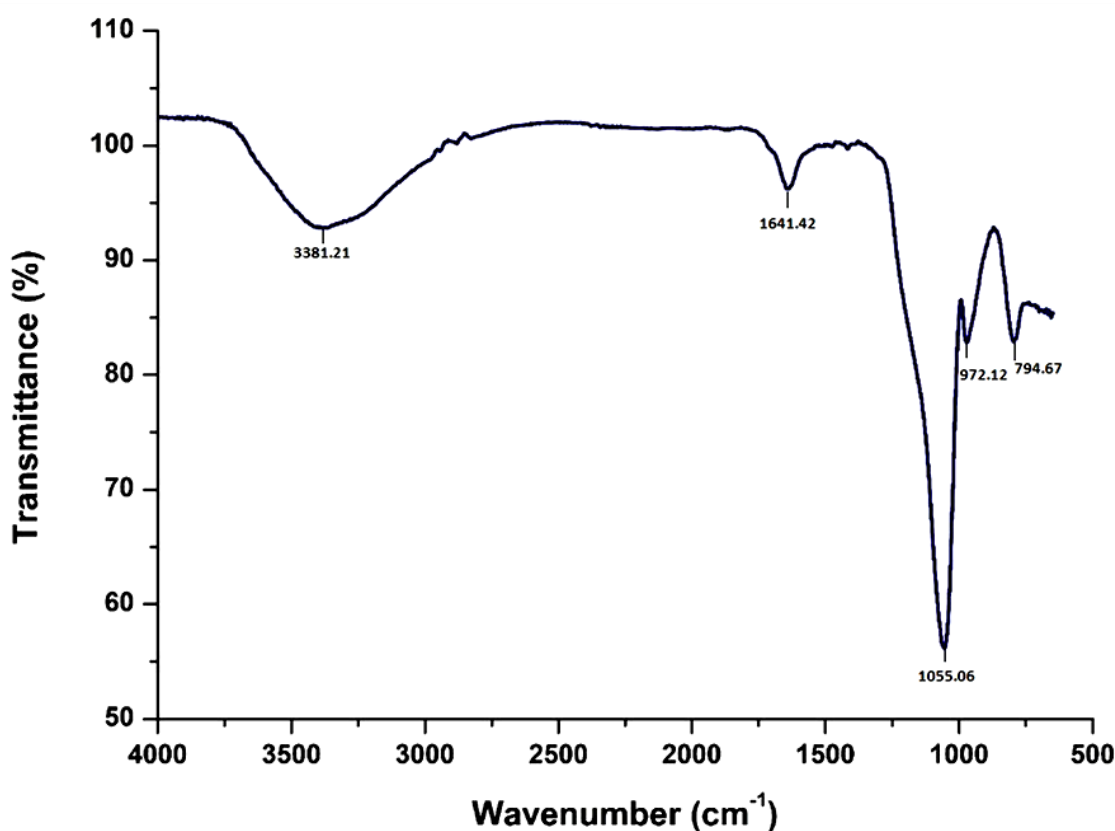
Figure 4.19 FTIR spectra of the synthesized MpAgNPs.

• **FTIR Study of CcAgNPs Biosynthesized using Cumin Seed Extract**

Figure 4.20 represents Fourier Transform Infrared (FTIR) spectrum of CcAgNPs. From the obtained data, an aliphatic primary amine (N-H) bond showes its meadium streating at 3373.50 cm^{-1}. The band at 1639.49 cm^{-1} indicates a strong alkene monosubstituted (C=C) stretching. The absorption peak at 1415.75 cm^{-1} could be identified as the -OH stretching of H$_2$O or ethanol present in the sample. The peak at 1058.92 cm^{-1} is due to the strong C-O stretching of primary alcohol vibration. The spectrum at 972.12 cm^{-1} represents a strong alkene disubstituted (trans) bond whereas the peak at 794.67 cm^{-1} is owing to the stretch of medium trisubstituted alkene (C=C) stretching and finally, 655 cm^{-1} is for strong C-Br stretching (halo compound).
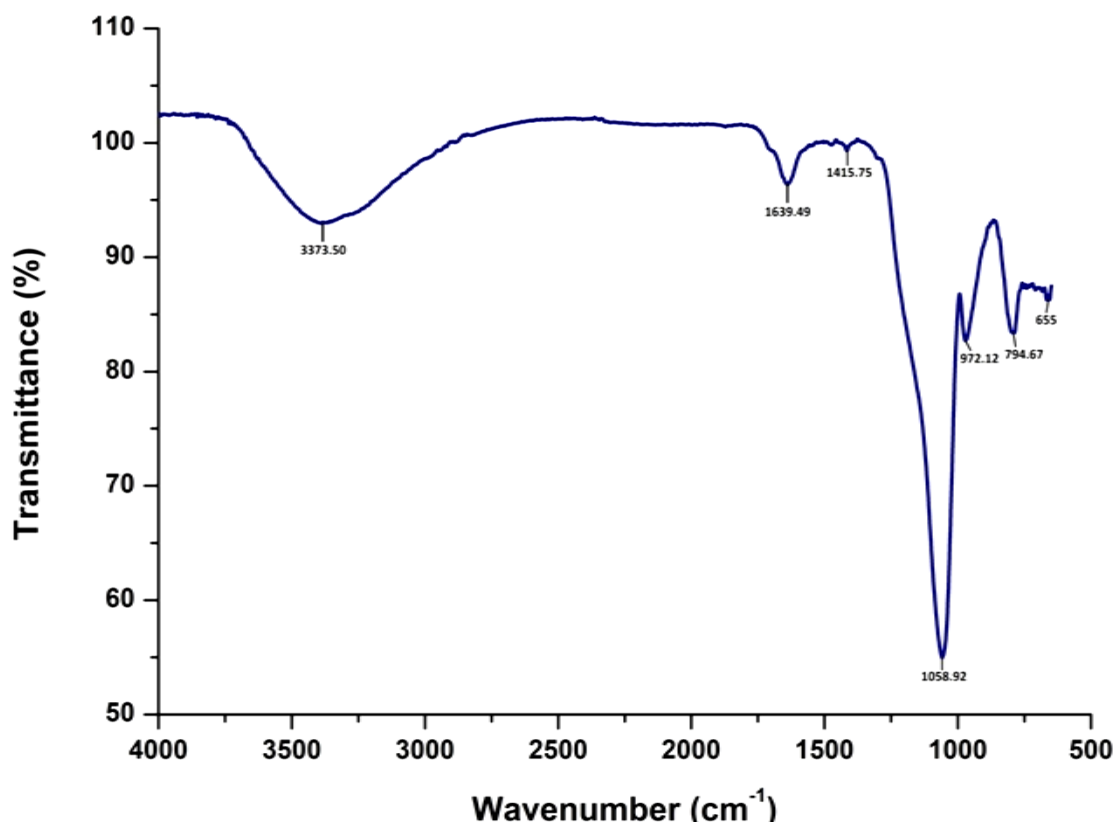
Figure 4.20 FTIR spectra of the synthesized CcAgNPs.

• **FTIR Study of ZoAgNPs Biosynthesized using Fresh Ginger Rhizome Extract**

The FTIR spectrum of ZoAgNPs (Figure 4.21) has demonstrated the band at 3365.78 cm^{-1} corresponds to aliphatic primary amine stretching (N-H). IR band has been detected mainly at 1637.56 cm^{-1} is responsible for strong alkene (C=C) monosubstituted stretching; whereas the spectrum at 1415.75 cm^{-1} could be identified as the -OH stretching of H_2O or ethanol present in the sample. A strong C-O stretching (primary alcohol) bond shows the peak at 1060.85 cm^{-1}. The peak at 966.34 cm^{-1} represents a strong alkene disubstituted (trans) bonds and finally, the stretch of medium alkene (C=C) trisubstituted at 800.86 cm^{-1}.

96
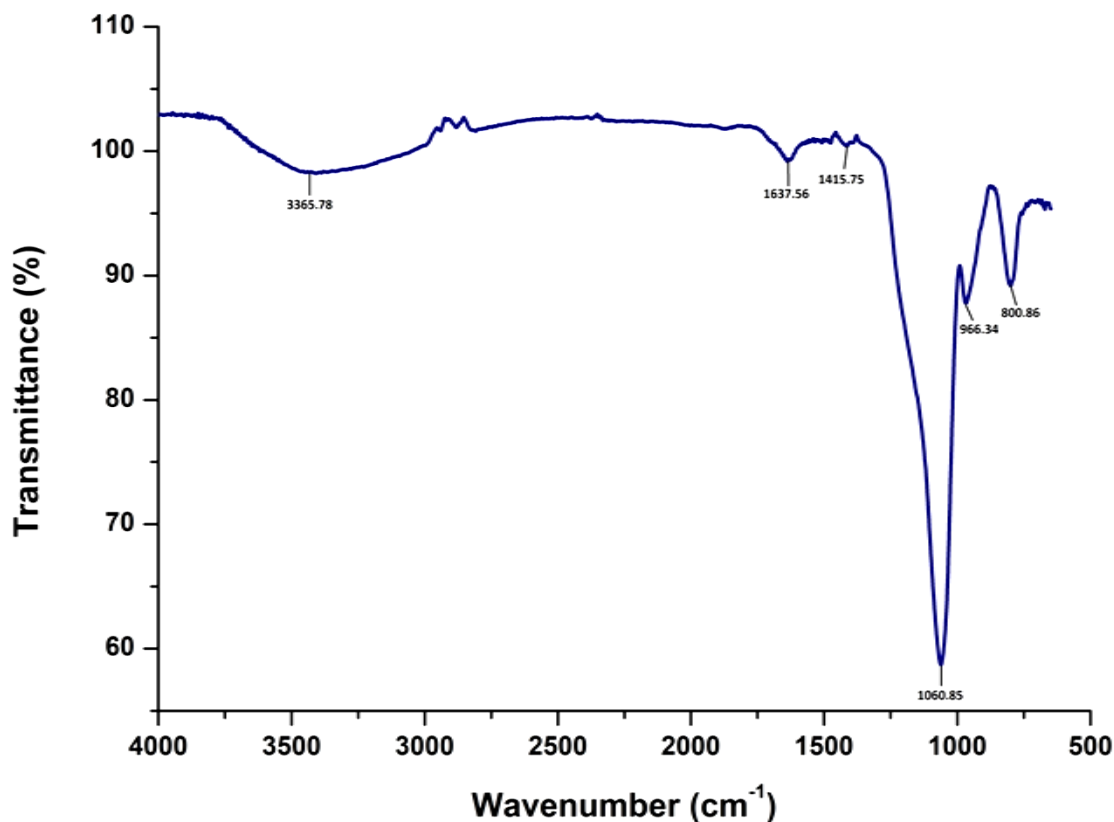
Figure 4.21 FTIR spectra of the synthesized ZoAgNPs.

• **FTIR Study of RsAgNPs Biosynthesized using Fresh Rose Petal Extract**

Figure 4.22 implies Fourier transform infrared (FTIR) spectrum of RsAgNPs. The band at 3446.79 cm^{-1} represents aliphatic primary amine stretching (N-H) bond. The spectrum at 2926.01 cm^{-1} is responsible for saturated alkane (-C-H) medium stretching and the spectrum at 1639.40 cm^{-1} could be allocated to the monosubstituted alkenyl (-C=C) strong bond. A strong stretching (C-O) of primary alcohol shows the peak at 1062.78 cm^{-1}. The band at 968.27 cm^{-1} represents a strong alkene disubstituted (trans) bonds; at 798.53 cm^{-1} is owing to -C=C alkenyl bond (trisubstituted) and ultimately, at 655 cm^{-1} is for strong C-Br stretching of halo compounds.
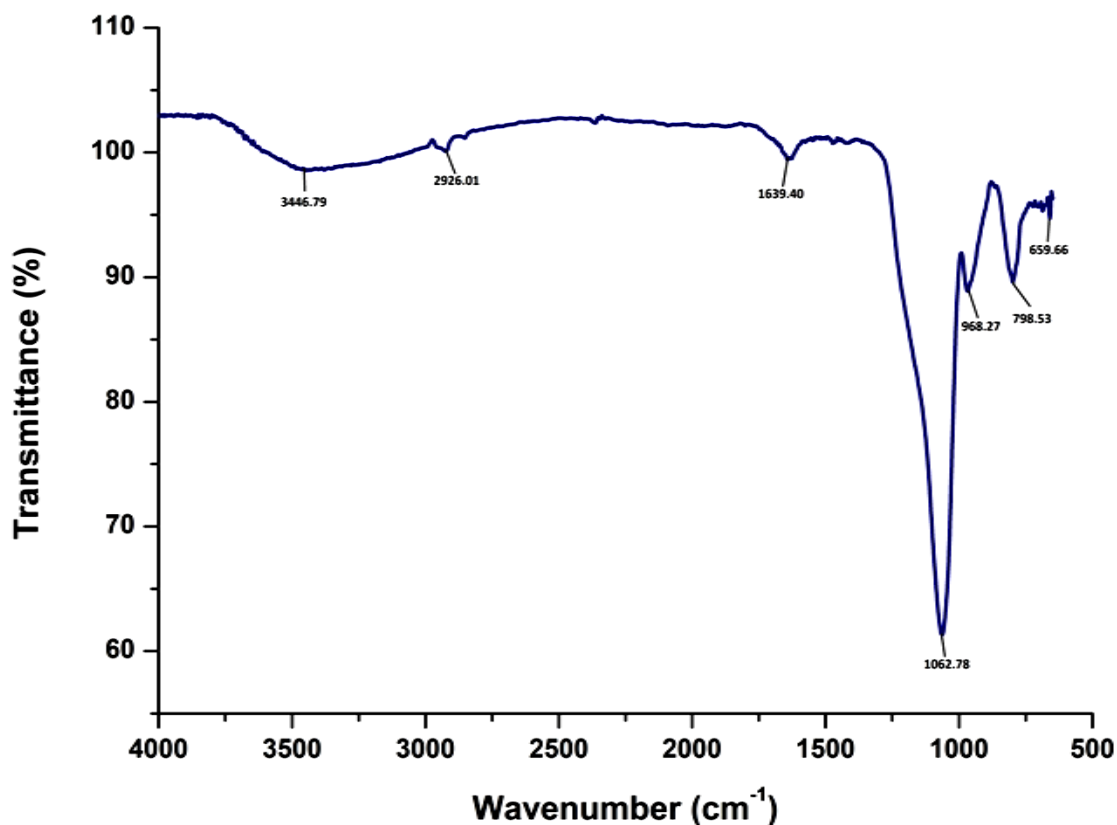
Figure 4.22 FTIR spectra of the synthesized RsAgNPs.

• **FTIR Study of ClAgNPs Biosynthesized using Lemon Peel Extract**

The FTIR spectrum of ClAgNPs (Figure 4.23) synthesized using lemon peel extract showed the band at 3392.79 cm^{-1} stands for the aliphatic primary amine bond (N-H). Peaks were observed mainly at 2926.01 cm^{-1} is responsible for saturated alkane (-C-H) medium stretching and the spectrum at 1641.42 cm^{-1} is responsible for strong alkene monosubstituted (C=C) stretching. A strong C-O stretching of primary alcohol bond represents at the peak of 1058.92 cm^{-1}; the spectrum at 974.05 cm^{-1} represents a strong alkene disubstituted (trans) bonds and finally, the peak at 786 cm^{-1} demonstrated medium alkene (C=C) trisubstituted bond.
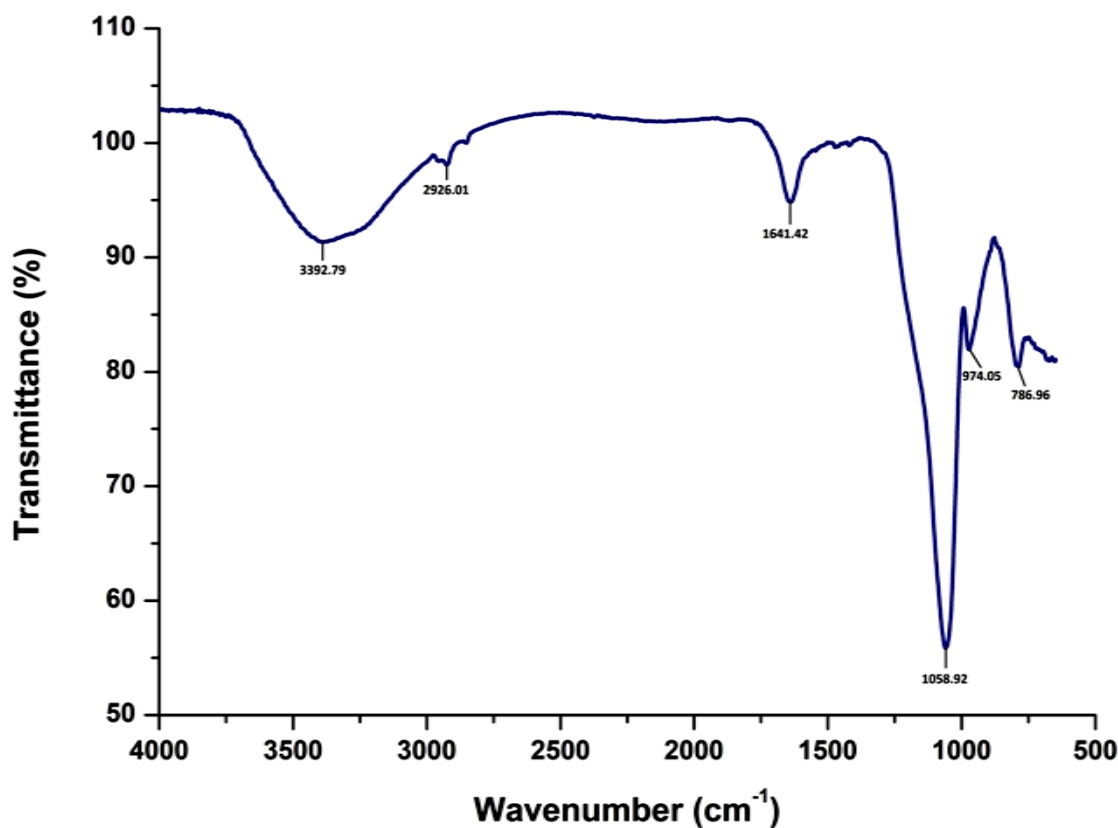
Figure 4.23 FTIR spectra of the synthesized of ClAgNPs.

• **FTIR Study of CsAgNPs Biosynthesized using Orange Peel Extract**

The FTIR procedure has been utilized to uncover the biomolecules along with their functional groups available in CsAgNPs (Figure 4.24). The bands at 3383.14 cm^{-1} stands for aliphatic primary amine (N-H) bond. Spectrum at 2931.80 cm^{-1} is responsible for saturated alkane (-C-H) medium stretching. The IR spectrum at 1639.49 cm^{-1} is because of strong alkene monosubstituted (C=C) stretching contrariwise a strong primary alcohol (C-O stretching) bond shows the peak at 1060.85 cm^{-1}. The spectrum at 970.19 cm^{-1} represents a strong alkene disubstituted (trans) bonds whereas the peak at 790.81 cm^{-1} is as a result of -C=C alkenyl (trisubstituted) stretching. Lastly, the adsorption at 653.87 cm^{-1} is showing the C-Br bond (halo compound).
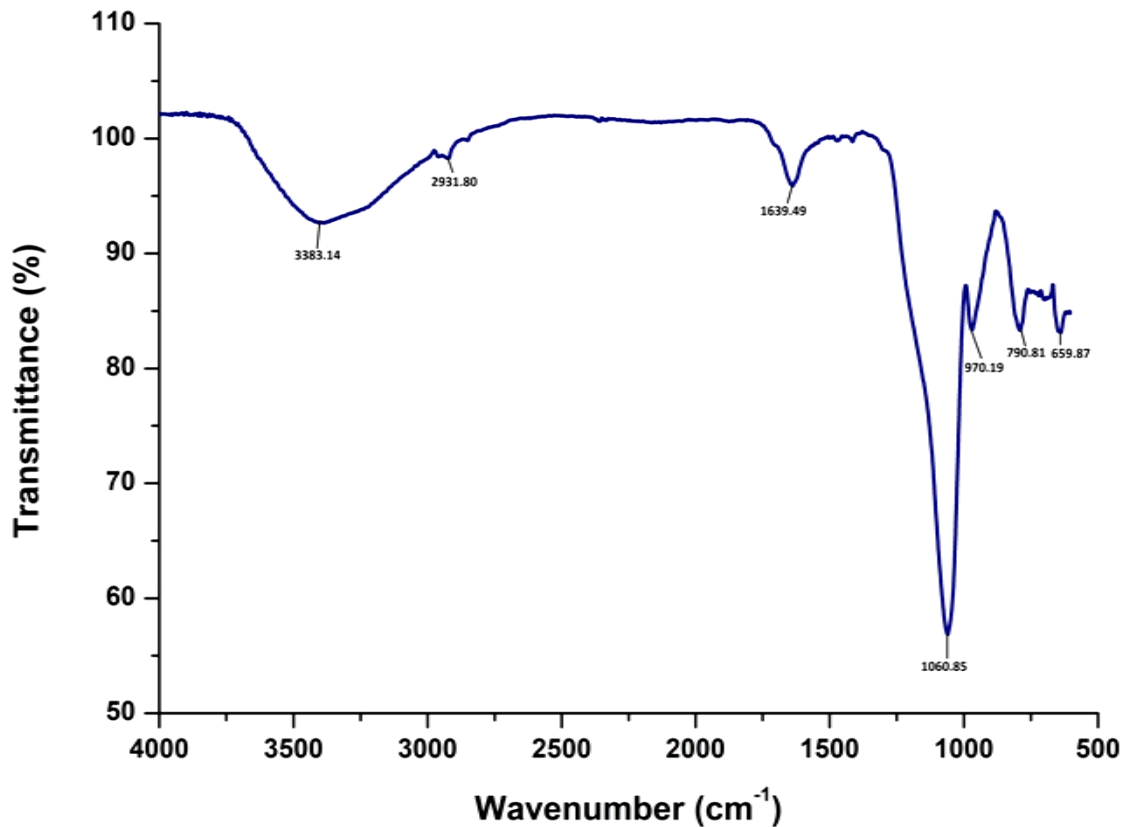
Figure 4.24 FTIR spectra of the synthesized CsAgNPs.

4.1.2.4 Particle Size Distribution and Zeta Potential Measurement

Particle size distribution and Zeta Potential measurement have been used to optimize the behaviour of the nanoparticles. The outcomes of Zeta-sizer have revealed the average size of phytosynthesized nanoparticles whereas the high zeta potential values have sustained long-term stability and excellent colloidal character of nanoparticles as a result of negative-negative repulsion [98]. Different powdered AgNPs samples have been diluted with ultra-purified water by ultrasonication process, to calculate the size distribution and Zeta Potential of the metallic silver nanoparticles. The average particle size in diameter (nm) has been recorded for all the six AgNPs samples from size distribution by number graph.

The zetasizer analysis of biosynthesized MpAgNPs by fresh yellow delicious apple (*Malus pumila*) extract has revealed that the average size was 22.70 nm whereas the average zeta potential value has been found as -25.80 mV as shown in Figure 4.25.
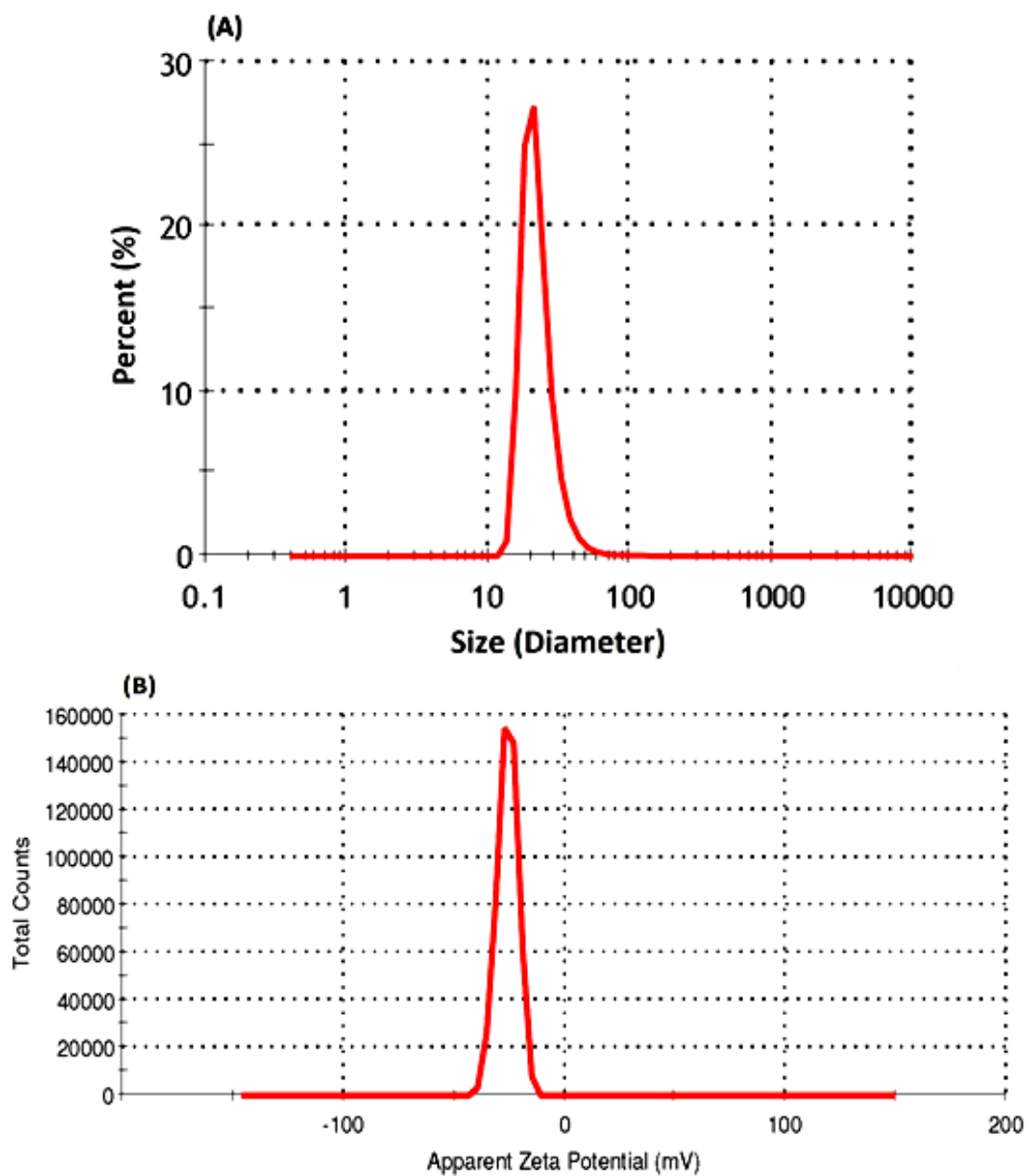
Figure 4.25 (A) Particle size by number and (B) zeta potential distribution of biosynthesized MpAgNPs.

The zetasizer analysis of biosynthesized CcAgNPs using cumin (*Cuminum cyminum*) seed extract has shown that the average size is 14.30 nm whereas the average zeta potential value has been found as -27.8 mV as shown in Figure 4.26.
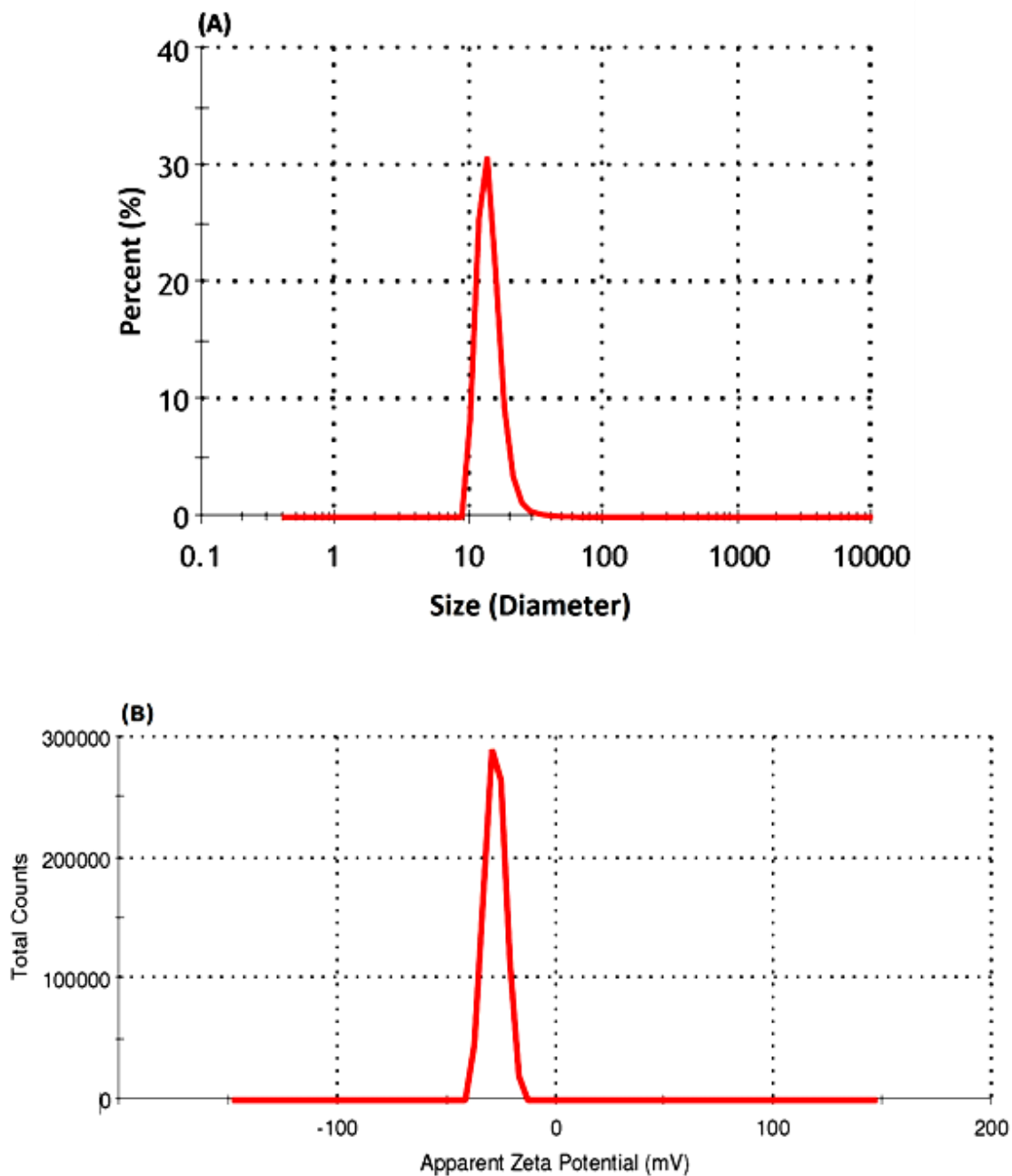
Figure 4.26 (A) Particle size by number and (B) zeta potential distribution of biosynthesized CcAgNPs.

The outcome of zetasizer has revealed that the average size of biosynthesized ZoAgNPs by fresh ginger (*Zingiber officinale*) rhizome extract has been recorded as 32.95 nm whereas the average zeta potential value has been found as -20.10 mV (Figure 4.27).
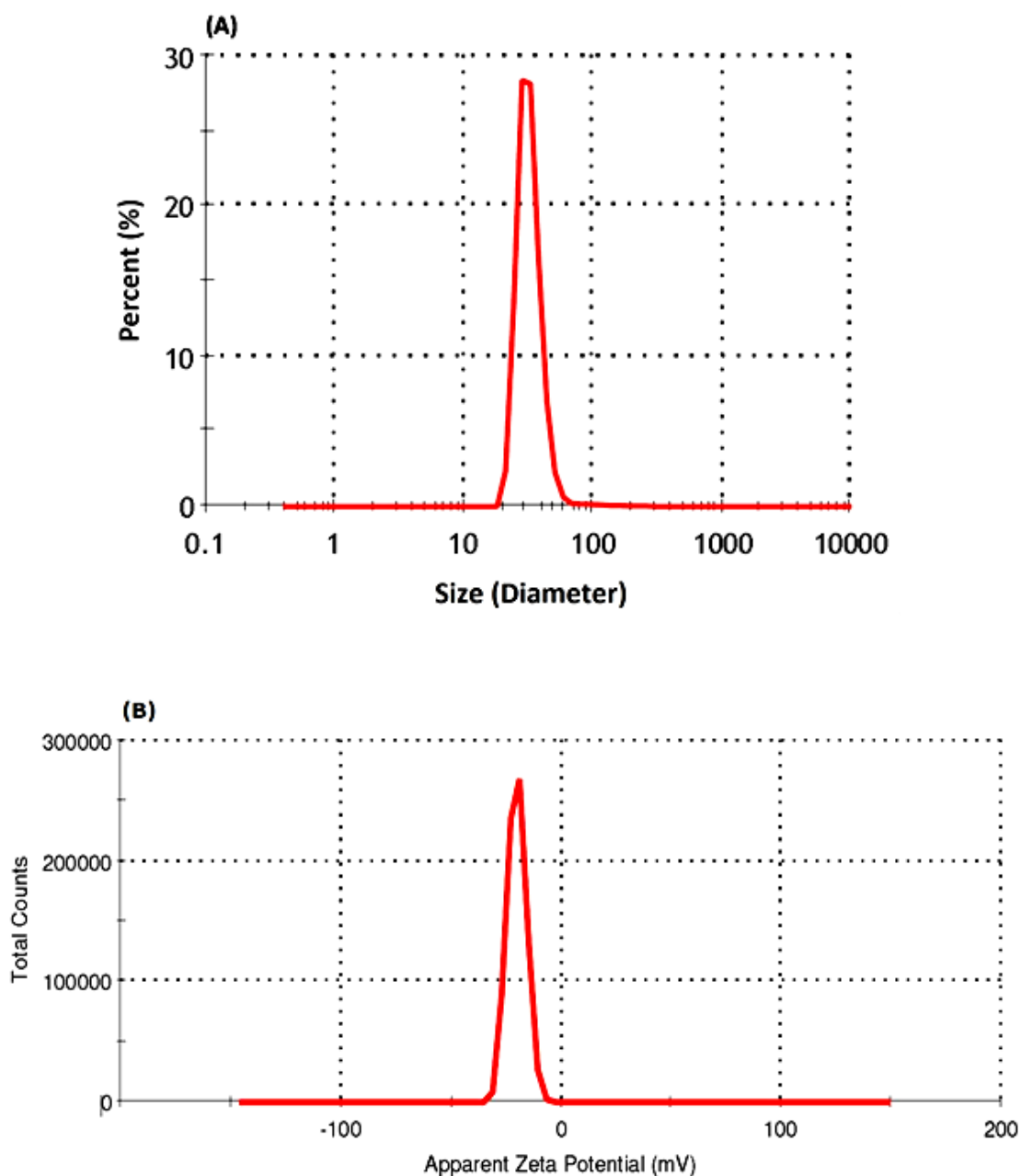
Figure 4.27 (A) Particle size by number and (B) zeta potential distribution of biosynthesized ZoAgNPs.

The zetasizer analysis of biosynthesized RsAgNPs by fresh rose (*Rosa santana*) petal extract has revealed that the z-average is 48.05 nm whereas the average zeta potential value has been found as -26.50 mV as shown in Figure 4.28.
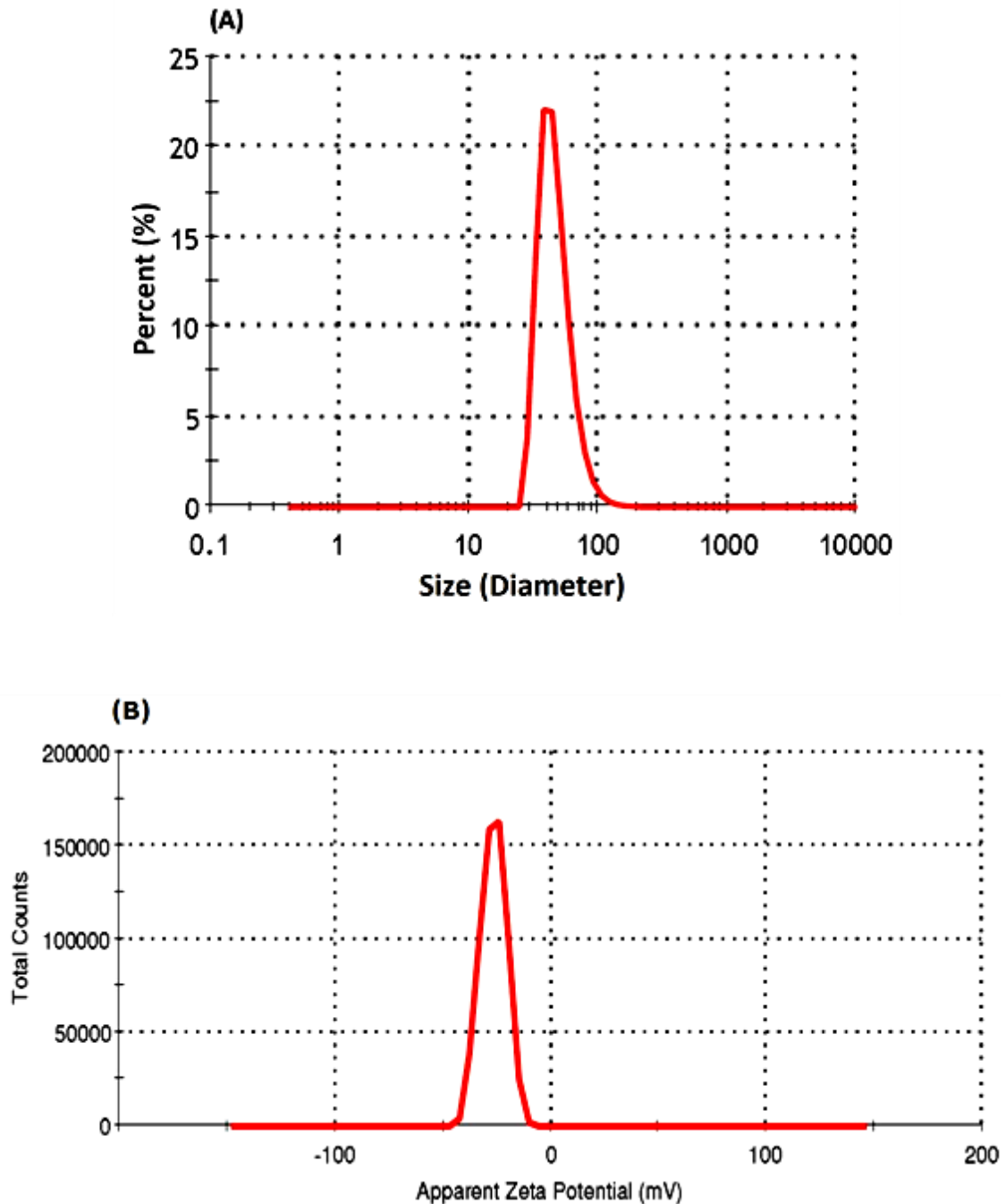
Figure 4.28 (A) Particle size by number and (B) zeta potential distribution of biosynthesized RsAgNPs.

The particle size distribution and Zeta potential analysis of the biosynthesized ClAgNPs using lemon (*Citrus limon*) peel extract are given in Figure 4.29. Z-average value for this AgNPs is 41.86 nm and the average zeta potential value has been found to be -18.70 mV.
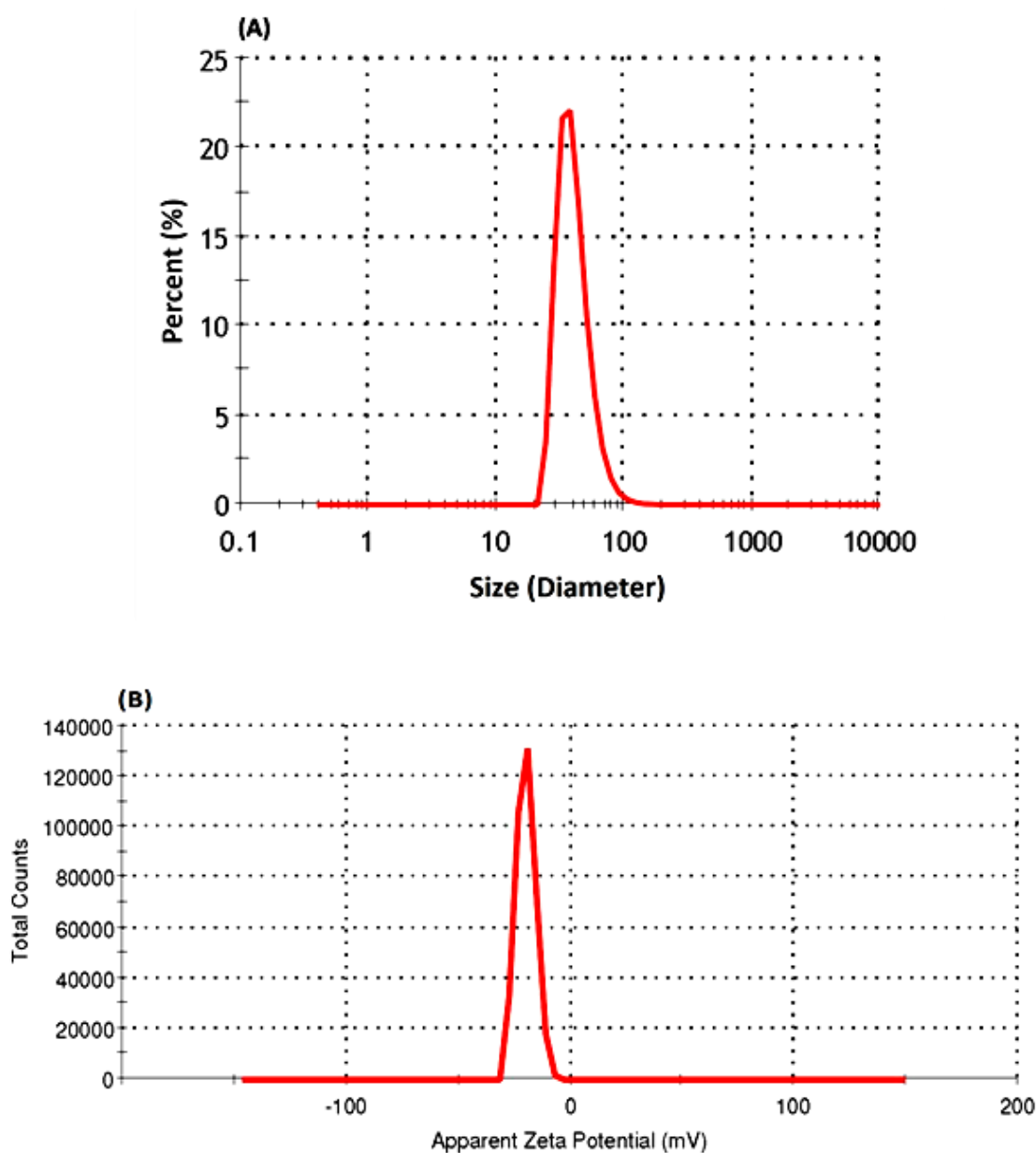
Figure 4.29 (A) Particle size by number and (B) zeta potential distribution of biosynthesized ClAgNPs.

As shown in Figure 4.30, the outcome of zetasizer revealed that the average size of biosynthesized CsAgNPs using orange (*Citrus sinensis*) peel extract has been observed as 40.23 nm whereas the average potential value has been indicated as -19.7 mV.
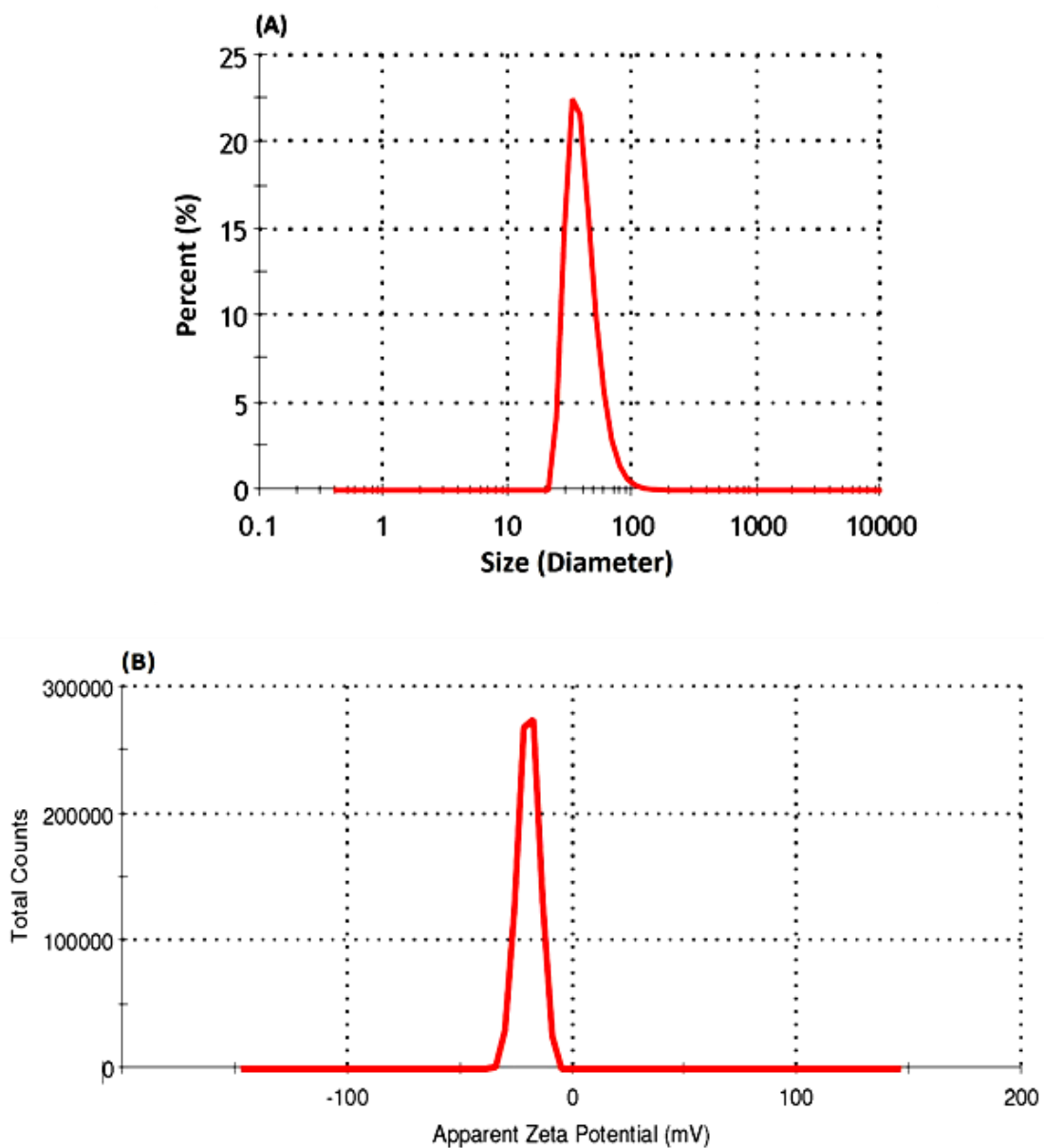
Figure 4.30 (A) Particle size by number and (B) zeta potential distribution of biosynthesized CsAgNPs.

4.1.2.5 TEM Analysis

TEM analysis has offered additional perception of the morphology and biochemical details of six different phytosynthesized silver nanoparticles at their nano level. TEM profiles also support the XRD results by confirming the crystalline nature of all silver nanoparticle samples.

TEM profile of biosynthesized MpAgNPs by fresh yellow delicious apple (*Malus pumila*) extract has shown that the nanoparticles have been morphology spherical or globular in shape with the distribution range of 7.46 nm to 21. 80 nm in diameter. The MpAgNPs are monodisperse, as illustrated in Figure 4.31.
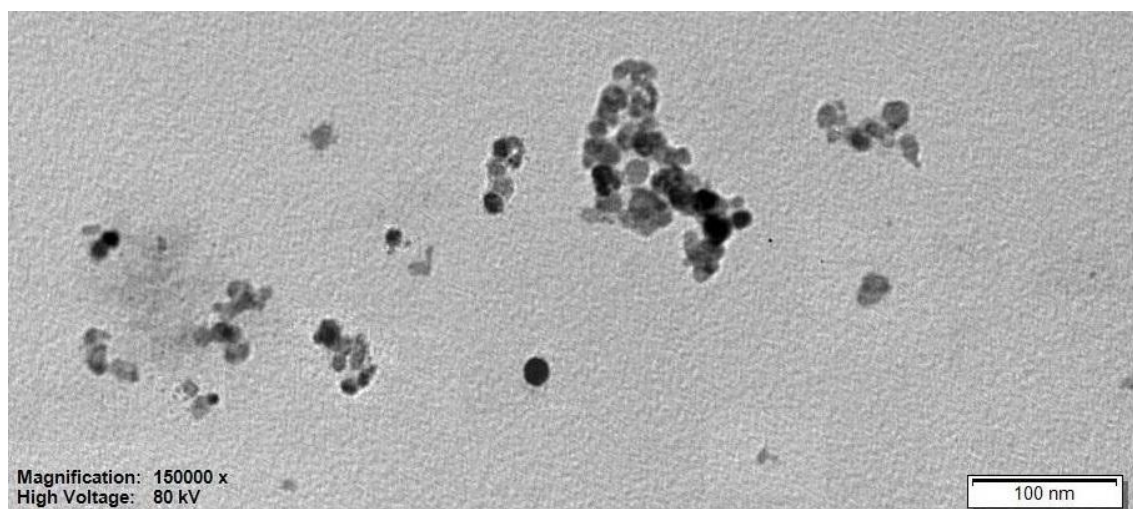
Figure 4.31 The TEM image of biosynthesized monodisperse MpAgNPs at 100 nm scales.

The TEM micrograph of the biosynthesized CcAgNPs using cumin (*Cuminum cyminum*) seeds extract at 50 nm scales has revealed in Figure 4.32. It has been found that CcAgNPs are almost globular shapes with maximum particles in the size ranged from 1.84 nm to 20. 57 nm.

Figure 4.33 illustrates TEM image that has been traced from the drop-coated specimen layer of ZoAgNPs, biosynthesized by using the fresh ginger (*Zingiber officinale*) rhizome extract. ZoAgNPs at 50 nm scales have dispersed approximately in the range of 2.68 nm to 42.69 nm with spherical and oval assemblies.
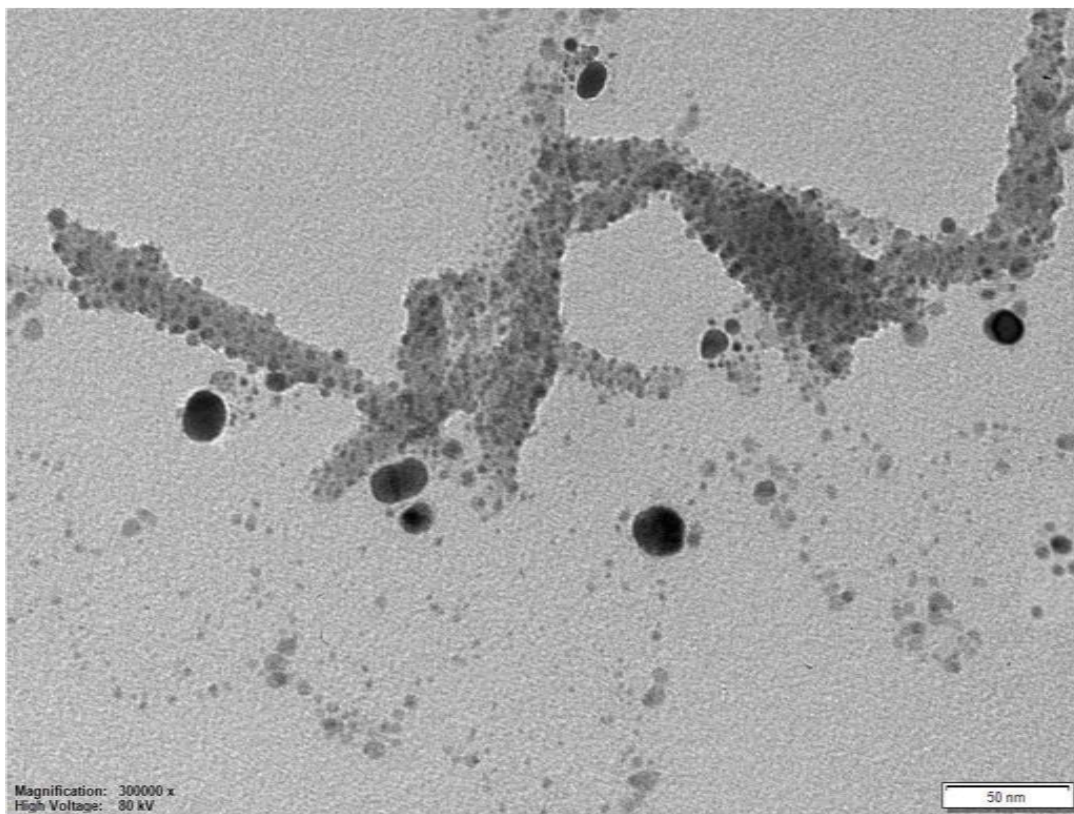
Figure 4.32 The TEM image of biosynthesized CcAgNPs at 50 nm scales.
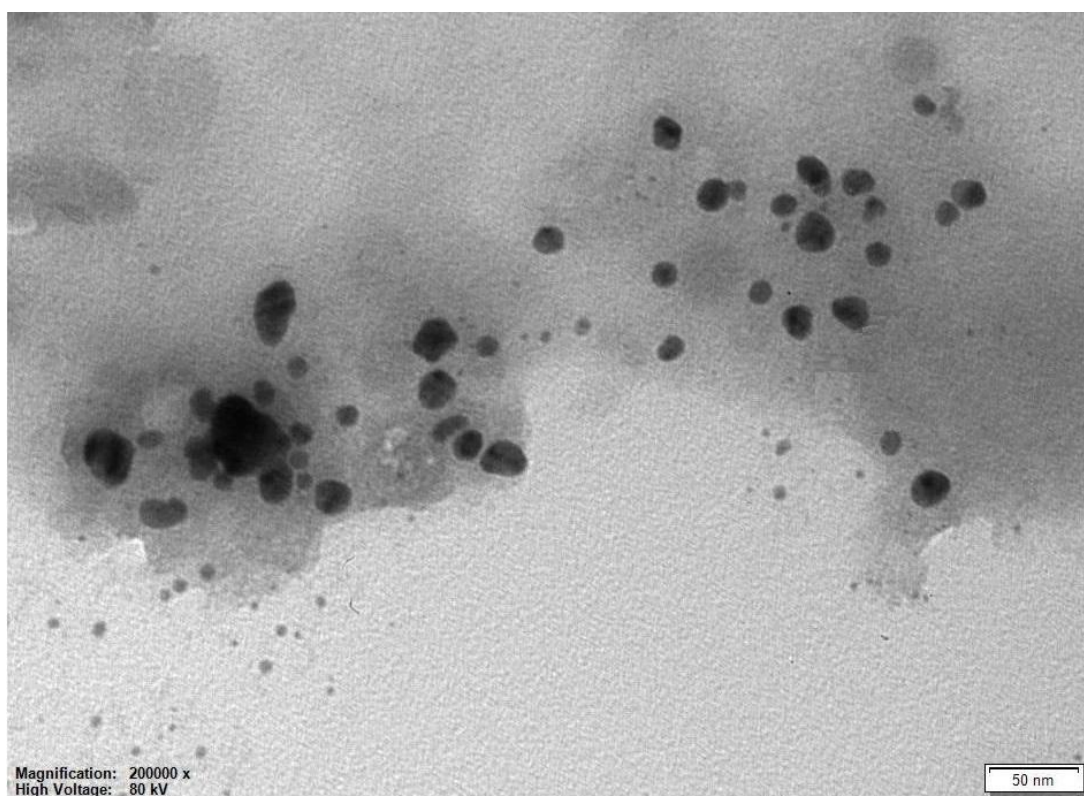
Figure 4.33 The TEM image of biosynthesized ZoAgNPs at 50 nm scales.

The size distribution of the phytosynthesized RsAgNPs using *R. santana* petal extract has been resolved by calculating the particle size of 100 randomly selected particles from TEM images. For RsAgNPs, The size distribution in diameter has been observed between 6.527 nm and 25.247 nm with a middling value of 14.48 nm (Figure 4.34). Nearly spherical shaped RsAgNPs are monodisperse in nature.
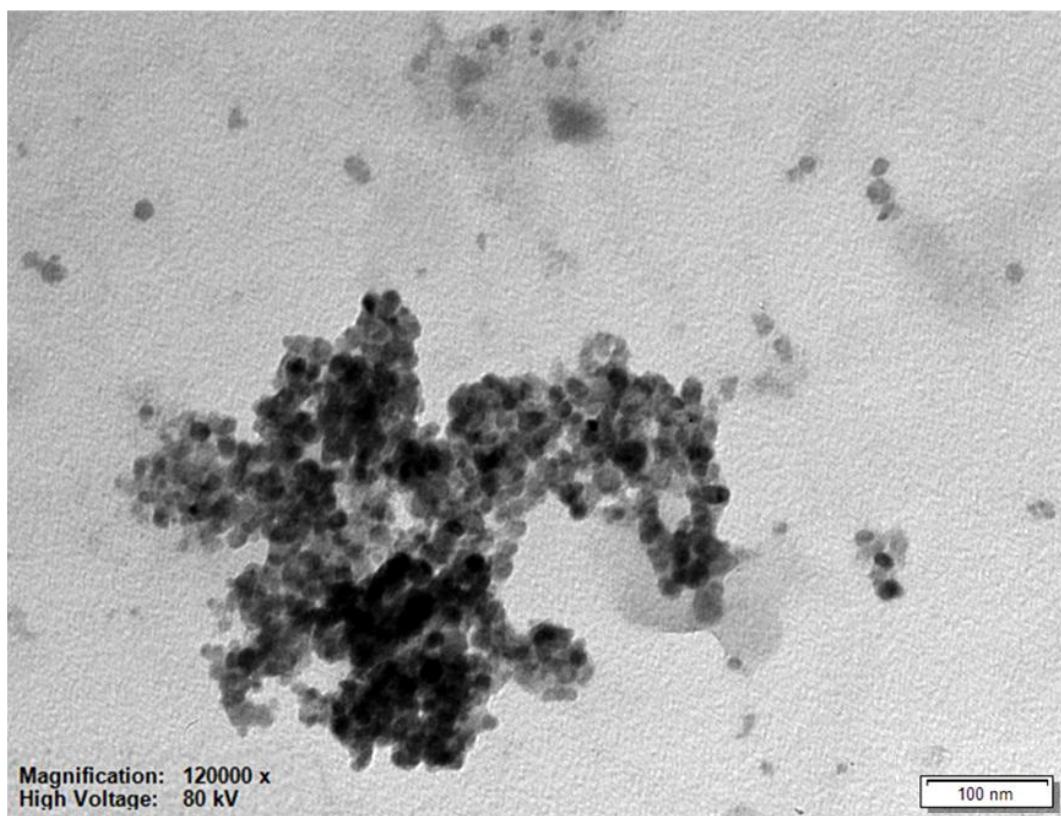
Figure 4.34 TEM image of biosynthesized RsAgNPs at 100 nm scales.

Figure 4.35 demonstrates a TEM image that has been traced from the drop-coated from the drop-coated specimen layer of the biosynthesized ClAgNPs using lemon (*Citrus limon*) peel extract. The ClAgNPs in the TEM image are dispersed as roughly globular, spherical and irregular in shape. The particle size was calculated in size range from 7.5 nm to 69.83 nm.

TEM has exposed the configuration of the biosynthesized CsAgNPs using orange (*Citrus sinensis*) peel extract (Figure 4.36). The particles were roughly spherical in shape and the largest particle size had a diameter of 60.44 nm while the smallest size was found to be around 4.79 nm.
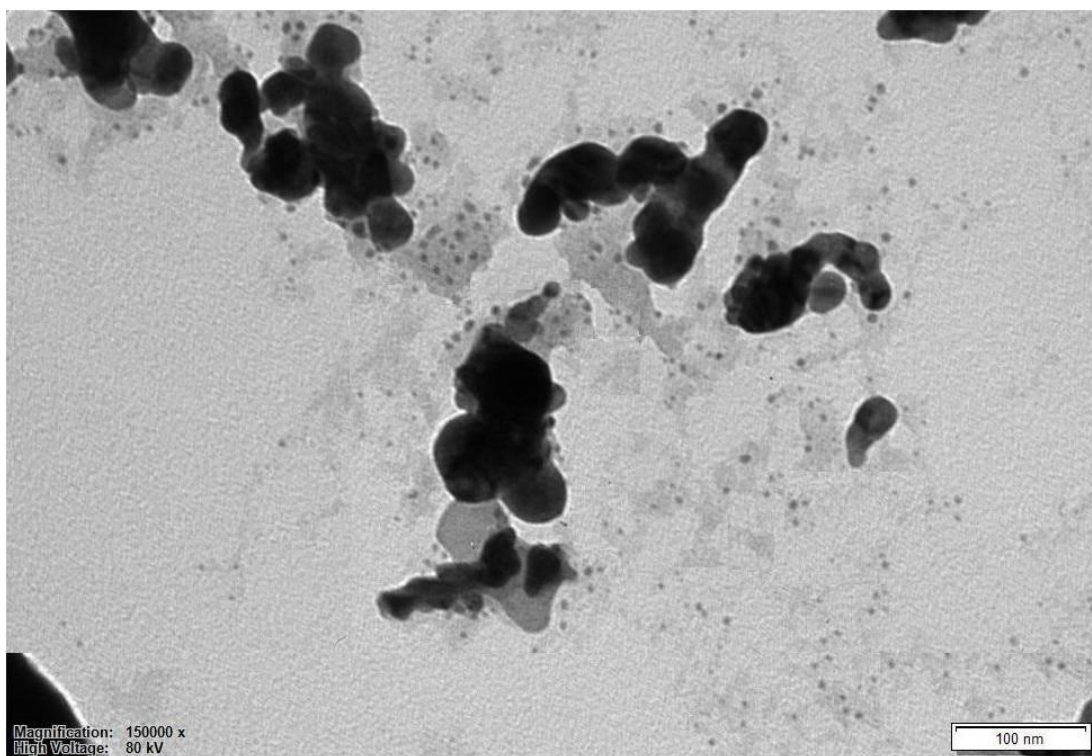
Figure 4.35 TEM image of biosynthesized ClAgNPs at 100 nm scales.
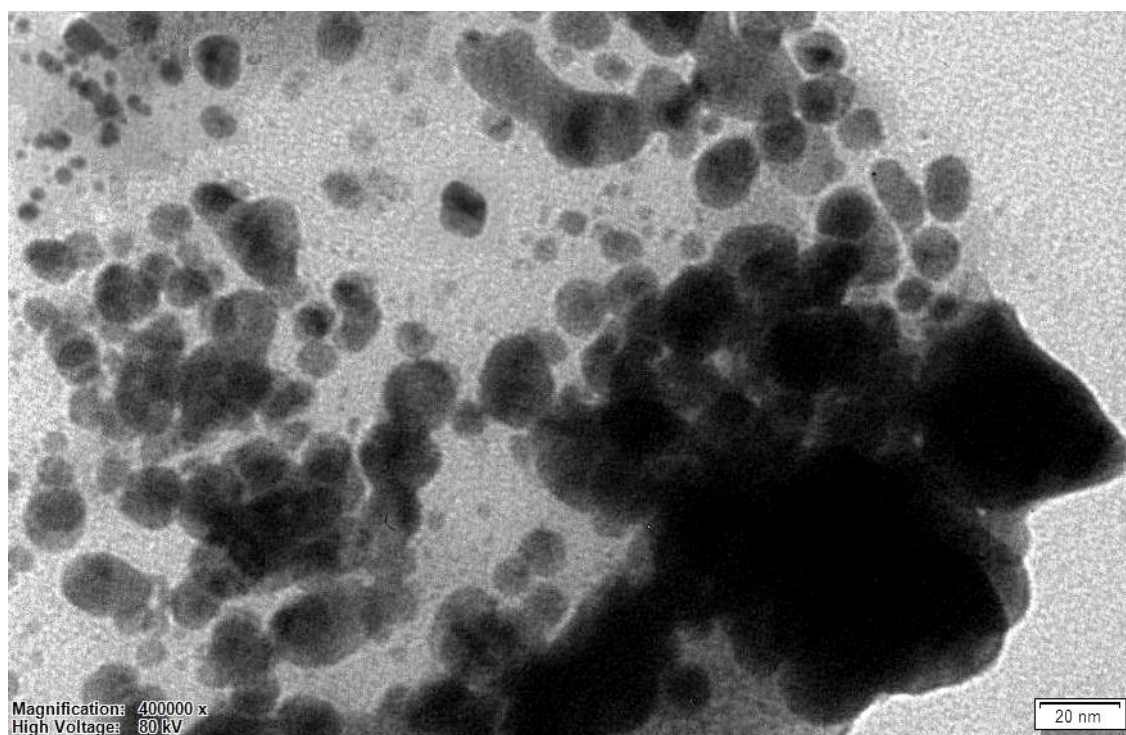
Figure 4.36 The TEM image of biosynthesized CsAgNPs at 20 nm scales.

4.2 Synthesis and Characterization of Copper Nanoparticles

Freshly acquired plant extracts have been used to fabricate copper nanoparticles. While plant extracts were mixed with Copper (II) sulphate pentahydrate salt ($CuSO_4.5H_2O$) solutions in desirable proportions, metal cooper ions have been reduced into copper nanoparticles. After synthesis, a variety of characterization techniques have been applied to evaluate the quantity and quality of phytosynthesized CuNPs.

4.2.1 Synthesis of Copper Nanoparticles

Fabrication of CuNPs has been followed by an immediate change in colour. Table 4.2 represents the initial colour changes of reaction mixture of CuNPs synthesis using various plant materials.

Table 4.2 Colour changes of solutions during copper nanoparticles synthesis using different plant extract.

Sr. No	Solution	Colour change		Colour intensity of synthesized solution
		Before synthesis	**After synthesis**	
1.	Fresh ginger (*Zingiber officinale*) rhizome extract	Pale yellow	Black (**Figure 4.37**)	+++
	1mM $CuSO_4.5H_2O$ solution	Blue		
2.	Green tea (*Camellia sinensis*) extract	Yellowish brown	Greenish black (**Figure 4.38**)	+++
	1mM $CuSO_4.5H_2O$ solution	Blue		
3.	Fresh orange *(Citrus sinensis)* juice	Yellow	Brownish black (**Figure 4.49**)	++
	1mM $CuSO_4.5H_2O$ solution	Blue		
4.	Turkish pine (*Pinus brutia*) bark extract	Pale Yellow	Brownish black (**Figure 4.40**)	+
	1mM $CuSO_4.5H_2O$ solution	Blue		

Colour intensity/potency: Light colour: +, Dark colour: ++, Deep dark colour: +++

111
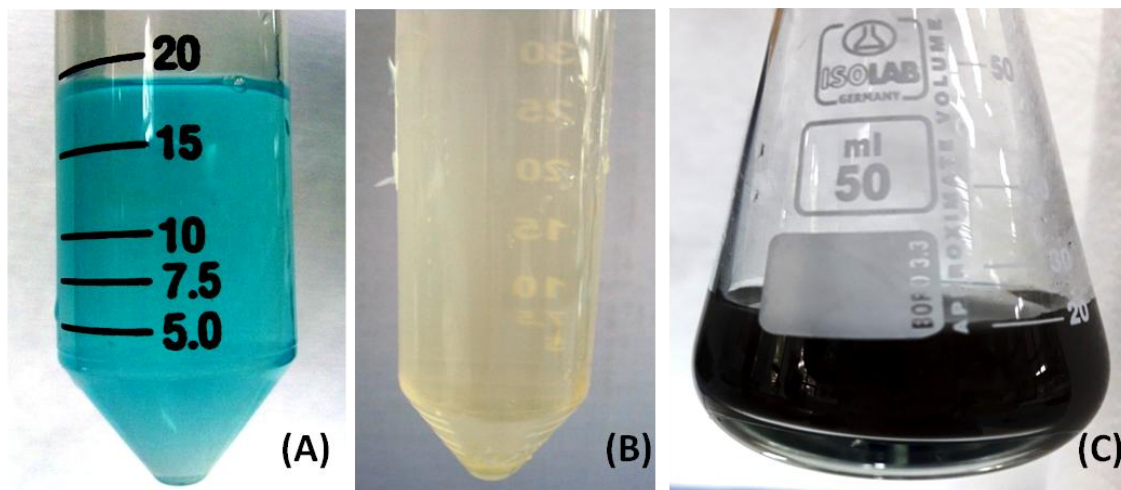
Figure 4.37 Photographic representation of copper nanoparticle synthesis. A. copper (II) sulphate pentahydrate solution; B. aqueous extract of fresh ginger rhizome; C. synthesized copper nanoparticles (ZioCuNPs).
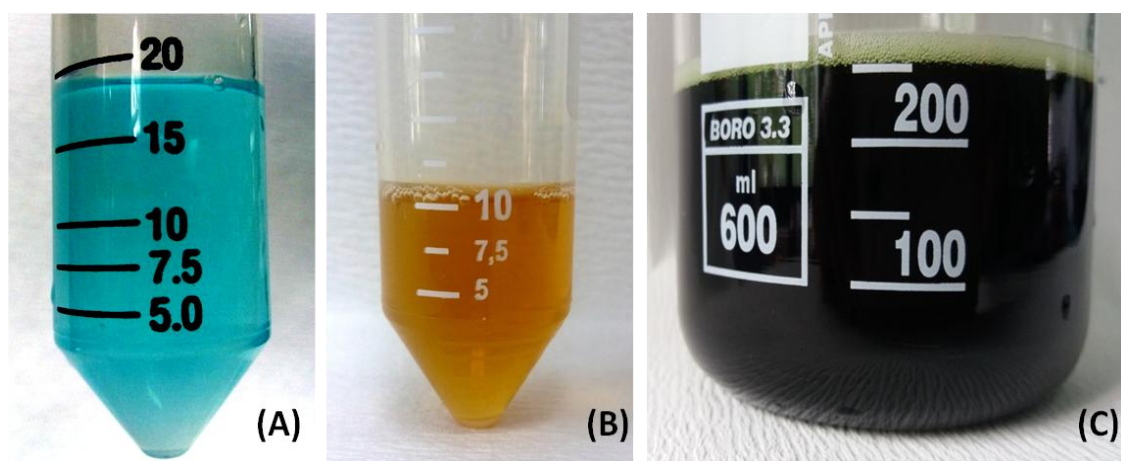
Figure 4.38 Photographic representation of copper nanoparticle synthesis. A. copper (II) sulphate pentahydrate solution; B. aqueous extract of green tea; C. synthesized copper nanoparticles (CasCuNPs).
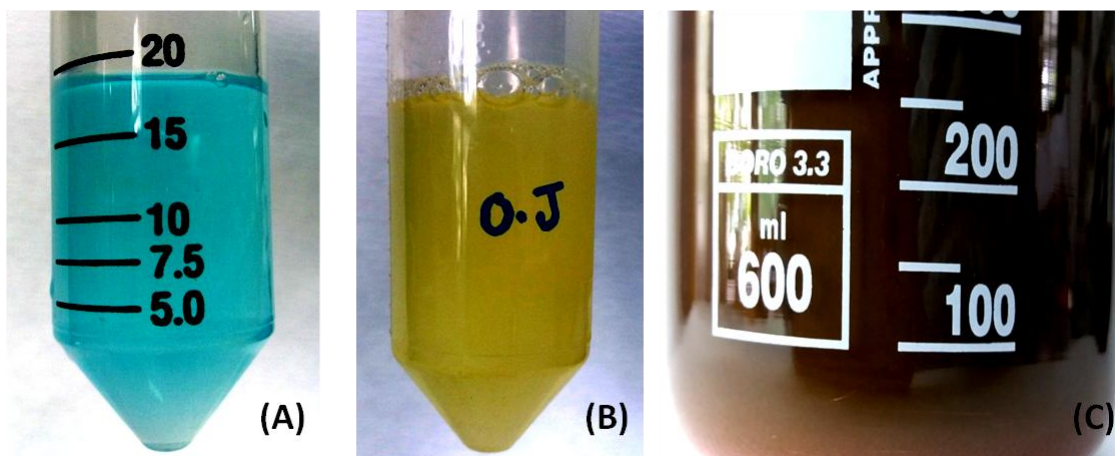
Figure 4.39 Photographic representation of copper nanoparticle synthesis. A. copper (II) sulphate pentahydrate solution; B. aqueous extract of orange juice; C. synthesized copper nanoparticles (CisCuNPs).
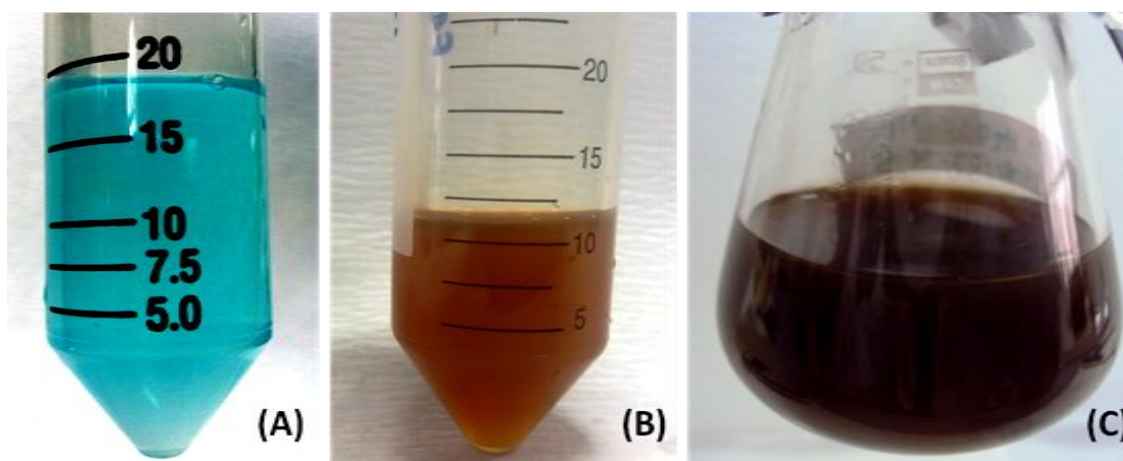
Figure 4.40 Photographic representation of copper nanoparticle synthesis. A. copper (II) sulphate pentahydrate solution; B. aqueous extract of Turkish pine bark extract; C. synthesized copper nanoparticles (PibCuNPs).

4.2.2 Copper Nanoparticle Characterizations

4.2.2.1 UV-Visible Absorption Spectroscopic Study

The progress of formation of copper nanoparticles has been screened by means of UV-Vis spectroscopy. Absorbance peaks between 500 nm and 600 nm is significant which have been exploited as an indicator to corroborate the formation of metallic copper nanoparticles from copper ions.

The sharp peaks of copper nanoparticles have been observed at 566 nm, 570 nm and 573 nm in case of ginger rhizome (ZioCuNPs), green tea (CasCuNPs.) and Turkish pine (PibCuNPs) extract, respectively (Figure 4.41, Figure 4.42 & Figure 4.44) whereas for orange juice extract (CisCuNPs) the band found at 560 nm (Figure 4.43).
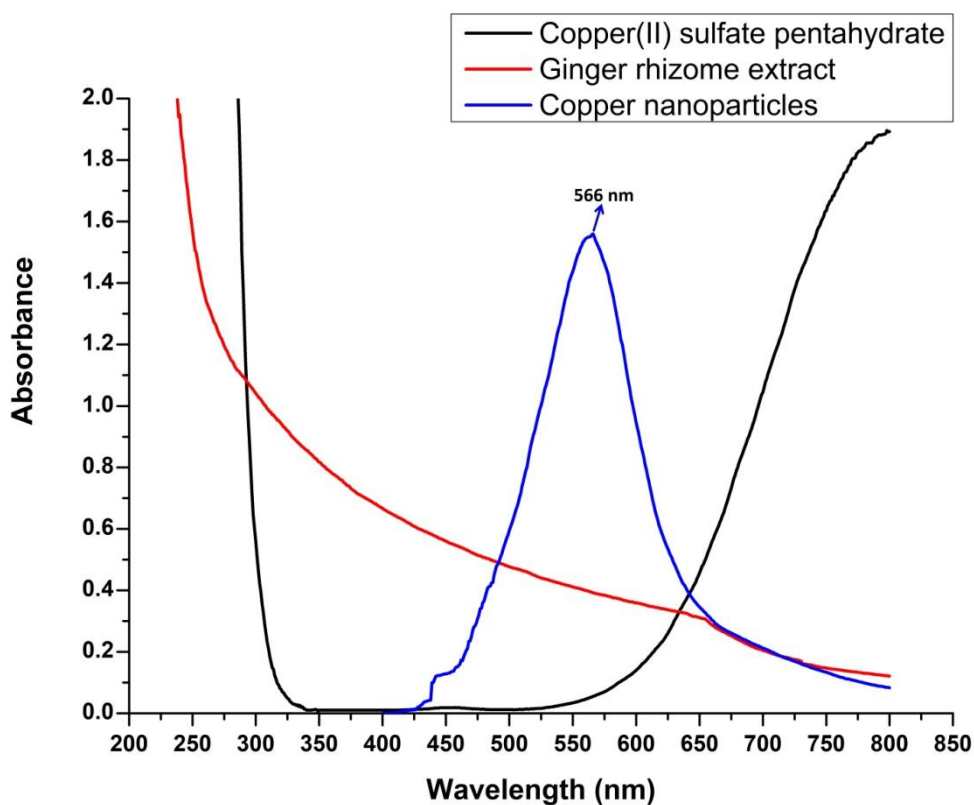
Figure 4.41 UV-visible absorbance maxima of phytosynthesized ZioCuNPs at 566 nm.
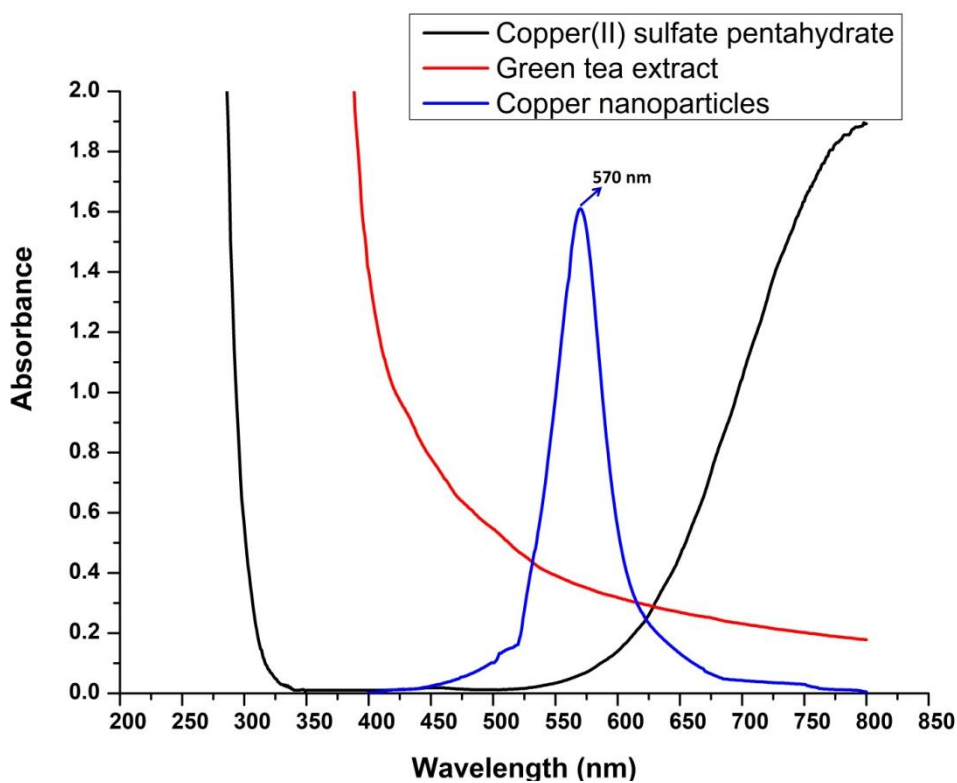
Figure 4.42 UV-visible absorbance maxima of phytosynthesized CasCuNPs at 570 nm.
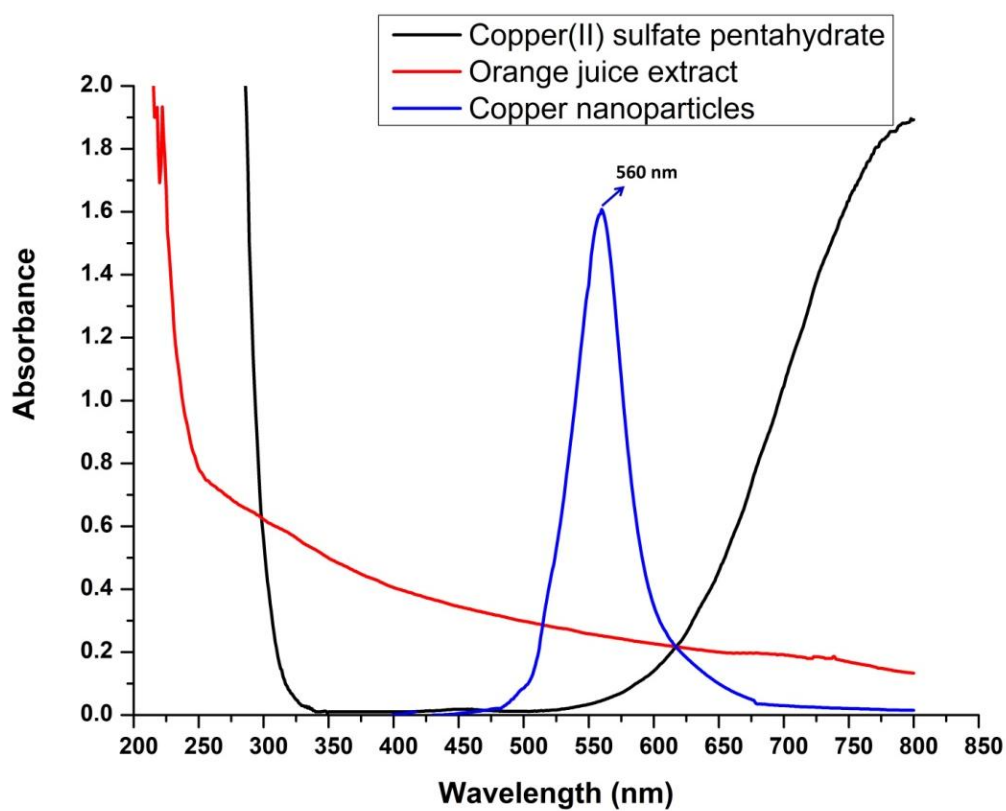
Figure 4.43 UV-visible absorbance maxima of phytosynthesized CisCuNPs at 560 nm.
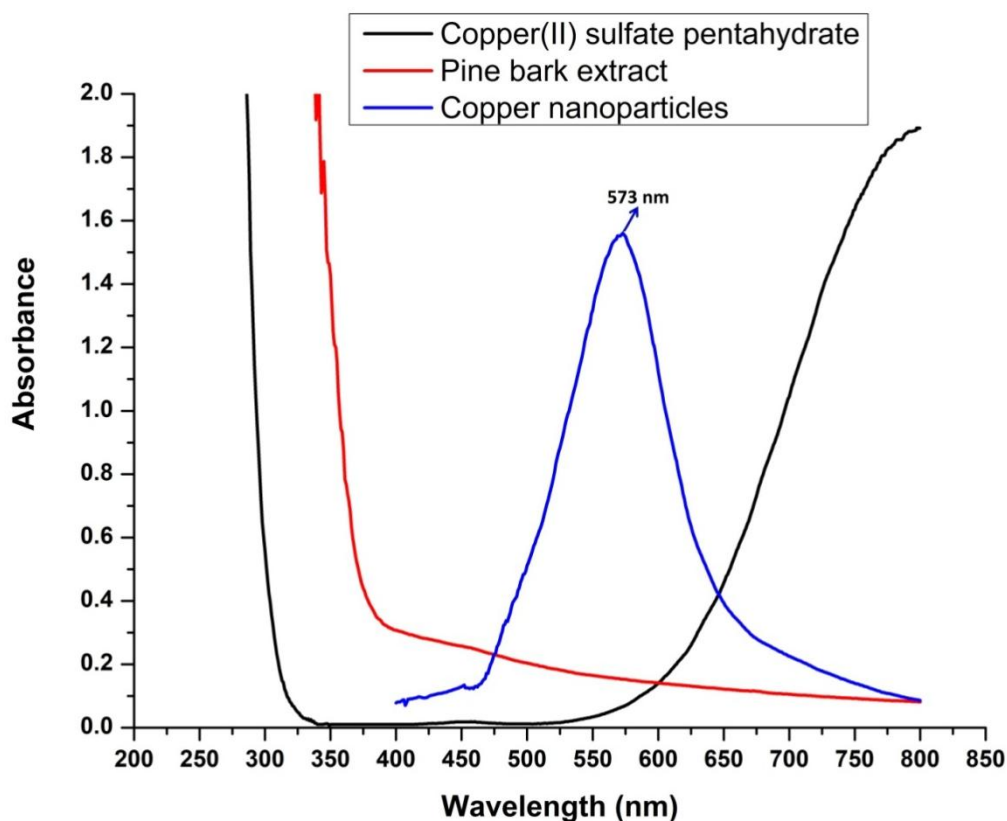
Figure 4.44 UV-visible absorbance maxima of phytosynthesized PibCuNPs at 573 nm.

4.2.2.2 X-ray Diffraction (XRD) Study

X-ray Diffraction (XRD) measurements of different reduced CuNPs samples have been recorded to identify the crystallinity of copper nanoparticles. The diffracted intensities have been documented from 20° to 100°.

The XRD pattern from various copper nanoparticle samples has confirmed five strong reflections correspond to the planes of (111), (200), (220), (311) and (222) corroborate the presence of metallic copper particles. As because, these planes are the characteristic Bragg's diffraction plans for copper with face-centered cubic crystalline structures which support or coordinate the database of the JCPDS (Joint Committee on Powder Diffraction Standards) file no: 04-0784 [269]. Moreover, a detail outline of XRD analysis of synthesized copper nanoparticle sample is describing below-

Using XRD spectrum analysis of biosynthesized ZioCuNPs by the fresh ginger (*Zingiber officinale*) rhizome extract, five different diffraction peaks at 43.54°, 50.54°, 74.42°, 90.28° and 95.52° are shown in Figure 4.45. The interplanar spacing (dcalculated) values are 2.082, 1.804, 1.277, 1.089 and 1.043Å.

116
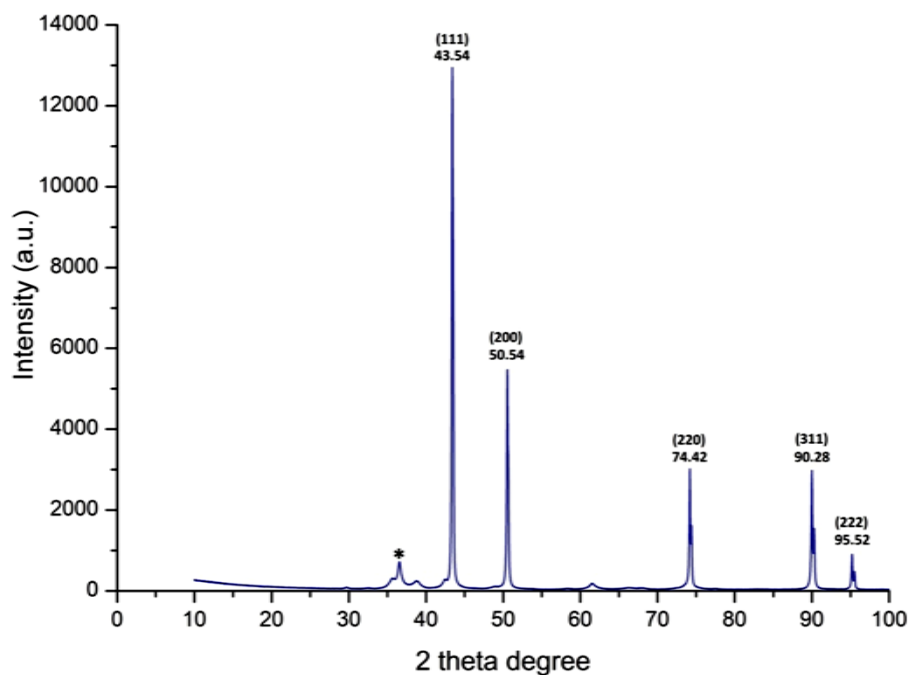
Figure 4.45 XRD pattern of biosynthesized ZioCuNPs.

Figure 4.46 exhibits the XRD pattern of biosynthesized CasCuNPs using green tea (*Camellia sinensis*) extract. Diffraction peaks have been appeared at 43.47°, 50.61°, 74.32°, 90.28° and 95.40° along with the interplanar spacing ($d_{calculated}$) values were 2.083, 1.804, 1.277, 1.089 and 1.043Å.
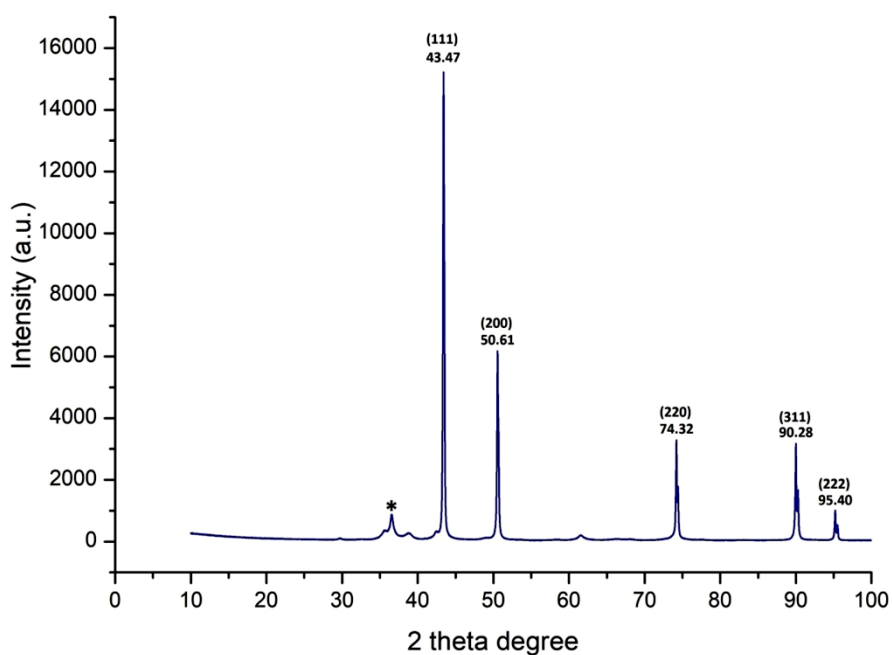
Figure 4.46 XRD pattern of biosynthesized CasCuNPs.

117

Figure 4.47 has revealed the XRD pattern of biosynthesized CisCuNPs using freshly squeezed orange (*Citrus sinensis*) juice extract. Five significant reflections have been observed at 43.49°, 50.64°, 74.38°, 90.25° and 95.48°. The interplanar spacing (dcalculated) values are 2.084, 1.806, 1.277, 1.090 and 1.043Å.
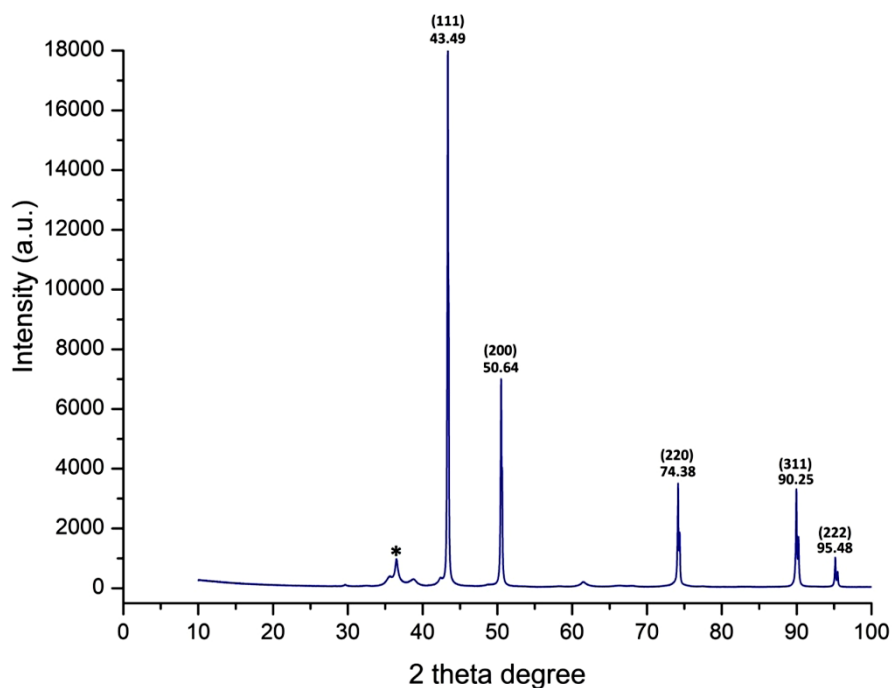
Figure 4.47 XRD pattern of biosynthesized CisCuNPs.

XRD analysis of biosynthesized PibCuNPs using Turkish pine (*Pinus brutia*) bark extract is demonstrated in Figure 4.48. Diffraction peaks have been found at 43.45°, 50.53°, 74.31°, 90.14° and 95.32° together with the interplanar spacing ($d_{calculated}$) values are 2.086, 1.807, 1.278, 1.091 and 1.044Å.
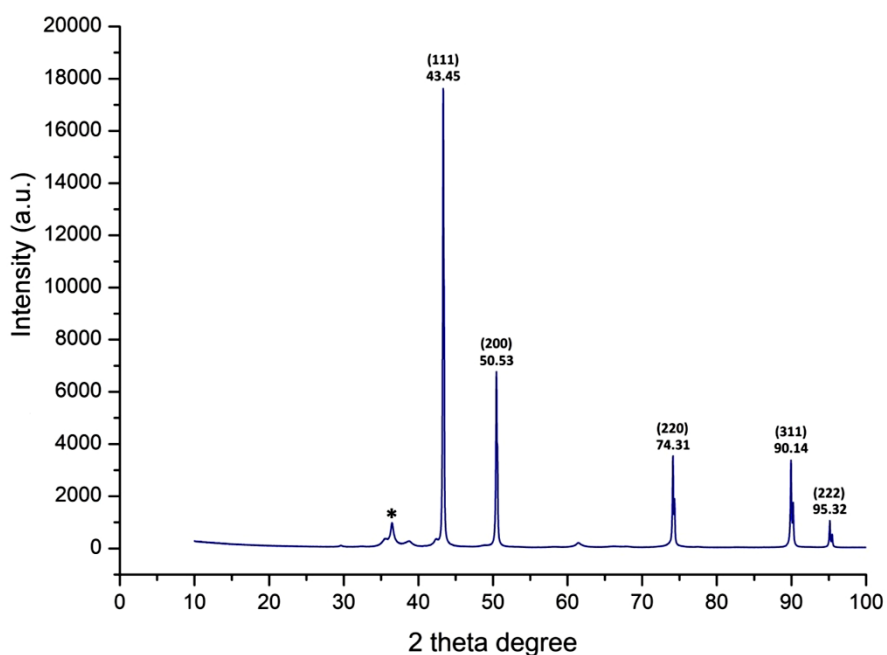
Figure 4.48 XRD pattern of biosynthesized PibCuNPs.

However, for all four CuNPs samples, a weak and broad reflection at ~36° marked with an asterisk (*) indicate the presence of minute amount of cuprous oxide (Cu_2O) = 36.5° as because the CuNPs have been exposed to the open air for a short time while transferring inside the XRD chamber during the sample loading into the instrument [270], [271].

4.2.2.3 Fourier-Transform Infrared Spectroscopic (FTIR) Analysis

FTIR spectroscopic analysis has been conducted to reveal the potential functional groups of biomolecules available in the fresh ginger (*Zingiber officinale*) rhizome, green tea (*Camellia sinensis*), freshly squeezed orange (*Citrus sinensis*) juice and Turkish pine (*Pinus brutia*) bark extracts which might have played as reducing agent as well as capping and stabilizing factors for the production of Cu nanoparticles from copper ions.

• FTIR Study of Biosynthesized ZioCuNPs by Fresh Ginger Rhizome Extract

Figure 4.49 represents FTIR spectrum of ZioCuNPs synthesized using fresh ginger rhizome extracts. The IR spectrum at 3563.10 cm^{-1} indicates the existence of O-H stretching whereas the peaks located mainly at 2,917.42 and 2,849.76 cm^{-1} are the representation of medium alkane C-H Stretch. The bands at 2,349.35 cm^{-1} is due to

absorption of atmospheric CO_2. Peaks observers at 1,629.34 cm^{-1} is for strong alkenyl monosaturated C=C stretch; whereas 1,096.37 cm^{-1} for strong C-O stretching alcohol bond. The adsorptions at 667.57 and 615.90 cm^{-1} are showing the C-X bond (X=bromide). Finally, The band at 420 cm-1 is related to metal ligand bond.
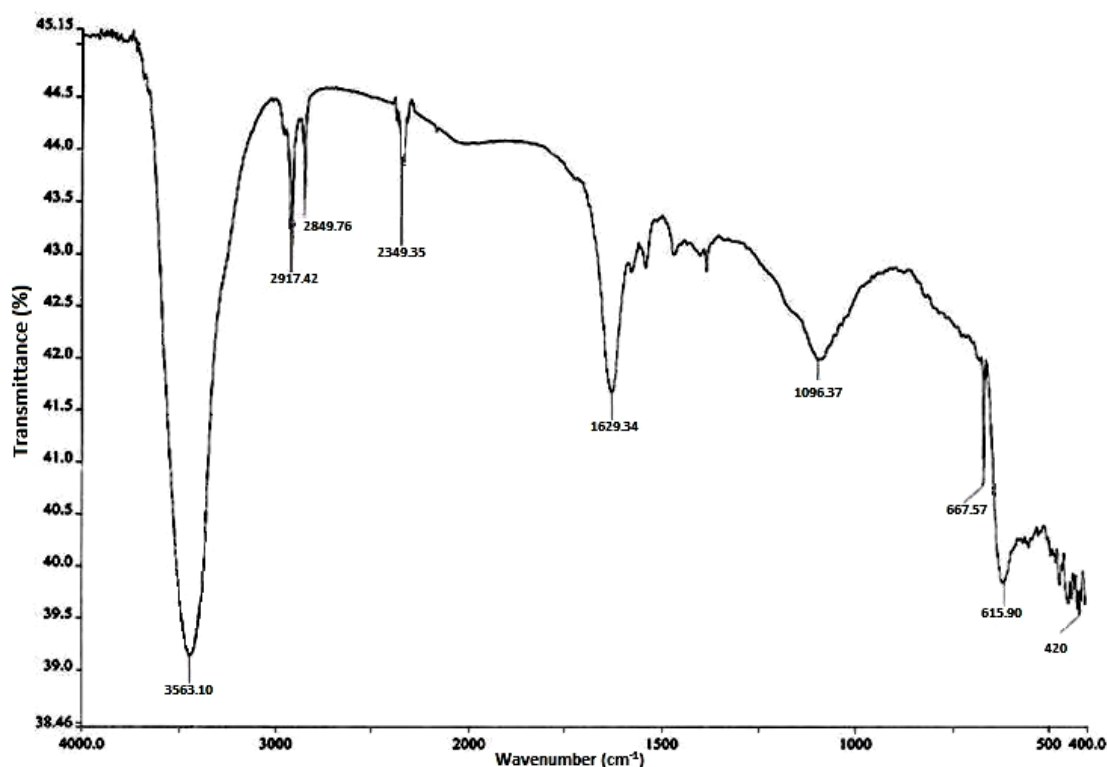
Figure 4.49 FTIR spectrum of the phytosynthesized ZioCuNPs.

• **FTIR Study of Biosynthesized CasCuNPs by Green Tea Extract**

Figure 4.50 represents FTIR spectra of CasCuNPs phytosynthesized via the green tree extracts. Peaks have been observed mainly at 3560.89 cm^{-1}for O-H stretching; 2,917.42 cm^{-1} for medium alkane C-H stretching; 1,631.24 cm^{-1} for strong alkene monosubstituted bond; 1,094.80 cm^{-1} for strong C-O stretching alcohol bond; 613.40 cm^{-1} for -C-X bond (X=bromide) and 426.90 cm^{-1} for metal ligand bond.
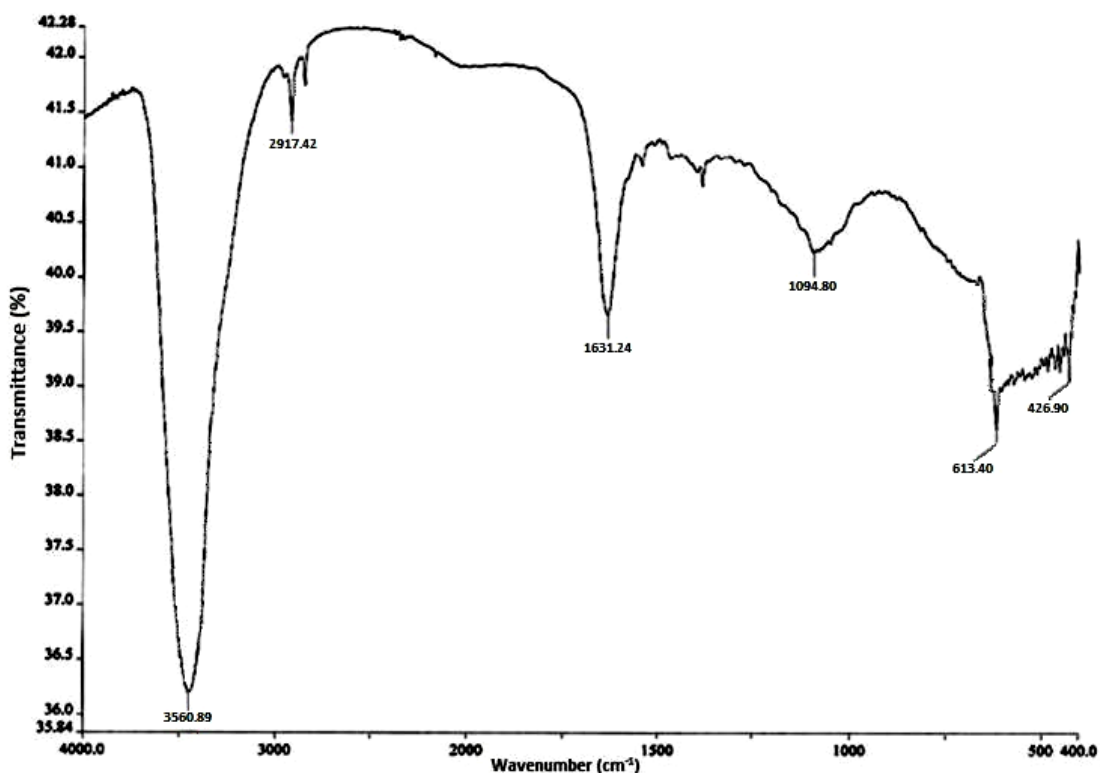
Figure 4.50 FTIR spectrum of the phytosynthesized CasCuNPs.

• **FTIR Study of Biosynthesized CisCuNPs by Freshly Squeezed Orange Juice**

Classification by FTIR has been utilized to uncover the biomolecules and their functional group available in the CisCuNPs phytosynthesized using fresh orange juice (Figure 4.51). The FTIR spectra of copper nanoparticles have showed the bands at 3540.76, 1634.81, 1033.14, 667.89 and 602.28 cm^{-1}. The absorption peak at 3540.76 cm^{-1} indicates the presence of O-H stretching. On the other hand, the band at 1,634.81 cm^{-1} matches up to strong alkenyl monosaturated (C=C) stretch. Another band at 1033.14 cm^{-1} has allocated as absorption peaks of strong sulfoxide (S=O stretching).The adsorptions at 667.89 and 602.28 cm^{-1} are showing the C-X bond (X=bromide).

121
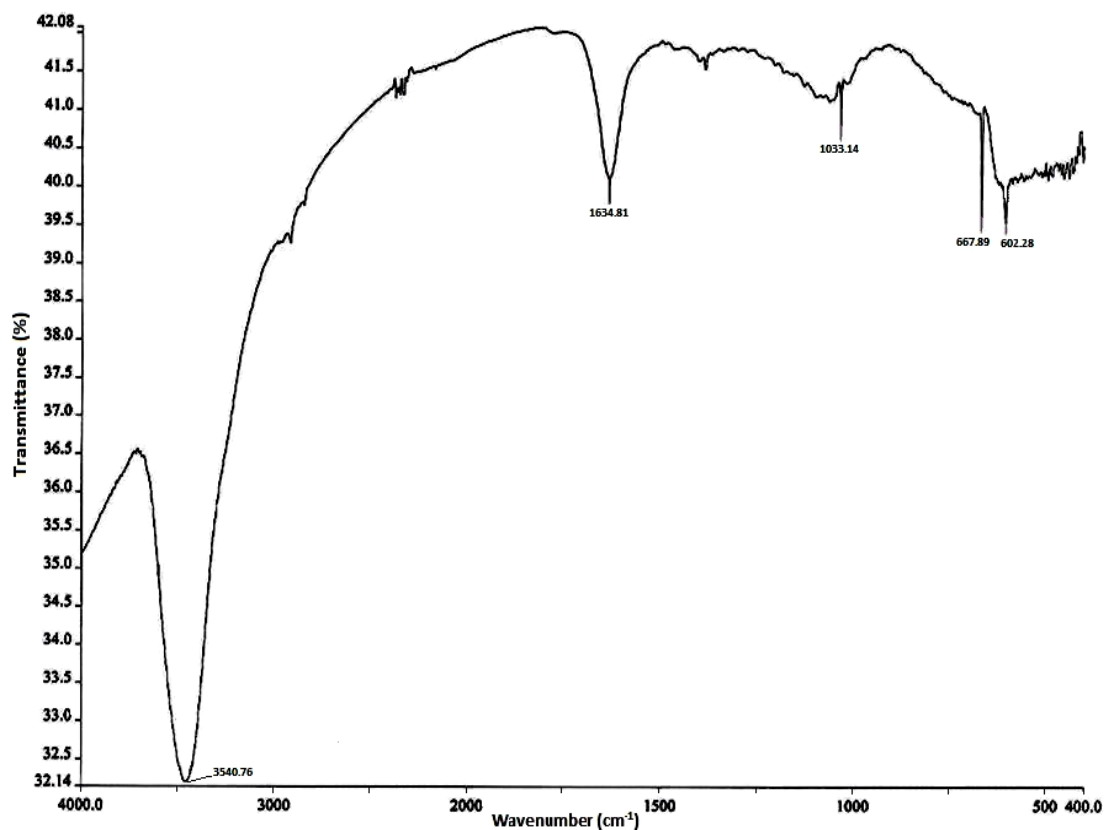
Figure 4.51 FTIR spectrum of the phytosynthesized CisCuNPs.

• **FTIR Study of Biosynthesized PibCuNPs by Turkish Pine Bark Extract**

Figure 4.52 represents Fourier transform infrared (FTIR) spectrum of PibCuNPs synthesized using the Turkish pine bark extract. The IR spectra at 3562.40 cm^{-1} specifies the existence of O-H stretching whereas the peaks located mainly at 2,917.30 and 2,849.67 cm^{-1} specify medium alkane C-H stretching alkane; 1,630.77 cm^{-1} for strong alkene monosubstituted C=C Stretch; 1,083.97 cm^{-1} for strong bond of C-O stretching found in primary alcohol; 667.90 and 616.05 cm^{-1} for -C-X bond (X=bromide) and finally 413.18 cm^{-1} is for metal ligand bond.

122
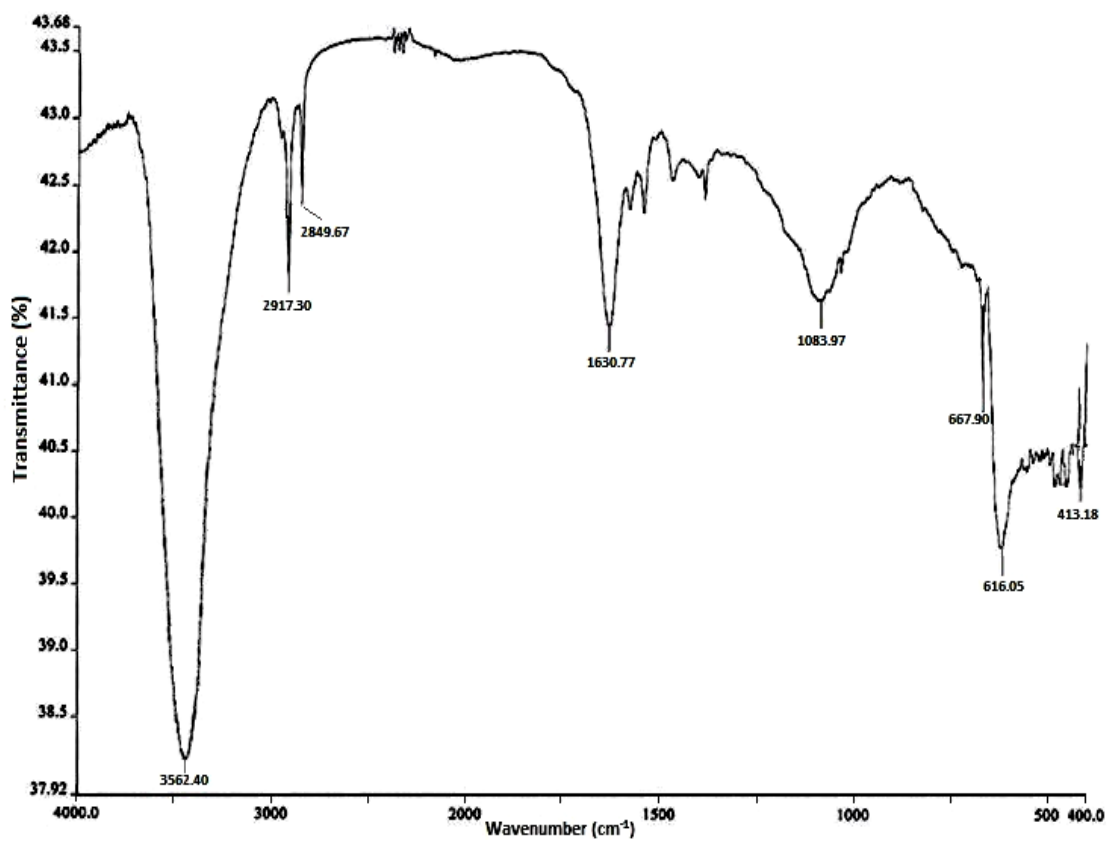
Figure 4.52 FTIR spectrum of the phytosynthesized PibCuNPs.

4.2.2.4 Particle Size Distribution and Zeta Potential Measurement

The comprehensive analysis of four different phytosynthesized copper nanoparticles have been carried out by particle size distribution and zeta potential measurement as described below-

Zeta-sizer analysis of biosynthesized ZioCuNPs by the fresh ginger (*Zingiber officinale*) rhizome extract revealed that the average size was 27.17 nm whereas the mean zeta potential value has been found as -24.40 mV as shown in Figure 4.53.
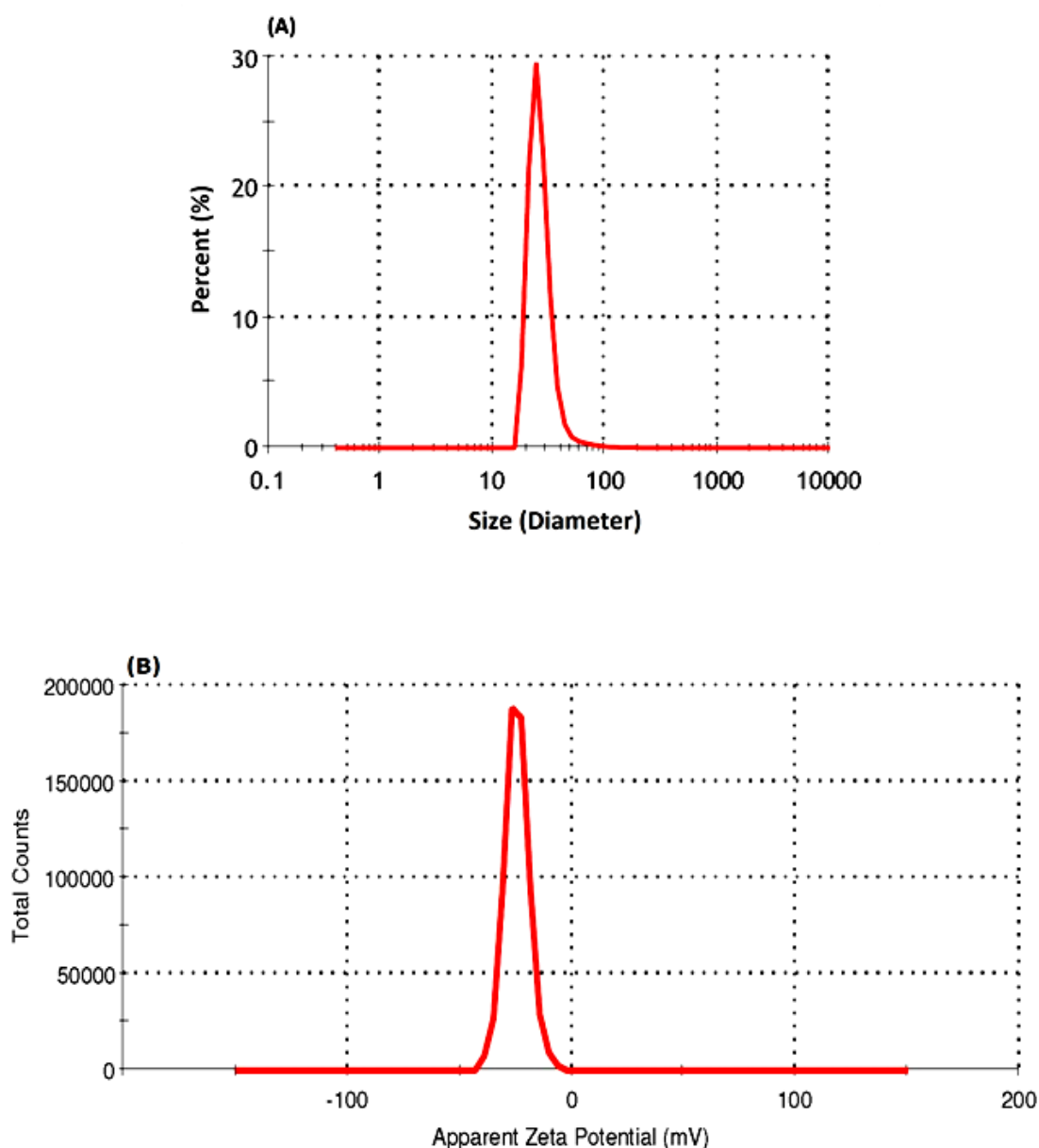
Figure 4.53 (A) Particle size by number and (B) zeta potential distribution of biosynthesized ZioCuNPs.

124

The particle size distribution and Zeta potential of the phytosynthesized CasCuNPs using green tea (*Camellia sinensis*) extract are revealed in Figure 4.54. Particle dimension distribution by number has revealed the z-average of CasCuNPs as 45.30 nm with the mean potential value of -19.0 mV.
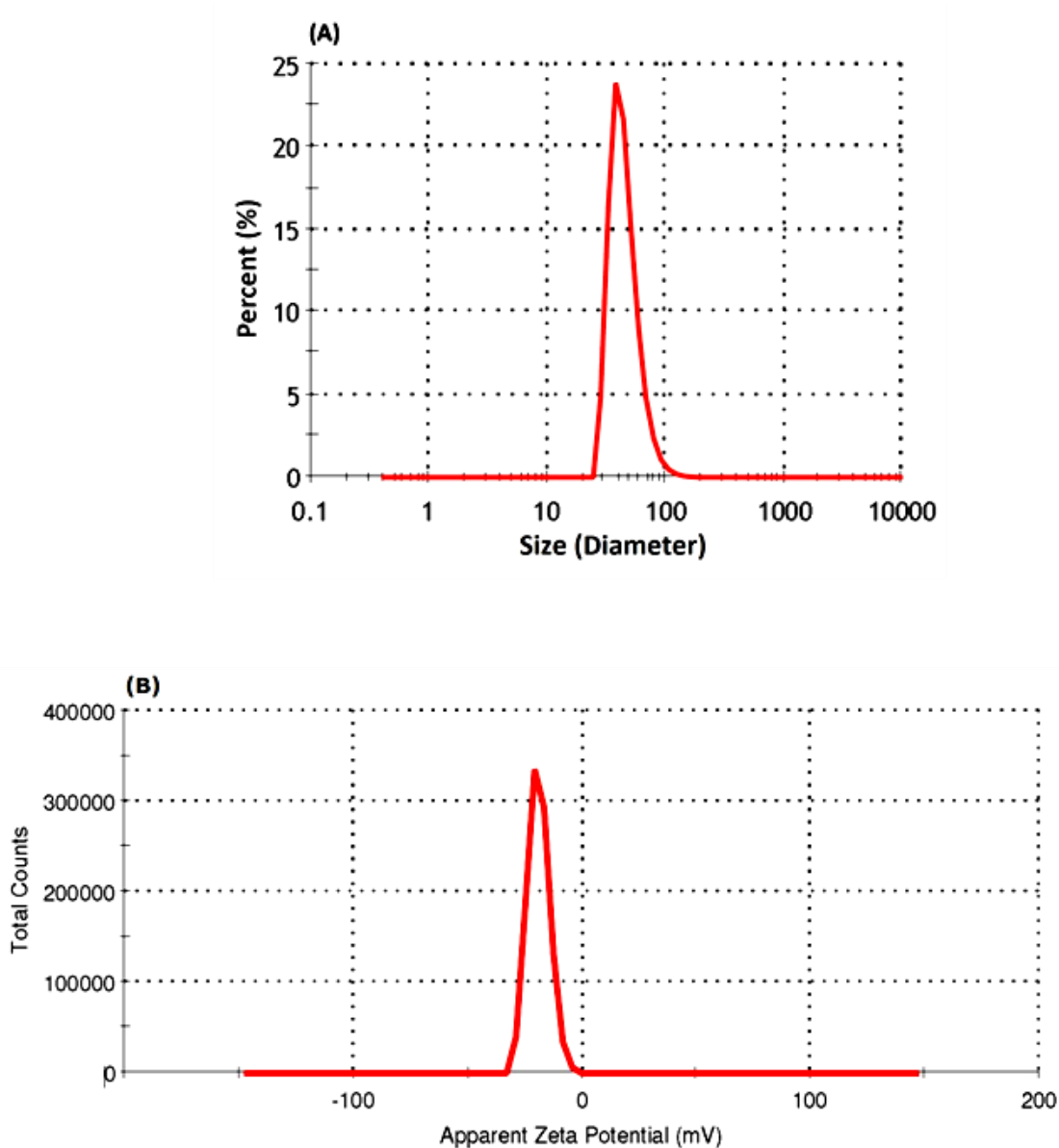
Figure 4.54 (A) Particle size by number and (B) zeta potential distribution of biosynthesized CasCuNPs.

The particle size distribution and Zeta potential of the phytosynthesized CisCuNPs using freshly squeezed orange (*Citrus sinensis*) juice extract are revealed in Figure 4.55. Particle dimension distribution by number has revealed the z-average of CisCuNPs as 17.58 nm. The mean potential value has been found as -25.60 mV for this copper NPs sample.
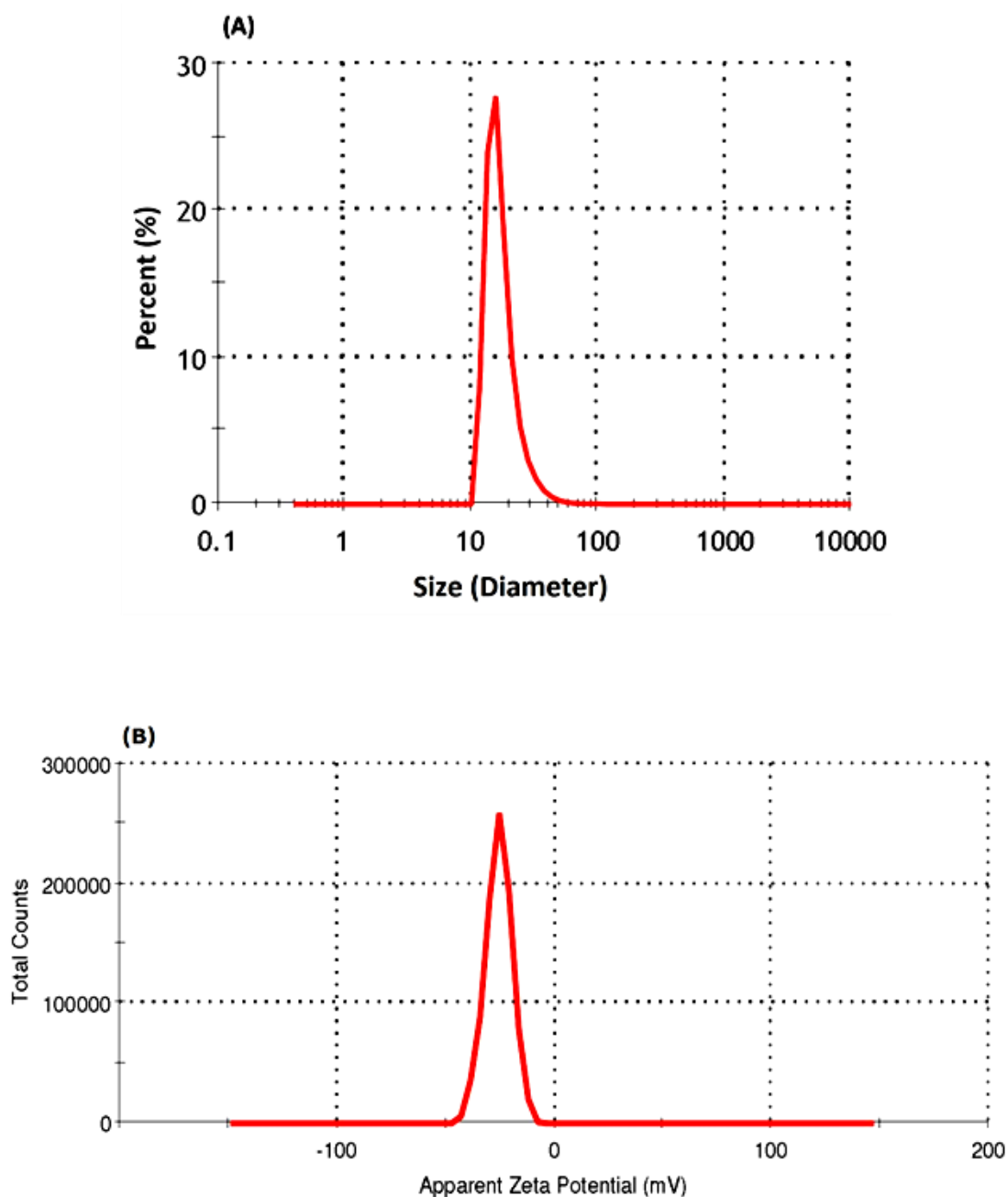
Figure 4.55 (A) Particle size by number and (B) zeta potential distribution of biosynthesized CisCuNPs.

The particle size distribution and Zeta potential of the phytosynthesized PibCuNPs using Turkish pine (*Pinus brutia*) bark extract are given in Figure 4.56. Z-average value for this copper nanoparticle sample has been recorded as 43.13 nm and the average potential value has been found to be -23.80 mV.
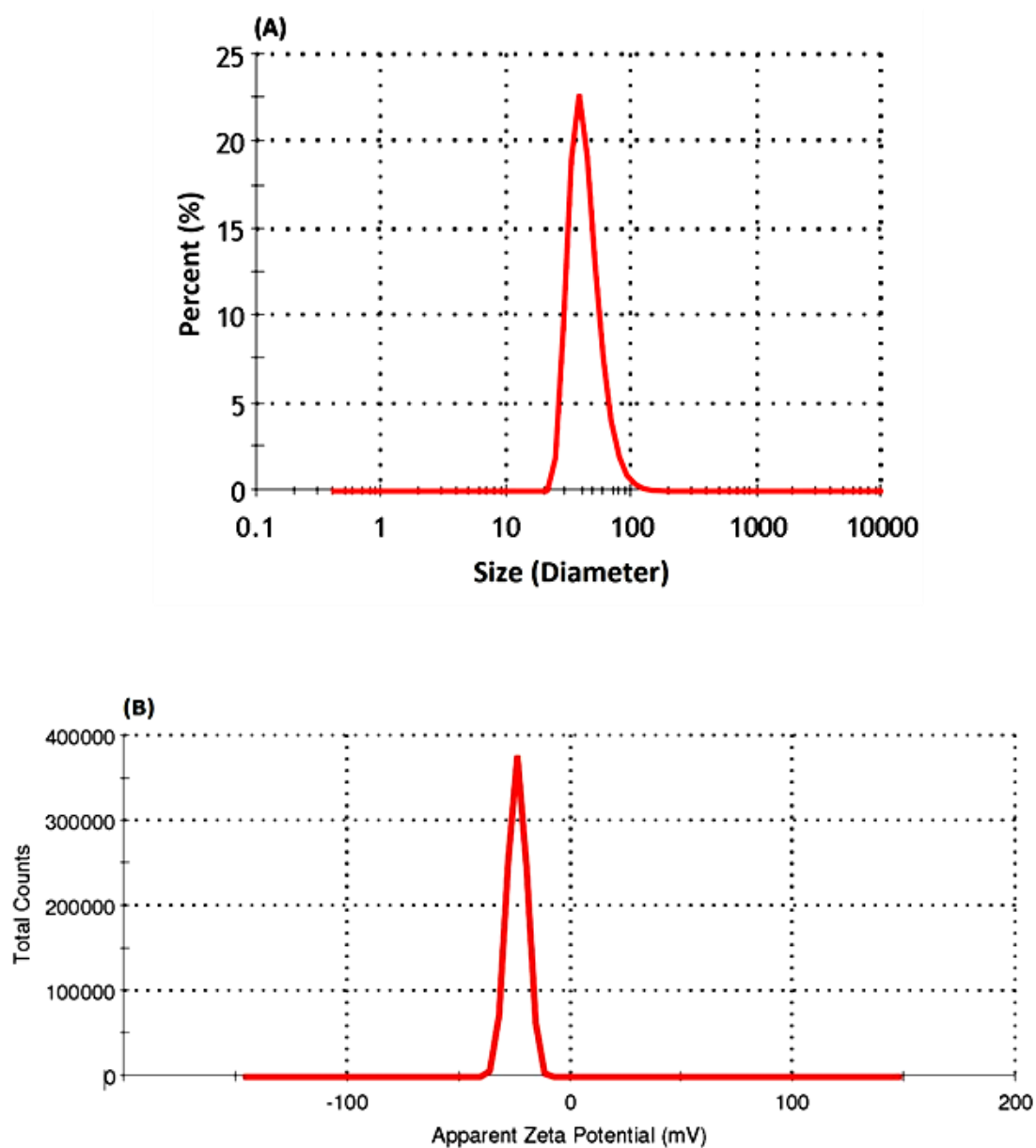
Figure 4.56 (A) Particle size by number and (B) zeta potential distribution of biosynthesized PibCuNPs.

4.2.2.6 TEM Analysis

TEM analysis has been performed for four different phytosynthesized copper nanoparticle samples to inspect the course of construction of CuNPs and to evaluate the morphology and size distribution of these NPs.

TEM profile of biosynthesized ZioCuNPs by the fresh ginger (*Zingiber officinale*) rhizome extract has revealed that the particles have been morphology roughly round or globular in shape with the distribution range of 11.32 nm to 33.70 nm in diameter (Figure 4.57).
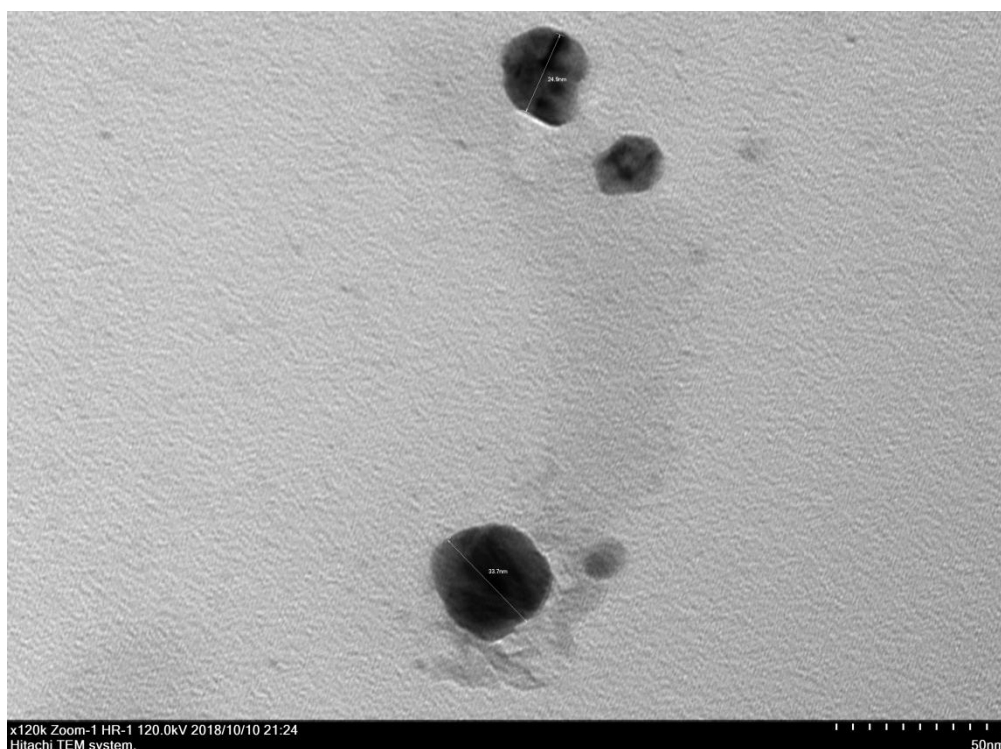
Figure 4.57 The TEM image of biosynthesized ZioCuNPs at 50 nm scales.

Figure 4.58 illustrates TEM image has been traced from the drop-coated specimen layer of the CasCuNPs, biosynthesized by treating the copper sulphate pentahydrate salt solution with green tea (*Camellia sinensis*) extract. CasCuNPs at 50 nm scales have dispersed approximately in between 17.59 nm and 149.92 nm by globular and oval assemblies.

TEM profile of biosynthesized CisCuNPs using freshly squeezed orange (*Citrus sinensis*) juice extract revealed that the monodisperse particles have been morphology

roughly round in shape with the distribution range of 6.93 nm to 20.70 nm in diameter (Figure 4.59).
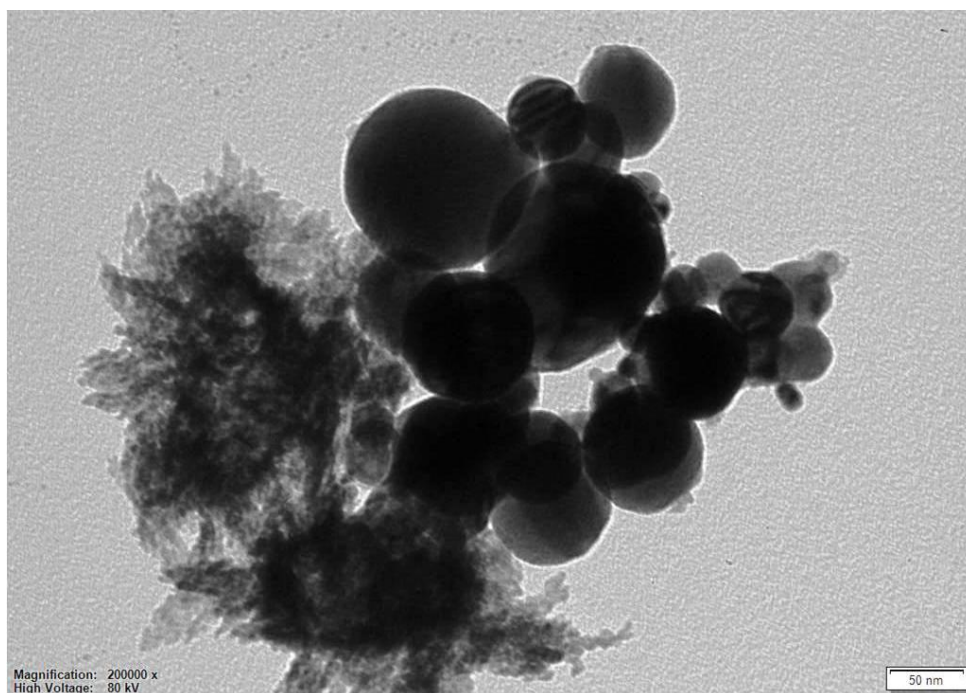
Figure 4.58 The TEM image of biosynthesized CasCuNPs at 50 nm scales.
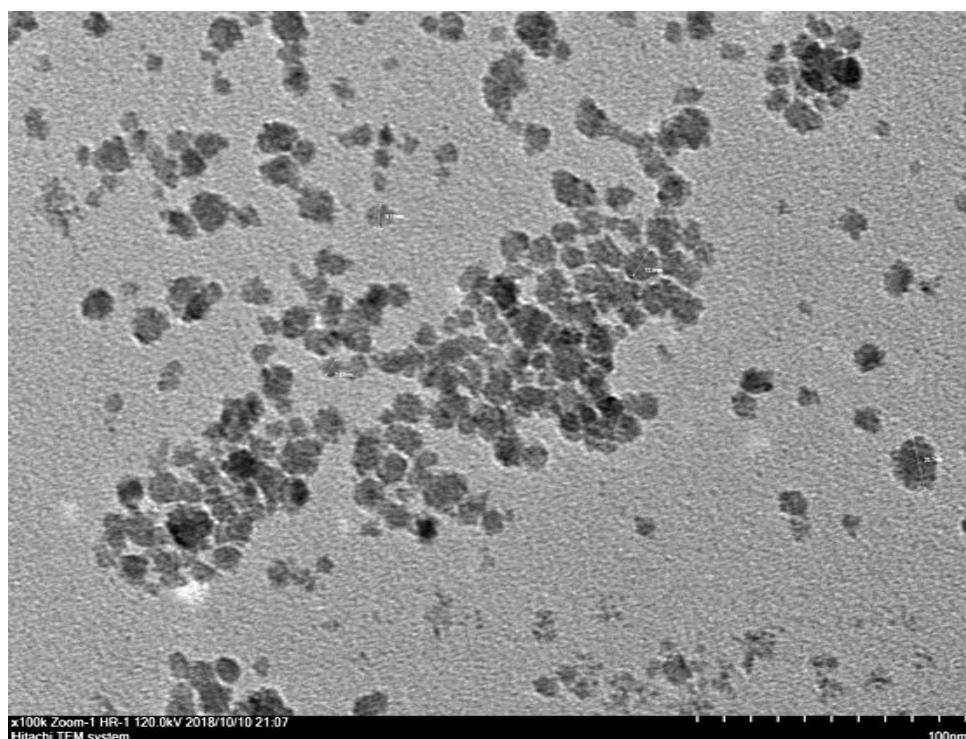
Figure 4.59 The TEM image of biosynthesized CisCuNPs at 100 nm scales.

TEM revealed the formation of the biosynthesized PibCuNPs using Turkish pine (*Pinus brutia*) bark extract (Figure 4.60). The nanoparticles are roughly oval in shape and approximately, the largest particle size is of 76.35 nm in diameter while the smallest size has been found to be around 27 nm.
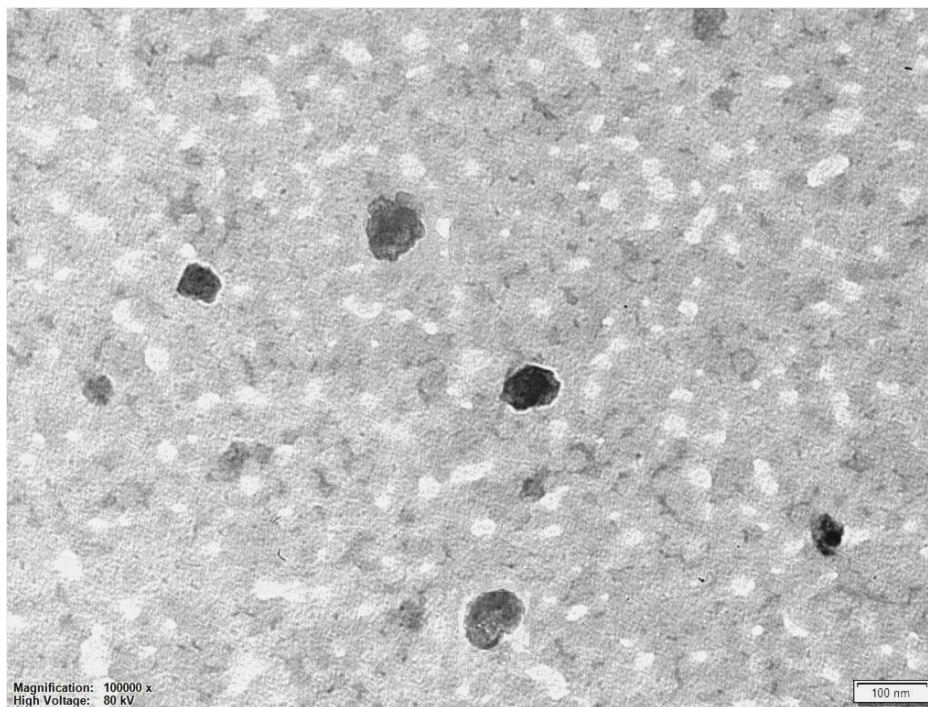
Figure 4.60 The TEM image of biosynthesized PibCuNPs at 100 nm scales.

4.3 Antimicrobial Study of Phytosynthesized Nanoparticles

Antibacterial effects of phytosynthesized silver and copper NPs have been studied against both Gram-Positive and Gram-negative bacteria. Lyophilized cultures of *Escherichia coli* (ATCC 25922) and *Staphylococcus aureus* (ATCC 25923) have been applied and designed for the antibacterial assays which were carried out by disc diffusion assay or agar diffusion assay method. 5 μg of each powdered nanoparticle samples have been suspended in 5 mL of ultra-purified deionized water that applied as the working concentration. In the Muller–Hinton agar plate medium, a volume of 50 μL of aliquot parts of nanoparticle solutions has been used to pour each medium well (7 mm in diameter). The antibacterial actions and potentials of both AgNPs and CuNPs have been resolute in contrast of standard antibiotic discs of gentamicin (10 μg discs; B.D., USA).

4.3.1 Antibacterial Potential of Phytosynthesized AgNPs

The results have disclosed that various biosynthesized silver nanoparticle samples have had efficient antibacterial potential. Remarkable inhibition zones have been observed in case of both Gram-positive (*S. aureus*) and Gram-negative (*E. coli*) bacterial strains by synthesized AgNPs, revealed in Table 4.3, Figure 4.61 and Figure 4.62.

Biosynthesized CcAgNPs using cumin seed extract with the inhibition zones of 12.53 ± 0.45 and 10.30 ± 0.36 mm and RsAgNPs by fresh rose petals extract with the inhibition zones of 11.73 ± 0.25 and 10.20 ± 0.36 mm have demonstrated highest antibacterial action against *S. aureus* and *E. coli* bacteria, respectively (Figure 4.61). Phytosynthesized MpAgNPs by fresh yellow delicious apple extract have also performed significant antibacterial activity against both bacteria with the inhibition zones of 10.20 ± 0.30 and 9.90 ± 0.50 (Table 4.3).

For ZoAgNPs by using fresh ginger rhizome extract, moderate zones of growth inhibition with 9.17 ± 0.70 mm have been observed against *S. aureus* bacterial strain whereas inhibition zones of 8.53 ± 0.32 and 8.27 ± 0.32 mm have intended for ClAgNPs and CsAgNPs using lemon peel and orange peel extracts, respectively. In case of *E. coli*, the growth inhibitions have been recorded as 8.47 ± 0.50 mm and 7.87 ± 0.35 mm, treating with ZoAgNPs and CsAgNPs, correspondingly (Table 4.3). However, the biosynthesized ClAgNPs did not show any noticeable inhibition zone against *E. coli* (Figure 4.61 and Figure 4.62).

Table 4.3 Zones of Inhibition (mm) in diameter of different AgNPs samples against experimented microorganisms by agar diffusion method.

Different samples of silver nanoparticle	Zones of inhibition (mm) against microorganisms	
	S. aureus	*E. coli*
MpAgNPs.	10.20 ±0.30	9.90 ± 0.50
CcAgNPs	12.53 ± 0.45	10.30± 0.36
ZoAgNPs	9.17± 0.70	8.47 ± 0.50
RsAgNPs	11.73± 0.25	10.20 ± 0.36
ClAgNPs	8.53 ± 0.32	_
CsAgNPs	8.27 ± 0.32	7.87 ± 0.35
Gentamicin	18.87 ± 0.70	21.20 ± 0.46

E. coli =Escherichia coli, S. aureus = Staphylococcus aureus. The individual data points have been articulated in the form of mean ± standard deviation (mean ± SD).

− Denotes no antibacterial activity.
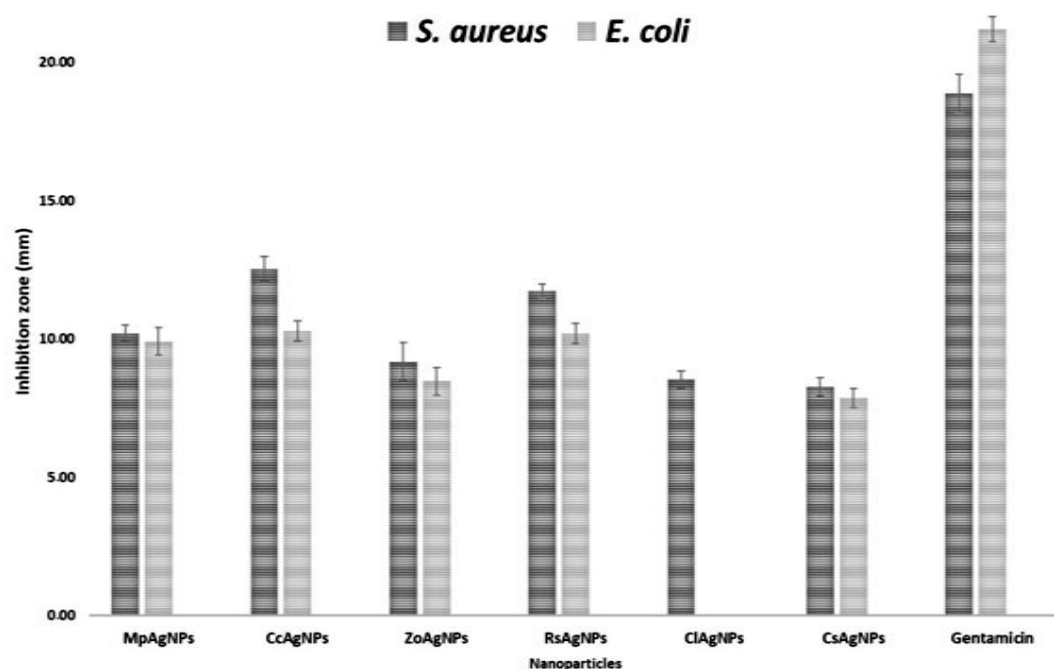
Figure 4.61 A comparative study of different AgNPs against two bacterial strains.
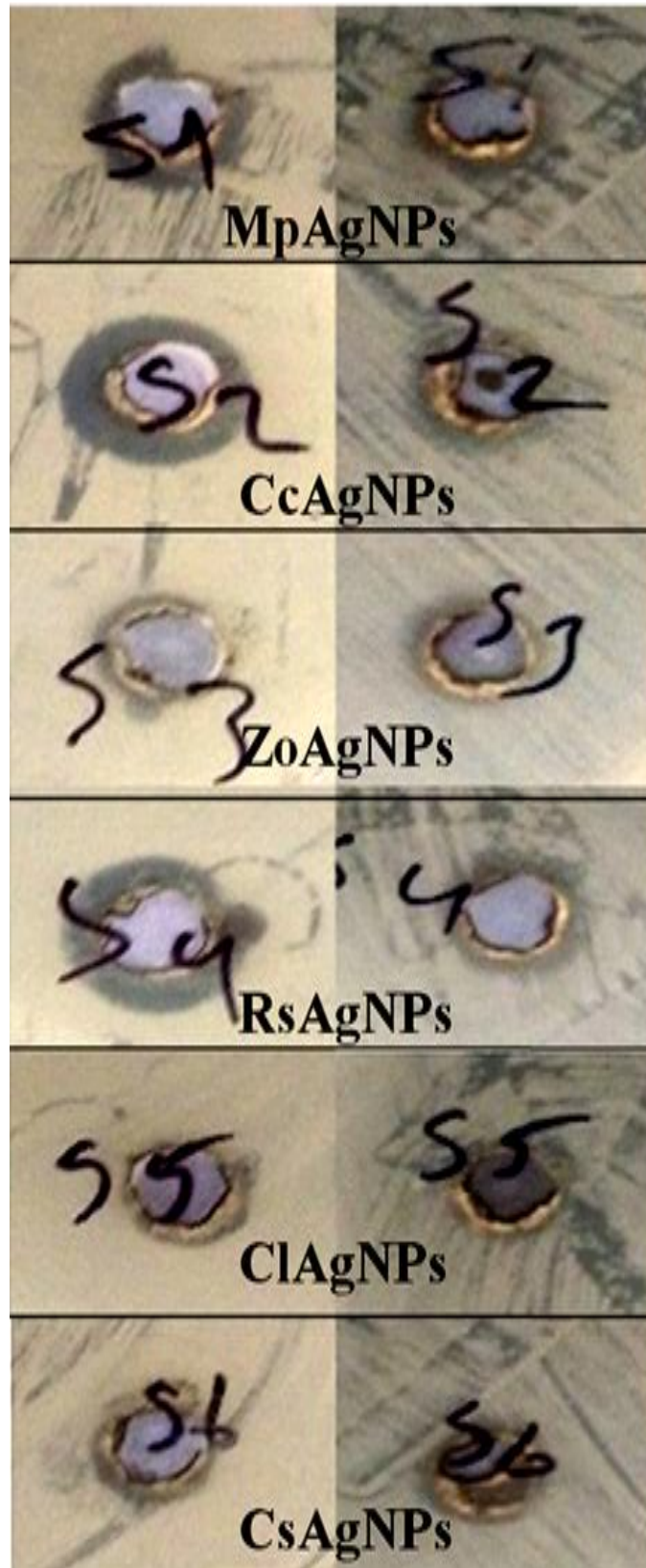
Figure 4.62 Inhibition zones of the AgNPs against tested microorganisms.

4.3.2 Antibacterial Potential of Phytosynthesized CuNPs

Four different copper nanoparticle samples have been used against both Gram-positive (*S. aureus*) and Gram-negative (*E. coli*) bacteria to evaluate their antibacterial capacity as given in Table 4.4, Figure 4.63 and Figure 4.64.

The biosynthesized CisCuNPs using freshly squeezed orange juice extract have showed the utmost antibacterial action against both *S. aureus* and *E. coli* with inhibition zones of 12.60 ± 0.20 and 10.83 ± 0.81 mm, respectively (Table 4.4). An effective zone of inhibition (12.07 ± 0.38 mm) has been found for *S. aureus* by phytosynthesized PibCuNPs using Turkish pine bark extract whereas this nanoparticle did not show any noticeable antibacterial action against *E. coli*. Biosynthesized ZioCuNPs by the fresh ginger rhizome extract with the inhibition zones of 8.27 ± 0.23 and 9.63 ± 0.31 mm have demonstrated extraordinary antibacterial potential against *S. aureus* and *E. coli* bacteria, correspondingly. Nevertheless, biosynthesized CasCuNPs using green tea extract did not showed any zone of inhibition against *S. aureus* and *E. coli* bacteria (Figure 4.63 & Figure 4.64).

Table 4.4 Zones of Inhibition (mm) in diameter of different CuNPs samples against experimented microorganisms by agar diffusion method.

Different samples of Copper nanoparticle	Zones of inhibition (mm) against microorganisms	
	S. aureus	*E. coli*
ZioCuNPs	8.27 ± 0.23	9.63 ± 0.31
CasCuNPs	–	–
CisCuNPs	12.60 ± 0.20	10.83 ± 0.81
PibCuNPs	12.07 ± 0.38	–
Gentamicin	18.87 ± 0.70	21.20 ± 0.46

E. coli = Escherichia coli, S. aureus = Staphylococcus aureus. The individual data points have been articulated in the form of mean ± standard deviation (mean ± SD).

– Denotes no antibacterial activity.
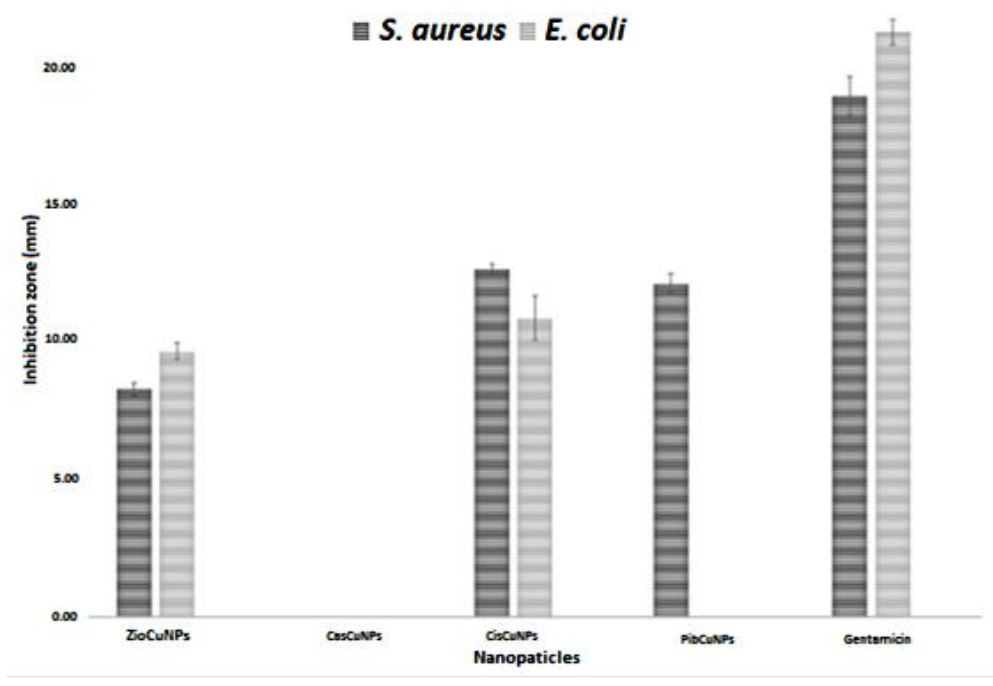
Figure 4.63 A comparative study of different CuNPs against two bacterial strains.
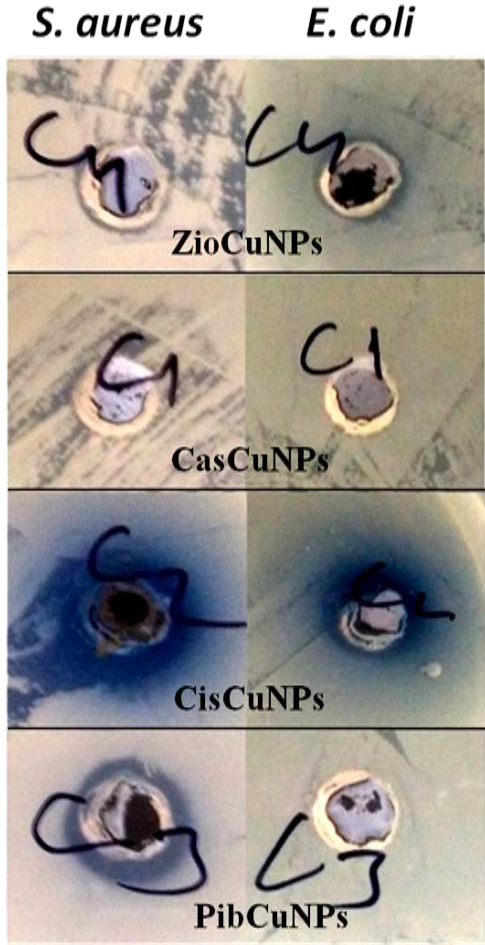
Figure 4.64 Inhibition zones of the CuNPs against tested microorganisms.

135

4.4 Cytotoxicity Study of Phytosynthesized Nanoparticles

The in-vitro cytotoxic effects of different samples of both AgNPs and CuNPs have been experimented against healthy regular mouse fibroblasts cell line (L929) through XTT cell viability assay.

As a consequence of mitochondrial activity, XTT changes to orange-coloured water-soluble dye which is the basic principle of XTT cell viability assay to test the cell viability. Simply, living and existing cells are capable of converting XTT reagent; hence, the optical absorbance peak value is directly related to cell viability.

The cell viability (%) has been calculated by using Equation 4.1 as follows:

$$\%\text{Cell viability} = \frac{\text{Optical density of sample}}{\text{Optical density of control}} \times 100 \tag{4.1}$$

Correspond to ISO 10993-5 standards, the percentage (%) of cell viability higher than 80% is measured as non-cytotoxic; in between 80% and 60% considered as weak cytotoxic; from 60% to 40% counted as moderate cytotoxic and beneath 40% estimated as strong cytotoxic [272], [273].

4.4.1 Cytotoxicity Study of Biosynthesized Silver Nanoparticles

Cytotoxic effect of phytosynthesized MpAgNPs by apple pulp extract, CcAgNPs by cumin seed extract, ZoAgNPs by fresh ginger rhizome extract, RsAgNPs by rose petal extract, ClAgNPs by lemon peel extract and CsAgNPs by orange peel extract have been examined in the given proportions (0.1μg/mL to 5μg/mL).

For all six silver nanoparticle samples, the percentage of cell viability is more than 90% in each concentration of nanoparticles. According to results, none of the nanoparticles has toxicity on L929 cells in given concentrations (Figures 4.65 to 4.70).
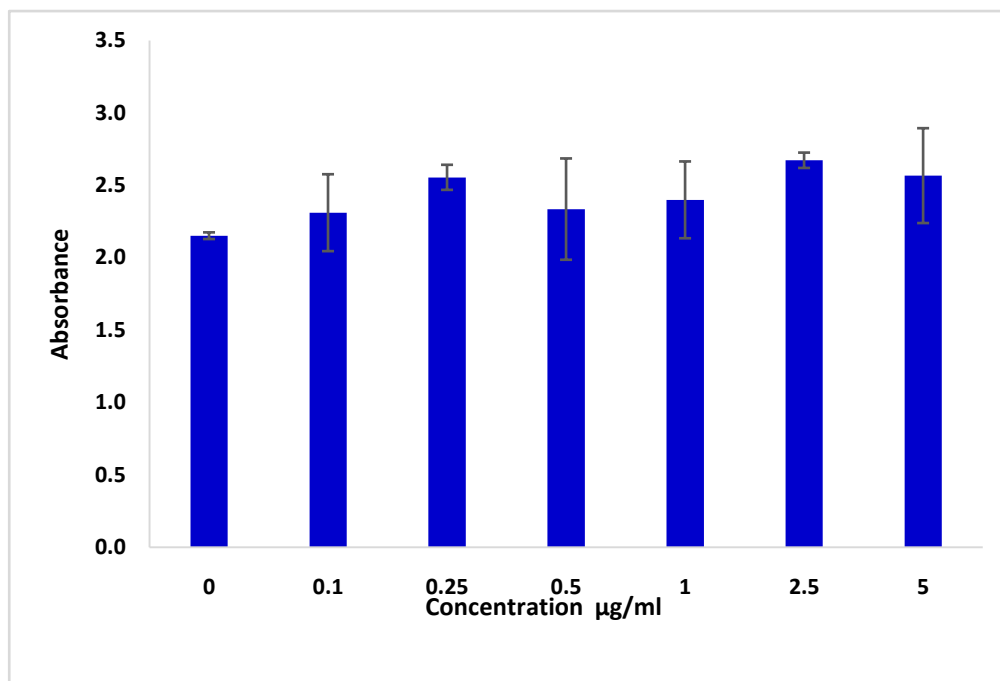
Figure 4.65 Cytotoxic effect of phytosynthesized MpAgNPs on L929 cells.
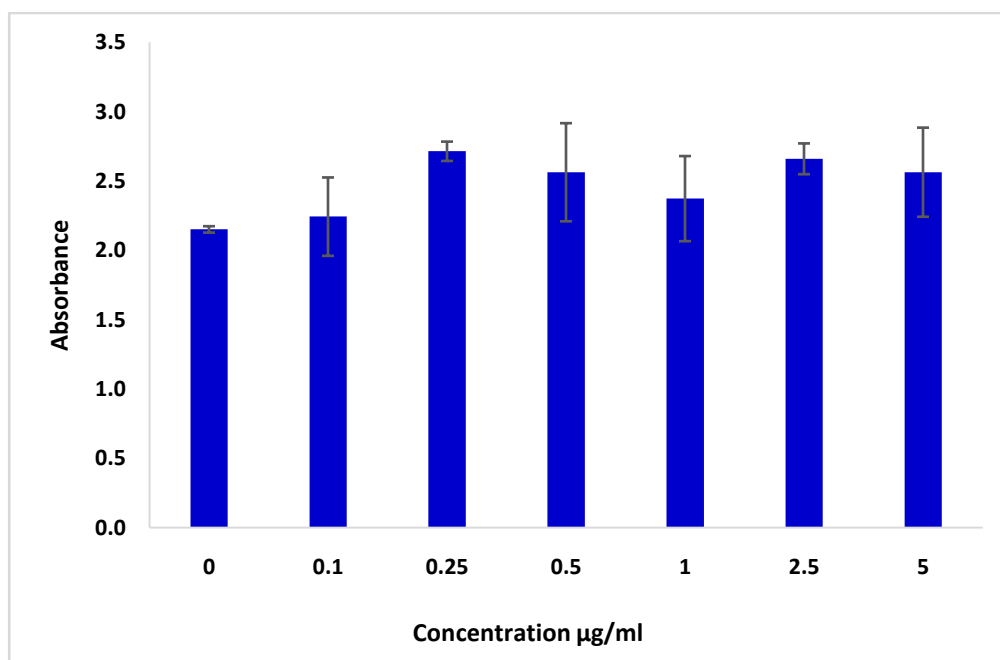
Figure 4.66 Cytotoxic effect of phytosynthesized CcAgNPs on L929 cells.
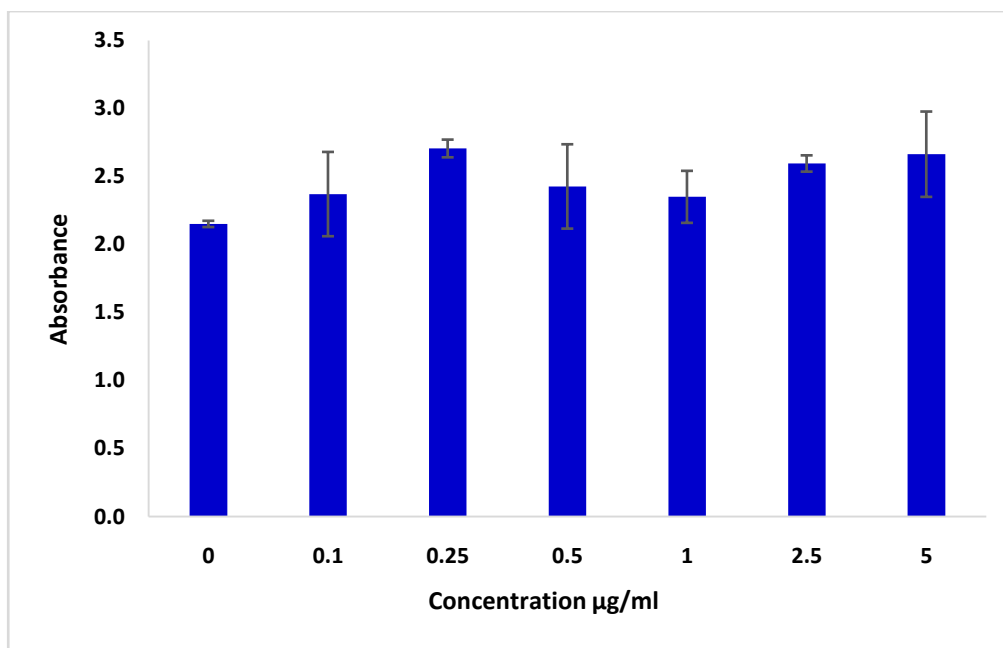
Figure 4.67 Cytotoxic effect of phytosynthesized ZoAgNPs on L929 cells.
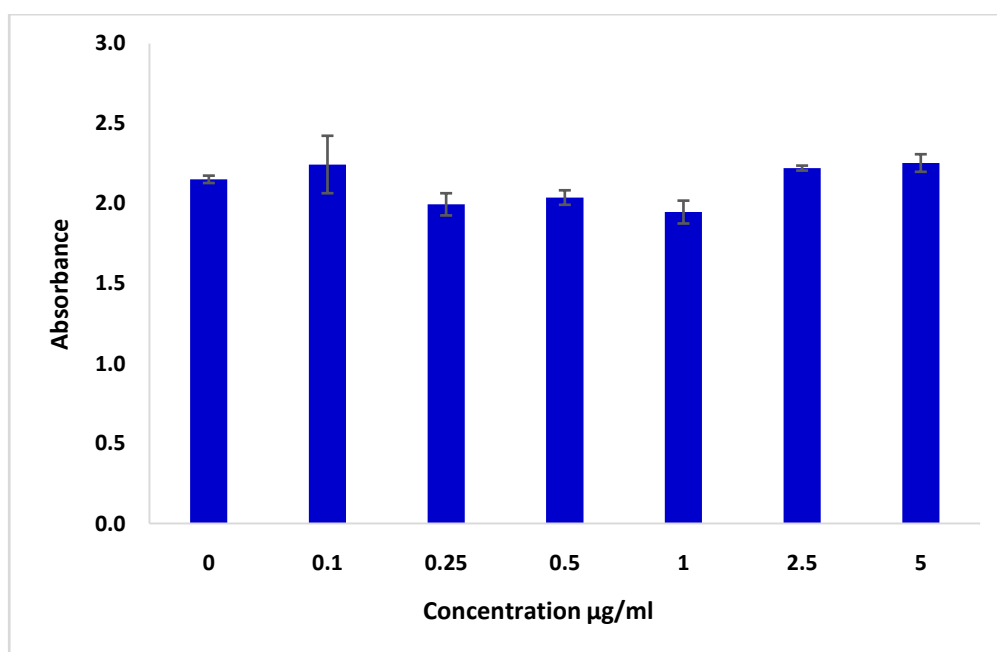
Figure 4.68 Cytotoxic effect of phytosynthesized RsAgNPs on L929 cells.
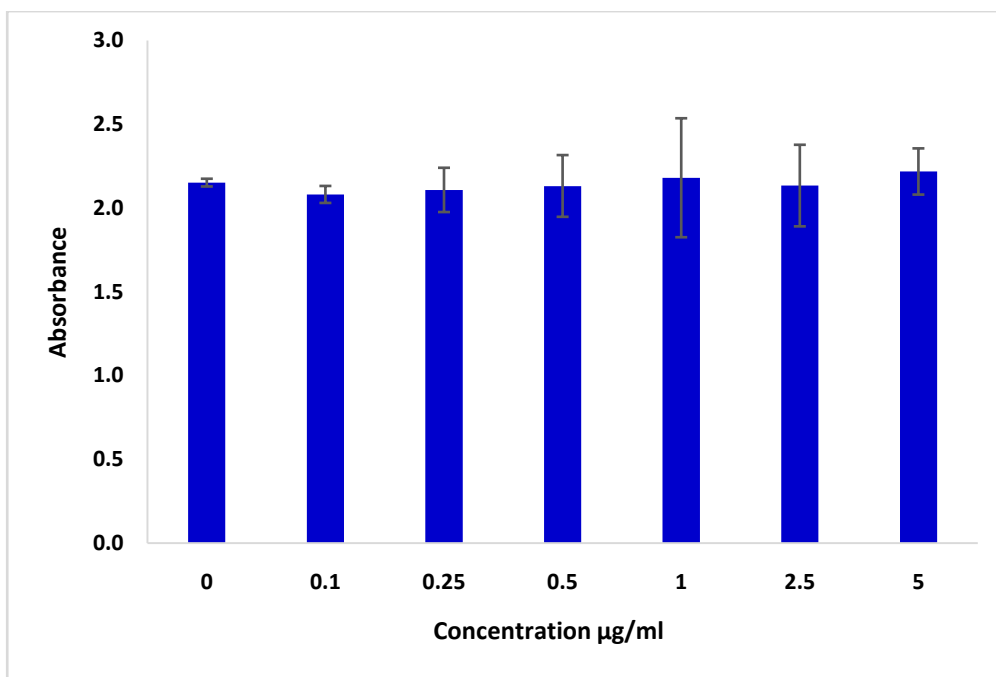
Figure 4.69 Cytotoxic effect of phytosynthesized ClAgNPs on L929 cells.
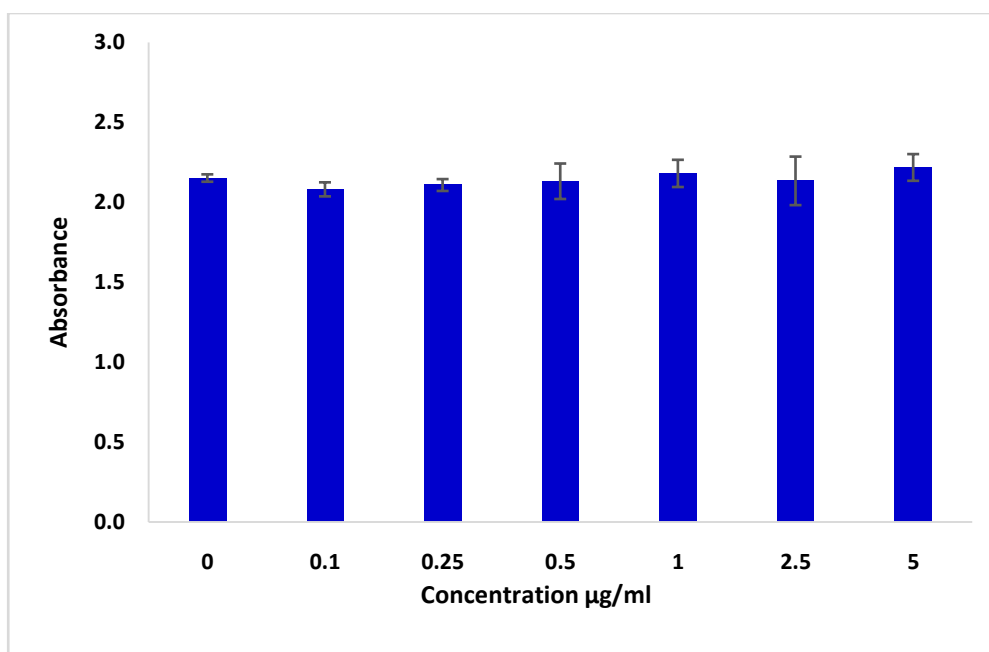
Figure 4.70 Cytotoxic effect of phytosynthesized CsAgNPs on L929 cells.

4.4.2 Cytotoxicity Study of Biosynthesized Copper Nanoparticles

In-vitro cytotoxic effect of phytosynthesized ZioCuNPs by the fresh ginger rhizome extract, CasCuNPs by green tea extract, CisCuNPs using freshly squeezed orange juice extract and PibCuNPs using Turkish pine bark extract were examined in the given proportions (0.1μg/mL to 5μg/mL).

The percentage of cell viability is more than 90% in each concentration of copper nanoparticles. According to results, none of the copper nanoparticle sample has toxicity on L929 cells in given concentrations (Figures 4.71 to 4.74).
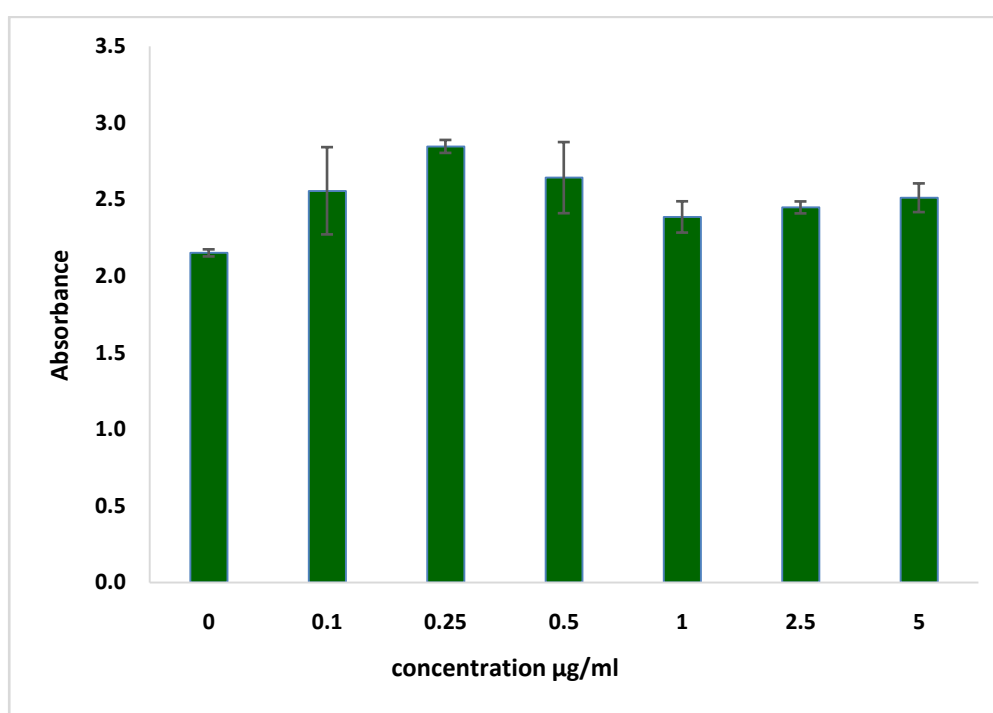
Figure 4.71 Cytotoxic effect of phytosynthesized ZioCuNPs on L929 cells.
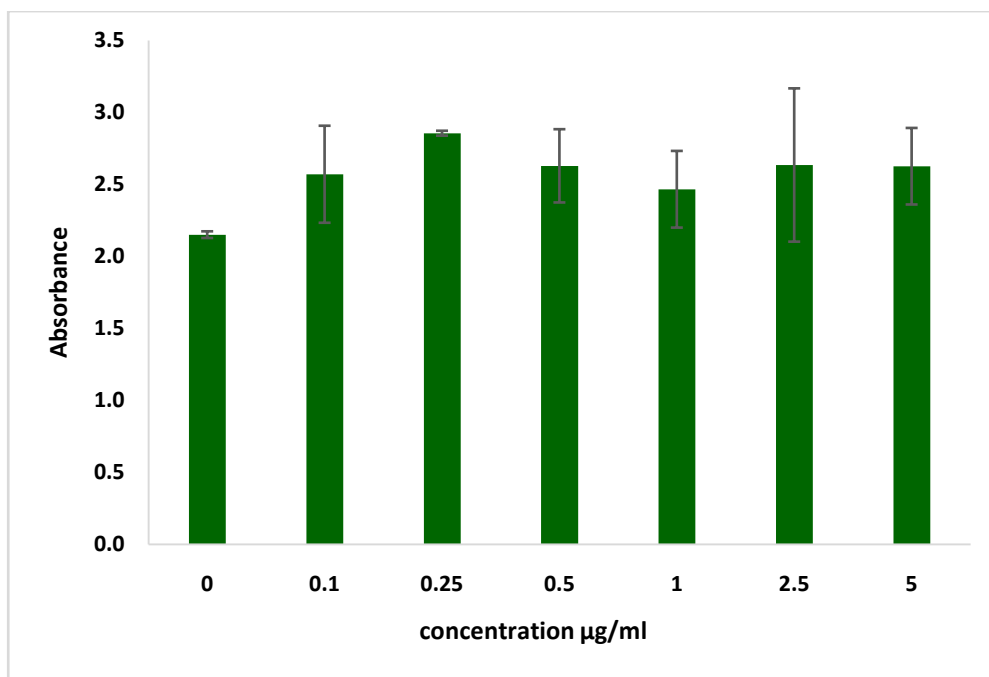
Figure 4.72 Cytotoxic effect of phytosynthesized CasCuNPs on L929 cells.
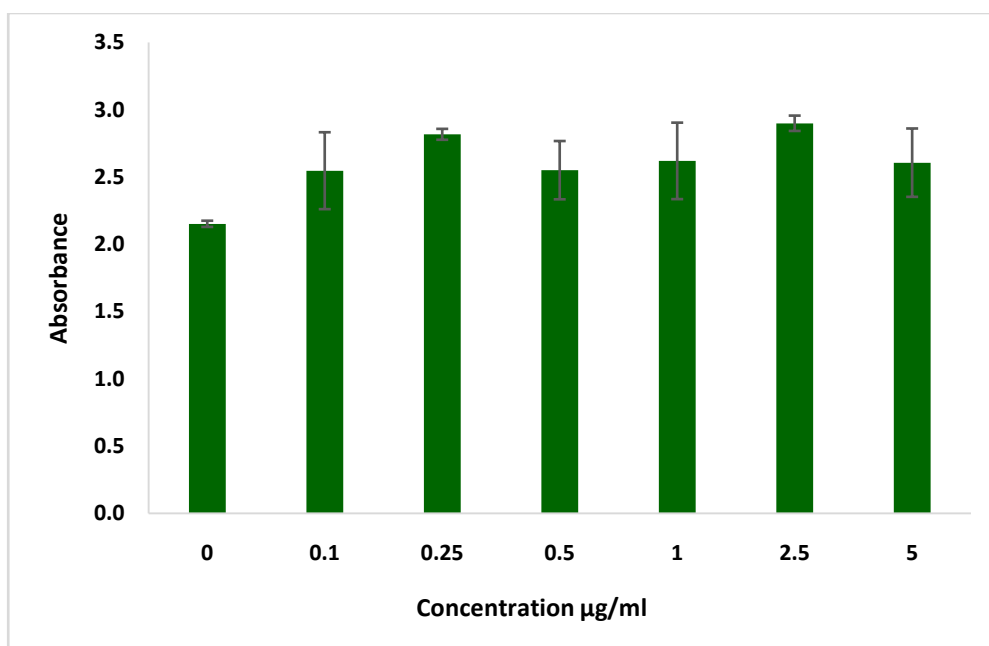
Figure 4.73 Cytotoxic effect of phytosynthesized CisCuNPs on L929 cells.
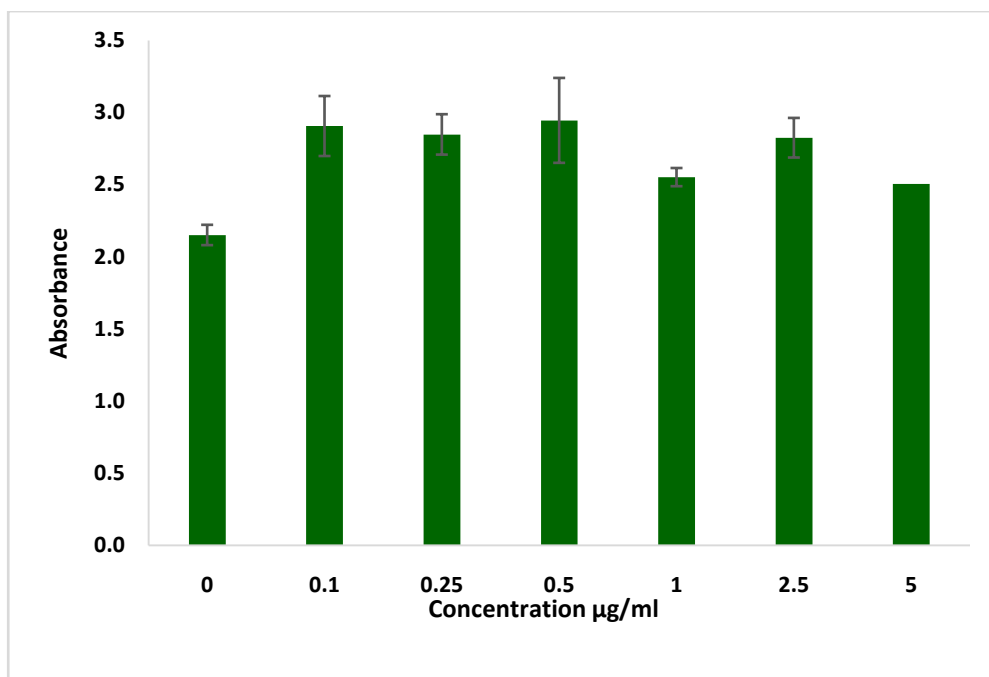
Figure 4.74 Cytotoxic effect of phytosynthesized PibCuNPs on L929 cells.

CHAPTER 5

CONCLUSIONS

The present investigation entitled "Green synthesis of metallic nanoparticles, their chemical and biochemical characterizations" has been conducted to study the phytosynthesis (plant based synthesis), characterization of silver (Ag) and copper (Cu) nanoparticles along with the evaluation of their antimicrobial and cytotoxicity potential. The study has reported the one-step microwave-irradiated biological fabrication of silver and copper nanoparticles. Using different aqueous plant extracts, metallic ions of silver and copper have been reduced to their metallic nanoparticles.

Moreover, in contrast to the conformist physical/mechanical and chemical protocols for the productions of metallic NPs, the bio-based scheme offers numerous benefits as because they utilize relatively inexpensive as well as comparatively simple and easily scaled-up nontoxic materials, in support of extensive production [60]. However, there are some considerable obstacles in conventional green synthesis procedure that might have an effect on the quantity and quality of biosynthesized nanoparticles. The most noticeable drawback of conventional green chemistry is that, in contrast of the chemical or physical methods, it requires much longer time for the synthesis which may influence the aggregation of NPs [274].

Considering these weakness, microwave-assisted green synthesis is an easy remedy to this problem. However, the green synthesis of nanoparticles with microwave-assisted heating technique offers some extra benefits in contrast to the conventional green synthesis. This is because of the fact that the microwave-assisted heating technique provides increased reaction kinetics and boosts reaction rates helping accelerate the higher yields along with the desirable quality.

It was reported that, in contrast to the conventional heating methods used in regular NPs synthesis process, microwave irradiated heating system produces nanoparticles of

privileged quality and quantity like the high crystallinity in NPs along with the narrower and smaller dimensions in the biosynthesis of NPs. By using microwave irradiation heating, it is possible to conduct a rapid synthesis which might offers controlled and desirable morphology of the nanostructured materials [274]. It is further reported from some previous studies that, in contrast to the conventional biosynthesis protocols, the microwave-assisted biosynthesis produce higher reaction kinetics that pilot to accelerated robust reactions by using equivalent synthesis temperatures as well as similar amount of time [275].

Microwave parameters have been optimized for two factors (i.e. time and temperature) in this study. Aqueous extracts of yellow delicious apple (*Malus pumila*) pulp, cumin (*Cuminum cyminum*) seeds, fresh ginger (*Zingiber officinale*) rhizome, fresh rose (*Rosa santana*) flower petals, lemon (*Citrus limon*) and orange (*Citrus sinensis*) peel have been used to synthesize AgNPs. On the other hand, CuNPs have been successfully synthesized by using the aqueous extracts from ginger (*Zingiber officinale*) rhizome, green tea (*Camellia sinensis*), freshly squeezed orange (*Citrus sinensis*) juice and Turkish pine (*Pinus brutia*) bark.

Using microwave technology, plant extracts have been mixed with silver nitrate (AgNO$_3$) and copper sulphate pentahydrate (CuSO$_4$.5H$_2$O) salt solutions in desirable proportions to reduce the silver and copper ions into AgNPs and CuNPs, respectively.

Meanwhile, during the syntheses, the fabrications of NPs have been followed by an immediate colour change of the aqueous extract medium. After successful syntheses of AgNPs and CuNPs, detailed chemical and biochemical characterizations of these metallic nanoparticles have been conducted by means of UV-Vis spectroscopy, X-Ray Diffraction (XRD) analysis, Fourier Transforms Infrared (FTIR) spectroscopy, Transmission Electron Microscopy (TEM) and particle size distribution and Zeta potential measurement.

Initially, the formations of both silver and copper nanoparticles have been monitored via UV-Vis spectroscopy. It is an important and reliable process of investigation for identifying the Surface Plasmon Resonance (SPR) features of NPs. This is due to the fact that every noble metal is known to exhibit unique and distinctive optical features because of the property of the SPR. In the UV−Vis analysis, the free electrons of metallic NPs could provide the distinctive SPR absorption bands while these free

electrons create a combined vibration with specific light wave of the ultraviolet-visible range [276].

By the UV–Vis absorption spectroscopy, six different biosynthesized silver nanoparticle samples showed sharp, strong and broad absorption bands from 435 nm to 445 nm. Different literatures also support that the development or fabrication of silver nanoparticles (AgNPs) were recorded by the UV–Vis absorption spectra at which showed SPR peak, ranged between 400 nm and 450 nm [277], [278]. Balashanmugam *et al.* (2014) investigated the synthesized silver nanoparticles from orange peel had a plasmon absorption band of 435 nm after 48 hrs [279]. Chauhan *et al.* (2011) used pomegranate fruit seeds for silver nanoparticles synthesis which revealed a peak of λ_{max} at 430 nm [280]. Iravani and Zolfaghari (2013) have reported that biosynthesized silver nanoparticles using *Pinus eldarica* bark extract showed absorbance maximum occurring at λ_{max} = 430 nm [281]. Furthermore, in the study by Premasudha *et al.* (2015), the biosynthesized AgNPs were verified by characteristic UV-vis bands from 400 nm to 440 nm [282]. Yallappa *et al.* (2013) studied microwave assisted biosynthesis of AgNPs using seed extract of Sweet Acacia (*Acacia farnesiana*) and have found that depending on the exposure time, the wavelength of the maximum absorption peaks varied from 430 to 450 nm [283].

Furthermore, In the UV-Vis spectra, all four copper nanoparticles showed the strong SPR peaks of λ_{max} from 560 nm to 573 nm. The UV-Vis results of CuNPs are also similar or closed to previous literatures. Dang *et al.* (2011) demonstrated that the absorption bands of the CuNPs varied from 562 to 572 nm, depending on the exposure time during synthesis [284]. Besides, Khodaie and Ghasemi (2018) studied green synthesis of CuNPs using *Eryngium campestre* leaf extract and found that the wavelength of the maximum absorption of metallic copper nanoparticles showed at 570 nm [285]. Basavarajappa and Neelagund (2016) used silkworm fecal matter for CuNPs synthesis which revealed a peak of λ_{max} at 560nm [286]. Usha *et al.* (2017) have reported that biosynthesized copper nanoparticles using tulasi (*Ocimum sanctum* L.) leaves extract showed absorbance maximum occurring at 560 nm (λ_{max}). [287]. Therefore, the abovementioned results of the UV–Vis absorption spectroscopy obtained from our study are in agreement with these studies for the fabrication of metallic nanoparticle; the silver and copper nanoparticles.

Furthermore, analyses by means of the FTIR (Fourier-Transform Infrared spectroscopic) of both biosynthesized silver and copper nanoparticles have revealed the possible biological molecule available in different aqueous plant extractions. This analysis also divulges the functional groups of these biomolecules which might play significant roles as reducing, synthesizing, capping and stabilizing factors for nanoparticle fabrications. Moreover, the frequent functional groups existing in the bio-extracts such as alkane (-C-H bending, C-H stretch) bonds, free hydroxyl (-OH) stretch, alkene (=CH bending, C=C stretch) bonds, carbonyl (C=O) and NH_2 groups have been verified through the standard IR-correlation table. Supporting theses exiting groups, FTIR data therefore have confirmed that these phytosynthesized nanoparticles were enclosed and attached by some reducing sugars, amino acid residues, proteins as well as some metabolites such as flavanones or terpenoids [288]. Besides that, IR spectra also has indicated that the protein molecules probably might create a coating layer encapsulating these metallic NPs (capping of both AgNPs and CuNPs) to prevent aggregation, and agglomeration as well as stabilizing these nanoparticles, which thereby are in agreement with the previous reports [289], [290]. Therefore, It can concluded that all those biological molecules of plant extracts could have carried out their binary functions for the fabrication as well as for the stabilization of silver (AgNPs) and copper (CuNPs) nanoparticles in the reaction medium.

Furthermore, different dried powder samples of both AgNPs and CuNPs have been identified through X-ray diffraction analysis. It has been considered as a very important key instrument to generate and evaluate the tertiary structures with mean size allocation over and above the crystallinity of particles at molecular levels [127]. XRD patterns have been utilized for confirming the crystallinity of phytosynthesized silver and copper nanoparticles. All silver nanoparticle samples have showed four strong reflections correspond to the planes of (111), (200), (220) and (311), whereas all copper nanoparticle samples have provided five strong reflections correspond to the planes of (111), (200), (220), (311) and (222). These planes are the characteristic Bragg's diffraction plans for silver and copper with face-centered cubic crystalline structures which support or coordinate the database of the JCPDS (Joint Committee on Powder Diffraction Standards) file no: 04–0783 and file no: 04-0784, respectively [268], [269], [291], [292].

Comprehensive analyses of both silver and copper nanoparticles have been carried out through TEM (Transmission Electron Microscopy) technique, zeta potential measurement with particle size distribution. TEM has provided direct images that help to determine the morphology and biochemical details of materials at nano level. This is due to the fact that TEM micrographs offered Informations at spatial resolution down to the level of atomic dimensions.

Conversely, Zeta sizer has been applied for perceiving the average particle size diameter (nm) of biosynthesized silver (AgNPs) and copper (CuNPs) nanoparticles. Besides, the interface extended net charges of the solid surface of nanoparticles have been calculated by the means of Zeta potential [98]. Likewise, zeta potential is also the effective electric charge on the nanoparticle surface and therefore it is needed to compute and evaluate the constancy and stability of metallic NPs by their potential values. Besides, the zeta potential charges of AgNPs and CuNPs are significantly essential for many appliance i.e. antimicrobial activities of NPs [293].

The TEM micrographs of both AgNPs and CuNPs have showed an organic coating layer around the NPs, possible came from biobased biochemical compounds. These surrounding layers the phytosynthesized nanoparticles might elucidate the excellent dispersion of these phytosynthesized NPs in solution [294].

The morphologic micrographs of all AgNPs and CuNPs generated by TEM analysis have showed the presence of nearly spherical or globular or oval shaped nanoparticles. However, for both biosynthesized AgNPs and CuNPs, the size range of the nanoparticles from TEM image and the mean dimensions of the particles from Zeta sizer analysis have varied for different plant samples. Besides, the nanoparticle samples with the smallest size ranges have showed the highest negative potential values.

Among all six silver nanoparticle samples, the smallest size range (1.84 nm - 20.57 nm) along with the mean diameter of 14.30 nm has been monitored for the biosynthesized CcAgNPs using cumin (*Cuminum cyminum*) seed extract. Moreover, CcAgNPs have also showed highest negative potential value and that is -27.8 mV. Besides, the largest size range (7.5 nm - 69.83 nm) along with the average diameter of 41.86 nm has been found for the biosynthesized ClAgNPs using lemon (*Citrus limon*) peel extract. The average zeta potential value of ClAgNPs has been observed as -18.70 mV which is the lowest among all AgNPs samples.

However, the average size diameter (48.05 nm), calculated for phytosynthesized RsAgNPs by using *R. santana* petal extract has exhibited as the highest value among all silver nanoparticle samples albeit showing smaller particle size range (6.527 nm to 25.247 nm) by TEM profile. However, it is remarkable that the z-average size destitution can be larger than the size distribution by surface imaging method i.e. TEM, SEM etc, unless the nanoparticles are all identical [293], [294].

Likewise, among all four copper nanoparticles, the smallest particle size range (6.93 nm to 20.70 nm) by the average size dimension of 17.58 nm in diameter has been observed for the biosynthesized CisCuNPs using freshly squeezed orange (*Citrus sinensis*) juice extract. CisCuNPs also has owned the highest negative potential value (-25.6 mV) among all CuNPs. On the other hand, the largest particle size range (17.59 nm to 149.92 nm) by the average size dimension of 45.30 nm in diameter has been found for the biosynthesized CasCuNPs using green tea (*Camellia sinensis*) extract. The average zeta potential value of CasCuNPs was -19.0 mV which is the lowest among all CuNPs samples.

Antibacterial potentials of both silver and copper nanoparticles have been examined against both Gram-Positive and Gram-negative bacterial strains. Lyophilized cultures of *Staphylococcus aureus* (ATCC 25923) and *Escherichia coli* (ATCC 25922) have been treated for the antibacterial assays by disc diffusion assay or agar diffusion assay method. 5 µg of the powdered nanoparticle samples have been suspended in 5 mL of ultra-purified deionized water that applied as the working concentration and a volume of 50 µL of aliquot parts of nanoparticle solution has been used to pour a single well of the medium.

Yet, the exact antimicrobial mechanisms of metallic nanoparticles toward the microorganisms have not evidently clear. The key mechanism of inhibitory action of NPs perhaps correlated to the amalgamation of metallic NPs to the negatively charged bacterial cell wall, where they are efficient at interacting with sulphur and phosphorus containing compounds. This interaction might alter the permeability of the plasma membrane; disrupt the shape; inhabit cell growth and ultimately leads to cell death [218].

For both AgNPs and CuNPs, it has been found that the nanoparticle samples with the smallest particle size ranges and highest potential values have showed the best

antibacterial activities. Hence, for silver nanoparticle sample, the highest bactericidal effects have been shown by the biosynthesized CcAgNPs using cumin (*Cuminum cyminum*) seed extract with the zones of inhibition, 12.53 ± 0.45 mm with 10.30 ± 0.36 mm in diameter against *S. aureus* and *E. coli* bacteria, respectively. In contrast, the biosynthesized ClAgNPs using lemon (*Citrus limon*) peel extract had moderate zone of inhibition (8.27 ± 0.32 nm) against *S. aureus* while has not showed any inhibition zone against *E. coli* (Gram-negative bacteria).

As a consequence, among the copper nanoparticle samples, the biosynthesized CisCuNPs using freshly squeezed orange (*Citrus sinensis*) juice extract have confirmed the utmost antibacterial potential against both *S. aureus* and *E. coli* with zones of inhibition, 12.60 ± 0.20 and 10.83 ± 0.81 mm in diameter, correspondingly. An effective zone of inhibition (12.07 ± 0.38 mm) in diameter has been found for *S. aureus* by phytosynthesized PibCuNPs by using Turkish pine bark extract whereas this nanoparticle has not demonstrated any noticeable activity against *E. coli*. Nevertheless, biosynthesized CasCuNPs using green tea extract has not showed any acttivity against *S. aureus* and *E. coli* bacteria.

Variations and dissimilarities in the results are probably responsible for the structural and chemical nature of bacterial cell wall. The reasons for some silver and copper nanparticle samples not showing bactericidal activity against Gram-negative bacteria (*E. coli*) are the presence of an additional external surface layer on top of the peptidoglycan. These outer layers of the bacteria have been distinguished as extremely resistant and impermeable that might interrupt the access of metallic ions into the bacterial cell [295]. However, Gram-positive bacteria have polysaccharides in their cell wall called teichoic acid, which is negatively charged and have facilitated the passage of the positive metal ions [295].

On the other hand, morphological and physiochemical properties of nanoparticles are also play vital factors for their bactericidal properties [223]. Nanoparticles with smaller size distribution have high reactive surface to volume ratio compared to their bulk macromolecules [218], [227]. This distinctive feature of NPs might facilitate them to contact and interrelate easily with other particles. Hence, they are capable of interacting with the bacterial cell and trend to show stronger antimicrobial effect [224], [225]. Furthermore, the potential values of NPs also influence their bactericidal properties.

Nano-metallic particles with high potential charge could rapidly bind with surfaces of bacterial cells which might increase of the bactericidal effect as well [226], [296].

Furthermore, it is noticeable that silver nanoparticles showed stronger antibacterial potential then copper nanoparticles. Handling metallic copper nanoparticles is quite challenging because of its intense susceptibility to the air. When copper nanoparticles expose to the air they trend to form an oxidized layer which may reduce their antimicrobial potential, remarkably [244], [248], [297]. Moreover, XRD analysis of CuNPs also support the theory by indicating the presence of minute amount of oxidation as because the CuNPs have been briefly exposed to the air when moving inside the XRD chamber during the sample preparation which might be the reason for some copper nanoparticle samples not showing any bactericidal activity.

The in-vitro cytotoxic effects of both AgNPs and CuNPs have been monitored against healthy regular mouse fibroblasts cell line (L929) through XTT cell viability assay. According to results, the cell viability has not extensively affected by raising concentrations (0.1 to 5μg/mL) of NPs; therefore, none of the phytosynthesized nanoparticles has toxicity on L929 cells in given concentrations.

At the end, it can be concluded that the present investigation offers an environment friendly, nontoxic, quick and cost-effective way to synthesize nontoxic silver and copper nanoparticles. Operating microwave-assisted procedure, extracts from most available plants have been utilized as both reducing and capping agent for successfull syntheses of metallic silver and copper NPs. The fabricated AgNPs and CuNPs in powdered form have been remained stable for a period of nine months without agglomeration of particles. Considering antibacterial potentials and the results of cytotoxic studies, it can be revealed that the one step microwave-assisted green synthesis method using various environmentally benign extract could be useful for future studies. Without threatening intervention from potentially harmful and toxic reagents, bio-based syntheses of silver and copper nanoparticles, might be suitable for immense exercise in therapeutic field, drug delivery systems, development of various biodevices and for other biological applications as well [156], [173].

REFERENCES

[1]   Kaur, G., Singh, T. and Kumar A., (2012). "Nanotechnology: A Review", International Journal of Education and Applied Research, 1(2): 50-53.

[2]   Goddard, W. A. et al., (eds.) (2007). Handbook on Nanoscience, Engineering and Technology, 2nd Ed., Taylor and Francis, Oxfordshire.

[3]   Salam, H.A., Rajiv, P., Kamaraj, M., Jagadeeswaran, P., Gunalan, S. and Sivaraj, R., (2012). "Plants: green route for nanoparticle synthesis", I. Res. J. Biological Sci., 1: 85-90.

[4]   Huang, J., Li. Q., Sun, D., Lu, Y., Su, Y., Yang, X., Wang, H., Wang, Y., Shao, W., He, N., Hong, J. and Chen, C., (2007). "Biosynthesis of silver and gold nanoparticles by novel sundried *Cinnamomum camphora* leaf", Nanotechnology, 18(10):105104-105115.

[5]   Safaepour M., Shahverdi A.R., Shahverdi H.R., Khorramizadeh M.R. and Gohari A.R., (2009). "Green synthesis of small silver nanoparticles using *Geraniol* and its cytotoxicity against Fibrosarcoma-Wehi 164", Avicenna J Med Biotech., 1:111-115.

[6]   Hutchison, J. E., (2008). "Greener nanoscience: a proactive approach to advancing applications and reducing implications of nanotechnology", ACS Nano., 2(3): 395-402.

[7]   Novack, B. and Bucheli, T.D., (2007). "Occurrence, behavior and effects of nanoparticles in the environment", Environ. Pollut., 150: 5-22.

[8]   Wang, Y. and Herron, N., (1991). "Nanometer-sized semiconductor clusters: materials synthesis, quantum size effects, and photophysical properties", J. Phys. Chem. A, 95: 525-532.

[9]   EPA, (2007). "Nanotechnology White Paper", Office of the Science Advisor, Science Policy Council, United States Environmental Protection Agency. https://www.epa.gov/sites/production/files/201501/documents/nanotechnology _whitepaper.pdf (Accessed on 08.15.2018).

[10]   Brill, R.H. and Cahill, N.D., (1988). "A red opaque glass from Sardis and some thoughts on red opaques in general", J. Glass Stud, 30: 16-27.

[11]   Rytwo, G., (2008). "Clay minerals as an Ancient nanotechnology: historical uses of clay organic interactions, and future possible perspectives", Macla., 9: 15-17.

[12]   Delgado, J., Vilarigues, M., Ruivo, A., Corregidor, V., da Silva, R.C. and Alves, L.C., (2011). "Characterisation of medieval yellow silver stained glass from Convento de Cristo in Tomar, Portugal.", Nucl. Instrum. Methods B2 (69): 2383-2388.

[13]   Stephen, W., (2002). A New Kind of Science, Wolfram Media Inc., Champaign.

[14]   Prasad, S. K., (2008). Modern Concepts in Nanotechnology, Discovery Publishing House, New Delhi.

[15]   Borisenko, V.E. and Tolochko, N.K., (2008). "Nanotechnologies: Stages of Development", Nauka i innovatsii (Minsk), 12: 66-68.

[16]   Manivasagan, P., Venkatesan, J., Sivakumar, K. and Kim, S.K., (2014). "Actinobacteria mediated synthesis of nanoparticles and their biological properties: a review", Crit. Rev. Microbiol., 28: 1-13.

[17]   Shin, W.K., Cho, J., Kannan, A.G., Lee, Y.-S. and Kim, D.W., (2016). "Cross-linked composite gel polymer electrolyte using mesoporous methacrylate-functionalized SiO_2 nanoparticles for lithium-ion polymer batteries", Sci. Rep., 6: 26332.

[18]   Skorokhod, V., Ragulya, A. and Uvarova, I., (2001). "Physico-chemical kinetics in nanostructured systems", Kyiv: Academperiodica, 43: 180-192.

[19]   Buzea, C., Pacheco, I. and Robbie, K., (2007). "Nanomaterials and nanoparticles: sources and toxicity", Biointerphases, 2: 17-71.

[20]   Gusev, A. I. (2007). Nanomaterials, Nanostructures, and Nanotechnologies (in Russian), Fizmatlit, Moscow.

[21]   Amin, G., (2012). ZnO and CuO Nanostructures: Low Temperature Growth, Characterization, their Optoelectronic and Sensing Applications, Dissertation, Department of Science and Technology, Linköping University, Linköping, Sweden.

[22]   Saeed, K. and Khan, I., (2016). "Preparation and characterization of single walled carbon nanotubes/nylon 6, 6 nanocomposites", Instrum Sci. Technol, 44: 435-444.

[23]   Ngoy, J.M., Wagner, N., Riboldi, L. and Bolland, O., (2014). "A CO_2 capture technology using multi-walled carbon nanotubes with polyaspartamide surfactant", Energy Procedia, 63: 2230-2248.

[24]   Mabena, L.F., Sinha, R. S., Mhlanga, S.D. and Coville, N.J., (2011). "Nitrogen-doped carbon nanotubes as a metal catalyst support", Appl. Nanosci., 1: 67-77.

[25]   Nahar, M., Dutta, T., Murugesan, S., Asthana, A., Mishra, D., Rajkumar, V., Tare, M., Saraf, S. and Jain, N.K., (2006). "Functional polymeric nanoparticles: an efficient and promising tool for active delivery of bioactives", Crit Rev Ther Drug Carrier Syst., 23(4): 259-318.

[26]   Sigmund, W., Yuh, J., Park, H., Maneeratana, V., Pyrgiotakis, G., Daga, A., Taylor, J. and Nino, J.C., (2006). "Processing and structure relationships in electrospinning of ceramic fiber systems", J. Am. Ceram. Soc., 89: 395-407.

[27] Thomas, S., Harshita, B.S.P., Mishra, P. and Talegaonkar, S., (2015). "Ceramic nanoparticles: fabrication methods and applications in drug delivery", Curr. Pharm. Des., 21: 6165-6188.

[28] Ali, S., Khan, I., Khan, S.A., Sohail, M., Ahmed, R., Rehman, A., Ur Ansari, M.S. and Morsy, M.A., (2017). "Electrocatalytic performance of Ni@Pt core–shell nanoparticles supported on carbon nanotubes for methanol oxidation reaction", J. Electroanal. Chem. 795: 17-25.

[29] Sun, S., (2000). "Monodisperse FePt nanoparticles and ferromagnetic FePt nanocrystal superlattices", Science, 80 (287): 1989-1992.

[30] Mansha, M., Qurashi, A., Ullah, N., Bakare, F.O., Khan, I. and Yamani, Z.H., (2016). "Synthesis of In_2O_3/graphene heterostructure and their hydrogen gas sensing properties", Ceram. Int., 42: 11490-11495.

[31] Puri, A., Loomis, K., Smith, B., Lee, J.H., Yavlovich, A., Heldman, E. and Blumenthal, R., (2009). "Lipid-based nanoparticles as pharmaceutical drug carriers: from concepts to clinic", Crit. Rev. Ther. Drug Carrier Syst., 26: 523-580.

[32] Gujrati, M., Malamas, A., Shin, T., Jin, E., Sun, Y. and Lu, Z.R., (2014). "Multifunctional cationic lipid-based nanoparticles facilitate endosomal escape and reduction-triggered cytosolic siRNA release", Mol. Pharm., 11: 2734-2744.

[33] Uddin, I., Poddar, P., Kumar, U. and Phogat, N., (2013). "A novel microbial bio-milling technique for the size reduction of micron sized Gd_2O_3 particles into nanosized particles", J. Green. Sci. Tech., 1: 48–53.

[34] Tai, C. Y., Tai, C., Chang, M. and Liu, H., (2007). "Synthesis of Magnesium Hydroxide and Oxide Nanoparticles Using a Spinning Disk Reactor", Ind. Eng. Chem. Res., 46 (17): 5536-5541.

[35] Mulvaney, P., (1996). "Surface plasmon spectroscopy of nanosized metal particles", Langmuir, 12: 788-800.

[36] Henglein, A., (1989). "Small-particle research: physiochemical properties of extremely small colloidal metal and semiconductor particles", Chem. Rev., 89: 1861-1873.

[37] Heiligtag, F. J. and Markus N., (2013). "The fascinating world of nanoparticle research", Materials Today, 16 (7-8): 262-271.

[38] Khanna, P.K., Gaikwad, S., Adhyapak, P.V., Singh, N. and Marimuthu, R., (2007). "Synthesis and characterization of copper nanoparticles", Mater. Lett., 61 (25): 4711-4714.

[39] Dhas, N.A., Raj, C.P. and Gedanken, A., (1998). "Synthesis, Characterization, and Properties of Metallic Copper Nanoparticles", Chem. Mater., 10 (5): 1446-1452.

[40] Moya, J. S., Pecharroman, C., Cubillo, A. and Montero, I., (2006). "Monodisperse and corrosion resistant metallic nanoparticles embedded into sepiolite particles for optical and magnetic applications", Journal of American Ceramic Society., 89 (10): 3043-3049.

[41]   Zia, F., Ghafoor, N., Iqbal M. and Mehboob, S., (2016). "Green synthesis and characterization of silver nanoparticles using *Cydonia oblong* seed extract. Appl. Nanosci., 6: 1023-1029.

[42]   Salavati-Niasari, M., Davar, F. and Mir, N., (2008). "Synthesis and characterization of metallic copper nanoparticles via thermal decomposition", Polyhedron, 27: 3514-8.

[43]   Yasin, S., Liu, L. and Yao, J. (2013). "Biosynthesis of silver nanoparticles by bamboo leaves extract and their antimicrobial activity", JFBI, 6: 77.

[44]   Rajoriya, P., (2017). "Green synthesis of silver nanoparticles, their characterization and antimicrobial potential", PhD Thesis, Sam Higginbottom University of Agriculture, Technology & Sciences, Allahabad, India. ID: 11PHBT108.

[45]   Iravani, S., (2011). "Green synthesis of metal nanoparticles using plants", Green Chemistry, 13(10):2638–2650. DOI: 10.1039/C1GC15386B

[46]   Magnusson, M.D., Malm, J. K., Bovin, J. and Samuelson, L., (1999). "Gold nanoparticles: production, reshaping, and thermal charging", J. Nanoparticle Res., 1: 243-251.

[47]   Jung, J. H., Oh H. C., Noh H.S., Ji, J. H. & Kim S. S., (2006). "Metal nanoparticle generation using a small ceramic heater with a local heating area", J. Aerosol Sci., 37: 1662-1670.

[48]   Mafune, F.K., Takeda, Y. J., Kondow, T. & Sawabe, H., (2001). "Formation of gold nanoparticles by laser ablation in aqueous solution of surfactant", J. Phys. Chem. B., 105: 5114-5120.

[49]   Tsuji, T.I., Watanabe, N. & Tsuji, M., (2002). "Preparation of silver nanoparticles by laser ablation in solution: influence of laser wavelength on particle size", Appl. Surf. Sci., 202: 80-85.

[50]   Parab, H., Jung, C., Woo, M.A. and Park, H.G., (2011). "An anisotropic snowflake-like structural assembly of polymer-capped gold nanoparticles", J. Nanopart Res., 13: 2173-2180.

[51]   Liu, D., Li, C., Zhou, F., Zhang, T., Zhang, H., Li, X., Duan, G., Cai, W. & Li, Y., (2015). "Rapid synthesis of monodisperse Au nanospheres through a laser irradiation -induced shape conversion, self-assembly and their electromagnetic coupling SERS enhancement", Sci. Rep., 5: 7686.

[52]   Yin, Y.L., Zhong, Z., Gates, B. & Venkateswaran, S., (2002). "Synthesis and characterization of stable aqueous dispersions of silver nanoparticles through the Tollens process", J. Mater. Chem., 12: 522-527.

[53]   Mohanpuria, P., Rana, N. K. and Yadav, S. K., (2008). "Biosynthesis of nanoparticles: technological concepts and future applications", Journal of Nanoparticle Research, 10(3): 507-517.

[54]   Parashar, U. K., Saxena, P. S. and Srivastava, A., (2009). "Bioinspired synthesis of silver nanoparticles", Digest Journal of Nanomaterials and Biostructures, 4(1):159-166.

[55] Tiwari, D. K., Behari, J. and Sen, P., (2008). "Time and dose-dependent antimicrobial potential of Ag nanoparticles synthesized by top-down approach", Current Science, 95(5): 647-655.

[56] Wang, Y. and Xia, Y., (2004). "Bottom-up and top-down approaches to the synthesis of monodispersed spherical colloids of low melting-point metals", NanoLett., 4: 2047-2050.

[57] Parashar, V., Parashar, R., Sharma, B. and Pandey, A. C., (2009). "*Partenium* leaf extract mediated synthesis of silver nanoparticles: a novel approach towards weed utilization", Digest Journal of Nanomaterials and Biostructures, 4(1): 45-50.

[58] Joerger, R., Klaus, T. and Granqvist, C.G., (2000). "Biologically produced silver carbon composite materials for optically functional thin film coatings", Advanced Materials, 12(6): 407-409.

[59] Anastas, P.T. and Warner, J.C., (2000). Green Chemistry: Theory and Practice, Oxford University Press, New York.

[60] Luechinger, N. A., Grass, R.N., Athanassiou, E. K. and Stark, W. J., (2010). "Bottom-up fabrication of metal/metal nanocomposites from nanoparticles of immiscible metals", Chemistry of Materials, 22(1): 155-160.

[61] Singh, P. Kim, Y-J., Zhang, D. and Yang, D-C., (2016). "Review: Biological Synthesis of Nanoparticles from Plants and Microorganisms", Trends in Biotechnology 34(7): 588-599.

[62] Konishi, Y., Ohno, K., Saitoh, N., Nomura, T. and Nagamine, S., (2004). "Microbial synthesis of gold nanoparticles by metal reducing bacterium", TransMater Res Soc Jpn., 29: 2341-2343.

[63] Li, X., Xu, H., Chen, Z-S. and Chen, G., (2011). "Biosynthesis of nanoparticles by microorganisms and their applications", J. Nanomaterials, 2011: 16.

[64] Loveley, J. F., Stolz, G. L., Nord, E. J. and Phillips, P., (1987). "Mechanisms for chelator stimulation of microbial Fe (III)-oxide reduction", Nature, 330: 252-254.

[65] Zhang, X., Yan, S., Tyagi, R.D. and Surampalli, R.Y., (2011). "Synthesis of nanoparticles by microorganisms and their application in enhancing microbiological reaction rates", Chemosphere, 82: 489-494.

[66] Hasan, S., Singh, S., Parikh, R.Y., Dharne, M.S., Patole, M.S., Prasad, B.L. and Shouche, Y.S., (2008). "Bacterial Synthesis of Copper/Copper Oxide Nanoparticles", Journal of Nanoscience and Nanotechnology, 8(6): 3191-3196.

[67] Kowshik, M., Ashtaputre, S., Kharrazi, S., Vogel, W., Urban, J., Kulkarni, S.K. and Paknikar, K.M., (2003). "Extracellular synthesis of silver nanoparticles by a silver-tolerant yeast strain MKY3", Nanotechnology, 14: 95-100.

[68] Dameron, C.T., Reese, R.N. and Mehra, R.K., (1989). "Biosynthesis of cadmium sulphide quantum semiconductor crystallites", Nature, 338 (13): 596–597. Doi: 10.1038/338596a0.

[69]   Sastry, M., Ahmad, A., Khan, I. and Kumar, R., (2003). "Biosynthesis of metal nanoparticles using fungi and actinomycetes", Curr Sci., 85(2): 162-170.

[70]   Mukherjee, P., Ahmad, A., Mandal, D., Senapati, S., Sainkar, S.R., Khan, M.I., Parischa, R., Ajaykumar, P.V., Alam, M., Kumar, R. and Sastry, M., (2001). "Fungus mediated synthesis of silver nanoparticles and their immobilization in the mycelial matrix: a novel biological approach to nanoparticle synthesis", Nano Letters, 1(10): 515–519. Doi: 10.1021/nl0155274.

[71]   Kumar, A. S., Abyaneh, M.K., Gosavi, S.W., Kulkarni, S.K., Pasricha, R., Ahmad, A. and Khan, M.I., (2007). "Nitrate reductase-mediated synthesis of silver nanoparticles from $AgNO_3$", Biotechnol. Lett. 29: 439-445. Doi: 10.1007/s10529-006-9256-7.

[72]   Mukherjee, P., Roy, M., Mandal, B.P., Dey, G.K., Mukherjee, P.K., Ghatak, J., Tyagi, A.K. and Kale, S.P., (2008). "Green synthesis of highly stabilized nanocrystalline silver particles by anon-pathogenic and agriculturally important fungus, *Trichoderma asperellum*", Nanotechnology, 19(75): 103-110. Doi: 10.1088/0957-4484/19/7/075103.

[73]   Honary, S., Barabadi, H., Fathabad, E.G. and Naghibi, F., (2012). "Green synthesis of copper oxide nanoparticles using *Penicillium aurantiogriseum*, *Penicillium citrinum* and *Penicillium wakasmanii*", Digest J. Nanomater Biostruct, 7: 999-1005.

[74]   Chakraborty, N., Banerjee, A., Lahiri, S., Panda, A., Ghosh, A.N. and Pal, R., (2009). "Biorecovery of gold using cyanobacteria and an eukaryotic alga with special reference to nano-gold formation: a novel phenomenon", J Appl Phycol., 21: 145-152.

[75]   Lengke, M., Fleet, M.E. and Southam, G., (2006). "Morphology of gold nanoparticles synthesized by filamentous cyanobacteria from gold (I)-thiosulfate and gold (III)-chloride complexes", Langmuir., 22: 2780-2787.

[76]   Niu, H. and Volesky, B., (2000). "Gold-cyanide biosorption with L-cysteine", J. Chem. Technol. Biotechnol., 75: 436-442.

[77]   Shahverdi, A.R., Minaeian, S., Shahverdi, H.R., Jamalifar, H. and Nohi, A., (2007). "Rapid synthesis of silver nanoparticles using culture supernatants of Enterobacteria: A novel biological approach", Process Biochemistry, 42: 919-923.

[78]   Lin, L., Wang, W. and Huang, J., (2010). "Nature factory of silver nanowires: Plant-mediated synthesis using broth of *Cassia fistula* leaf", Chemical Engineering Journal, 162: 852-858. Doi: 10.1016/j.cej.2010.06.023.

[79]   Abboud, Y., Eddahbi, A, El B.A., Aitenneite, H., Brouzi, K. and Mouslim, J., (2013). "Microwave-assisted approach for rapid and green phytosynthesis of silver nanoparticles using aqueous onion (*Allium cepa*) extract and their antibacterial activity", J. Nanostruct. Chem., 3(1): 1-7.

[80]   Noruzi, M., (2015). "Biosynthesis of gold nanoparticles using plant extracts", Bioprocess Biosyst. Eng., 38: 1-14.

[81]   Chandran, S.P., Chaudhary, M., Pasricha, R., Ahmad, A. and Sastry, M., (2006). "Synthesis of gold nanotriangles and silver nanoparticles using *Aloe vera* plant extract", Biotechnol. Prog., 22: 577-583.

[82]   Kasthuri, J., Kanthiravan, K. and Rajendiran, N., (2009). "Phyllanthin-assisted biosynthesis of silver and gold nanoparticles: a novel biological approach", J. Nanopart Res., 15: 1075-1085.

[83]   Raveendran, P., Fu, J. and Wallen, S.L., (2003). "Completely "green" synthesis and stabilization of metal nanoparticles.", J. Am. Chem. Soc., 125: 13940-13941.

[84]   Philip, D., Unni, C., Aromal, S.A. and Vidhu, V.K., (2011). "*Murraya koenigii* leaf-assisted rapid green synthesis of silver and gold nanoparticles", Spectrochim. Acta A Mol. Biomol. Spectrosc, 78: 899-904. Doi: 10.1016/j.saa.2010.12.060.

[85]   Makarov, V.V., Love, A.J., Sinitsyna, O.V., Makarova, S.S., Yaminsky, I.V., Taliansky, M.E. and Kalinina, N.O., (2014). "Green nanotechnologies: synthesis of metal nanoparticles using plants", Acta. Naturae., 6(1): 35-44.

[86]   Mittal, A. K., Chisti, Y. and Banerjee, U. C., (2013). "Research review Paper: Synthesis of metallic nanoparticles using plant extracts", Biotechnology Advances, 31: 346-356.

[87]   Nasrollahzadeh, M. and Sajadi, S.M., (2015). "Green synthesis of copper nanoparticles using *Ginkgo biloba* L. leaf extract and their catalytic activity for the Huisgen [3+2] cycloaddition of azides and alkynes at room temperature", J. Colloid Interface Sci., 457: 141-147. Doi: 10.1016/j.jcis.2015.07.004.

[88]   Poopathi, S., Britto, L.J.D., Praba, V.L. Mani, C. and Praveen, M. (2015). "Synthesis of silver nanoparticles from *Azadirachta indica*–a most effective method for mosquito control", Environ. Sci. Pollut. Res. Int., 22: 2956-2963.

[89]   Velmurugan, P., Park, J-H., Lee, S-M., Jang, J-S., Lee, K-J., Han, S-S., Lee, S-H., Cho, M. and Oh, B-T., (2015). "Synthesis and characterization of nanosilver with antibacterial properties using *Pinus densiflora* young cone extract", J. Photochem. Photobiol., 147: 63-68. Doi: 10.1016/j.jphotobiol.2015.03.008.

[90]   Hyllested E. J., Palanco, M.E., Hagen, N., Mogensen, K. B. and Kneip, K. (2015). 'Green preparation and spectroscopic characterization of plasmonic silver nanoparticles using fruits as reducing agents", Beilstein. J. Nanotechnol., 6: 293-299. Doi:10.3762/bjnano.6.27.

[91]   Santhoshkumar, T., Rahuman, A.A., Rajakumar, G., Marimuthu, S., Bagavan, A, and Jayaseelan, C., (2011). "Synthesis of silver nanoparticles using *Nelumbo nucifera* leaf extract and its larvicidal activity against malaria and filariasis vectors", Parasitol Res., 108: 693-702.

[92]   Von, W.G., Kerscher, P., Brown, R.M., Morella, J.D., McAllister, W., Dean, D. and Kitchens, C.L., (2012). "Green synthesis of robust, biocompatible silver nanoparticles using garlic extract", J. Nanomater., 2: 1-12.

[93]   Moosa, A.A., Ridha, A.M. and Al-Kaser, M., (2015). "Process parameters for green synthesis of silver nanoparticles using leaves extract of *Aloe vera* plant", IJMCR, 3: 966-975.

[94]   Shende, S., Ingle, A.P., Gade, A. and Rai, M., (2015). "Green synthesis of copper nanoparticles by *Citrus medica* Linn. (Idilimbu) juice and its antimicrobial activity", World J. Microbiol. Biotechnol., 31: 865-873. Doi: 10.1007/s11274-015-1840-3.

[95]   Naseem, T. and Farrukh, M.A., (2015). "Antibacterial activity of green synthesis of iron nanoparticles using *Lawsonia inermis* and *Gardenia jasminoides* leaves extract", Journal of Chemistry, 2015: 912342. Doi: 10.1155/2015/912342.

[96]   Suresh, D., Shobharani, R.M., Nethravathi, P.C., Pavan K.M.A., Nagabhushana, H. and Sharma, S.C., (2015). "*Artocarpus gomezianus* aided green synthesis of ZnO nanoparticles: luminescence, photocatalytic and antioxidant properties", Spectrochim. Acta A Mol. Biomol. Spectrosc., 141: 128-134. Doi: 10.1016/j.saa.2015.01.048.

[97]   Valodkar, M., Nagar, P.S., Jadeja, R.N., Thounaojam, M.C., Devkar, R.V. and Thakore, S., (2011). "*Euphorbiaceae* latex induced green synthesis of non-cytotoxic metallic nanoparticle solutions: a rational approach to antimicrobial applications", Colloids Surf A., 384: 337-44.

[98]   Kaviya, S., Santhanalakshmi, J., Viswanathan, B., Muthumar, J. and Srinivasan, K., (2011). "Biosynthesis of silver nanoparticles using *Citrus sinensis* peel extract and its antibacterial activity", Spectrochimica Acta Part A: Molecular and Biomolecular Spectroscopy, 79(3): 594-598. DOI: 10.1016/j.saa.2011.03.040.

[99]   Dubey, S.P., Lahtinen, M. and Sillanpaa, M., (2010a). "Green synthesis and characterizations of silver and gold nanoparticles using leaf extract of *Rosa rugosa*", Colloids Surf A., 364: 34-41.

[100]   Jain, D., Daima, H.K., Kachhwaha, S. and Kothari, S., (2009). "Synthesis of plant-mediated silver nanoparticles using papaya fruit extract and evaluation of their antimicrobial activities", Dig J Nanomater Biostruct., 4: 557-563.

[101]   Shankar, S.S., Rai, A., Ahmad, A. and Sastry, M., (2005). "Controlling the optical properties of lemongrass extract synthesized gold nanotriangles and potential application in infrared-absorbing optical coatings", Chem Mater. 17: 566-572.

[102]   Joglekar, S., Kodam, K., Dhaygude, M. and Hudlikar, M., (2011). "Novel route for rapid biosynthesis of lead nanoparticles using aqueous extract of *Jatropha curcas* L. latex", Mater Lett., 65: 3170-3172.

[103]   Ali, D.M., Thajuddin, N., Jeganathan, K. and Gunasekaran, M., (2011). "Plant extract mediated synthesis of silver and gold nanoparticles and its antibacterial activity against clinically isolated pathogens", Colloids Surf B Biointerfaces, 85: 360-365.

[104]   Banerjee, J. and Narendhirakannan, R., (2011). "Biosynthesis of silver nanoparticles from *Syzygium cumini* (L.) seed extract and evaluation of their in vitro antioxidant activities", Dig J Nanomater Biostruct, 6: 961-968.

[105]   Bankar, A., Joshi, B., Kumar, A.R. and Zinjarde, S., (2010). "Banana peel extract mediated novel route for the synthesis of silver nanoparticles", Colloids Surf A., 368: 58-63.

[106]   Shankar, S.S., Ahmad, A. and Sastry, M., (2003). "*Geranium* leaf assisted biosynthesis of silver nanoparticles", Biotechnol Prog., 19: 1627-1631.

[107]   Baker, S., Rakshith, D., Kavitha, K. S., Santosh, P., Kavitha, H. U., Rao, Y. and Satish, S. (2013). "Plants: emerging as nanofactories towards facile route in synthesis of nanoparticles", BioImpacts, 3(3): 111-117. Doi: 10.5681/bi.2013.012.

[108]   Kharissova, O. V., Dias, H. V. R., Kharisov, B. I., P´erez, B. O. and. P´erez, V. M. J, (2013). "The greener synthesis of nanoparticles", Trends in Biotechnology, 31(4): 240-248.

[109]   Vadlapudi, V. and Kaladhar, D. S. V. G. K., (2014). "Review: green synthesis of silver and gold nanoparticles", Middle-East Journal of Scientific Research, 19(6): 834-842.

[110]   Dubey, S.P., Lahtinen, M. and Sillanpaa, M., (2010b). "Tansy fruit mediated greener synthesis of silver and gold Nanoparticles", Process Biochem., 45: 1065-1071.

[111]   Armendariz, V., Herrera, I., Peralta-Videa, J. R., Jose-yacaman, M., Troiani, H., Santiago, P. and Gardea-Torresdey, J. L., (2004). "Size controlled gold nanoparticle formation by *Avena sativa* biomass: use of plants in nanobiotechnology", Journal of Nanoparticle Research, 6(4): 377-382.

[112]   Soni, N. and Prakash, S., (2011). "Factors affecting the geometry of silver nanoparticles synthesis in *Chrysosporium tropicum* and *Fusarium oxusporum*", American Journal of Nanotechnology, 2(1): 112-121. Doi: 10.3844/ajnsp.2011.112.121.

[113]   Prathna, T.C., Chandrasekaran, N., Raichur, A.M. and Mukherjee, A., (2011). "Kinetic evolution studies of silver nanoparticles in a bio-based green synthesis process", Colloids Surf., 377: 212-216. Doi: 10.1016/j.colsurfa.2010.12.047.

[114]   Rai, A., Singh, A., Ahmad, A. and Sastry, M., (2006). "Role of halide ions and temperature on the morphology of biologically synthesized gold nanotriangles", Langmuir, 22(2): 736-741. Doi: 10.1021/la052055q.

[115]   Gericke, M. and Pinches, A., (2006). "Biological synthesis of metal nanoparticles", Hydrometallurgy, 83: 132-140. Doi: 10.1016/j.hydromet.2006.03.019.

[116]   Nagy, A. and Mestl, G., (1999). "High temperature partial oxidation reactions over silver catalysts", Appl Catal A., 188: 337. Doi: 10.1016/S0926-860X(99)00246-X.

[117]   Darroudi, M., Ahmad, M. B., Zamiri, R., Zak, A. K., Abdullah, A. H. and Ibrahim, N. A., (2011). "Time-dependent effect in green synthesis of silver nanoparticles", International Journal of Nanomedicine, 6 (1): 677-681. Doi: 10.2147/IJN.S17669.

[118]   Baer, D. R., (2011). "Surface characterization of nanoparticles: critical needs and significant challenges", J. Surf. Anal., 17(3): 163-169.

[119] Ahmad, N. and Sharma, S., (2012). "Green synthesis of silver nanoparticles using extracts of Ananas comosus", Gr. Sustain. Chem., 2: 141-147. Doi: 10.3390/ma8115377.

[120] Abhilash, B. D. P., (2012). "Synthesis of zinc-based nanomaterials: a biological perspective", IET Nanobiotechnology, 6(4): 144-148.

[121] Tran, Q. H., Nguyen, V. Q. and Le, A. T., (2013). "Silver nanoparticles: synthesis, properties, toxicology, applications and perspectives", Advances in Natural Sciences: Nanoscience and Nanotechnology, 4, Article ID 033001.

[122] Huang, J., Li, Q., Sun, D., Lu, Y., Su, Y., Yang, X., Wang, H., Wang, Y., Shao, W., He, N., (2007). "Biosynthesis of silver and gold nanoparticles by novel sundried *Cinnamomum camphora* leaf", Nanotechnology, 18: 1-11.

[123] Park, Y., Hong, Y. N., Weyers, A., Kim, Y. S. and Linhardt, R. J., (2011). "Polysaccharides and phytochemicals: a natural reservoir for the green synthesis of gold and silver nanoparticles", IET Nanobiotechnology, 5(3): 69-78. Doi: 10.1049/iet-nbt.2010.0033.

[124] Haverkamp, R. G., Marshall, A. T. and Van, D. A., (2007). "Pick your carats: nanoparticles of gold-silver-copper alloy produced in vivo", Journal of Nanoparticle Research, 9(4): 697-700.

[125] Sarathy, V., Tratnyek, P. G., Nurmi J. T., Baer, D. R., Amonette, J. E., Chun, C., Penn, L. and Reardon, E. J., (2008). "Aging of iron nanoparticles in aqueous solution: effects on structure and reactivity", The Journal of Physical Chemistry C., 112(7): 2286-2293. Doi: 10.1021/jp0777418.

[126] Patri, A.K., Dobrovolskaia, M. A., Stern, S. T. and McNeil, S. E., (2007). Nanotechnology for cancer therapy: Preclinical characterization of engineered nanoparticles intended for cancer therapeutics, CRC Press, Florida.

[127] Sapsford, K.E., Tyner, K.M., Dair, B.J., Deschamps, J.R. and Medintz, I.L., (2011). "Analyzing nanomaterial bioconjugates: A review of current and emerging purification and characterization techniques", Anal. Chem., 83: 4453-4488. Doi: 10.1021/ac200853a.

[128] Daniel, M.C. and Astruc, D., (2004). "Gold nanoparticles: assembly, supramolecular chemistry, quantum-size-related properties, and applications toward biology, catalysis, and nanotechnology", Chemical Reviews, 104(1): 293-346. Doi: 10.1021/cr030698+.

[129] Akbari, B., Tavandashti, M. P. and Zandrahimi, M., (2011). "Particle size characterization of nanoparticles—a practical approach", Iranian Journal of Materials Science and Engineering, 8(2): 48-56.

[130] Jiang, X., Jiang, J., Jin, Y., Wang, E. and Dong, S., (2004). "Effect of colloidal gold size on the conformational changes of adsorbed cytochrome c: probing by circular dichroism, UV–visible, and infrared spectroscopy", Biomacromolecules, 6: 46-53. Doi: 10.1021/bm049744l.

[131] Chauhan, R. P. S., Gupta, C. and Prakash, D., (2012). "Methodological advancements in green nanotechnology and their applications in biological synthesis of herbal nanoparticles", International Journal of Bioassays, 1(7): 6-10.

[132]   Faraji, M., Yamini, Y. and Rezaee, M., (2010). "Magnetic nanoparticles: synthesis, stabilization, functionalization, characterization, and applications", Journal of the Iranian Chemical Society, 7(1): 1-37.

[133]   Liu, H. and Webster, T.J., (2007). "Nanomedicine for implants: a review of studies and necessary experimental tools", Biomaterials, 28: 354-369. Doi: 10.1016/j.biomaterials.2006.08.049.

[134]   Hind, A.R., Bhargava, S.K., and McKinnon A., (2001). "At the solid/liquid interfaces: FTIR/ATR—the tool of choice", Adv Colloid Interface Sci., 93: 91-114.

[135]   Johal, M.S., (2011). Understanding nanomaterials, Boca Raton: CRC Press, Boca Raton, Florida.

[136]   Cantor, C.R. and Schimmel, P.R., (1980). Techniques for the study of biological structure and function, WH Freeman and Co., Oxford.

[137]   Gupta, V., Gupta, A. R. and Kant, V., (2013). "Synthesis, characterization and biomedical application of nanoparticles", Science International, 1(5): 167-174. Doi: 10.5567/sciintl.2013.167.174.

[138]   Klug, H.P. and Alexander, L.E., (1974). X-ray Diffraction Procedures for Poly-crystallite and Amorphous Materials, 2nd ed., Wiley, New York.

[139]   Zanchet, D., Hall, B.D. and Ugarte, D., (2001). Characterization of nanophase materials: X-ray characterization of nanoparticles, Edited by Zhong Lin Wang, Wiley-VCH Verlag: GmbH, New York.

[140]   Cao, G., (2004). Nanostructures and nanomaterials: synthesis, properties and applications, Imperial College Press, London.

[141]   Doniach, S., (2001). "Changes in biomolecular conformation seen by small angle X-ray scattering", Chem Rev., 101: 1763-1778. Doi: 10.1021/cr990071k.

[142]   Corbari, L., Cambon-Bonavita, M.-A., Long, G. J., Grandjean, F., Zbinden, M., Gaill, F. and Compère, P., (2008). "Iron oxide deposits associated with the ectosymbiotic bacteria in the hydrothermal vent shrimp *Rimicaris exoculata*", Biogeosciences. 5 (5): 1295-1310. Doi: 10.5194/bgd-5-1825-2008.

[143]   Prasad, K. S., Pathak, D., Patel, A., Dalwadi, P., Prasad, R., Patel, P. and Selvaraj, K., (2011). "Biogenic synthesis of silver nanoparticles using *Nicotiana tobaccum* leaf extract and study of their antibacterial effect", African Journal of Biotechnology, 10(41): 8122-8130. Doi: 10.5897/AJB11.394.

[144]   Domingos, R.F., Baalousha, M.A., Ju-Nam, Y., Reid, M.M., Tufenkji, N., Lead, J.R., (2009). "Characterizing manufactured nanoparticles in the environment: multi-method determination of particle sizes", Environ Sci Technol., 43: 7277-7284.

[145]   Wang, Z.L., (2001). Characterization of nanophase materials: Transmission electron microscopy and spectroscopy of nanoparticles, Edited by Zhong Lin Wang, Wiley-VCH Verlag: GmbH, New York.

.

[146]   Brice-Profeta, S., Arrio, M.A., Tronc, E., Menguy, N., Letard, I., Cartier dit Moulin, C., Nogue`s, M., Chane´ac, C., Jolivet, J.-P. and Sainctavita, P., (2005). "Magnetic order in γ-Fe2O3 nanoparticles: a XMCD study", Journal of Magnetism and Magnetic Materials, 288: 354-365. Doi:10.1016/j.jmmm.2004.09.120.

[147]   Mallikarjuna, K., Narasimha, G., Dillip, G. R., Praveen, B., Shreedhar, B., Lakshmi, C. S, Reddy, B. V. S. and Raju, B. D. P., (2011). "Green synthesis of silver nanoparticles using *Ocimum* leaf extract and their characterization", Digest Journal of Nanomaterials and Biostructures, 6(1): 181-186.

[148]   Saxena, A., Tripathi, R. M. and. Singh, R. P, (2010). "Biological synthesis of silver nanoparticles by using onion (*Allium cepa*) extract and their antibacterial activity", Digest Journal of Nanomaterials and Biostructures, 5(2): 427-432.

[149]   Hall, J.B., Dobrovolskaia, M.A., Patri, A.K. and McNeil, S.E., (2007). "Characterization of nanoparticles for therapeutics", Nanomedicine (London), 2: 789-803. Doi: 10.2217/17435889.2.6.789.

[150]   Ianoul, A. and Johnston, L.J., (2007). "Near-field scanning optical microscopy to identify membrane microdomains", Methods Mol. Biol., 400: 469-480.

[151]   Bogner, A., Thollet, G., Basset, D., Jouneau, P.H. and Gauthier, C., (2005). "Wet STEM: a new development in environmental SEM for imaging nano-objects included in a liquid phase", Ultramicroscopy, 104: 290-301. Doi: 10.1016/j.ultramic.2005.05.005.

[152]   Ranjbar, B., and Gill, P., (2009). "Circular dichroism techniques: biomolecular and nanostructural analyses — a review", Chem. Biol. Drug Des., 74: 101-120. Doi: 10.1111/j.1747-0285.2009.00847.x.

[153]   Rao, C.N. and Biswas, K., (2009). "Characterization of nanomaterials by physical methods", Annu. Rev. Anal. Chem., 435-462. Doi: 10.1146/annurev-anchem-060908-155236.

[154]   Bonnell, D., (2001). Scanning probe microscopy and spectroscopy: theory, techniques, and applications, Wiley-VCH, New York.

[155]   Bootz, A., Vogel, V., Schubert, D. and Kreuter, J., (2004). "Comparison of scanning electron microscopy, dynamic light scattering and analytical ultracentrifugation for the sizing of poly (butyl cyanoacrylate) nanoparticles", Eur. J. Pharm. Biopharm., 57: 369-375. Doi: 10.1016/S0939-6411(03)00193-0.

[156]   Rao, P.V. and Gan, S.H., (2015). "Recent advances in nanotechnology- based diagnosis and treatments of diabetes", Curr. Drug Metab., 16: 371-375.

[157]   Keat, C.L., Aziz, A., Ahmad, M. E. and Elmarzugi, N.A., (2015). "Review: Biosynthesis of nanoparticles and silver nanoparticles", Bioresour. Bioprocess., 2: 47.

[158]   Peng, H.I. and Miller, B.L., (2011). "Recent advancements in optical DNA biosensors: exploiting the plasmonic effects of metal nanoparticles", Analyst, 136: 436-447. Doi: 10.1039/c0an00636j.

[159] Walter, E.C., Penner, R.M., Liu, H., Ng, K.H., Zach, M.P. and Favier, F., (2002). "Sensors from electrodeposited metal nanowires", Surf. Interface Anal., 34: 409-412. Doi: 10.1002/sia.1328.

[160] Selid, P.D., Xu, H., Collins, E.M., Face-Collins, M.S. and Zhao, J.X., (2009). "Sensing mercury for biomedical and environmental monitoring", Sensors (Basel), 9: 5446–5459. Doi: 10.3390/s90705446.

[161] Koren, K., Brodersen, K.E., Jakobsen, S.L. and Kühl, M., (2015). "Optical sensor nanoparticles in artificial sediments–a new tool to visualize O_2 dynamics around the rhizome and roots of seagrasses", Environ. Sci. Technol., 49: 2286-2292. Doi: 10.1021/es505734b.

[162] Kavitha, K.S., Baker, S., Rakshith, D., Kavitha, H.U., Rao, Y. H.C., Harini, B.P. and Satish, S., (2013). "Plants as Green Source towards Synthesis of Nanoparticles", International Research Journal of Biological Sciences, 2(6): 66-76.

[163] Raffaelle, R. P., Castro, S. L., Hepp, A. F. and Bailey, S. G., (2002). "Quantum dot solar cell", Prog. Photovolt. Res. Appl., 10: 433-439. Doi: 10.1002/pip.452.

[164] Rai, M., Ingle, A.P., Birla, S., Yadav, A. and Santos, C.A., (2016). "Strategic role of selected noble metal nanoparticles in medicine", Crit. Rev. Microbiol., 42(5):696-719. Doi: 10.3109/1040841X.2015.1018131.

[165] Huang, X., Jain, P.K., El-Sayed, I.H. and El-Sayed, M.A., (2007). "Gold nanoparticles: interesting optical properties and recent applications in cancer diagnostics and therapy", Nanomedicine (London), 2(5): 681-93. Doi: 10.2217/17435889.2.5.681.

[166] Iv, M., Telischak, N., Feng, D., Holdsworth, S.J., Yeom, K.W. and Daldrup-Link, H.E., (2015). "Clinical applications of iron oxide nanoparticles for magnetic resonance imaging of brain tumors", Nanomedicine (Lond), 10(6):993-1018. Doi: 10.2217/nnm.14.203.

[167] Khlebtsov, N. and Dykman, L., (2011). "Biodistribution and toxicity of engineered gold nanoparticles: a review of *in vitro* and *in vivo* studies", Chem. Soc. Rev., 40: 1647-1671. Doi: 10.1039/c0cs00018c.

[168] Ambika, S. and Sundrarajan, M., (2015). "Green biosynthesis of ZnO nanoparticles using *Vitex negundo* L. extract: spectroscopic investigation of interaction between ZnO nanoparticles and human serum albumin", J. Photochem. Photobiol., B., 149: 143-148. Doi:10.1016/j.jphotobiol.2015.05.004.

[169] Zahir, A.A., Chauhan, I.S., Bagavan, A., Kamaraj, C., Elango, G., Shankar, J., Arjaria, N., Roopan, S.M., Rahuman, A.A. and Singh, N., (2015). "Green synthesis of silver and titanium dioxide nanoparticles using *Euphorbia prostrata* extract shows shift from apoptosis to G0/G1 arrest followed by necrotic cell death in *Leishmania donovani*.", Antimicrob. Agents Chemother., 59: 4782-4799. doi: 10.1128/AAC.00098-15.

[170] Ahamed, M., Alsalhi, M.S. and Siddiqui, M.K., (2010). "Silver nanoparticle applications and human health", Clin. Chim. Acta., 411: 1841-1848. Doi: 10.1016/j.cca.2010.08.016.

[171]   Momeni, S. and Nabipour, I., (2015). "A simple green synthesis of palladium nanoparticles with *Sargassum* alga and their electrocatalytic activities towards hydrogen peroxide", Appl. Biochem. Biotechnol., 176(7): 1937-1949. Doi: 10.1007/s12010-015-1690-3.

[172]   Waki, M., Sugiyama, E., Kondo, T., Sano, K. and Setou, M., (2015). "Nanoparticle-assisted laser desorption/ionization for metabolite imaging", Methods Mol. Biol., 1203: 159-173. Doi: 10.1007/978-1-4939-1357-2_16.

[173]   Mittal, A. K., Chisti, Y. and Banerjee, U. C., (2013). "Synthesis of metallic nanoparticles using plant extracts", Biotechnology Advances, 31: 346-356. DOI:10.1016/j.biotechadv.2013.01.003.

[174]   Nel, A., Xia, T., Mädler, L. and Li. N., (2006). "Toxic potential of materials at the nano level", Science, 311(5761): 622-627. DOI: 10.1126/science.1114397.

[175]   Jahan, I., Erci, F. and Isildak, I., (2019). "Microwave-assisted green synthesis of non-cytotoxic silver nanoparticles using the aqueous extract of *Rosa santana* (rose) petals and their antibacterial activity", Analytical Letters, Doi:10.1080/00032719.2019.1572179.

[176]   Kim, J.S., Kuk, E., Yu, K.N., Kim, J.H., Park, S.J., Lee, H.J., Kim, S.H., Park, Y.K., Park, Y.H., Hwang, C.Y., Kim, Y.K., Lee, Y.S., Jeong, D.H. and Cho, M.H., (2007). "Antimicrobial effects of silver nanoparticles", Nanomed Nanotechno Biol Med, 3: 95-101. Doi: 10.1016/j.nano.2006.12.001.

[177]   Furno, F., Morley, K.S., Bong, B., Sharp, B.L., Arnold, P.L., Howdle, S.M., (2004). "Silver nanoparticle and polymeric medical device: A new approach to prevention of infection", J. Anti. Chemo., 54: 1019-1024.

[178]   Blaser, S.A., Scheringer, M., MacLeod, M. and Hungerbühler, K., (2008). "Estimation of cumulative aquatic exposure and risk due to silver: contribution of nano-functionalized plastics and textiles", Sci Total Environ., 390(2-3): 396-409.

[179]   Zhang, Xi-F., Liu, Zhi-G., Shen W. and Gurunathan S., (2016). "Silver Nanoparticles: Synthesis, Characterization, Properties, Applications, and Therapeutic Approaches", Int. J. Mol. Sci., 17: 1534.

[180]   Gurunathan, S., Park, J.H., Han, J.W. and Kim, J.H., (2015). "Comparative assessment of the apoptotic potential of silver nanoparticles synthesized by *Bacillus tequilensis* and *Calocybe indica* in MDA-MB-231 human breast cancer cells: Targeting p53 for anticancer therapy", Int. J. Nanomed., 10: 4203-4222.

[181]   Chernousova, S. and Epple, M., (2013). "Silver as antibacterial agent: Ion, nanoparticle, and metal", Angew. Chem. Int. Ed., 52: 1636-1653.

[182]   Tien, D.C., Liao, C.Y., Huang, J.C., Tseng, K.H., Lung, J.K., Tsung, T.T., Kao, W.-S., Tsai, T.-H., Cheng, T.-W., Yu, B.-S., Lin, H.-M. and Stobinski, L. (2008). "Novel technique for preparing a nano-silver water suspension by the arc-discharge method". Rev. Adv. Mater. Sci., 18: 750-756.

[183]   Jain, P. and Pradeep, T., (2005). "Potential of silver nanoparticle-coated polyurethane foam as an antibacterial water filter", Biotechnol. Bioeng., 90: 59-63.

[184] Moran, J.R., Elechiguerra, J.L., Camacho, A., Holt, K., Kouri, J.B., Ramirez J.T., and Yacaman, M.J., (2005). "The bactericidal effect of silver nanoparticles", Nanotech, 16: 2346-2353.

[185] Noorden, R. V., (2006). "Nano-hype comes out in the wash", Chemistry World. https://www.chemistryworld.com/news/nano-hype-comes-out-in-the-wash/3002657.article (Accessed on 08.28.2018).

[186] Mallik, K., Mandal M., Pradhan N., and Pal T., (2001). "Seed mediated formation of bimetallic nanoparticles by UV irradiation: a photochemical approach for the preparation of "coreshell" type structures", Nano Lett., 1 (6): 319-322.

[187] Esteban-Cubillo, A., Pecharroman, C., Agilar, E., Santaren, J. and Moya, J., (2006). "Antibacterial activity of copper monodispersed nanoparticles into sepiolite", Journal of Material Science., 41: 5208-5221.

[188] Guduru, R. K., Murty, K. L., Youssef, K. M., Scattergood, R. O. and Koch, C. C., (2007). "Mechanical behavior of nanocrystalline copper", Materials Science and Engineering A., 463 (1-2): 14-21.

[189] Eastman, J. A., Cho S. U., Yu, W. and Thompson, L. J., (2001). "Anomalously increased effective thermal conductivity of ethylene glycol-based nanofluids containing copper nanoparticles", Applied Physics Letters., 78 (6): 718-720.

[190] Kang, X., Mai, Z., Zou, X., Cai, P. and Mo, J., (2007). "A sensitive non-enzymatic glucose sensor in alkaline media with a copper nanocluster/multiwall carbon nanotubes-modified glassy carbon electrode", Analytical Biochemistry., 363: 143-150.

[191] Kantam, M. L., Jaya, V. S., Lakshmi, M. J., Reddy, B. R., Choudary, B. M. and Bhargava, S. K., (2007). "Alumina supported copper nanoparticles for aziridination and cyclopropanation reactions", Catalysis Communications., 8: 1963-1968.

[192] Clasen, T., (2010). "Household Water Treatment and the Millennium Development Goals: Keeping the Focus on Health Environ", Sci. Technol., 44(19): 7357-7360.

[193] Dankovich T.A. and Smith J. A., (2014). "Incorporation of copper nanoparticles into paper for point-of-use water purification", Water Res., 63: 245-251.

[194] Ruparelia, J. P., Chatterjee, A. K., Duttagupta, S. P. and Mukherji, S., (2008). "Strain specificity in antimicrobial activity of silver and copper nanoparticles", Acta Biomater, 4 (3): 707-716.

[195] Brunel, F., ElGueddari, N.E. and Moerschbacher, B.M., (2013). "Complexation of copper (II) with chitos an nanogels: Toward control of microbial growth", Carbohydrate Polymers, 92: 1348-1356.

[196] Esteban-Tejeda, L., Malpartida, F., Esteban-Cubillo, A., Pecharromn, C. and Moya, J. S., (2009). "Antibacterial and antifungal activity of a soda-lime glass containing copper nanoparticles", Nanotechnology, 20: 505701.

[197] Wei, Y., Chen, S., Kowalczyk, B., Huda, S., Gray, T. P. and Grzybowski, B. A., (2010). "Synthesis of Stable, Low-Dispersity Copper Nanoparticles and

Nanorods and Their Antifungal and Catalytic Properties", J. Phys. Chem. C., 114: 15612-15616.

[198]   Nasirian, A. (2012). "Synthesis and characterization of Cu nanoparticles and studying of their catalytic properties", Int. J. Nano. Dim., 2(3): 159-164.

[199]   Luo, X., Morrin, A., Killard, A. J. and Smyth, M. R., (2006). "Application of Nanoparticles in Electrochemical Sensors and Biosensors", Electroanalysis, 18: 319-326.

[200]   Yetisen, A. K., Montelongo, Y., Vasconcellos, F. D. C., Martinez-Hurtado, J., Neupane, S., Butt, H., Qasim, M.M., Blyth, J., Burling, K.,. Carmody, J. B., Evans, M., Wilkinson, T.D., Kubota, L.T., Monteiro, M. J. and Lowe, C. R., (2014). "Reusable, Robust, and Accurate Laser-Generated Photonic Nanosensor", Nano Letters., 14: 3587-3593. Doi: 10.1021/nl5012504.

[201]   Dizaj, S.M., Lotfipour, F., Barzegar-Jalali, M., Zarrintan, M.H. and Adibkia, K., (2014). "Antimicrobial activity of the metals and metal oxide nanoparticles", Mater. Sci. Eng. C Mater. Biol. Appl., 44: 278-284.

[202]   Bui, V., Park, D. and Lee, Y-C., (2017). "Chitosan Combined with ZnO, TiO$_2$ and Ag Nanoparticles for Antimicrobial Wound Healing Applications: A Mini Review of the Research Trends", Polymers, 9: 21.

[203]   Besinis, A., De Peralta, T. and Handy, R.D., (2014). "The antibacterial effects of silver, titanium dioxide and silica dioxide nanoparticles compared to the dental disinfectant chlorhexidine on Streptococcus mutans using a suite of bioassays". Nanotoxicology, 8: 1-16.

[204]   Azam, A., Ahmed, A.S., Oves, M., Khan, M.S., Habib, S.S. and Memic, A., (2012). "Antimicrobial activity of metal oxide nanoparticles against Gram-positive and Gram-negative bacteria: A comparative study", Int. J. Nanomed., 7: 6003-6009.

[205]   Lemire, J.A., Harrison, J.J. and Turner, R.J., (2013). "Antimicrobial activity of metals: Mechanisms, molecular targets and applications", Nat. Rev. Microbiol., 11: 371-384.

[206]   Shleeva, S., Tkac, J., Christenson, A., Ruzgas, T., Yaropolov, A.I., Whittaker, J.W. and Gorton, L., (2005). "Direct electron transfer between copper-containing proteins and electrodes", Biosens. Bioelectron., 20: 2517-2554.

[207]   Prabhu, S. and Poulose, E.K., (2012). "Silver nanoparticles: Mechanism of antimicrobial action, synthesis, medical applications, and toxicity effects", Int. Nano Lett., 32: 2-10.

[208]   Kim, J.D., Yun, H., Kim, G.C., Lee, C.W. and Choi, H.C., (2013). "Antibacterial activity and reusability of CNT-Ag and GO-Ag nanocomposites", Appl. Surf. Sci., 283: 227-233.

[209]   Applerot, G., Lellouche, J., Lipovsky, A., Nitzan, Y., Lubart, R., Gedanken, A. and Banin, E., (2012). "Understanding the antibacterial mechanism of CuO nanoparticles: Revealing the route of induced oxidative stress" Small, 8: 3326-3337.

[210]   Palza, H., (2015). "Antimicrobial polymers with metal nanoparticles", International journal of molecular science, 16(1): 2099-2116.

166

[211] Wahid, F., (2017). "Review: recent advances in antimicrobial hydrogels containing metal ions and metals/metal oxide nanoparticles", Polymers, 9: 636.

[212] Gaetke, L.M. and Chow, C.K., (2003). "Copper toxicity, oxidative stress, and antioxidant nutrients", Toxicology, 189: 147-163.

[213] Bremner, I., (1988). "Manifestations of copper excess", Am. J. Clin. Nutr., 67: 1069S-1073S.

[214] Buettner, G.R. and Jurkiewicz, B.A., (1996). "Catalytic metals, ascorbate and free radicals: Combinations to avoid", Radiat. Res., 145: 532-541.

[215] Grass, G., Rensing, C. and Solioz, M., (2011). "Metallic copper as an antimicrobial surface", Appl. Environ. Microbiol., 77: 1541-1548.

[216] Zhang, Y.M. and Rock, C.O., (2008). "Membrane lipid homeostasis in bacteria", Nat. Rev. Microbiol., 6: 222-233.

[217] Sondi, I. and Salopek-Sondi, B., (2004). "Silver nanoparticles as antimicrobial agent: A case study on *E. coli* as a model for Gram-negative bacteria", J. Colloid Interface Sci., 275: 177-182.

[218] Matsumura, Y., Yoshikata, K., Kunisaki, S. and Tsuchido, T., (2003). "Mode of bactericidal action of silver zeolite and its comparison with that of silver nitrate", Applied and Environmental Microbiology, 69(7): 4278-4281. DOI: 10.1128/AEM.69.7.4278-4281.2003.

[219] Morones, J.R., Elechiguerra, J.L., Camacho, A., Holt, K., Kouri, J.B., Ramirez, J.T. and Yacaman, M.J., (2005). "The bactericidal effect of silver nanoparticles", Nanotechnology, 16: 2346-2353.

[220] Hatchett, D.W. and Henry, S., (1996). "Electrochemistry of sulfur adlayers on low-index faces of silver", J. Phys. Chem., 100: 9854-9859.

[221] Bera, R., Mandal, S. and Raj, C.R., (2014). "Antimicrobial activity of fluorescent Ag nanoparticles", Lett. Appl. Microbiol., 58: 520-526.

[222] Xia, X., Xie, C., Cai, S., Yang, Z. and Yang, X., (2006). "Corrosion characteristics of copper microparticles and copper nanoparticles in distilled water", Corros. Sci., 48: 3924-3932.

[223] Mohammadi, G., Valizadeh, H., Barzegar-Jalali, M., Lotfipour, F., Adibkia, K., Milani, M., Azhdarzadeh, M., Kiafar, F. and Nokhodchi, A., (2010). "Development of azithromycin–PLGA nanoparticles: Physicochemical characterization and antibacterial effect against *Salmonella typhi*", Colloids Surf. B Biointerfaces, 80: 34-39. Doi: 10.1016/j.colsurfb.2010.05.027.

[224] Fellahi, O., Sarma, R.K., Das, M.R., Saikia, R., Marcon, L., Coffinier, Y., Hadjersi, T., Maamache, M. and Boukherroub, R., (2013). "The antimicrobial effect of silicon nanowires decorated with silver and copper nanoparticles", Nanotechnology, 24: 495101.

[225] Mohammadi, G., Nokhodchi, A., Barzegar-Jalali, M., Lotfipour, F., Adibkia, K., Ehyaei, N. and Valizadeh, H., (2011). "Physicochemical and anti-bacterial performance characterization of clarithromycin nanoparticles as colloidal drug delivery system", Colloids Surf. B. Biointerfaces, 88: 39-44.

[226] Seil, J.T. and Webster, T.J., (2012). "Antimicrobial applications of nanotechnology: Methods and literature". Int. J. Nanomed., 7: 2767.

[227] Pal, S., Tak, Y.K. and Song, J.M., (2007). "Does the antibacterial activity of silver nanoparticles depend on the shape of the nanoparticle? A study of the gram-negative bacterium *Escherichia coli*", Appl. Environ. Microbiol., 73: 1712-1720.

[228] Ingle, A.P., Duran, N. and Rai, M., (2014). "Bioactivity, mechanism of action, and cytotoxicity of copper-based nanoparticles: a review", Appl. Microbiol. Biotechnol., 98: 1001-1009.

[229] Umer, A., Naveed, S., Ramzan, N., Rafique, M.S., Imran, M., (2014). "A green method for the synthesis of copper nanoparticles using L-ascorbic acid", Rev Matér., 19: 197-203.

[230] Li, Z., Lee, D., Sheng, X., Cohen, R.E. and Rubner, M.F., (2006). "Two-level antibacterial coating with both release-killing and contact-killing capabilities", Langmuir, 22: 9820-9823.

[231] Zewde, B., Ambaye, A., Stubbs, J., (2016). "A review of stabilized silver nanoparticles – synthesis, biological properties, characterization, and potential areas of applications", JSM Nanotechnology & Nanomedicine, 4(2): 1043.

[232] Cho, K., Park, J., Osaka, T. and Park, S., (2005). "The study of antimicrobial activity and preservative effects of nanosilver ingredient", Electrochim Acta., 51: 956-960.

[233] Peiris, M.K., Gunasekara, C.P., Jayaweera, P. M., (2017). "Biosynthesized silver nanoparticles: are they effective antimicrobials", Mem. Inst. Oswaldo Cruz, 112(8): 537-543.

[234] Wright, J.B., Lam, K., Hanson, D. and Burrell, R.E., (1999). "Efficacy of topical silver against fungal burn wound pathogens", Am. J. Infect. Control, 27(4): 344-350.

[235] Rao, M. L. and Savithramma, N., (2011). "Biological synthesis of silver nanoparticles using *Svensonia hyderabadensis* leaf extract and evaluation of their antimicrobial efficacy", J. Pharm. Sci. & Res., 3(3): 1117-1121.

[236] Zhang, Y., Yang, D., Kong, Y., Wang, X., Pandoli, O. and Gao, G., (2010). "Synergetic antibacterial effects of silver nanoparticles@*Aloe vera* prepared via a green method", Nano. Biomed. Eng., 2(4): 252-257.

[237] Mariselvam, R., Ranjitsingh, A.J.A., Nanthini, U. R. A., Kalirajan, K., Padmalatha, C. and Selvakumar, M. P., (2014). "Green synthesis of silver nanoparticles from the extract of the inflorescence of *Cocos nucifera* (Family: Arecaceae) for enhanced antibacterial activity", Spectrochim Acta. Part A.: Mol. Biomol. Spectrosc., 129: 537-541.

[238] Suna, Q., Cai, X., Li, J., Zheng, M., Chenb, Z. and Yu, C.P., (2014). "Green synthesis of silver nanoparticles using tea leaf extract and evaluation of their stability and antibacterial activity", Colloid Surf A.: Physicochem Eng. Aspects, 444: 226-231.

[239] Kumar, D.A., Palanichamy, V. and Roopan, S.M., (2014). "Green synthesis of silver nanoparticles using *Alternanthera dentata* leaf extract at room

temperature and their antimicrobial activity", Spectrochim Acta Part A: Mol Biomol Spectrosc, 127: 168-171.

[240] Geetha, N., Geetha, T.S., Manonmani, P. and Thiyagarajan, M., (2014). "Green synthesis of silver nanoparticles using *Cymbopogan Citratus* (Dc) Stapf. Extract and its antibacterial activity", Aus. J. Basic. Appl. Sci., 8(3): 324-331.

[241] Gopinatha, V., Ali, M.D., Priyadarshini, S., Priyadharsshini, N.M., Thajuddinb, N. and Velusamy, P., (2012). "Biosynthesis of silver nanoparticles from *Tribulus terrestris* and its antimicrobial activity: a novel biological approach", Colloid Surf B.: Biointerface, 96: 69-74.

[242] Kumar, P.N.V., Pammi, S.V.N., Kollu, P., Satyanarayana, K.V.V. and Shameem, U., (2014). "Green synthesis and characterization of silver nanoparticles using *Boerhaavia diffusa* plant extract and their anti-bacterial activity", Ind. Crops Prod. 52: 562-566.

[243] Letfullin, R.R., Iversen, C.B., George, T.F., (2011). "Modeling nanophotothermal therapy: kinetics of thermal ablation of healthy and cancerous cell organelles and gold nanoparticles", Nanomed: Nanotechnol. Biol. Med., 7: 137-145.

[244] Chatterjee, A. and Chakra, R., (2014). "Mechanism of antibacterial activity of copper nanoparticles", Nanotechnology, 25(13):1-23. DOI:10.1088/0957-4484/25/13/135101.

[245] Wang, L., Hu, C. and Shao, L. (2017). "The antimicrobial activity of nanoparticles: present situation and prospects for the future", Int. J. Nanomed, 12: 1227-1249.

[246] Beyth, N., Houri-Haddad, Y., Domb, A., Khan, W. and Hazan, R., (2015). "Alternative antimicrobial approach: Nano-antimicrobial materials", Evid-Based Complement Altern. Med., 2015: 246012.

[247] Yoon, K., Byeon, J.H., Park, J. and Hwang, J. (2007). "Susceptibility constants of *Escherichia coli* and *Bacillus subtilis* to silver and copper nanoparticles", Sci. Total Environ., 373: 572-575.

[248] De Alba-Montero, I., Guajardo-Pacheco, J., Morales-Sánchez, E., Araujo-Martínez, R., Loredo-Becerra, G.M., Martínez-Castañón, G.-A., Ruiz, F. and Jasso, M. E. C., (2017). "Antimicrobial properties of copper nanoparticles and amino acid chelated copper nanoparticles produced by using a soya extract", Bioinorg Chem. Appl., 2017 (1064918). Doi: 10.1155/2017/1064918.

[249] Edelstein, A. S. and Cammaratra, R. C., (1998). Nanomaterials: synthesis, properties and applications, 2nd edition, CRC Press, New York.

[250] Staggers, N., McCasky, T., Brazelton, N. and Kennedy, R., (2008), "Nanotechnology: the coming revolution and its implications for consumers, clinicians, and informatics", Nursing Outlook, 56 (5): 268–274.

[251] Klaine, S. J., Alvarez, P. J. J., Batley, G. E., Fernandes, T.F., Handy, R.D., Lyon, D.Y., Mahendra, S., McLaughlin, M.J. and Lead, J.R., (2008). "Nanomaterials in the environment: behavior, fate, bioavailability and effects", Environmental Toxicology and Chemistry, 27(9): 1825–1851.

[252] Schulte, P., Geraci, C., Zumwalde, R., Hoover, M. and Kuempel, E., (2008). "Occupational risk management of engineered nanoparticles", Journal of Occupational and Environmental Hygiene, 5(4): 239–249.

[253] Li, J.J., Muralikrishnan, S., Ng, C.T., Yung, L.Y. and Bay, B.H., (2010). "Nanoparticle-induced pulmonary toxicity", Exp. Biol. Med. (Maywood), 235:1025-1033.

[254] Lee, J.C., Son, Y.O., Pratheeshkumar, P. and Shi, X., (2012). "Oxidative stress and metal carcinogenesis", Free Radic. Biol. Med., 53:742-757.

[255] Panda, K.K., Achary, V.M., Krishnaveni, R., Padhi, B.K., Sarangi, S.N., Sahu, S.N. and Panda, B.B., (2011). "*In vitro* biosynthesis and genotoxicity bioassay of silver nanoparticles using plants", Toxicology in Vitro, 25:1097- 1105. Doi: 10.1016/j.tiv.2011.03.008.

[256] Teodoro, J.S., Simões, A.M., Duarte, F.V., Rolo, A.P., Murdoch, R.C., Hussain, S.M. and Palmeira, C.M., (2011). "Assessment of the toxicity of silver nanoparticles in vitro: A mitochondrial perspective", Toxicology in Vitro, 25:664 -670. Doi: 10.1016/j.tiv.2011.01.004.

[257] Park, M.V., Neigh, A.M., Vermeulen, J.P., de la Fonteyne, L.J., Verharen, H.W., Briedé, J.J., van Loveren, H. and de Jong, W.H., (2011). "The effect of particle size on the cytotoxicity, inflammation, developmental toxicity and genotoxicity of silver nanoparticles", Biomaterials, 32(36):9810-7. Doi: 10.1016/j.biomaterials.2011.08.085.

[258] Chaudhry, Q., Schotter, M., Blackburn, J., Ross, B., Boxall, A., Castle, L., Aitken, R. and Watkins, R., (2008). "Applications and implications of nanotechnologies for the food sector", Food Addit. Contam. 25(3):241–258.

[259] Ingle, A.P., Duran, N. and Rai, M., (2013). "Bioactivity, mechanism of action, and cytotoxicity of copper-based nanoparticles: a review", Appl. Microbiol. Biotechnol., 98:1001–1009. Doi: 10.1007/s00253-013-5422-8.

[260] Prabhu, B.M., Ali, S.F., Murdock, R.C., Hussain, S.M. and Srivatsan, M., (2010). "Copper nanoparticles exert size and concentration dependent toxicity on somatosensory neurons of rat", Nanotoxicology, 4(2):150–160.

[261] Liu, W., Chaurand, P., Di Giorgio, C., De Méo, M., Thill, A., Auffan, M., Masion, A., Borschneck, D., Chaspoul, F., Gallice, P., Botta, A., Bottero, J.Y. and Rose, J., (2012). "Influence of the length of imogolite-like nanotubes on their cytotoxicity and genotoxicity toward human dermal cells", Chem Res Toxicol, 25: 2513- 2522.

[262] Wonsawat, W., (2014). "Determination of vitamin C (ascorbic acid) in orange juices product", International Journal of Materials and Metallurgical Engineering, 8(6): 623- 625.

[263] Baird, R.B., Eaton, A.D., and Rice, E.W., (2015). "Standard methods for the examination of water and waste water", 23rd ed., APHA, Washington, D.C.

[264] Lapage, S., Shelton, J. and Mitchell, T., (1970). "Methods in Microbiology", Academic Press, London. Vol. 3A.

[265] Haltiner, R.C., Migneault, P.C. and Roberston, R.G., (1980). "Incidence of thymidine-dependent Enterococci detected on Mueller-Hinton agar with low thymidine content", Anti. Ag. and Chemo., 18(3): 365-368.

[266] Mueller, J. H. and Hinton, J., (1941). "A protein-free medium for primary isolation of the *Gonococcus* and *Meningococcus*", Experimental Biology and Medicine, 48 (1): 330–333.

[267] Cockerill, F. R., (2012). "Methods for dilution antimicrobial susceptibility tests for bacteria that grow aerobically", Approved Standard—Ninth Edition. CLSI, 32(2):12.

[268] Hamedi, S., Shojaosadati, S.A. and Mohammadi, A., (2017). "Evaluation of the catalytic, antibacterial and anti-biofilm activities of the *Convolvulus arvensis* extract functionalized silver nanoparticles", Journal of Photochemistry and Photobiology B: Biology, 167: 36-44. Doi: 10.1016/j.jphotobiol.2016.12.025.

[269] Otte, H. M., (1961). "Lattice parameter determinations with an x-ray spectrogoniometer by the debye-scherrer method and the effect of specimen condition", J. Appl. Phys., 32:1536–1546.

[270] Rice, K. P., Walker, E. J., Stoykovich, M. P. and Saunders, A. E., (2011). "Solvent-dependent surface plasmon response and oxidation of copper nanocrystals", J. Phys. Chem. C 115, 1793–1799 (2011). Doi: 10.1021/jp110483z

[271] Dabera, G.D.M.R., Walker, M., Sanchez, A.M., Pereira, H.J., Beanland, R. and Hatton, R.A., (2017). "Retarding oxidation of copper nanoparticles without electrical isolation and the size dependence of work function", Nature Communications, 8:1894. Doi: 10.1038/s41467-017-01735-6.

[272] López-García, J., Lehocký, M., Humpolíček, P. and Sáha, P., (2014). "HaCaT keratinocytes response on antimicrobial atelocollagen substrates: extent of cytotoxicity, cell viability and proliferation", Journal of functional biomaterials, 5(2): 43-57. Doi: 10.3390/jfb5020043.

[273] ANSI/AAMI/ISO 10993-5:2009, (2009). Biological Evaluation of Medical Devices. Part 5: Tests for In Vitro Cytotoxicity, International Organization for Standardization: Geneva, Switzerland.

[274] Tsuji, M., Hashimoto, M., Nishizawa, Y., Kubokawa, M. and Tsuji, T., (2005). "Microwave-assisted synthesis of metallic nanostructures in solution", Chemistry, 11(2): 440-452. Doi: 10.1002/chem.200400417.

[275] Jiang, H., Moon, K.-s., Zhang, Z., Pothukuchi, S. and Wong, C. P., (2006). "Variable frequency microwave synthesis of silver nanoparticles", Journal of Nanoparticle Research, 8(1):117-124. Doi: 10.1007/s11051-005-7522-6.

[276] Bindhu, M.R., Umadevim M., (2013). "Synthesis of monodispersed silver nanoparticles using *Hibiscus cannabinus* leaf extract and its antimicrobial activity", Spectrochimica Acta Part A: Molecular and Bimolecular Spectroscopy, 101: 184-190. DOI: 10.1016/j.saa.2012.09.031

[277] Dong, C., Zhou, K., Zhang, X., Cai, H., Xiong, G., Chuanliang, C. and Chen, Z. (2014). "*Semen cassiae* extract mediated novel route for the preparation of

silver nanoparticles", Materials Letters, 120:118–121. Doi: 10.1016/j.matlet.2014.01.039.

[278] Karuppiah, M. and Rajmohan, R., (2013). "Green synthesis of silver nanoparticles using *Ixora coccinea* leaves extract", Materials Letters, 97: 141–143.

[279] Balashanmugam, P., Nandhini, R., Vijayapriyadharshini, V. and Kalaichelvan, P.T., (2014) "Biosynthesis of silver nanoparticles from orange peel extract and its antibacterial activity against fruit and vegetable pathogens", International Journal of Innovative Research in Science & Engineering (IJIRSE), ISSN (Online): 2347-3207.

[280] Chauhan, S., Upadhyay, M. K., Rishi, N. and Rishi, S., (2011). "Phytofabrication of silver nanoparticles using pomegranate fruit seeds", International Journal of Nanomaterials and Biostructures, 1 (2):17-21.

[281] Iravani, S. and Zolfaghari, B., (2013). "Green synthesis of silver nanoparticles using *Pinus eldarica* bark extract", BioMed Research International, 2013: Article ID 639725.

[282] Premasudha, P., Venkataramana, M., Abirami, M., Vanathi, P., Krishna, K. and Rajendran, R., (2015). "Biological synthesis and characterization of silver nanoparticles using *Eclipta alba* leaf extract and evaluation of its cytotoxic and antimicrobial potential", Bull. Mater. Sci., 38(4): 965–973.

[283] Yallappa, S., Manjanna, J., Peethambar, S., K., Rajeshwara, A., N. and Satyanarayan, N., D., (2013). "Green synthesis of silver nanoparticles using *Acacia farnesiana* (sweet Acacia) seed extract under microwave irradiation and their biological assessment", J Clust Sci, 24:1081–1092.

[284] Dang, T.M.D., Le1, T.T.T., Fribourg-Blanc, E. and Dang, M.C., (2011). "Synthesis and optical properties of copper nanoparticles prepared by a chemical reduction method", Advances in Natural Sciences: Nanoscience and Nanotechnology, 2 (015009): 6pp.

[285] Khodaie, M. and Ghasemi, N., (2018). "Green synthesis and characterization of copper nanoparticles using *Eryngium campestre* leaf extract", Bulgarian Chemical Communications, 50(Special Issue L): 244 – 250.

[286] Basavarajappa, A. and Neelagund, S.E., (2016). "An investigation on antibacterial efficacy of biosynthesized novel copper nanoparticles using silkworm fecal matter", Imperial Journal of Interdisciplinary Research (IJIR), 2(12): 1501-1507.

[287] Usha, S., Ramappa, K.T., Hiregoudar, S., Vasanthkumar, G.D. and Aswathanarayana, D.S., (2017). "Biosynthesis and characterization of copper nanoparticles from tulasi (*Ocimum sanctum* L.) leaves", International Journal of Current Microbiology and Applied Sciences, 6 (11): 2219-2228.

[288] Bar, H., Bhui, D.K., Sahoo, G.P., Sarkar, P., De, S.P. and Misra, A., (2009). "Green synthesis of silver nanoparticles using latex of *Jatropha curcas* ", Colloids and Surfaces a: Physicochemical Engineering Aspects, 339: 134-139.

[289] Daniel, K., Kumar, R., Sathish, V., Sivakumar, M. and Sironmani, A., (2011)."Green Synthesis (*Ocimum tenuiflorum*) of Silver Nanoparticles and

Toxicity Studies in Zebra Fish (Danio rerio)", International Journal of NanoScience and Nanotechnolog, 2 (2): 103-117.

[290]   Zhou Y., Lin W., Huang J., Wang W., Gao Y., Lin L., Li Q. and Du M. (2010) Biosynthesis of Gold Nanoparticles by Foliar Broths: Roles of Bio compounds and Other Attributes of the Extracts. Nanoscale Research Letter, 5: 1351-1359.

[291]   Theivasanthi, T. and Alagar, M., (2012). "Electrolytic Synthesis and Characterization of Silver Nanopowder", Nano Biomedicine and Engineering, 4(2), 58-65. DOI: 10.5101/nbe.v4i2.p58-65.

[292]   Suresh, Y., Annapurna, S., Bhikshamaiah, G. and Singh, A.K., (2014). "Copper Nanoparticles: Green Synthesis and Characterization", International Journal of Scientific & Engineering Research, 5(3): 156-160.

[293]   Haider, M. J. and Mehdi, M. S., (2014). "Study of morphology and Zeta Potential analyzer for the Silver Nanoparticles", International Journal of Scientific & Engineering Research, 5(7): 381-387.

[294]   Kahrilas, G. A., Wally, L. M., Fredrick, S. J., Hiskey, M., Prieto, A.L. and Owens, J. E., (2014). "Microwave-assisted green synthesis of silver nanoparticles using orange peel extract", ACS Sustainable Chemistry & Engineering, 2014, 2 (3): 367–376. DOI: 10.1021/sc4003664.

[295]   Arthur, L.K., (2003). "Bacterial wall as target for attack: past, present, and future research", Clinical Microbiology Reviews, 16(4): 673-687. DOI: 10.1128/CMR.16.4.673-687.2003.

[296]   Mukherjee, S., Chowdhury, D., Kotcherlakota, R., Patra, S., Vinothkumar, B., Bhadra, M.P., Sreedhar, B. and Patra, C.R., (2014). "Potential theranostics application of bio-synthesized silver nanoparticles (4-in-1 system)", Theranostics, 4(3): 316-335. Doi:10.7150/thno.7819.

[297]   Fernando, S.S.N., Gunasekara, T.D.C.P., Holton, J., (2018). "Antimicrobial Nanoparticles: applications and mechanisms of action", Sri Lankan Journal of Infectious Diseases, 8 (1):2-11. DOI: http://dx.doi.org/10.4038/sljid.v8i1.8167.

CURRICULUM VITAE

PERSONAL INFORMATION

Name Surname   : Israt JAHAN

Date of birth and place : 26. 10. 1984 / Narsingdi, Bangladesh

Foreign Languages   : English, Turkish

E-mail   : sonia.israt@yahoo.com

EDUCATION

Degree	Department	University	Date of Graduation
Master	Department of Botany	Jahangirnagar University	2010
Undergraduate	Department of Botany	Jahangirnagar University	2008

WORK EXPERIENCE

Year	Corporation/Institute	Enrolment
2010-2012	Bangladesh Council of Scientific and Industrial Research (BCSIR), Bangladesh.	Post graduate research fellow
2009-2012	Cytogenetics Lab., Department of Botany,	Researcher

Dhaka University, Bangladesh.

	Plant Breeding and Crop Improvement Lab.,	
2007-2009	Department of Botany, Jahangirnagar	Researcher
	University, Bangladesh.	

PUBLISHMENTS
Papers

1.   **Israt Jahan**, Fatih Erci & Ibrahim Isildak (2019). Microwave-assisted green synthesis of non-cytotoxic silver nanoparticles using the aqueous extract of *Rosa santana* (rose) petals and their antimicrobial activity. ***Analytical Letters***, DOI:10.1080/00032719.2019.1572179.

2.   Sheikh Shamimul Alam, Ruhina Tasmin, **Israt Jahan**, Md. Ahashan Habib & Syeda Sharmeen Sultana (2013). Fluorescent banding and RAPD analysis of five varieties in *Vigna unguiculata* ssp. *sesquipedalis* (L.) Verdc. ***Cytologia***, 78(1), 73-79. DOI:10.1508/cytologia.78.73.

3.   **Israt Jahan**, Md. Ahashan Habib, Nazmul Alam & Sheikh Shamimul Alam (2012). Karyotype and RAPD analysis in 3 commercial varieties of *Cucurbita maxima* Duch. ***Cytologia***, 77(2), 149-154. DOI:10.1508/cytologia.77.149.

Conference Papers

1.   **Israt Jahan** (2011). Karyotype and RAPD analysis in 3 commercial varieties of *Cucurbita maxima* Duch. *5th International Botanical Conference*, December 9 - 11, 2011, Dhaka.

Projects

1.   TAGEM (09/2014 – 09/2016), Farkli Nanopartiküllerin Yeşil

Sentezi ve Bitkilere Etkileri, **Assistant Researcher**

2.   TAGEM (09/2014 – 09/2016), Seralarda Bitki Hastaliklarinin Erken Tespiti Için Kalsiyumve Salisilik Asit Seçici Sensörlerinin Geçirilmesi ve Uygulanmasi, **Assistant Researcher**

AWARDS

1.   **Doctoral Scholarship**, Türkiye Burslari Ali Kuşçu Bilim ve Teknoloji Burs Programı, Yurtdışı Türkler ve Akraba Topluluklar Başkanlığı (YTB), October, 2012 – September, 2018.

2.   **Postgraduate Research Fellowship**, Bangladesh Council of Science and Industrial Research (BCSIR), 2010-2012.

3.   **First Class 1st in Masters Program**, Department of Botany, Faculty of Life Science, Jahangirnagar University, 2010

4.   **First Class 1st in Undergraduate Program**, Department of Botany, Faculty of Life Science, Jahangirnagar University, 2008.